THERMAL STRATIFICATION IN SOLAR STORAGE TANKS

A thesis submitted for the degree of doctor of philosophy of the Council for National Academic Awards

by

ELSAYED ABD ELHAY ELDESSOUKY M.Sc.

School of Architecture

Leicester Polytechnic

Leicester

September 1981

Any pages, tables, figures or photographs, missing from this digital copy, have been excluded at the request of the university.

DECLARATION

I declare that no material contained in the thesis "Thermal stratification in solar storage tanks" has been used in any other submission for an academic award.

Acknowledgements of assistance received are listed at the front of the thesis document.

ACKNOWLEDGEMENT

I wish to express my deepest gratitude to Dr. N. Bowman, who supervised this research, for his guidance, helpful suggestions and constructive criticism throughout the thesis program. Tribute must be paid to his enthusiasm for the field of solar energy and its application.

My thanks are due to Mr. J. Croft who was a major source of help and inspiration throughout all of the laboratory investigations.

I am sincerely indebted to Professor B. Farmer, head of the School of Architecture, for his encouragement throughout the entire course of this program.

I am also indebted to Professor R. Maw, Polytechnic of Central London, Dr. B. Redferne, School of Building, Dr. P. Few, School of Mechanical Engineering, Dr. D. Armitage, School of Chemistry, and computer staff.

I am also indebted to Mr. P. Laughton, School of Electrical Engineering for his assistance with the simulator.

My thanks are also due to Mr. L. Tibbs and Mr. R. Smith, School of Mechanical Engineering and Mr. S. Berry and Mr. M. Geraghty, School of Architecture for their technical assistance.

The continuous encouragement and support of my wife has been greatly appreciated. The financial assistance of Leicestershire County Council is gratefully acknowledged.

ABSTRACT

The purpose of the work was to investigate the thermal stratification in solar storage containers. Three domestic thermally stratified hot water storage containers were designed with the main object of improving and stabilizing thermal stratification of the stored water as a means of improving the overall efficiency of solar water heating systems. Testing of the three storage containers was carried out under similar conditions and the results showed that TYPE I storage container behaves as a three-segment stratified system, TYPE II storage container behaves as a two-segment stratified system with a thermocline occupying approximately half of the height of the storage container, and TYPE III storage container behaves as a two-segment stratified system with a thermocline occupying two thirds of the height of the storage container. It was found that TYPE I storage container, with a L/D equal to 3/1, gave the best results in terms of heat collected, and also had the maximum stratification which is the main goal of this study.

The effect of each of three flow rates (0.01 kg/Sm^2, 0.015 kg/Sm^2, 0.02 kg/Sm^2) on stratification was studied and it was found that the flow rate of 0.01 kg/Sm^2 of collector area gave the better result.

A low-cost simulator for studying the performance of solar energy storage containers was designed. The design was based on a relatively inexpensive micro-computer linking into a mains power regulator with an 8-bit digital control system. Meteorological data was used to compute radiation income on any inclined plane and the output to the power regulator is controlled by the computed instantaneous rate of energy gain from the collector system undergoing simulation.

A comparison has been made between some of the experimental and theoretical results for TYPE I storage container. The theoretical prediction was based on two mathematical models of Duffie and Beckman[2], and Close[44]. A computer system model has been developed to assist in the design of a solar water heating system.

CONTENTS

* publication

List of Tables

List of Figures

List of photographic prints

INTRODUCTION

In general it is clear that thermal stratification may produce an improvement in the overall performance of solar water and space heating systems. Other secondary benefits, such as a smaller system size may be realized in solar heating systems where the stratification of the storage fluid is maintained. While these benefits may serve to increase the efficiency and cost effectiveness of solar water and space heating systems, there is little design information available which can answer questions such as:

- How can stratification be achieved and maintained?
- What are the factors which effect stratification in the solar storage container?
- What is the most suitable design for a solar heat store, which will also improve thermal stratification?
- How does the fluid input and output of the storage container effect stratification?

The main aim of this thesis was to investigate under controlled laboratory conditions thermal stratification in solar storage containers, on a scale which has hitherto not been attempted, to begin to answer these questions as a basis for improving the overall efficiency of solar water heating systems. In particular this thesis has concentrated on water heating systems of domestic scale, e.g. for a family of four, and a collector area of 5 m^2 has been assumed.

In summary the main objectives of the investigation were:

1. To design a solar energy simulator to model the solar collection profile of any solar water heating system at any latitude, orientation, tilt and time of year.

2. To study the formation and stability of vertical temperature gradients in storage containers as a basis for improving the overall efficiency of a solar water heating system.

3. To provide information about those factors which affect stratification and make recommendations for optimising the design of storage containers.

4. To develop a computer system model for the solar water heating systems undergoing investigation.

The thesis is divided into nine chapters, each dealing with a particular aspect of the work.

Chapter 1: a state-of-the-art review of thermal stratification literature.

Chapter 2: describes the characteristics of solar radiation and meteorological data is used to compute radiation income on the tilted collector surface.

Chapter 3: describes the flat-plate solar collector and its mathematical treatment. A computer model is developed and used to compute the instantaneous rate of energy gain from the collector system undergoing simulation.

Chapter 4: describes the design of a suitable simulator for this study, which is intended to be representative of the long term energy delivery averaged over most cloud conditions and incident angles. This chapter also describes the experimental equipment.

Chapter 5: considers the problem of thermal energy storage. The problem is divided into three parts:

(i) The choice of storage medium

(ii) The determination of the storage capacity

(iii) The storage container design.

Chapter 6: describes the main body of the experimental work and presents the results in a variety of ways.

Chapter 7: describes the computer model of a stratified storage container based on two mathematical models of (i) Duffie and Beckman[2], and (ii) Close[44]. A comparison is made between some of the experimental and theoretical results.

Chapter 8: describes the computer system model for the solar water heating system undergoing investigation.

Chapter 9: gives the conclusions and suggestions for future work.

CHAPTER 1. THERMAL STRATIFICATION: STATE-OF-THE-ART REVIEW

The advantages of stratification have been illustrated by Brumleve[1] in the form of calculations comparing stratified and mixed storage under conditions of fixed return temperatures from the load and from the collector. Additionally a quantitative comparison was reported by Duffie and Beckman[2] who simulated the operation of a solar water heating system over a one week period. They found a 6% increase in the fraction of the total load served by solar energy when a three-segment stratified storage tank was substituted for a mixed tank.

Sharp and Lockrke[3], have simulated the operation of solar water heating, space heating and air conditioning systems. The performance of comparable systems with mixed and stratified storage was determined in terms of the fraction of the total load supplied by solar energy. Their results show that significant improvements in system performance (5-15%) may be realized if stratification can be maintained in the storage tank, and the magnitude of improvement is greatest, and the sensitivity to design variables smallest, in hot water services applications.

Davis and Bartera[4] experimentally studied the effects of temperature stratification in a water storage tank used in a hot water system for an apartment complex. They presented data which illustrated the performance of solar water heating systems for two types of fluid input and output configurations. In one case a thermocline was formed having a width which was 20 to 30 percent of the height of the tank.

With the second configuration, no thermocline was formed, thus illustrating the sensitivity of the system to the fluid removal and input configuration.

Brinkworth[5] has pointed out that one of the most interesting current problems in liquid storage is how to produce and sustain thermal gradients so as to minimize the change of entropy and maintain the thermodynamic availability of the energy stored. Where the input comes from solar collectors; the existence of temperature gradients also allows the collectors to be fed with fluid having a temperature lower than the mean temperature of the store, with some further benefit to the efficiency of collection. Sheridan et al[6] have solved simple cases of stratified storage tanks using an analogue computer, while Gutierrez et al[7] have produced solutions to a number of cases involving water heating, on a hybrid computer. The differences in predicted system performance using an unstratified model as compared to a stratified model may be significant, depending on the nature of the application. These differences are most pronounced when a two- or three-segment tank is substituted for a one-section tank.

Loehrke, Gari, Sharp and Haberstroh[8] have studied two possible approaches to the design of an inlet distributor as a passive technique for enhancing thermal stratification in liquid storage tanks. One employs a fixed, vertical, porous manifold; the other approach employs a lightweight, flexible hose with one end attached to the inlet and the other end is free to move vertically within the tank in response to the buoyance force. They pointed out that the latter

method had the advantage of preventing mixing between fluids of unlike temperature, while the former is potentially more reliable since it is fixed and self-purging of entrapped air. Model tests show that even a small amount of entrapped air seriously degrades the performance of a flexible-hose distributor. Thus their attention was concentrated on the rigid, porous manifold.

Sharp and Loehrke[9] carried out simulation studies to compare the predicted performance of a system using stratified storage with that of the same system using well-mixed storage in a solar space heating application. They pointed out that the benefit due to stratification, as measured by the increase in the fraction of the total heating load supplied by solar energy, ranged from about 5 to 15 percent.

Van Koppen, Fischer and Dijkmans[10] concluded that the systematic use of thermal stratification generally leads to an increase in the heat gain of solar heating installations of the order of 15%. Moreover the dimensions of several components of the installation can be substantially reduced.

Lavan and Thompson[11] have carried out studies on small-scale model stratified hot water storage containers, and their results showed that stratification can be maintained in cylindrical water storage containers, and the effect of length to diameter ratio (L/D) of storage containers is a trade-off between performance and cost. An L/D between 3 and 4 was suggested to be a reasonable compromise. Additionally they concluded that stratification improves with increasing length to diameter ratio, inlet and outlet port diameter, and it

decreases with increasing flow rates.

Mrs Carter[12] showed that thermal stratification could be maintained in large storage containers. She recommended that the proportion of storage container volume to collector area no longer had to be limited to 40 litre/m^2 of collecting area, which is the recommended[13] ratio in conventionally constructed solar water heating systems, but that a large storage volume, to cover at least 2 or 3 days, is justifiable (e.g. > 200 litre/m^2). She justifies her claim in three ways:

(i) in exceptionally hot weather there will be room for an exceptionally large volume of hot water.

(ii) in mediocre weather a reserve of warm water can be built up so that when the sun does come out hot water can be obtained fairly quickly.

(iii) Cold water can be kept in the very bottom of the storage container so that in bad weather it stands the best chances of collecting some heat.

Lin and Sha[14] have developed a computer model COMMIX-SA (COMponent MIXing-Solar Applications) to investigate the effects of baffles on thermal stratification in thermocline storage containers. Their results showed that a tall and slender storage container with vertical concentric cylindrical baffles and a ring distributor gave discharge and charge efficiencies in excess of 90%.

Hamaker, Hoekstra, Van Koppen and Van Wolde[15] have designed a short-term storage vessel at the Eindhoven University of Technology.

The main feature of the vessel is a floating inlet (a flexible thin walled plastic hose) which automatically discharges the water from the collector at the correct level in the storage container. The floating inlet makes 5% more energy available to the whole solar heating system. There is also a possibility of reducing the dimensions and costs of some parts of the solar heating system.

Van Koppen, Simon Thomas and Veltkamp[16] have concluded that a more widespread utilisation of thermally stratified storage in combination with much lower collector flow rates than usual will lead to considerable improvements in the performance of solar space heating and hot water supply systems.

Lin, Sha and Michaels[17] pointed out that thermal stratification improves storage efficiency as well as collector efficiency, and the efficiency of one component may effect that of another and hence the overall system efficiency may be a complicated function of all the component efficiencies. The authors claim that thermal stratification in a storage unit leads to an improvement of the overall system performance for two primary reasons:

(i) it improved the storage discharge efficiency

(ii) it improved the storage charge efficiency, and hence the collector efficiency.

Han and Wu[18] carried out a numerical simulation of a solar hot water application for an apartment by using the general transient system simulation program, TRNSYS with a mixed and a stratified water storage tank model. Their simulation results show that solar energy

collection efficiency can be increased up to 6% by using a stratified model, compared with that of a mixed model and the difference of the total solar energy collected between a mixed and a stratified model depends strongly on temperature stratification regardless of the system parameters.

Loehrke, Holzer, Gari and Sharp[19] carried out a series of experiments to compare the performance of inlets of different design to cylindrical steel tank with vertical axis. The tank was 2.27 m^3 (600 gal), 1.16 m (45.6 in) diameter and well-insulated. They studied the effect of each of three different inlet configurations (vertical jet, nozzle matrix and distribution manifold) on stratification. Their results show that when the flow is introduced through a vertical jet little stratification is obtained, while better stratification is obtained with the nozzle matrix. Overall the best stratification, with more uniform distribution, was obtained from the distribution manifold.

Much of this work is of interest and has a direct bearing on the direction of this thesis. In particular the author has noted the range of "efficiencies" claimed in association with the benefits from stratification; a summary of the more important findings has been given in Table 1.

TABLE 1. The range of "efficiencies" claimed in association with the benefits from stratification

AUTHOR(S)	PREDICTED IMPROVEMENT IN SYSTEM PERFORMANCE
Duffie and Beckman[2]	6%
Sharp and Lockrke[3]	5-15%
Han and Wu[18]	6%
Van Koppen, Fisher and Dijkmans[10]	15%

CHAPTER 2. THE CHARACTERISTICS OF SOLAR RADIATION AND THE COMPUTATION OF HOURLY RADIATION ON A TILTED SURFACE

2.1 Introduction

Before any attempt can be made to predict quantitatively the performance of a flat-plate solar energy collector the intensity of solar radiation incident on the surface of the collector must be known.

Although there are meteorological stations where solar radiation is regularly measured, these measurements are primarily limited to total radiation (direct plus diffuse) on a horizontal surface only. As the efficient operation of a solar collector generally requires orientation of the collector to a position other than horizontal, the horizontal incidence data of these meteorological stations must be converted to its equivalent on a tilted surface. Meteorological data was used to compute radiation income on a tilted plane (the collector surface).

2.2 Solar Radiation in the U.K.

Brinkworth[20] has pointed out that although the British climate is renowned for its lack of sunshine, it is interesting to note that the U.K. receives more than half the solar energy available in Australia or two thirds of that in the United States. However solar radiation in the U.K. is characterized by:

(i) More than 50 percent of diffuse radiation.

(ii) A large summer to winter variation (6:1).

The performance of all solar energy systems is dependent upon the weather. The weather may be interpreted as the time-dependent forcing functions exerted upon solar energy systems. These forcing functions are unique in that they are neither completely random nor deterministic, they are best described as irregular functions of time, both on a small (e.g. hourly or daily) and large (e.g. seasonally or yearly) time scale.

It is this irregular behaviour of the forcing functions (i.e. the weather) which complicates the analyses of solar energy systems. However, the work carried out at Sheffield University by Professor Page[21] has concentrated on providing reliable solar radiation data for the purpose of predicting accurately the solar inputs. Similar work has been carried out by Munroe[22], who has made a comparison between observed and estimated daily values for solar radiation on a horizontal surface from U.K. average meteorological data. His results showed that the computed values for daily radiation on a horizontal surface agree well with observed values for March and June, but the error is larger for September and December.

Page[23] and Heywood[24] have pointed out that the importance of the diffuse radiation to design should never be underrated, especially in cloudy climates and especially at higher latitudes such as U.K. This diffuse radiation is by no means negligible in magnitude, and whilst on a clear bright day it may only

amount to 10 per cent of the total radiation on a horizontal surface, on partially cloudy days it may amount to more than 50 per cent. On completely cloudy days however it comprises the total radiation.

Another point which complicates the analysis of any solar energy system is that the nonlinear dependence of system performance upon climatic conditions increases the difficulty of determining the effect that design variables have upon system performance.

2.3 Influence of surface orientation on the incident energy

An inclined surface will receive solar energy from three points:- (a) directly from the sun, (b) indirectly from the sky as diffuse radiation and (c) as reflected radiation from the ground. The tilt angle selection influences the performance of the solar system, furthermore the radiative and convection losses will also be affected by the choice of the tilt angle, as will be the reflected heat gain.

Ideally the collector should always be normal to the direct sunlight but the flat-plate collector is, by definition, fixed, and the best compromise position has to be decided upon. The tilt angle must itself be a compromise because winter performance is improved if it is large and the collector is inclined near the vertical. In summer a nearly horizontal collector is preferable. Important in the design of the system is the optimisation of tilt

to get high efficiency and good overall economy. One of the difficulties in such studies is the lack of a detailed description of the solar radiation climate on the slopes in question. Direct, diffuse and reflected energy have all to be considered in such optimisation processes. There is little data on solar radiation on inclined surfaces, as the meteorological networks generally measure only radiation on a horizontal surface. Svendsen[25] has pointed out that a programme has been carried out for continuous measurement of the inclined surface irradiance at University College, Cardiff. This programme is in progress and will provide the basis for a considerable range of studies applicable to the utilization of solar energy.

The optimization of tilt angle has been discussed in detail by Page[23], and has pointed out that much attention should be given to optimisation of tilt angle. However, the optimum slope depends on the period of the year over which the optimization is to be made, as well as on the precise use to which the energy is put. Figure 1 is presented by reference 26 and indicates the mean monthly daily values of total irradiation on slopes of 45^{o}, 60^{o} and 90^{o} at Kew, compared with horizontal surface, estimated from horizontal surface data 1957-1971. It can be seen from figure 1 that the 45^{o} tilt appears to offer the best collection possibility all year round. A similar study has been carried out by Courtney[27], and has confirmed that an angle of about 50^{o} to the horizontal results in the largest interception of direct radiation per unit area of collector in the U.K.

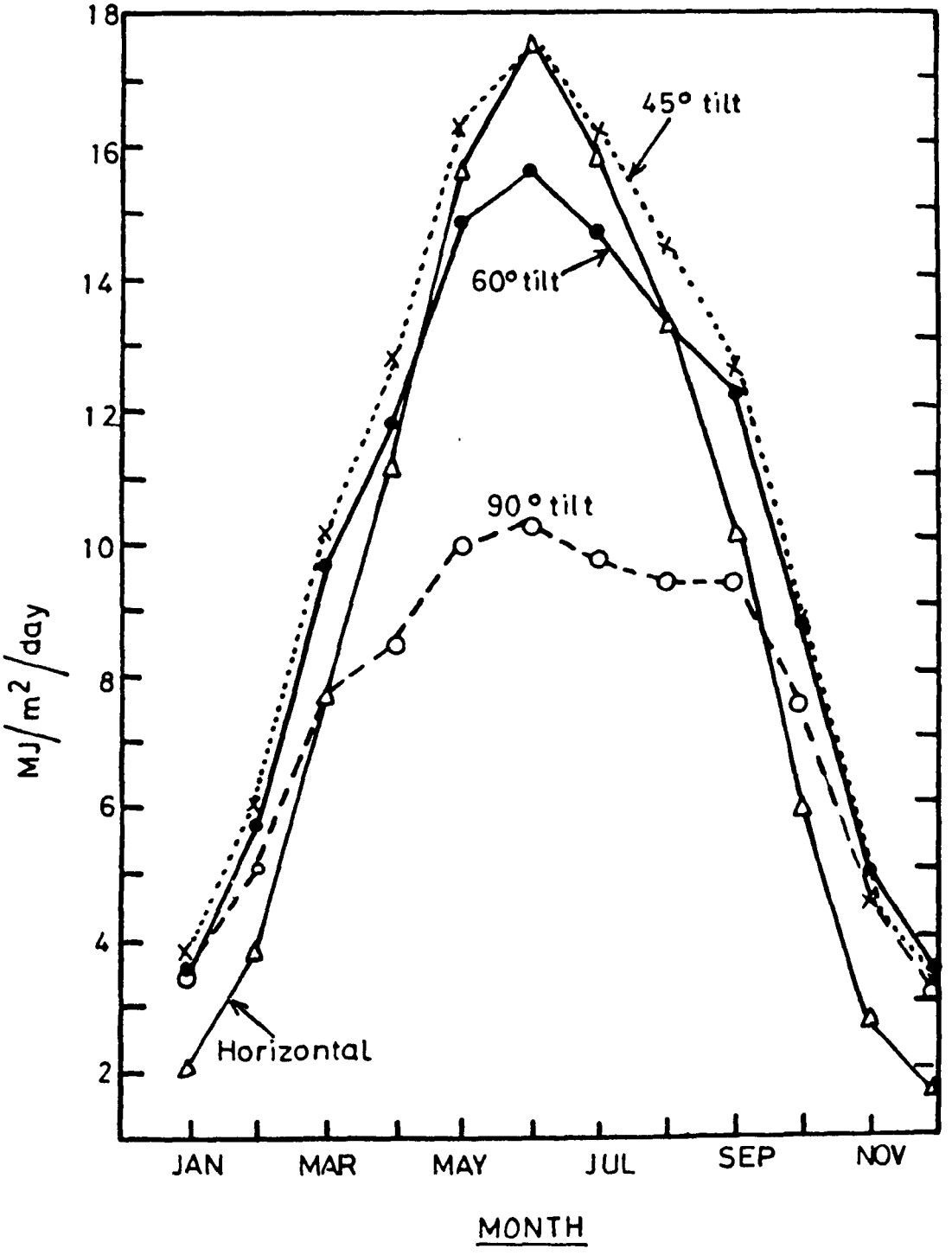

Figure 1

Mean monthly daily values of total irradiation on slopes of 45°, 60° and 90° at Kew compared with horizontal surface, estimated from horizontal surface data 1957-1971.

2.4 Hourly radiation data on a horizontal surface

The hourly radiation data on a horizontal surface at Leicester was needed for the computation of hourly radiation on a 45 degree plane. Unfortunately, there was no meteorological station at Leicester. McVeigh[28] has pointed out that the averaged radiation data from any meteorological station within 150 km will be perfectly adequate in the U.K., therefore it was decided to look for the nearest meteorological station to Leicester. It was found that the nearest one to Leicester is Bracknell, and the nearest place to Leicester which the radiation statistics were recorded is Cambridge, therefore the averaged radiation data from Cambridge was used for Leicester, also Cambridge is located at almost the same latitude as Leicester.

On that basis an average of ten years (1962-1971) hourly radiation data on a horizontal surface was specially purchased for this investigation.

Certain previous studies, e.g. Buchberg and Roulet[29], Lof and Tybout[30] have used no more than one year of radiation data. However, the adequacy of using a single year of data to provide an estimate of long-term system performance has not been justified in their studies. Therefore it was decided to incorporate weather data representative of long-term behaviour, ten years (1962-1971) hourly radiation of data were used to provide an estimate of long-term system performance. Since

solar radiation data are generally presented by meteorological stations on an hourly basis, therefore the total radiation received during a given hour instead of the radiation intensity at an instant was converted as shown in section 2.5.

2.5 Estimation and computation of hourly radiation on a tilted surface

The collector model described in chapter 3 requires a knowledge of R_T, the rate of radiation incident on the tilted collector surface per unit area. Unfortunately, measurements of R_T are generally unavailable and as a result, R_T must be estimated from measurements of the hourly radiation incident on a horizontal surface.

R_T can be estimated from measurements of radiation on a horizontal surface by separately treating the beam, diffuse and reflected components of the radiation as shown by Duffie and Beckman[2]. For beam components this can be done as follows:

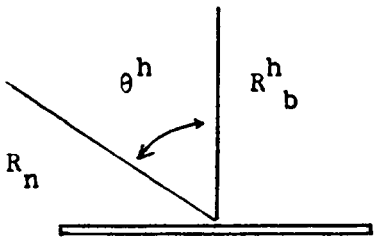

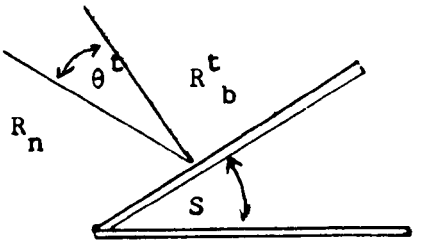

$$R_b = \frac{R^t_b}{R^h_b} = \frac{R_n \cos\theta^t}{R_n \cos\theta^h} = \frac{\cos\theta^t}{\cos\theta^h}$$

$$\therefore \quad R^t_b = R^h_b \frac{\cos\theta^t}{\cos\theta^h} \qquad (2.1)$$

Where,

R^t_b = the ratio of radiation on the tilted surface

R^h_b = the ratio of radiation on the horizontal surface

R_n = Radiation normal to the beam

θ^t = the angle of incidence on the tilted plane

θ^h = the angle of incidence on the horizontal plane.

For diffuse component this can be done as follows:

A surface tilted at a slope from the horizontal sees a portion of the sky dome given by 1 + Cos tilt/2.

If it is assumed that diffuse radiation is uniformly distributed over the sky, an assumption which generally results in a conservative estimate of the radiation on tilted surfaces,

$$\text{then } R^t_d = R^h_d \times \frac{1 + \text{Cos (tilt)}}{2} \qquad (2.2)$$

It is assumed that the reflected radiation is negligible.

From equations (2.1) and (2.2) the total radiation on the tilted surface at any time is

$$R^t = R^t_b + R^t_d = R^h_b \frac{\text{Cos } \theta^t}{\text{Cos } \theta^h} + R^h_d \frac{1 + \text{Cos (tilt)}}{2} \qquad (2.3)$$

and

$$\text{Cos } \theta^t = (\text{Cos } (\theta - S)\text{Cos}\delta \text{ Cos}\omega + \text{Sin } (\phi - S) \text{ Sin}\delta \qquad (2.4)$$

and

$$\text{Cos}\ \theta^h = \text{Cos}\phi\ \text{Cos}\ \delta\ \text{Cos}\omega + \text{Sin}\phi\ \text{Sin}\ \delta \qquad (2.5)$$

Where,

θ^t = the angles of incidence on the tilted plane

θ^h = the angles of incidence on the horizontal plane

R^t_b = the beam radiation on the tilted surface

R^h_b = the beam radiation on the horizontal surface

R^t_d = the diffuse radiation on the tilted surface

R^h_d = the diffuse radiation on the horizontal surface

Tilt = the angle between the collector and the horizontal plane

ϕ = latitude (north positive)

δ = declination (i.e. the angular position of the sun at solar noon with respect to the plane of the equator) (north positive)

$$= 23.45\ \text{Sin}\left[360\ \frac{284 + n}{365}\right] \qquad (2.6)$$

where n is the day of the year

S = the angle between the horizontal and the plane (i.e. the slope) south positive.

ω = hour angle, solar noon being zero, and each hour equalling 15^o of longitude with morning positive and afternoons negative e.g.

$\omega = +15$ for 11.00, and

$\omega = -37.5$ for 14.30.

2.6 The computation procedure for the radiation model

The computation procedure is shown in figure 2 which illustrates the flow chart for the radiation model. This model was used to compute radiation income on a tilted plane (the collector surface) using the meteorological data described in section 2.4.

2.7 Results

The results of the computation are shown in tables 2-13. Each table shows the mean monthly hourly radiation (KJ/m^2) on a horizontal surface and on a 45 degree plane, at Leicester (latitude $52^{o}37'$ N) for each month. It can be seen from these tables that the sum total of such hourly values over a period of a day should give radiation on the sloped surface for the day.

The results of the computation were used to generate a series of radiation profiles on a 45 degree plane (the collector surface) as shown in figures 3-14.

A histogram plot of mean monthly daily radiation on a 45^{o} plane at Leicester is shown in figure 15. It can be seen that the maximum mean monthly daily radiation on 45 degree plane at Leicester is in June, and the minimum is in December.

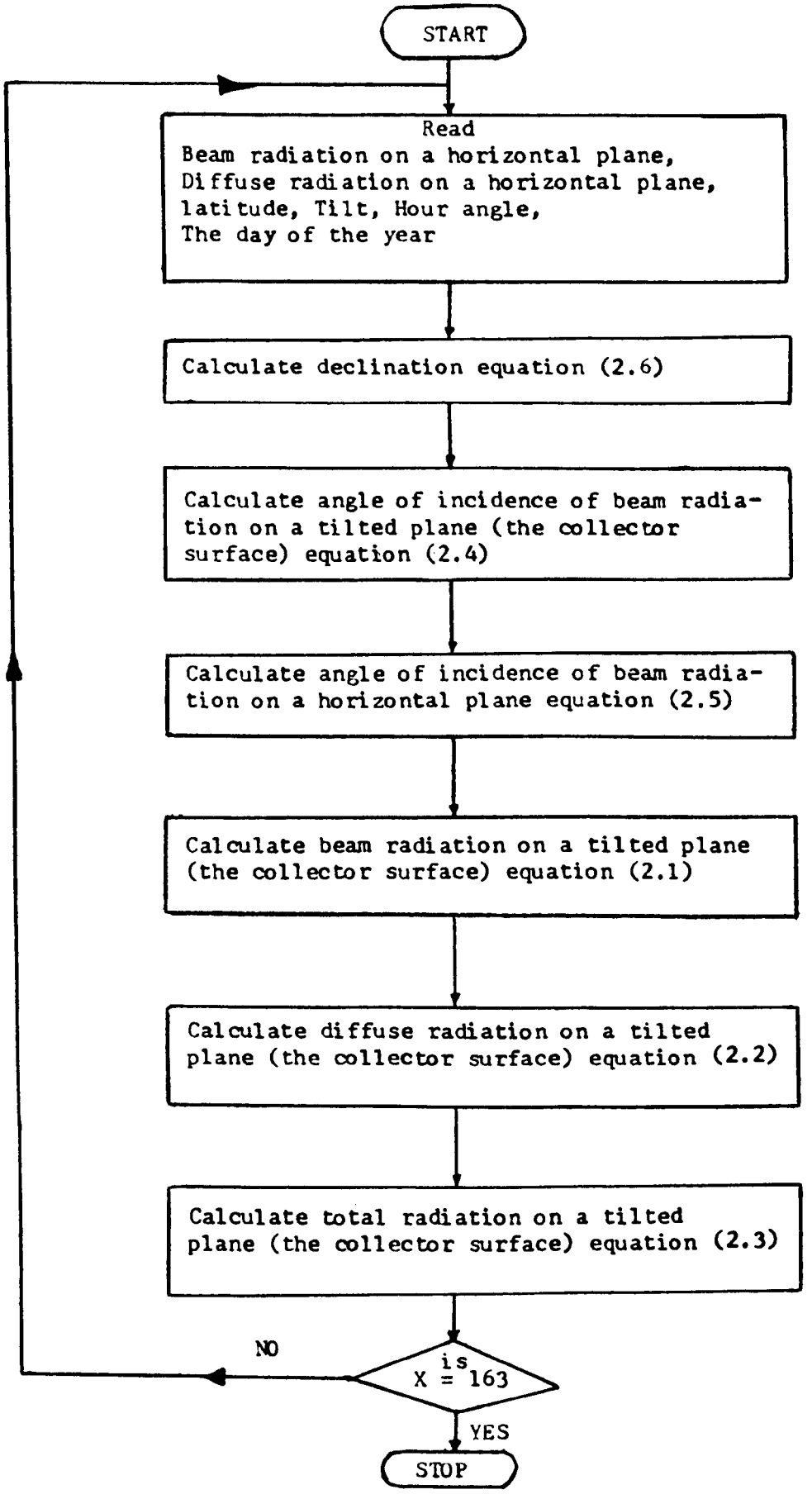

Figure 2

Flow chart for the radiation model

TABLE 2. 15 January: mean monthly hourly radiation (KJ/m^2) on a horizontal surface and on a 45^o plane, latitude $52^o37'$ N and orientation due south.

Hour	Mean monthly Hourly Radiation					
	Horizontal surface			45 degree plane		
	Beam	Diffuse	Total	Beam	Diffuse	Total
7 - 8	000	010	010	000.0	008.5	008.5
8 - 9	020	060	080	183.2	051.2	234.4
9 - 10	070	170	240	298.5	145.1	443.6
10 - 11	120	260	380	412.2	221.9	634.1
11 - 12	160	310	470	509.2	264.6	773.8
12 - 13	160	310	470	509.2	264.6	773.8
13 - 14	130	260	390	446.5	221.9	668.4
14 - 15	070	170	240	298.5	145.1	443.6
15 - 16	010	070	080	091.6	059.8	151.4
16 - 17	000	010	010	000.0	008.5	008.5
Daily Total	740	1630	2370	2748.9	1391.2	4140.1

TABLE 3. 15 February: mean monthly hourly radiation (KJ/M^2) on a horizontal surface and on a 45^o plane, latitude $52^o37'$ N and orientation due south.

Hour	Mean monthly Hourly Radiation					
	Horizontal surface			45 degree plane		
	Beam	Diffuse	Total	Beam	Diffuse	Total
7 - 8	010	060	070	078.0	051.2	0129.2
8 - 9	070	190	260	220.2	162.2	0382.4
9 - 10	160	320	480	411.0	273.1	0684.1
10 - 11	240	430	670	568.7	367.0	0935.7
11 - 12	280	490	770	643.1	418.2	1061.3
12 - 13	270	480	750	620.1	409.7	1029.8
13 - 14	230	410	640	545.1	350.0	0895.1
14 - 15	160	310	470	411.0	264.6	0675.6
15 - 16	070	190	260	220.2	162.2	0382.4
16 - 17	020	060	080	155.9	051.2	0207.1
17 - 18	000	010	010	000.0	008.5	0008.5
Daily Total	1510	2950	4460	3873.3	2517.9	6391.2

TABLE 4. 15 March: mean monthly hourly radiation (KJ/m^2) on a horizontal surface and on a 45^o plane, latitude $52^o37'$ N and orientation due south.

Hour	Mean monthly Hourly Radiation					
	Horizontal surface			45 degree plane		
	Beam	Diffuse	Total	Beam	Diffuse	Total
5 - 6	000	010	0010	000.0	008.5	0008.5
6 - 7	020	060	0080	061.3	051.2	0112.5
7 - 8	100	210	0310	193.0	179.3	0372.3
8 - 9	240	370	0610	433.5	315.8	0749.3
9 - 10	380	510	0890	669.7	435.3	1105.0
10 - 11	470	610	1080	819.0	520.7	1339.7
11 - 12	490	660	1150	849.9	563.4	1413.3
12 - 13	480	650	1130	832.6	554.8	1387.4
13 - 14	440	590	1030	766.7	503.6	1270.3
14 - 15	330	490	0820	581.5	418.2	0999.7
15 - 16	210	370	0580	379.3	315.8	0695.1
16 - 17	110	210	0320	212.2	179.3	0391.5
17 - 18	010	070	0080	030.6	059.8	0090.4
18 - 19	000	010	0010	000.0	008.5	0008.5
Daily Total	3280	4820	8100	5829.3	4114.2	9943.5

TABLE 5. 15 April: mean monthly hourly radiation (KJ/m^2) on a horizontal surface and on a 45^o plane, latitude $52^o37'N$ and orientation due south.

Hour	Mean monthly Hourly Radiation					
	Horizontal surface			45 degree plane		
	Beam	Diffuse	Total	Beam	Diffuse	Total
4 - 5	000	010	0010	000.0	008.5	0008.5
5 - 6	010	070	0080	000.0	059.8	0059.8
6 - 7	110	220	0330	078.9	187.8	0266.7
7 - 8	260	390	0650	286.6	332.9	0619.5
8 - 9	380	560	0940	474.0	478.0	0952.0
9 - 10	460	700	1160	606.2	597.5	1203.7
10 - 11	510	810	1320	690.4	691.4	1381.8
11 - 12	540	860	1400	739.5	734.1	1473.6
12 - 13	550	870	1420	753.2	742.6	1495.8
13 - 14	500	820	1320	676.9	699.9	1376.8
14 - 15	410	720	1130	540.3	614.6	1154.9
15 - 16	320	570	0890	399.2	486.5	0885.7
16 - 17	190	390	0580	209.6	332.9	0542.5
17 - 18	080	210	0290	057.4	179.3	0236.7
18 - 19	010	070	0080	000.0	059.8	0059.8
19 - 20	000	010	0010	000.0	008.5	0008.5
Daily Total	4330	7280	11610	5512.2	6214.1	11726.3

TABLE 6. 15 May: mean monthly hourly radiation (KJ/m^2) on a horizontal surface and on a 45^o plane, latitude $52^o37'$ N and orientation due south

Hour	Mean monthly Hourly Radiation					
	Horizontal surface			45 degree plane		
	Beam	Diffuse	Total	Beam	Diffuse	Total
4 - 5	000	0050	0050	000.0	042.7	0042.7
5 - 6	060	0190	0250	000.0	162.2	0162.2
6 - 7	220	0370	0590	109.8	315.8	0425.6
7 - 8	420	0540	0960	354.6	460.9	0815.5
8 - 9	570	0730	1300	577.6	623.1	1200.7
9 - 10	670	0880	1550	740.8	751.1	1491.9
10 - 11	750	0960	1710	866.9	819.4	1686.3
11 - 12	780	1030	1810	919.1	879.2	1798.3
12 - 13	780	1020	1800	919.1	870.6	1789.7
13 - 14	690	0970	1660	797.6	828.0	1625.6
14 - 15	600	0870	1470	663.4	742.6	1406.0
15 - 16	470	0710	1180	476.3	606.0	1082.3
16 - 17	340	0570	0910	287.1	486.5	0773.6
17 - 18	180	0380	0560	089.8	324.4	0414.2
18 - 19	070	0190	0260	000.0	162.2	0162.2
19 - 20	010	0050	0060	000.0	042.7	42.7
Daily Total	6610	9510	16120	6802.1	8117.4	14919.5

TABLE 7. 15 June: mean monthly hourly radiation (KJ/m^2) on a horizontal surface and on a 45° plane, latitude $52^{\circ}37'$ N and orientation due south

Hour	Mean monthly Hourly Radiation					
	Horizontal surface			45 degree plane		
	Beam	Diffuse	Total	Beam	Diffuse	Total
3 - 4	000	0010	0010	000.0	008.5	0008.5
4 - 5	030	0090	0120	000.0	076.8	0076.8
5 - 6	130	0250	0380	000.0	213.4	0213.4
6 - 7	300	0430	0730	132.7	367.0	0499.7
7 - 8	510	0620	1130	387.3	529.2	0916.5
8 - 9	670	0780	1450	621.5	665.8	1287.3
9 - 10	810	0920	1730	829.1	785.3	1614.4
10 - 11	890	1000	1890	958.5	853.6	1812.1
11 - 12	880	1060	1940	969.0	904.8	1873.8
12 - 13	870	1060	1930	958.0	904.8	1862.8
13 - 14	830	0990	1820	893.9	845.0	1738.9
14 - 15	700	0900	1600	716.5	768.2	1484.7
15 - 16	570	0760	1330	528.8	648.7	1177.5
16 - 17	450	0600	1050	341.7	512.1	0853.8
17 - 18	300	0420	0720	132.7	358.5	0491.2
18 - 19	130	0260	0390	000.0	221.9	0221.9
19 - 20	020	0100	0120	000.0	085.4	0085.4
20 - 21	000	0010	0010	000.0	008.5	0008.5
Daily Total	8090	10260	18350	7469.7	8757.5	16227.2

TABLE 8. 15 July: mean monthly hourly radiation (KJ/m^2) on a horizontal surface and on a 45^o plane, latitude $52^o37'$ N and orientation due south

Hour	Mean monthly Hourly Radiation					
	Horizontal surface			45 degree plane		
	Beam	Diffuse	Total	Beam	Diffuse	Total
4 - 5	020	0060	0080	000.0	051.2	0051.2
5 - 6	090	0210	0300	000.0	179.3	0179.3
6 - 7	230	0400	0630	106.4	341.4	0447.8
7 - 8	370	0590	0960	292.7	503.6	0796.3
8 - 9	520	0750	1270	499.3	640.2	1139.5
9 - 10	640	0900	1540	675.2	768.2	1443.4
10 - 11	670	1020	1690	741.9	870.6	1612.5
11 - 12	670	1060	1730	757.7	904.8	1662.5
12 - 13	680	1070	1750	769.0	913.3	1682.3
13 - 14	630	1020	1650	697.6	870.6	1568.2
14 - 15	580	0900	1480	611.9	768.2	1380.1
15 - 16	480	0750	1230	460.9	640.2	1101.1
16 - 17	350	0580	0930	276.9	495.1	0772.0
17 - 18	230	0400	0630	106.4	341.4	0447.8
18 - 19	090	0230	0320	000.0	196.3	0196.3
19 - 20	020	0070	0090	000.0	059.8	0059.8
Daily Total	6270	10010	16280	5995.9	8544.2	14540.1

TABLE 9. 15 August: mean monthly hourly radiation (KJ/m^2) on a horizontal surface and on a 45° plane, latitude $52^{\circ}37'$ N and orientation due south.

Hour	Mean monthly Hourly Radiation					
	Horizontal surface			45 degree plane		
	Beam	Diffuse	Total	Beam	Diffuse	Total
4 - 5	000	010	0010	000.0	008.5	0008.5
5 - 6	040	100	0140	000.0	085.4	0085.4
6 - 7	150	260	0410	088.6	221.9	0310.5
7 - 8	320	450	0770	308.4	384.1	0692.5
8 - 9	480	620	1100	540.7	529.2	1069.9
9 - 10	620	750	1370	750.4	640.2	1390.6
10 - 11	630	850	1480	790.4	725.5	1515.9
11 - 12	630	920	1550	802.7	785.3	1588.0
12 - 13	620	910	1530	789.9	776.7	1566.6
13 - 14	560	860	1420	702.6	734.1	1436.7
14 - 15	450	760	1210	544.6	648.7	1193.3
15 - 16	380	620	1000	428.1	529.2	0957.3
16 - 17	230	460	0690	221.7	392.6	0614.3
17 - 18	110	280	0390	065.0	239.0	0304.0
18 - 19	030	100	0130	000.0	085.4	0085.4
19 - 20	000	010	0010	000.0	008.5	0008.5
Daily Total	5250	7960	13210	6033.1	6794.3	12827.4

TABLE 10. 15 September: mean monthly hourly radiation (KJ/m^2) on a horizontal surface and on a 45^o plane, latitude $52^o37'$ N and orientation due south.

Hour	Mean monthly Hourly Radiation					
	Horizontal surface			45 degree plane		
	Beam	Diffuse	Total	Beam	Diffuse	Total
5 - 6	000	020	0020	0000.0	017.1	0017.1
6 - 7	050	130	0180	0061.1	111.0	0172.1
7 - 8	180	310	0490	0263.0	264.6	0527.6
8 - 9	360	460	0820	0547.2	392.6	0939.8
9 - 10	540	610	1150	0834.1	520.7	1354.8
10 - 11	610	710	1320	0949.4	606.0	1555.4
11 - 12	650	740	1390	1014.9	631.6	1646.5
12 - 13	640	720	1360	0999.3	614.6	1613.9
13 - 14	560	680	1240	0871.6	580.4	1452.0
14 - 15	460	580	1040	0710.5	495.1	1205.6
15 - 16	320	450	0770	0486.4	384.1	0870.5
16 - 17	160	290	0450	0233.8	247.5	0481.3
17 - 18	040	120	0160	0048.9	102.4	0151.3
18 - 19	000	020	0020	0000.0	017.1	0017.1
Daily Total	4570	5840	10410	7020.2	4984.8	12005.0

TABLE 11. 15 October: mean monthly hourly radiation (KJ/m^2) on a horizontal surface and on a 45^o plane, latitude $52^o37'$ N and orientation due south

Hour	Mean monthly Hourly Radiation					
	Horizontal surface			45 degree plane		
	Beam	Diffuse	Total	Beam	Diffuse	Total
6 - 7	000	020	020	000.0	017.1	0017.1
7 - 8	040	110	150	145.8	093.9	0239.7
8 - 9	140	260	400	345.8	221.9	0567.7
9 - 10	260	390	650	572.0	332.9	0904.9
10 - 11	360	500	860	754.0	426.8	1180.8
11 - 12	420	550	970	862.7	469.5	1332.2
12 - 13	420	540	960	862.7	460.9	1323.6
13 - 14	350	480	830	733.1	409.7	1142.8
14 - 15	270	380	650	596.9	324.4	0921.3
15 - 16	140	260	400	345.8	221.9	0567.7
16 - 17	040	110	150	145.8	093.9	0239.7
17 - 18	000	020	020	000.0	017.1	0017.1
Daily Total	2440	3620	6060	5364.6	3090	8454.6

TABLE 12. 15 November: mean monthly hourly radiation (KJ/m^2) on a horizontal surface and on a 45^o plane, latitude $52^o37'$ N and orientation due south.

Hour	Mean monthly Hourly Radiation					
	Horizontal surface			45 degree plane		
	Beam	Diffuse	Total	Beam	Diffuse	Total
7 - 8	010	010	020	000.0	008.5	008.5
8 - 9	040	100	140	238.0	085.4	323.4
9 - 10	120	220	340	431.8	187.8	619.6
10 - 11	180	320	500	549.3	273.1	822.4
11 - 12	210	360	570	603.4	307.3	910.7
12 - 13	200	360	560	574.6	307.3	881.9
13 - 14	160	310	470	488.3	264.6	752.9
14 - 15	110	210	320	392.5	179.3	571.8
15 - 16	030	100	130	178.5	085.4	263.9
16 - 17	010	010	020	000.0	008.5	008.5
Daily Total	1070	2000	3070	3456.4	1707.2	5163.6

TABLE 13. 15 December: mean monthly hourly radiation (KJ/m^2) on a horizontal surface and on a 45^o plane, latitude $52^o37'$ N and orientation due south.

Hour	Mean monthly Hourly Radiation					
	Horizontal surface			45 degree plane		
	Beam	Diffuse	Total	Beam	Diffuse	Total
8 - 9	000	040	040	000.0	034.1	034.1
9 - 10	050	130	180	262.6	111.0	373.6
10 - 11	110	220	330	433.0	187.8	620.8
11 - 12	130	260	390	464.3	221.9	686.2
12 - 13	130	260	390	464.3	221.9	686.2
13 - 14	100	210	310	393.7	179.3	573.0
14 - 15	050	130	180	262.6	111.0	373.6
15 - 16	000	040	040	000.0	034.1	034.1
Daily Total	570	1290	1860	2280.5	1101.1	3381.6

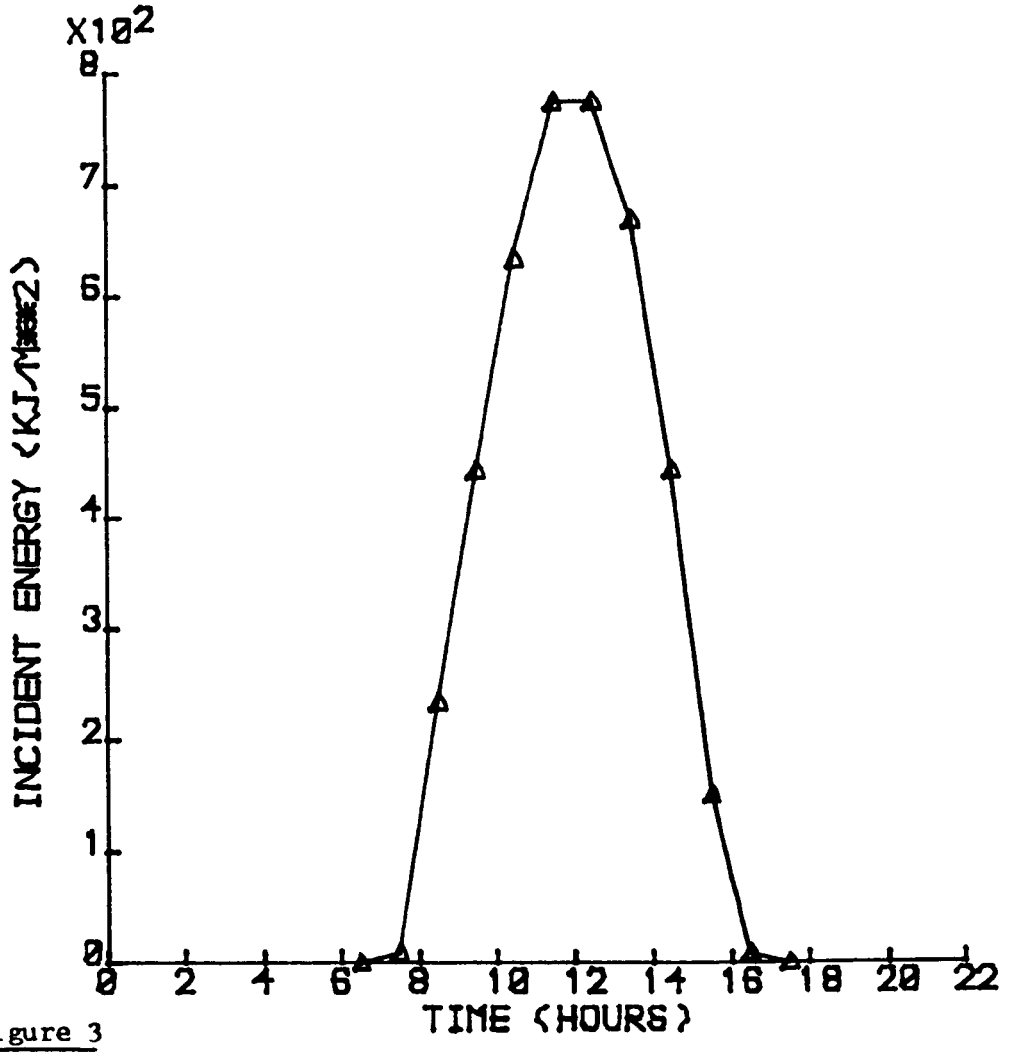

Figure 3

MEAN MONTHLY HOURLY RADIATION ON 45 DEGREE PLANE AT LEICESTER FOR 15TH JANUARY

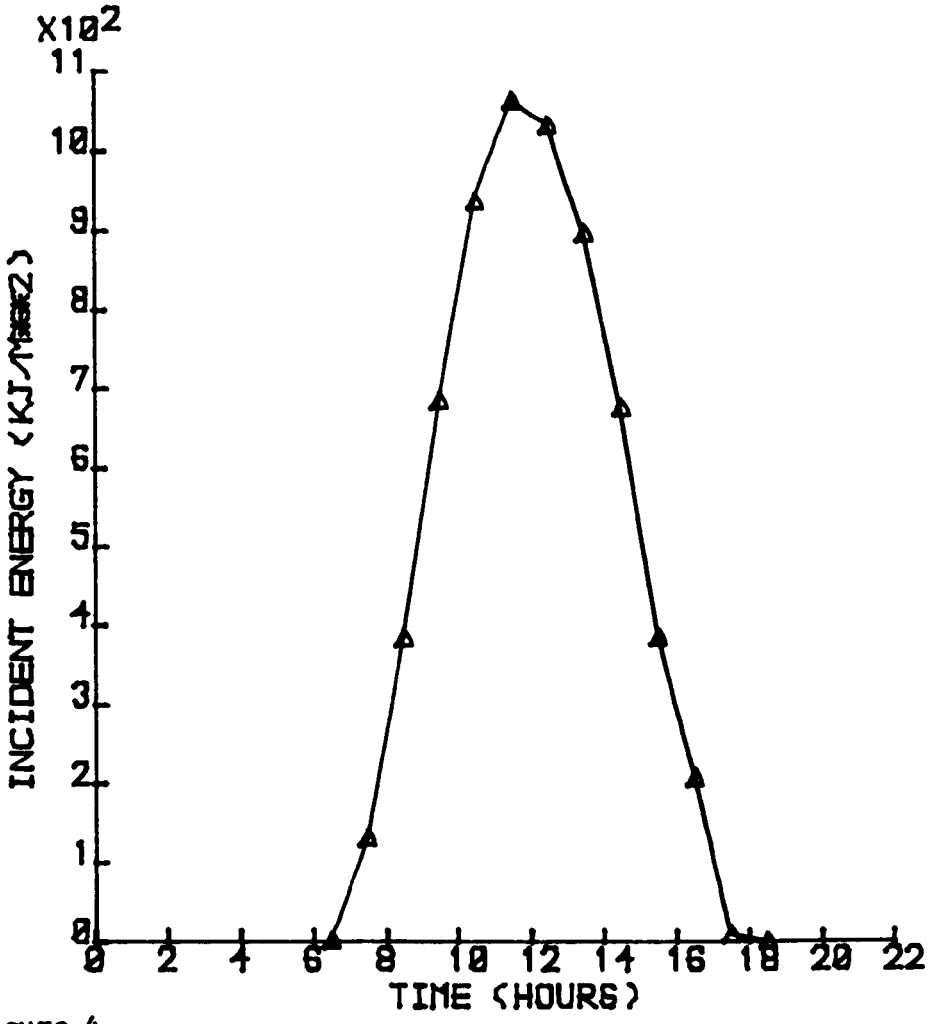

Figure 4

MEAN MONTHLY HOURLY RADIATION ON 45 DEGREE PLANE AT LEICESTER FOR 15TH FEBRUARY

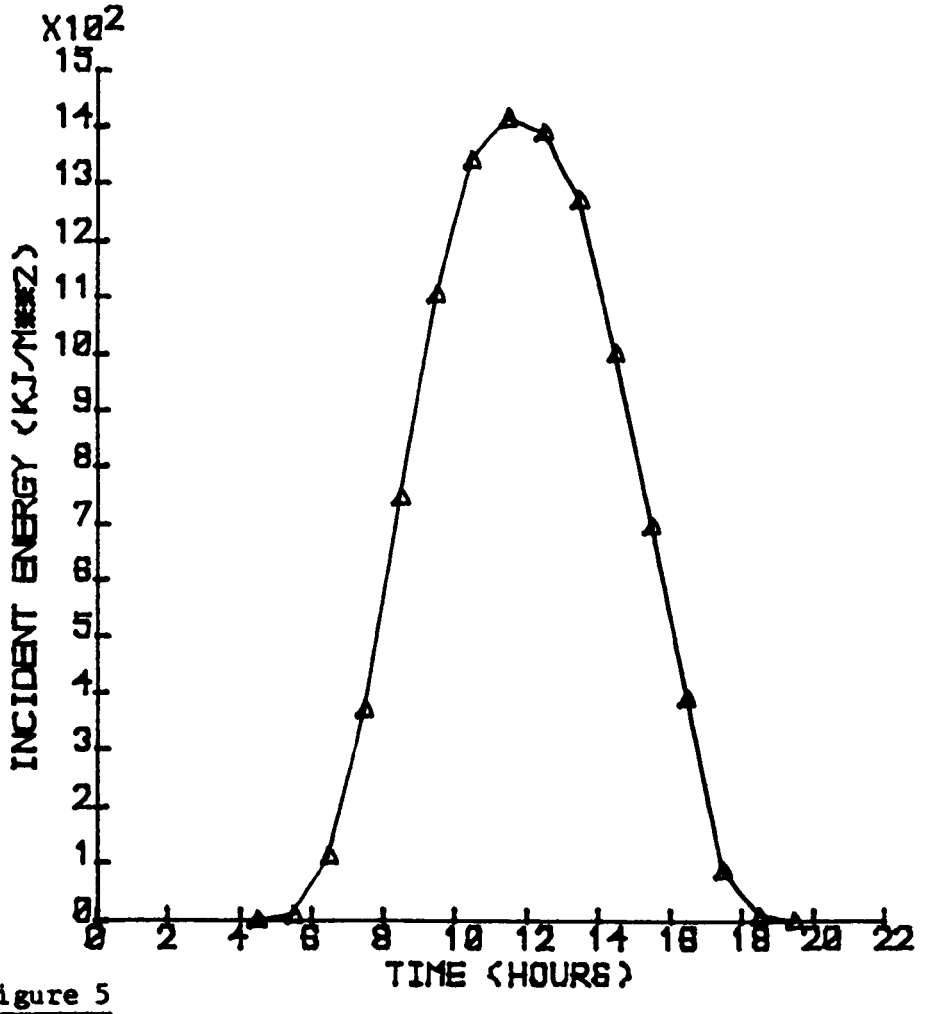

Figure 5

MEAN MONTHLY HOURLY RADIATION ON 45 DEGREE PLANE AT LEICESTER FOR 15TH MARCH

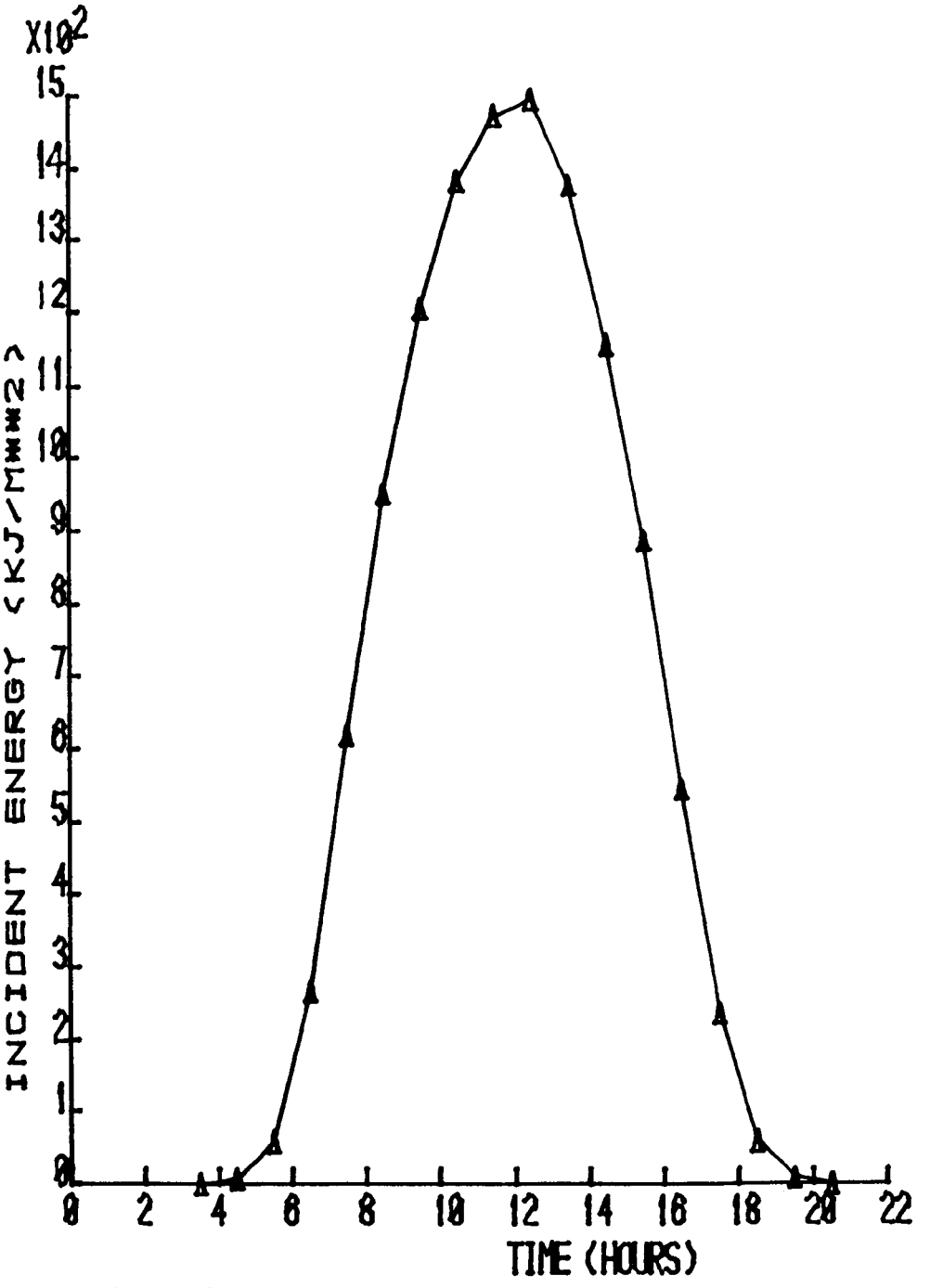

Figure 6

MEAN MONTHLY HOURLY RADIATION ON 45 DEGREE PLANE AT LEICESTER FOR 15TH APRIL

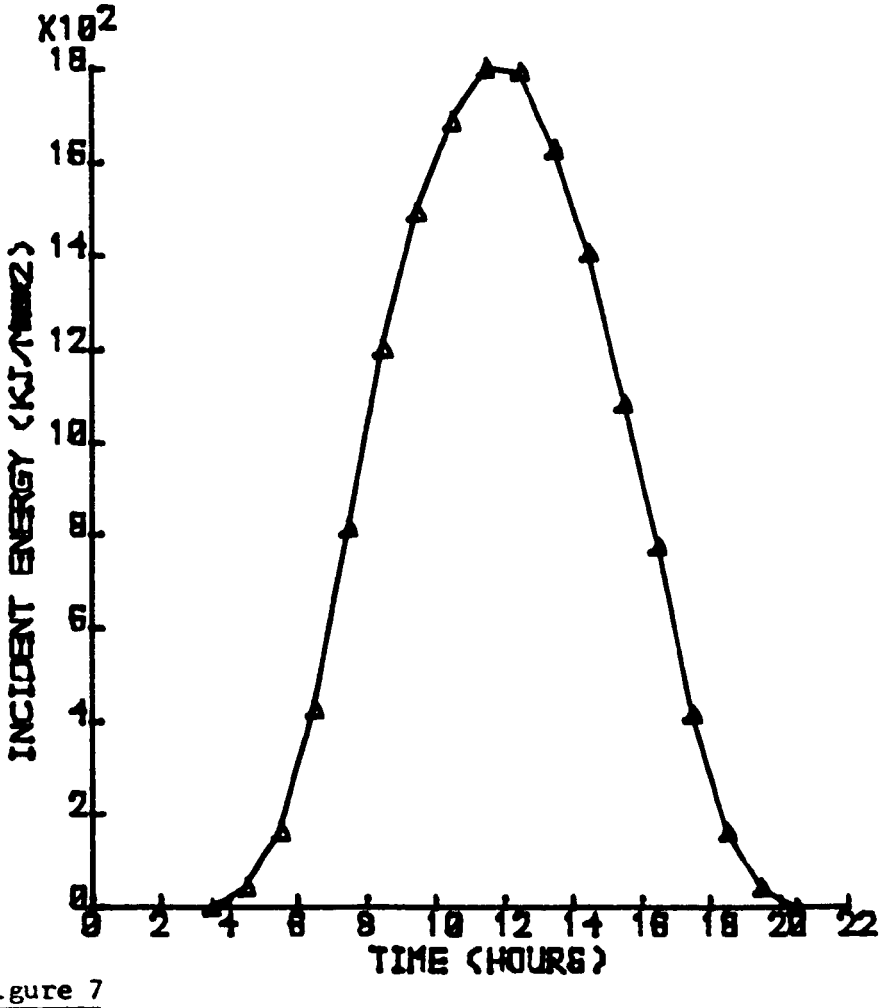

Figure 7

MEAN MONTHLY HOURLY RADIATION ON 45 DEGREE PLANE AT LEICESTER FOR 15TH MAY

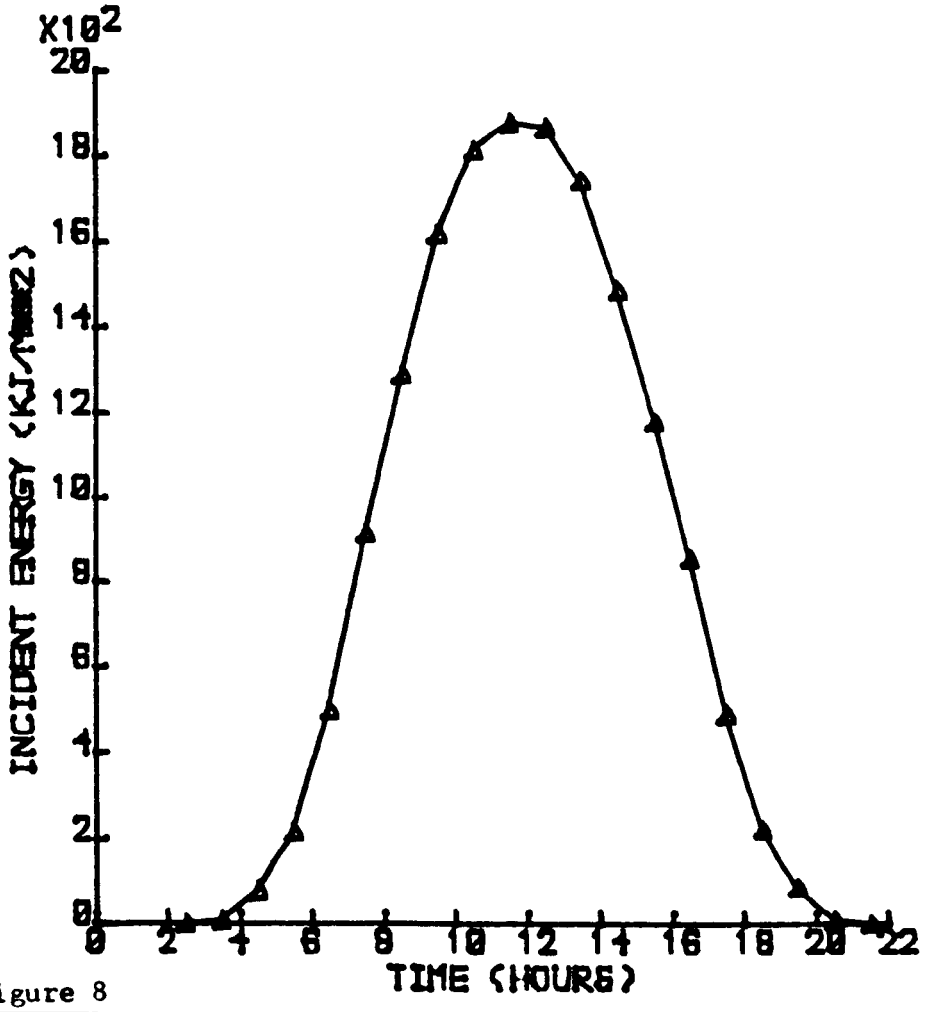

Figure 8

MEAN MONTHLY HOURLY RADIATION ON 45 DEGREE PLANE AT LEICESTER FOR 15TH JUNE

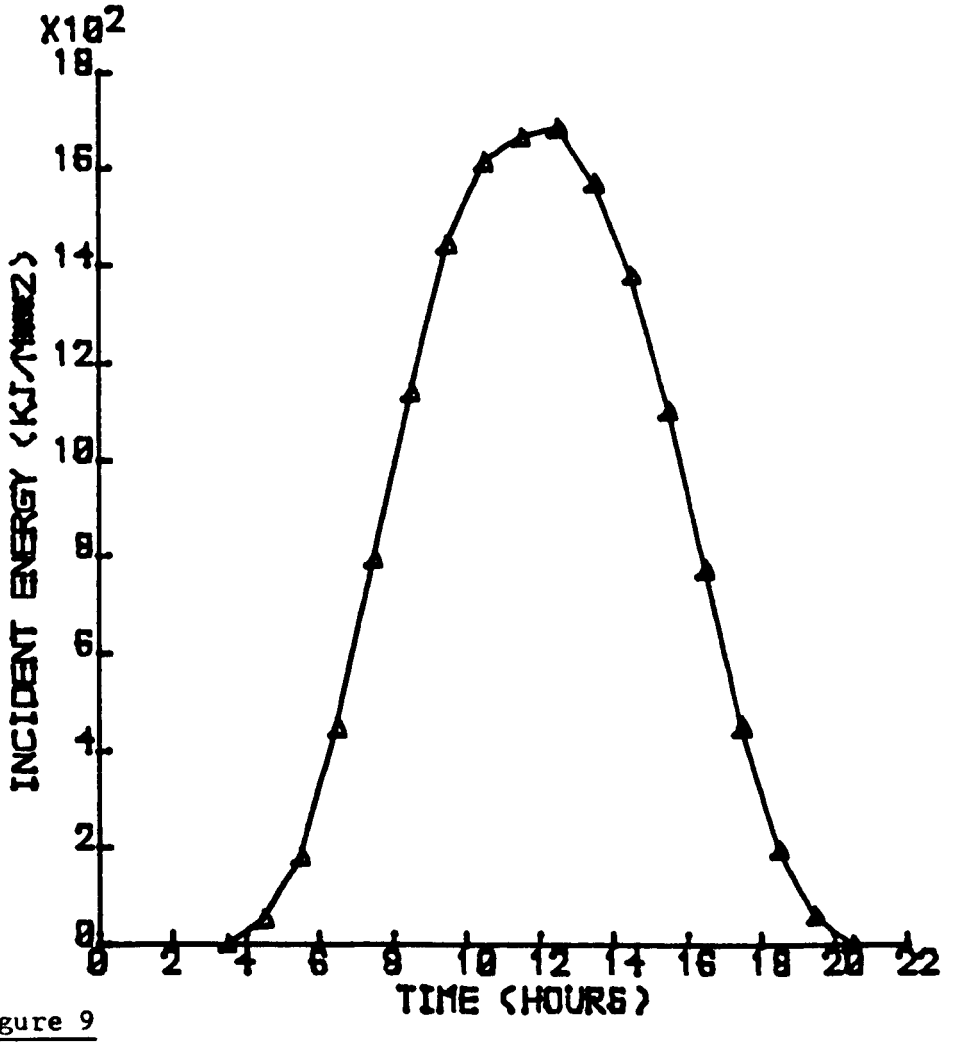

Figure 9

MEAN MONTHLY HOURLY RADIATION ON 45 DEGREE PLANE AT LEICESTER FOR 15TH JULY

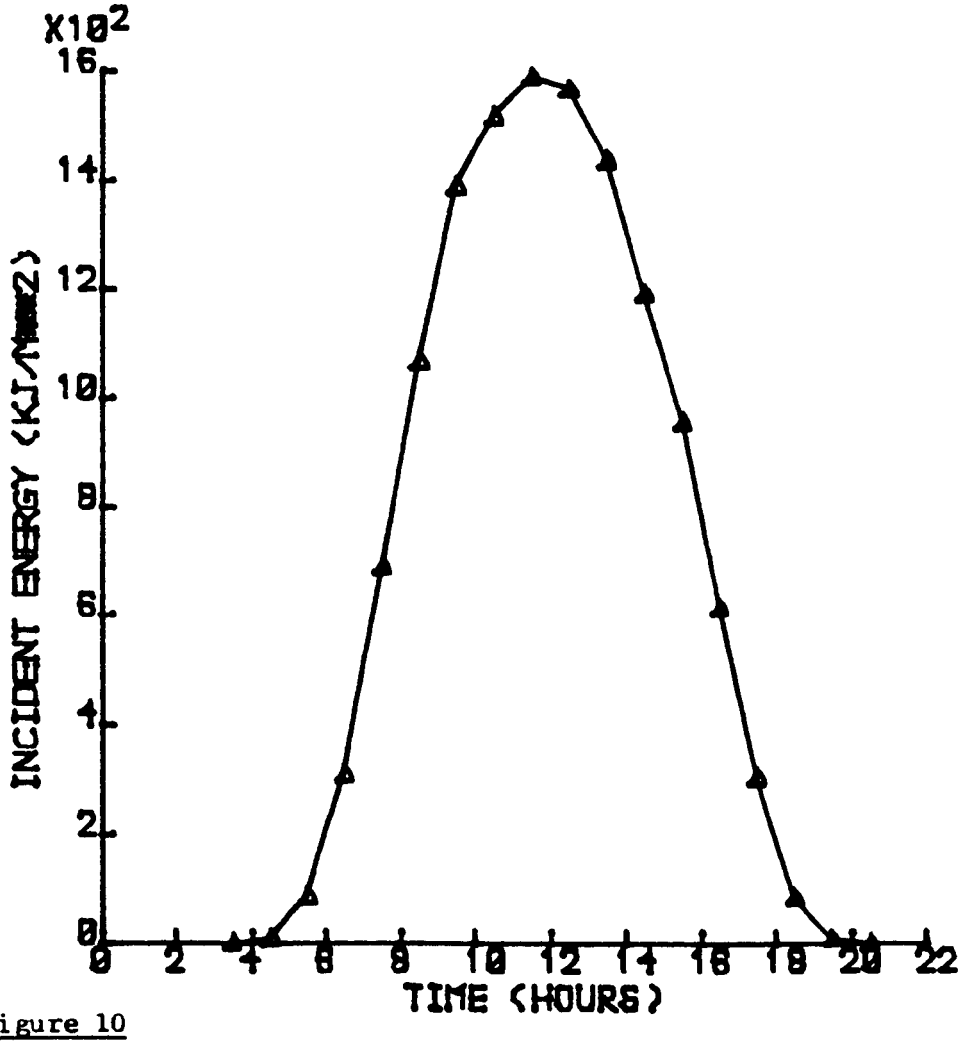

Figure 10

MEAN MONTHLY HOURLY RADIATION ON 45 DEGREE PLANE AT LEICESTER FOR 15TH AUGUST

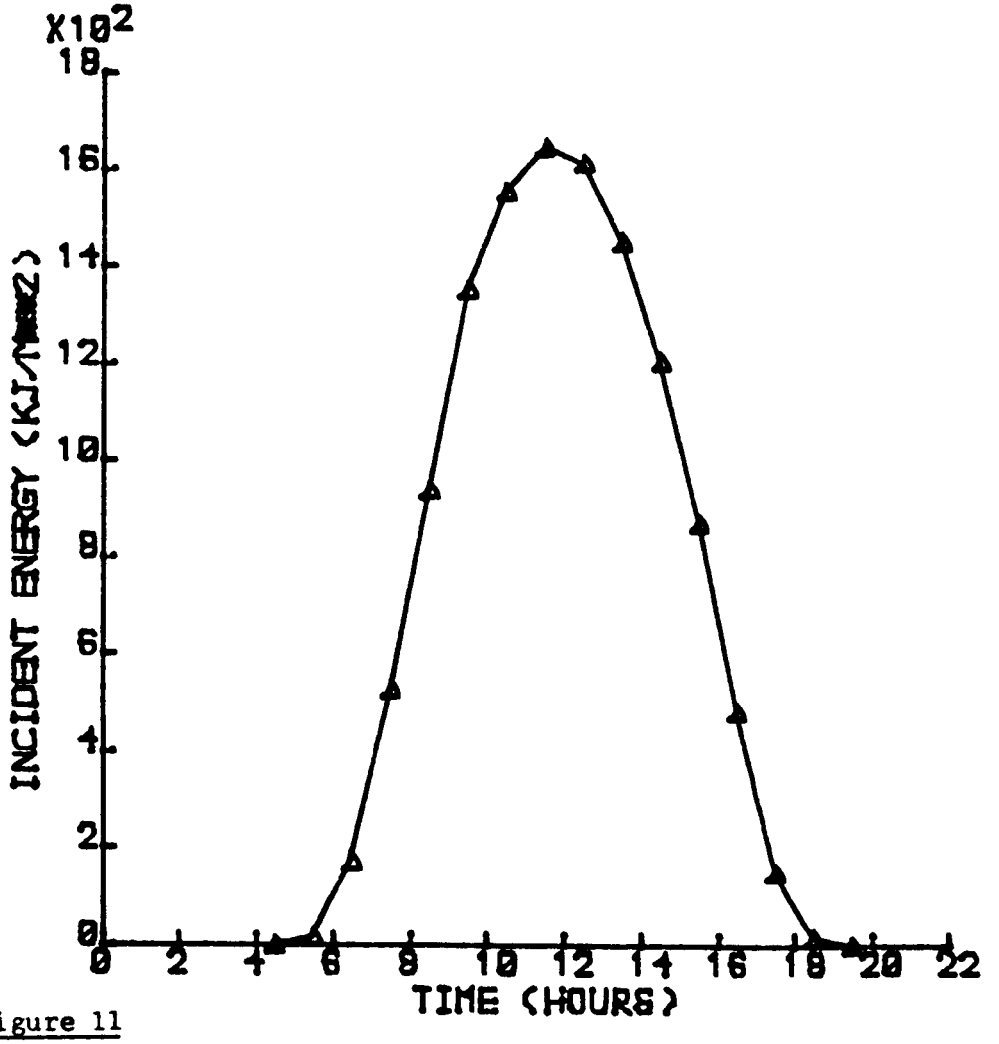

Figure 11

MEAN MONTHLY HOURLY RADIATION ON 45 DEGREE PLANE AT LEICESTER FOR 15TH SEPTEMBER

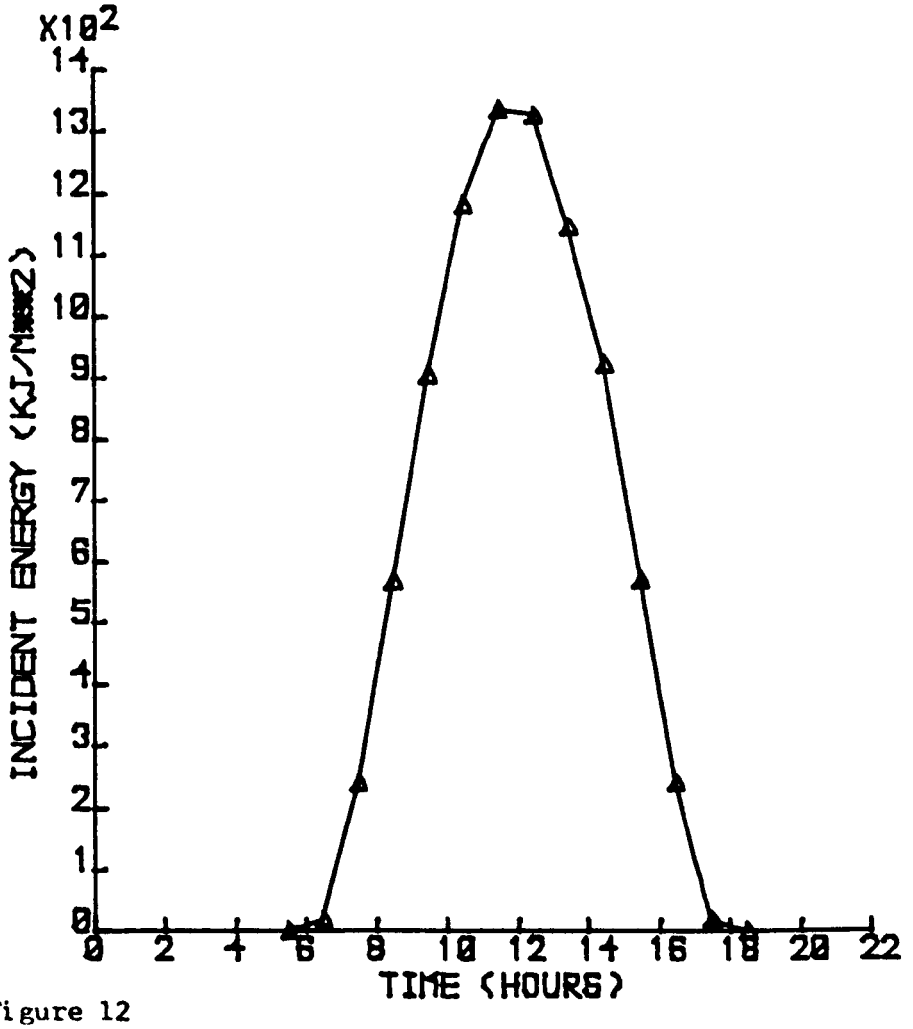

Figure 12

MEAN MONTHLY HOURLY RADIATION ON 45 DEGREE PLANE AT LEICESTER FOR 15TH OCTOBER

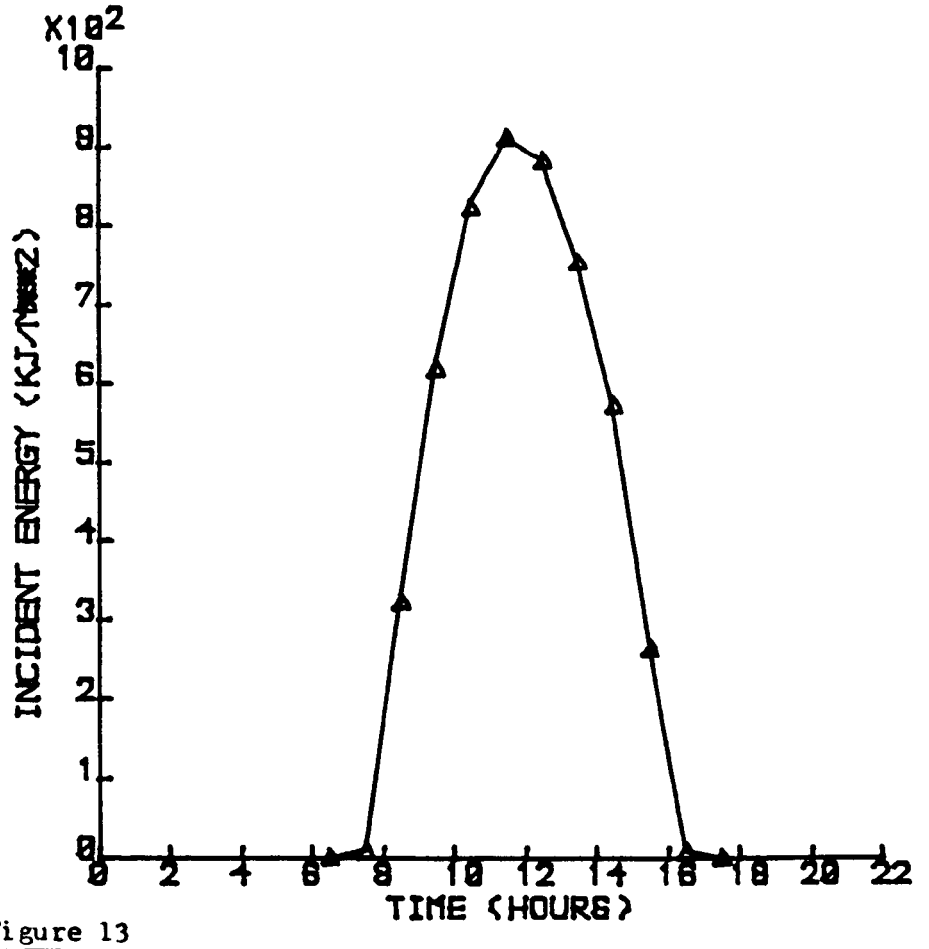

Figure 13

MEAN MONTHLY HOURLY RADIATION ON 45 DEGREE PLANE AT LEICESTER FOR 15TH NOVEMBER

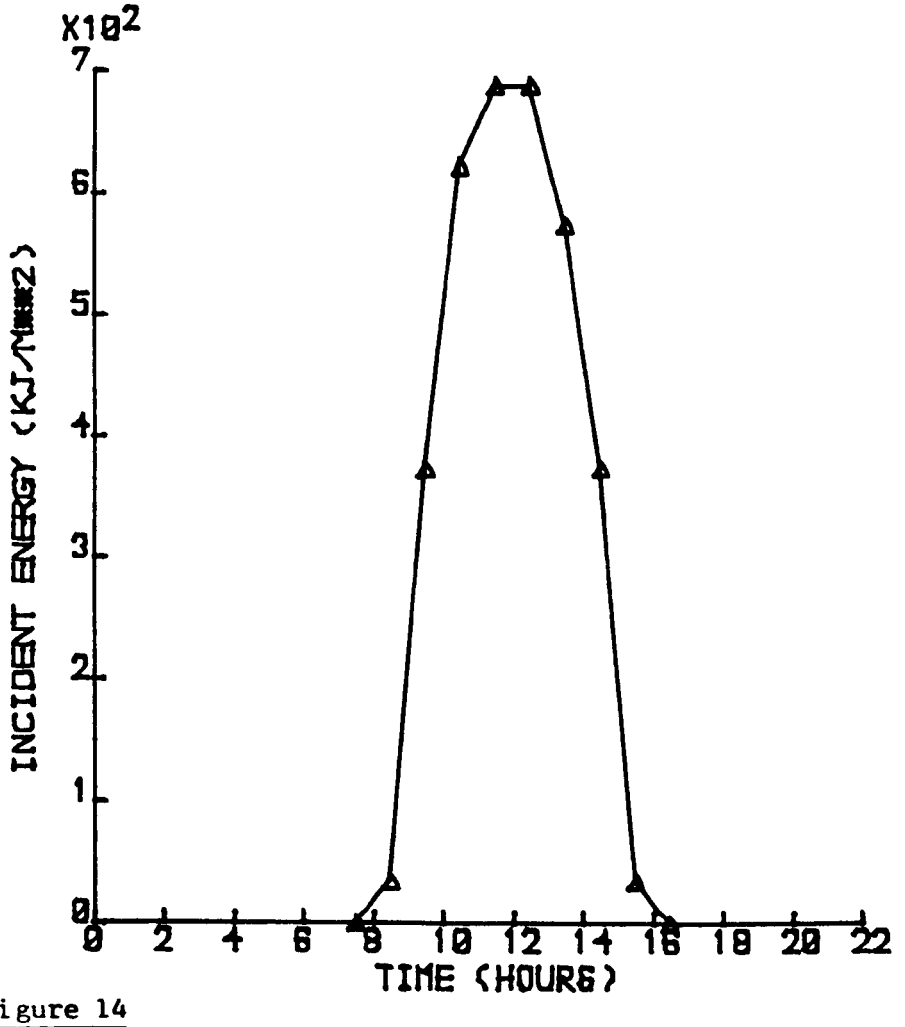

Figure 14

MEAN MONTHLY HOURLY RADIATION ON 45 DEGREE PLANE AT LEICESTER FOR 15TH DECEMBER

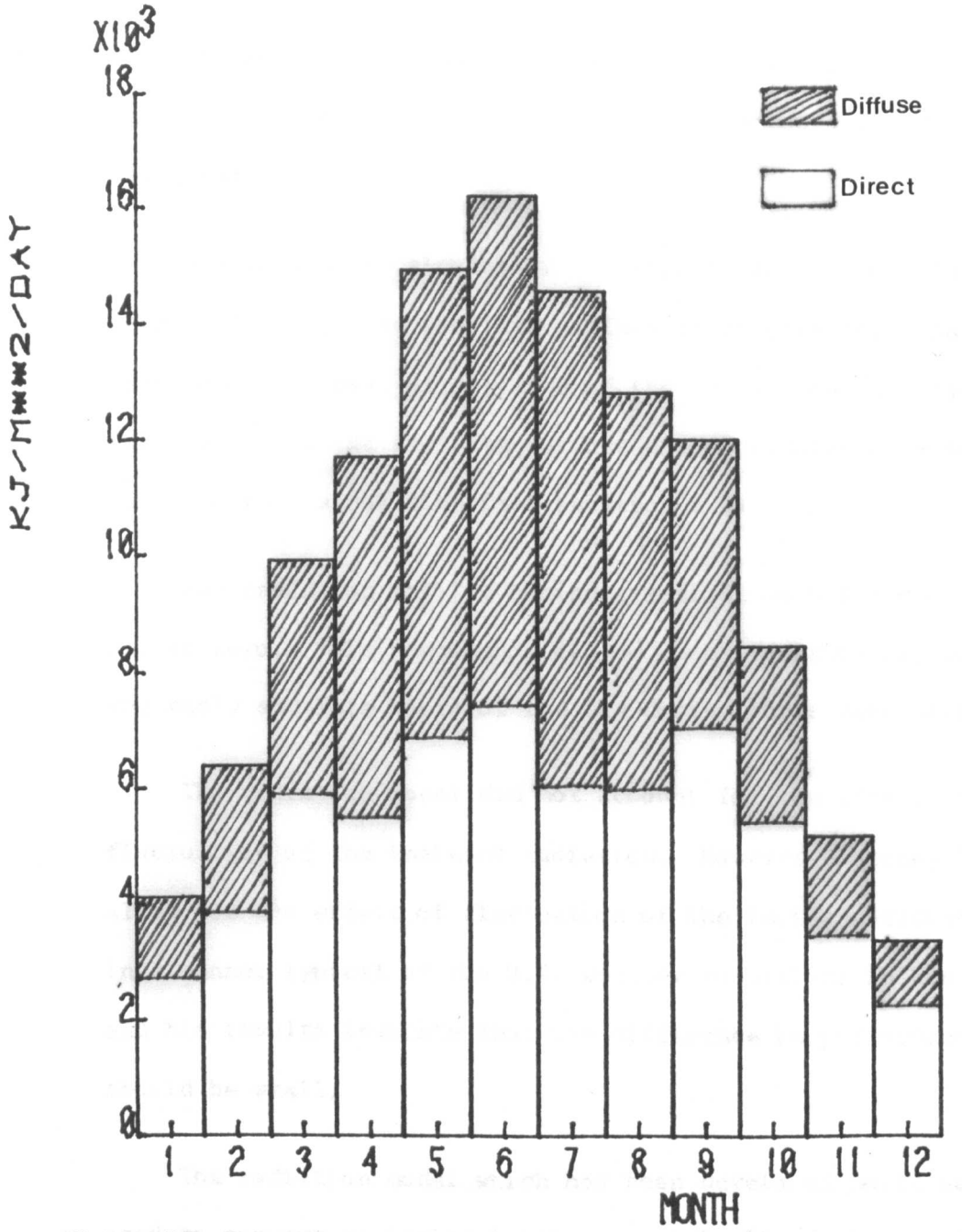

Figure 15

MEAN MONTHLY DAILY RADIATION AT LEICESTER ON 45 DEGREE PLANE

2.8 Discussion

The calculations were carried out on the basis of one square meter of collector area so that the results could be adapted to collectors of different sizes.

The method of calculation is based on the direct radiation which will reach the inclined surface under consideration, throughout the day, at any time of the year. However, radiation falling behind the inclined surface could produced a negative value in the calculation (see equation 2.1).

Any radiation falling behind a surface must therefore be set at zero. This phenomenon can be observed primarily during the early and late hours of the day during the summer months.

The radiation model did not account for the effect of fluctuation of the incident radiation. However Courtney[31] did allow for the effect of fluctuation of the incident radiation in a manner typical of the U.K. weather conditions in his model, and his results indicate that the difference in performance should be small.

The radiation model which has been developed could be used to convert radiation income on any inclined plane and at any latitude.

CHAPTER 3. THE FLAT PLATE COLLECTOR AND ITS COMPUTER MODEL

3.1 Introduction

Having generated a series of radiation profiles on a tilted plane (the collector surface) as described in chapter 2, the next stage was to determine the efficiency of collection and hence the useful energy gain, from the collector undergoing simulation, using this series of radiation profiles.

The effect of flow rates on useful energy gain had to be investigated. A computer model has been developed using the equations described in this chapter concerning the thermal analysis and the geometrical construction of the collector undergoing simulation.

The method adopted for the evaluation of the useful energy gain from the collector undergoing simulation, using the computer program which has been developed for that purpose, is based on a well established technique[2].

3.2 Description of the flat plate collector

The major component of a solar heating system is the collector, which converts the sun's radiation into useful energy and then transfers that to a working fluid. The fluid transports the thermal energy to the storage tank for later use.

The main components of the collector are:

(a) A blackened or otherwise treated absorber plate (usually metal) one of whose principal functions is to absorb the incident solar radiation and to convert it to heat.

(b) Fluid passages through which a heat transfer fluid flows, in good thermal contact with the absorber plate. Heat conducted from the absorber plate is transferred to this fluid which subsequently transfers it to water contained i.e. the storage tank.

(c) A glass cover whose principal functions are to help to insulate the collector plate from the cooler ambient air, and to provide weatherproofing.

(d) Insulation material behind the collector plate, whose function is sometimes one of providing some mechanical support for the collector plate as well as preventing heat loss. Often a highly reflective metal foil is placed immediately behind the collector plate to help reduce heat loss.

(e) An enclosing box whose principal functions are to hold the other components of the collector in their correct respective positions.

3.3 Collector Thermal Analysis

The flat-plate collector model developed by Hottel and Woertz[32], Whillier[33], and Hottel and Whillier[34] relates the

instantaneous rate of energy gain Q_u, to the design parameters of the collector and the meteorological conditions as follows:

$$\dot{Q}_u = F_R A[R_T(\tau\alpha)_e - U_L(T_{in} - T_a)] \qquad 3.1$$

where,

F_R = the overall collector efficiency factor

A = the collector area

R_T = the rate of total radiation incident on the collector surface

$(\tau\alpha)_e$ = the effective product of the transmittance of transparent covers and the absorbance of the collector plate

U_L = the collector overall energy loss coefficient

T_{in} = the temperature of the fluid at the collector inlet

T_a = the ambient temperature.

Their model gives a simplified assumption because they did not take into account the effects of the thermal capacitance of the collector. However Lof and Tybout[30] did take this into account, and they concluded that such effects are negligible for all common flat-plate collector constructions.

Klein[35] has carried out a much more rigorous analysis in his model than Lof and Tybout, and has arrived at essentially the same conclusion.

On the basis of Lof and Tybout, and Klein's conclusion,it appears that despite the simplified assumptions used by Hottel

and Whillier, their model has been found to compare quite favourably with more complex models.

Equation 3.1 can be written:

$$\eta = \frac{\dot{Q}_u/A}{R_T} = F_R(\tau\alpha)_e - F_R U_L(T_{in} - T_a)/R_T \qquad 3.2$$

Where η is the collector efficiency, and is defined as the amount of useful energy extracted from the collector as a percentage of the solar energy incident upon the collector during the same period.

3.3.1 Collector Overall loss coefficient (U_L)

The overall loss heat transfer coefficient is an important factor affecting the collector performance. Klein[36] has developed an empirical equation for the overall loss coefficient (U_L) following the basic procedure of Hottel and Woertz[32]. This equation is as follows:

$$U_L = \left[\frac{N}{(344/T_p)[T_p - T_a]/(N + f)]^{0.31}} + \frac{1}{h_w}\right]^{-1} + \frac{\sigma\,(T_p + T_a)(T_p^2 + T_a^2)}{[\varepsilon_p + 0.0425N(1 - \varepsilon_p)]^{-1} + [(2N + f - 1)/\varepsilon_g]^{-N}} + U_b \qquad 3.3$$

Where,

N = number of glass covers

$f = (1.0 - 0.04\,h_w + 5.0 \times 10^{-4} h_w^2)(1 + 0.058N)$

σ = Stefon-Boltzman constant

ε_g = emittance of glass (0.88)

ε_p = emittance of plate

T_a = ambient temperature

T_p = plate temperature

h_w = wind heat transfer coefficient

= 5.7 x 3.8V

V = wind velocity

U_b = The bottom loss coefficient

$= \frac{K}{L}$

K = insulation thermal conductivity

L = insulation thickness.

However, Klein has pointed out that on evidence from his equation, the collector overall energy loss coefficient (U_L) is a complicated function of both the collector construction and its operating conditions. Klein also has carried out an examination of graphs of theoretical values of U_L against temperatures and windspeed and his analysis indicates that the functional dependence of U_L upon the operating conditions is not very strong, particularly for collectors with selective absorber plate surfaces. In addition, the single straight line relationship between collector efficiency and $(T_{in} - T_a)/R_T$ obtained in many collector performance tests, such as those presented by Simon[37], suggest that the experimentally measured value of U_L, may be considered to be constant within experimental error, provided that U_L is evaluated at the estimated average

operating conditions, the error in the long-term collector performance incurred by assuming U_L to be constant will be small.

Duffie and Beckman[2] have pointed out that the mean plate temperature changes slightly as Q_u changes throughout the day, but the influence on U_L will be small. Therefore, if the dependence of U_L upon operating conditions is ignored, U_L is a constant for a specified collector; its value can be determined (at the estimated average operating conditions) from the information given in Duffie and Beckman[2].

3.3.2 Collector Geometry Efficiency Factor (F')

The collector geometry efficiency factor F' is another important parameter affecting the collection efficiency. The higher the value of the collector efficiency factor, the greater is the useful gain given to the working fluid, therefore the overall collection efficiency is increased.

A physical interpretation for the collector efficiency factor is that, at a particular location it represents the ratio of the useful energy gain to the useful energy gain if the collector absorbing surface had been at the local fluid temperature, and it is essentially a constant for any collector design and fluid flow rate.

The collector geometry efficiency factor is primarily a function of the collector construction and it can be determined

in the manner described by Whillier[30] or Duffie and Beckman[2].

For conventional tube-in-sheet construction

$$F' = \frac{1/U_L}{w\,\frac{1}{U_L[D_o + (w - D_o)F]} + \frac{1}{C_b} + \frac{1}{\pi D_i h_{fi}}} \qquad 3.4$$

Where:

$$F = \frac{\tan h\,[m(w - D_o)/2]}{m(w - D_o)/2} \qquad 3.5$$

$$m = \sqrt{U_L/K_p\delta p} \qquad 3.6$$

w = the distance between tube centres

D_o = the outside tube diameter

D_i = the inside tube diameter

K_p = the conductivity of the plate material

δ_p = the plate thickness

C_b = the bond conductance between the tubes and plate

h_{fi} = the convection heat transfer coefficient between the fluid and the tube wall

U_L = the collector overall loss coefficient.

The bond conductance C_b can be a very important parameter in accurately describing collector performance, and the bond resistance can be reduced by having good metal-to-metal contact and so improving collector performance. Increase in the heat transfer coefficient inside the tubes (i.e. forced convection) increases the collector efficiency F'. This also increases with both material thicknesses and thermal conductivity and decreases with increased tube centre to centre distance.

3.3.3 Heat Removal Factor (F_R) and Flow Factor (F")

A very important parameter affecting the total useful energy gain of the collector is the heat removal factor F_R. The higher the heat removal factor, the higher the useful energy gain is, and therefore the greater the collector efficiency. The heat removal factor (F_R) can be determined in the manner described by Duffie and Beckman[2].

$$F_R = \frac{GC_p}{U_L}\left(1 - e^{-\left[U_L F'/GC_p\right]}\right) \qquad 3.7$$

Where,

G = flow rate per unit collector area

C_p = specific heat of fluid

U_L = the collector overall loss coefficient

F' = the collector geometry efficiency factor.

From the collector useful energy equation, defined by equation 3.1, it can be seen that the effect of multiplier F_R, is to reduce the calculated useful energy gain from what it would have been had the whole collector been at $T_{F,i}$ to what it actually is, using a fluid that increases in temperature as it flows through the collector.

From equation 3.7 it can be seen that for a given collector construction and a specified flow rate, F_R is essentially constant.

By defining a new variable, the flow factor (F") = $\frac{F_R}{F'}$, and examining its variation with the function $\frac{GC_p}{U_L F'}$ as shown in figure 16,

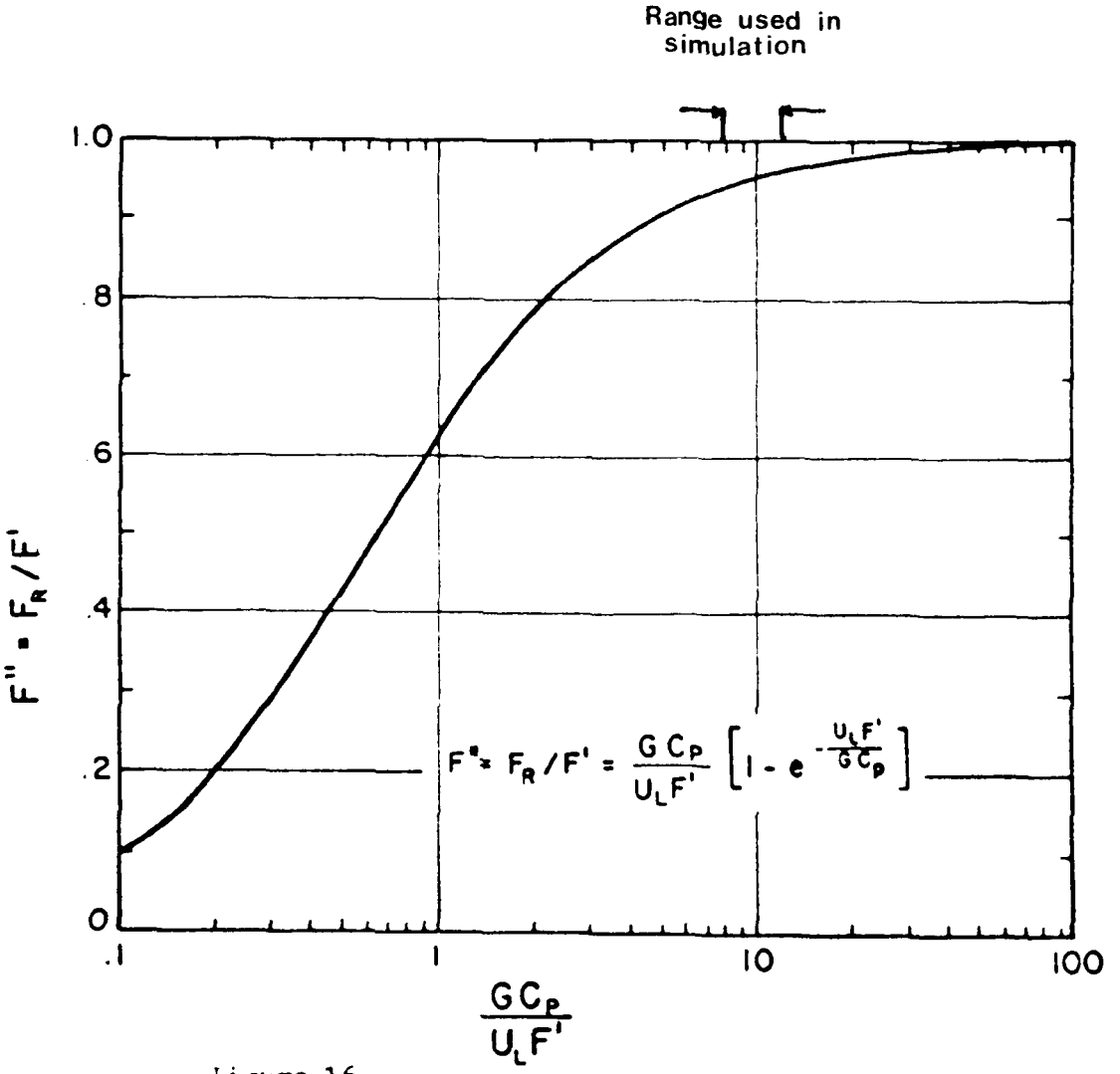

Figure 16

Collector flow factor F'' as a function of GC_p/U_LF'.

the significance of these factors can be fully appreciated. As the flow rate (G) per square metre of collector area increases, the temperature rise through the collector decreases, causing lower losses and a corresponding increase in the useful energy gain.

This increase in Q_u is reflected by an increase in the collector heat removal factor F_R as the mass flow rate increases.

Therefore an increase in the flow rate increases the heat removal factor (F_R) which improves the overall collector performance. It can be seen that the function $\frac{GC_p}{U_L F'}$ beyond about 50 has little marginal benefit for a specified collector as shown in figure 16.

For the maximum energy collection in a solar collector it is necessary that it operates as closely as possible to the collector inlet temperature.

Very high fluid flow rates are needed to maintain a collector-absorber surface nearly isothermal at the collector inlet temperature.

Although high flows maximize energy collection, practical and economic constraints put an upper limit on useful flow rates.

However very high flows require large pumps and excessive power consumption and lead to fluid conduit erosion.

In practice, liquid flows in the range of 50-75 kg/m^2hr of collector area ($\sim$ 10-15 lb/hr ft^2) of water equivalent are the best compromise among collector heat transfer coefficient, fluid pressure drop, and energy delivery[38,39]. British Standards draft[40] recommends that flow rates in the region of 36 - 72 kg/m^2hr of collector area ($\sim$ 7.2 - 14.4 lb/hr ft^2). However, the desired flow rate also depends on whether the storage tank is stratified or mixed.

For a mixed storage tank, a large flow rate will deliver the most energy if pumping power is ignored.

For a stratified storage tank, a lower flow rate is desired, since high flow destroys stratification.

3.3.4 Effective Transmittance-Absorptance product $(\tau\alpha)_e$

The effective transmittance-absorptance product $(\tau\alpha)_e$ represents the complex interaction of optical properties in the solar radiation wave length. It is somewhat larger than the direct product of the cover transmittance and the absorber absorptance, because some of the radiation reflected from the absorber is returned to it due to cover reflectance. The increase is typically about 5 percent. However, the effective transmittance-absorptance product is influenced by cover transmittance, number of covers, absorptance of the absorber plate, and solar angle of incidence.

The effective transmittance-absorptance for a cover system

of n identical plates can be determined in the manner described by Duffie and Beckman[2].

$$(\tau\alpha)_e = (\tau\alpha) + (1 - \tau_a)\sum_{i=1}^{n} a_i \tau^{i-1} \qquad 3.8$$

Where,

$$(\tau\alpha) = \frac{\tau\alpha}{1 - (1 - \alpha)\rho_d} \qquad 3.9$$

$$\tau_a = e^{-KL} \quad \text{at normal angle of incidence} \qquad 3.10$$

$$\tau_a = e^{-KL/\cos\theta_2} \quad \text{at another angle of incidence} \qquad 3.11$$

$$\tau = \tau_r \tau_a \qquad 3.12$$

$(\tau\alpha)$ = the transmittance-absorptance product

ρ_d = the reflectance of the transparent covers for diffuse radiation

α = the absorptance of the absorber plate

τ = the transmittance (considering absorption and reflection)

τ_a = the transmittance considering only absorption

L = the actual path of the radiation through the medium

K = the extinction coefficient

θ_2 = the refraction angle

τ_r = the transmittance considdring only reflection

a_i = the ratio of the overall loss coefficient to the loss coefficient from the ith cover to the surrounding.

Duffie and Beckman [2] recommended that ρ_d be calculated from the Fresnel equation with an incidence angle of 60^o.

The Fresnel equation is

$$= \frac{1}{2}\left[\frac{\sin^2(\theta_2 - \theta_1)}{\sin^2(\theta_2 + \theta_1)} + \frac{\tan^2(\theta_2 - \theta_1)}{\tan^2(\theta_2 + \theta_1)}\right] \qquad 3.13$$

Where,

θ_1 = the angle of incidence

θ_2 = the angle of refraction.

The angles θ_1 and θ_2 are related to the indices of refraction by Snell's law.

Snell's law is:

$$\frac{n1}{n2} = \frac{\sin \theta_2}{\sin \theta_1} \qquad 3.14$$

and

$$\tau_{r,1} = \frac{1 - \rho}{1 + \rho} \qquad 3.15$$

Where,

ρ = the reflectances of one interface.

3.4 Evaluation of the instantaneous efficiency of the collector under investigation

The next stage in the simulation was to determine the

efficiency of collection, and hence the useful energy gain from the collector. Tleimat[41] has suggested that the average diurnal efficiency can be used as a measure of collector performance but this approach would seem to be inappropriate when attempting to assess long term system performance.

The preferred method was that given by Duffie and Beckman[2], whereby the instantaneous efficiency is computed in terms of the instantaneous rate of energy gain.

Other system variables used in the computation are given below.

a) Ambient air temperature: ten years (1962-1971) mean monthly hourly dry bulb temperatures were used, corresponding to the same period used for the radiation data.

b) Water supply temperature: reliable records of water supply temperature were not forthcoming and the data used in the computation is based on the three year survey of Brinkworth[42], a mean value being taken for each month as follows:

$$Tc_w = 9 - 3\,\mathrm{Cos}\left(\frac{2\pi}{365}\ (D + 11.25)\right)$$

where D is the day number (January 1 = 1).

c) Fluid flow rates: A British Standard[40] recommends the rate to be in the region of 0.01 - 0.02 kg/Sm^2.

d) Collector overall loss coefficient (U_L): It was evaluated from the information given by Duffie and Beckman[2], at the estimated average operating condition as shown in figure 17.

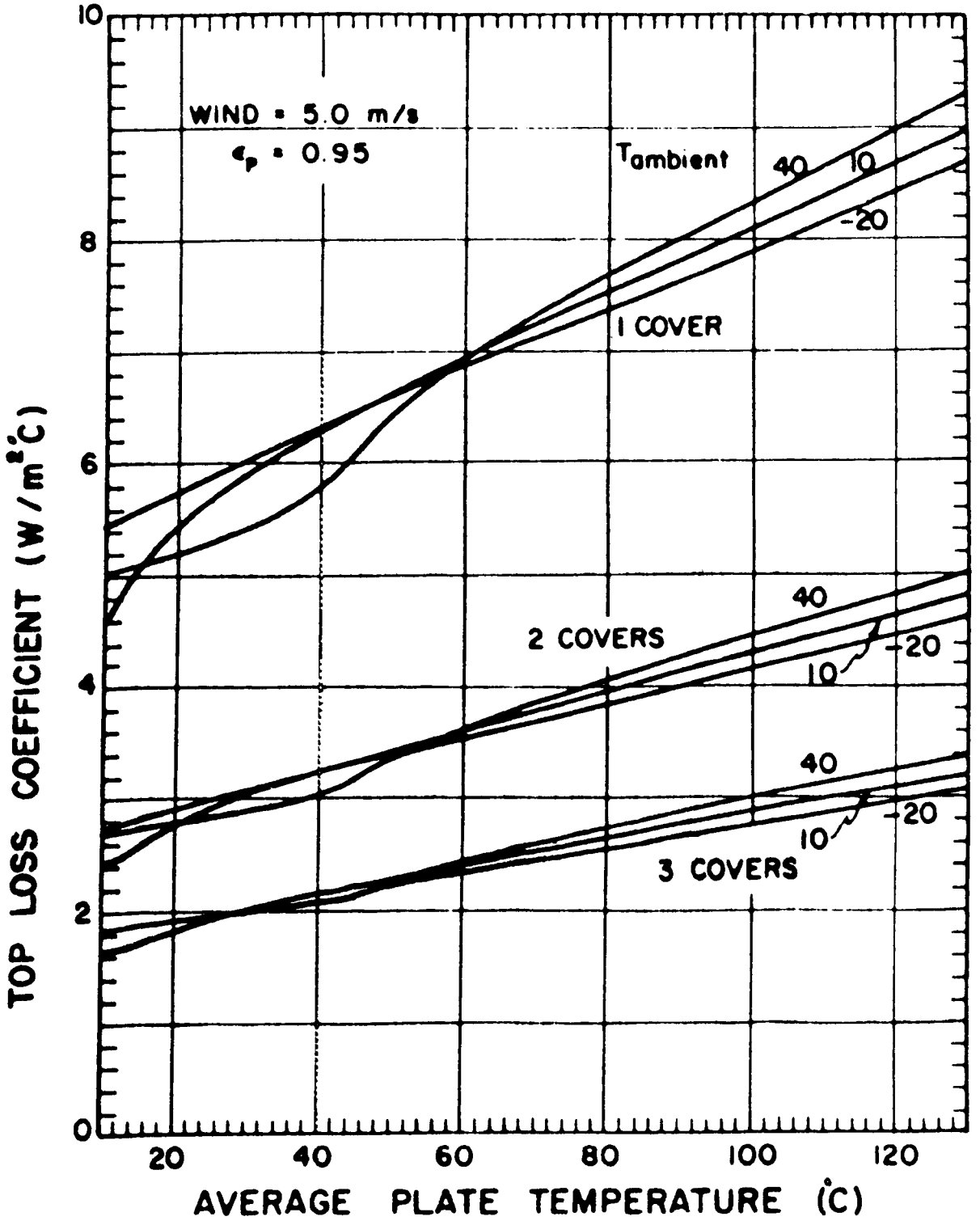

Figure 17

Top loss coefficient for slope of 45 degree

e) Optical characteristics of 4 mm float glass: the calculation of the optical characteristics of 4 mm float glass based on information given by Pilkington Brothers Limited, Solar Energy Advisory Service and Duffie and Beckman[2] as shown in figure 18.

f) The collector undergoing simulation was a typical tube and sheet solar collector with single cover, in which the particular set of parameters concerning the geometry and the heat transfer coefficient were as follows:

Collector overall loss coefficient (U_L)

$= 28.78\ KJhr^{-1}m^{-2}\ ^oC^{-1}$

plate thickness (δ_p) = 0.0005 m

plate conductivity (K_p) = $755.4\ KJhr^{-1}m^{-1}\ ^oC^{-1}$

The distance between tube centres (W) = 0.15 m

Outside tube diameter (D_o) = 0.015 m

Inside tube diameter (D_i) = 0.013 m

Bond conductivity (c_b) = ∞

The convection heat transfer coefficient between the fluid and the tube wall (h_{fi}) = $5395.68\ KJhr^{-1}m^{-2}\ ^oC^{-1}$

Specific heat of fluid (C_p) = $4.187\ KJkg^{-1}\ ^oC^{-1}$

Number of covers (N) = 1

Collector area (A) = $1\ m^2$

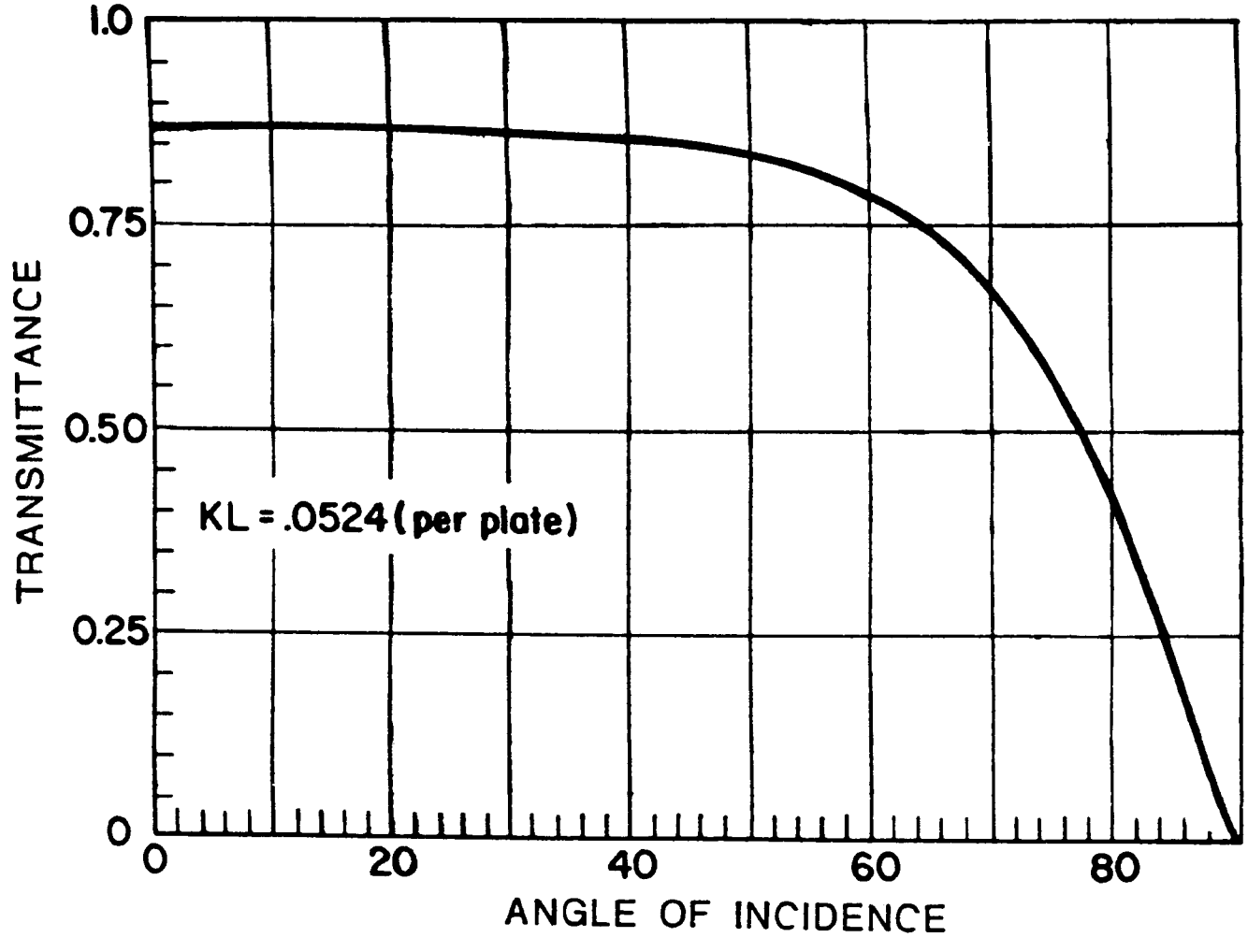

Figure 18

Transmittance neglecting absorption (due to reflection only) of one cover

The absorptance of the absorber plate (α) = 0.95 and is independent of direction.

The ratio of the overall loss coefficient to the loss coefficient from the 1th cover to the surrounding (a_i) = 0.27.

The reflectance of the transparent covers for diffuse radiation (ρ_d) = 0.16.

3.5 The Computation procedure for the collector model

The computation procedure is shown in figure 19 which illustrates the flow chart for the collector model.

3.6 Results

The results of the computation are shown in tables 14-25. Each table shows the useful energy gain as a function of mass flow rate for each month.

It can be seen from these tables that the effect of mass flow rate, 0.01 kg/Sm^2, 0.015 kg/Sm^2 and 0.02 kg/Sm^2, in useful energy gain, indicate that as the flow rates increase from 0.01 kg/Sm^2 to 0.015 kg/Sm^2 and 0.02 kg/Sm^2 there was a corresponding increase in useful energy gain.

The results of the computation were used to generate a series of useful heat gain profiles, and these profiles formed the basic input data to the simulator as described in chapter 4.

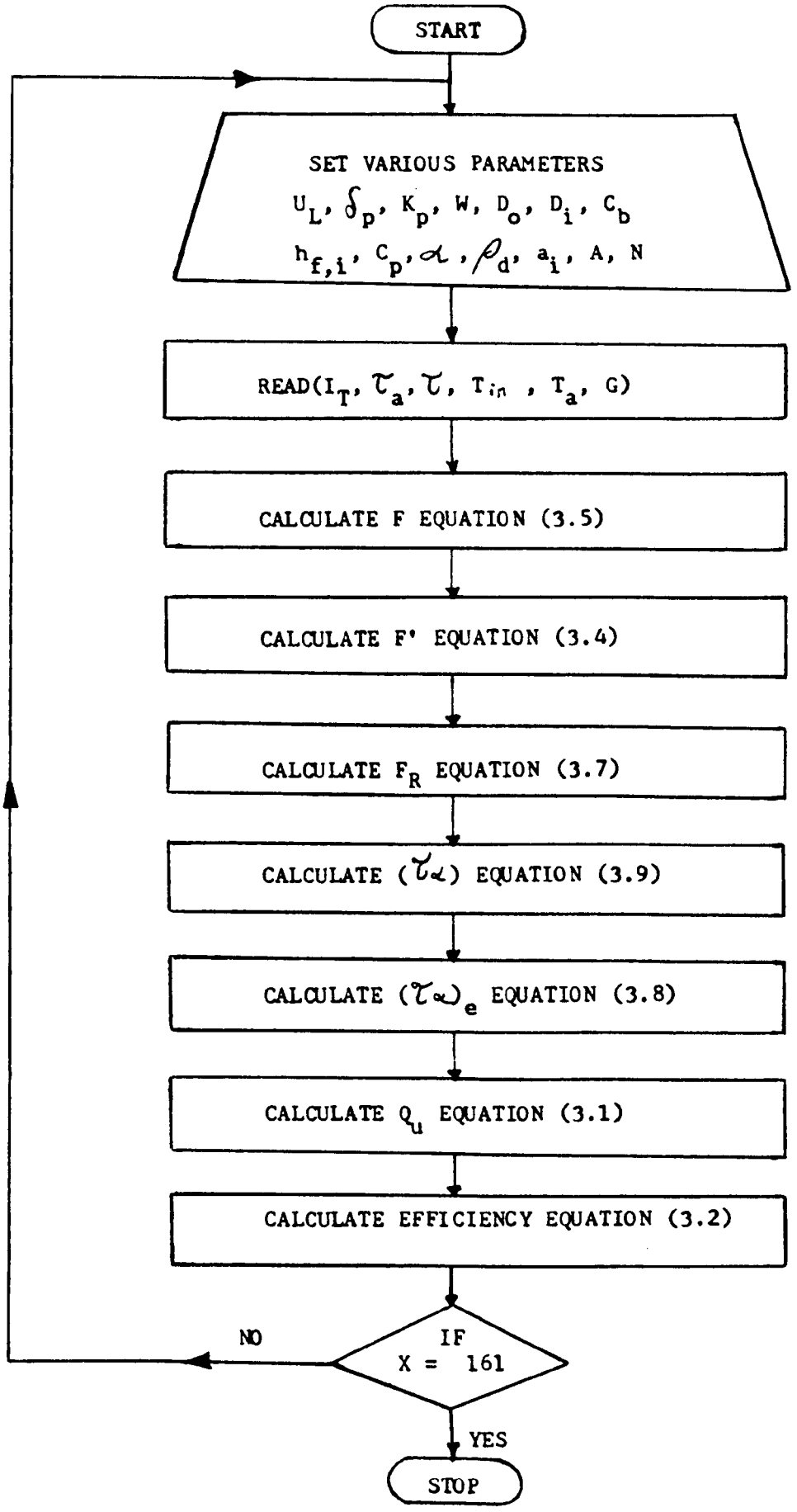

Figure 19

Flow chart for the collector model

TABLE 14 15 January: useful energy as a function of mass flow rate.

Time hours	Ambient Temperature ^{o}C	Incident Energy KJ/m^2	Useful energy KJ/m^2		
			Flow rate		
			0.01 kg/Sm^2	0.015 kg/Sm^2	0.02 kg/Sm^2
7 - 8	2.47	008.5	0	0	0
8 - 9	2.59	234.4	0	0	0
9 - 10	3.15	443.6	227.0	233.3	236.6
10 - 11	3.78	634.1	378.3	389.0	394.4
11 - 12	4.27	773.8	486.2	499.8	506.9
12 - 13	4.65	773.8	495.2	509.1	516.2
13 - 14	4.78	668.4	425.6	437.6	443.7
14 - 15	4.74	443.6	264.5	272.0	275.8
15 - 16	4.32	151.4	0	0	0
16 - 17	3.85	008.5	0	0	0
Total		4140.1	2276.8	2340.8	2373.6

TABLE 15. 15 February: useful energy as a function of mass flow rate

Time Hours	Ambient Temperature °C	Incident Energy KJ/m^2	Useful energy KJ/m^2		
			Flow rate		
			0.01 kg/Sm^2	0.015 kg/Sm^2	0.02 kg/Sm^2
7 - 8	1.81	0129.2	0	0	0
8 - 9	2.24	0382.4	130.6	134.2	136.1
9 - 10	3.12	0684.1	368.7	379.1	384.4
10 - 11	3.76	0935.7	561.3	577.1	585.2
11 - 12	4.28	1061.3	660.1	678.6	688.2
12 - 13	4.64	1029.8	646.8	665.0	674.4
13 - 14	4.84	0895.1	558.8	574.5	582.6
14 - 15	4.83	0675.6	403.3	414.6	420.4
15 - 16	4.62	0382.4	186.8	192.0	194.7
16 - 17	4.12	0207.1	000.0	000.0	000.0
17 - 18	3.61	0008.5	0	0	0
Total		6391.2	3516.4	3615.1	3666

TABLE 16. 15 March: useful energy as a function of mass flow rate

Time Hours	Ambient Temperature ^{o}C	Incident Energy KJ/m^2	Useful energy KJ/m^2		
			Flow rate		
			0.01 kg/Sm^2	0.015 kg/Sm^2	0.02 kg/Sm^2
5 - 6	2.46	0008.5	0	0	0
6 - 7	2.53	0112.5	0	0	0
7 - 8	3.18	0372.3	82.9	085.2	0086.4
8 - 9	4.11	0749.3	392.4	403.4	0409.1
9 - 10	5.12	1105.0	675.4	694.4	0704.2
10 - 11	5.97	1339.7	860.2	884.4	0896.8
11 - 12	6.62	1413.3	926.0	952.1	0965.5
12 - 13	7.00	1387.4	917.8	943.7	0956.9
13 - 14	7.30	1270.3	843.7	867.5	0879.7
14 - 15	7.34	0999.7	655.5	673.9	0683.4
15 - 16	7.16	0695.1	428.2	440.2	0446.4
16 - 17	6.74	0391.5	178.0	183.0	0185.5
17 - 18	6.13	0090.4	0	0	0
18 - 19	5.25	0008.5	0	0	0
Total		9943.5	5960.1	6127.8	6213.9

TABLE 17. 15 April: useful energy as a function of mass flow rate

Time Hours	Ambient Temperature °C	Incident Energy KJ/m^2	Useful energy KJ/m^2		
			Flow rate		
			0.01 kg/Sm^2	0.015 kg/Sm^2	0.02 kg/Sm^2
4 - 5	4.44	0008.5	0	0	0
5 - 6	4.46	0059.8	0	0	0
6 - 7	5.35	0266.7	0	0	0
7 - 8	6.40	0619.5	0267.5	0275.0	0278.8
8 - 9	7.33	0952.0	0566.8	0582.7	0590.9
9 - 10	8.28	1203.7	0782.7	0804.7	0816.0
10 - 11	9.00	1381.8	0924.0	0950.0	0963.3
11 - 12	9.56	1473.6	0999.9	1028.0	1042.5
12 - 13	10.05	1495.8	1026.8	1055.6	1070.5
13 - 14	10.37	1376.8	0952.9	0979.7	0993.5
14 - 15	10.46	1154.9	0800.6	0823.1	0834.7
15 - 16	10.37	0885.7	0594.3	0611.0	0619.6
16 - 17	10.17	0542.5	0312.0	0320.7	0325.2
17 - 18	9.65	0236.7	0000.0	0000.0	0000.0
18 - 19	8.63	0059.8	0	0	0
19 - 20	7.23	0008.5	0	0	0
Total		11726.3	7227.5	7430.5	7535

TABLE 18. 15 May: useful energy as a function of mass flow rate

Time Hours	Ambient Temperature ^{o}C	Incident Energy KJ/m^2	Useful energy KJ/m^2		
			Flow rate		
			0.01 kg/Sm^2	0.015 kg/Sm^2	0.02 kg/Sm^2
4 - 5	7.23	0042.7	0	0	0
5 - 6	7.89	0162.2	0	0	0
6 - 7	9.15	0425.6	0073.7	0075.7	0076.8
7 - 8	10.20	0815.5	0451.9	0464.6	0471.2
8 - 9	11.12	1200.7	0794.3	0816.6	0828.1
9 - 10	12.07	1491.9	1041.8	1071.1	1086.2
10 - 11	12.78	1686.3	1195.3	1228.9	1246.2
11 - 12	13.34	1798.3	1285.4	1321.5	1340.1
12 - 13	13.82	1789.7	1290.8	1327.1	1345.7
13 - 14	14.14	1625.5	1185.5	1218.8	1236.0
14 - 15	14.31	1406.0	1035.6	1064.7	1079.7
15 - 16	14.27	1082.3	0789.6	0811.8	0823.2
16 - 17	13.96	0773.6	0516.0	0530.5	0538.0
17 - 18	13.46	0414.2	0172.0	0176.9	0179.4
18 - 19	12.59	0162.2	0000.0	0000.0	0000.0
19 - 20	11.60	0042.7	0000.0	0000.0	0000.0
Total		14919.5	9831.9	10108.2	10250.6

TABLE 19. 15 June: useful energy as a function of mass flow rate

Time Hours	Ambient Temperature °C	Incident Energy KJ/m^2	Useful energy KJ/m^2		
			Flow rate		
			0.01 kg/Sm^2	0.015 kg/Sm^2	0.02 kg/Sm^2
3 - 4	10.09	0008.5	0	0	0
4 - 5	10.28	0076.8	0	0	0
5 - 6	11.21	0213.4	0	0	0
6 - 7	12.36	0499.7	0170.6	0175.4	0177.9
7 - 8	13.40	0916.5	0574.3	0590.5	0598.8
8 - 9	14.36	1287.3	0916.1	0941.9	0955.2
9 - 10	15.34	1614.4	1189.4	1222.8	1240.0
10 - 11	16.19	1812.1	1349.9	1387.8	1407.3
11 - 12	16.72	1873.8	1404.5	1444.0	1464.3
12 - 13	17.32	1862.8	1411.1	1450.8	1471.2
13 - 14	17.54	1738.9	1331.2	1368.7	1387.9
14 - 15	17.61	1484.7	1153.8	1186.2	1202.9
15 - 16	17.57	1177.5	0918.6	0944.5	0957.7
16 - 17	17.41	0853.8	0632.1	0649.8	0659.0
17 - 18	16.99	0491.2	0277.3	0285.0	0289.1
18 - 19	16.14	0221.9	0102.0	0104.9	0106.4
19 - 20	15.08	0085.4	0000.0	0000.0	0000.0
20 - 21	14.09	0008.5	0000.0	0000.0	0000.0
Total		16227.2	11430.9	11751.5	11917.7

TABLE 20. 15 July: useful energy as a function of mass flow rate

Time Hours	Ambient Temperature °C	Incident Energy KJ/m^2	Useful energy KJ/m^2		
			Flow rate		
			0.01 kg/Sm^2	0.015 kg/Sm^2	0.02 kg/Sm^2
4 - 5	11.79	0051.2	0000.0	0000.0	0000.0
5 - 6	12.49	0179.3	0000.0	0000.0	0000.0
6 - 7	13.65	0447.8	0190.2	0195.6	0198.3
7 - 8	14.68	0796.3	0539.6	0554.7	0562.5
8 - 9	15.61	1139.5	0852.6	0876.6	0888.9
9 - 10	16.53	1443.4	1105.8	1136.9	1152.9
10 - 11	17.28	1612.5	1243.8	1278.8	1296.7
11 - 12	17.77	1662.5	1289.5	1325.7	1344.4
12 - 13	18.36	1682.3	1317.1	1354.1	1373.2
13 - 14	18.70	1568.2	1246.8	1281.8	1299.8
14 - 15	18.83	1380.1	1116.6	1148.0	1164.2
15 - 16	18.77	1101.1	0901.6	0926.9	0940.0
16 - 17	18.56	0772.0	0616.9	0634.2	0643.1
17 - 18	18.13	0447.8	0296.0	0304.4	0308.6
18 - 19	17.25	0196.3	0133.3	0137.1	0139.0
19 - 20	16.24	0059.8	0000.0	0000.0	0000.0
Total		14540.1	10849.8	11154.8	11311.6

TABLE 21. 15 August: useful energy as a function of mass flow rate

Time Hours	Ambient Temperature °C	Incident energy KJ/m^2	Useful energy KJ/m^2		
			Flow rate		
			0.01 kg/Sm^2	0.015 kg/Sm^2	0.02 kg/Sm^2
4 - 5	11.54	0008.5	0000.0	0000.0	0000.0
5 - 6	11.84	0085.4	0000.0	0000.0	0000.0
6 - 7	12.88	0310.5	0144.2	0148.3	0150.4
7 - 8	14.00	0692.5	0486.1	0499.8	0506.8
8 - 9	14.99	1069.9	0815.3	0838.3	0850.0
9 - 10	15.97	1390.6	1082.0	1112.4	1128.1
10 - 11	16.74	1515.9	1188.2	1221.7	1238.8
11 - 12	17.36	1588.0	1251.9	1287.1	1305.2
12 - 13	17.84	1566.6	1248.5	1283.6	1301.7
13 - 14	18.14	1436.7	1166.6	1199.4	1216.3
14 - 15	18.28	1193.3	1000.6	1028.8	1043.3
15 - 16	18.20	0957.3	0816.0	0838.9	0850.7
16 - 17	17.91	0614.3	0532.3	0547.3	0555.0
17 - 18	17.4	0304.0	0249.0	0256.0	0259.6
18 - 19	16.32	0085.4	0000.0	0000.0	0000.0
19 - 20	15.21	0008.5	0000.0	0000.0	0000.0
Total		12827.4	9980.7	10261.6	10405.9

TABLE 22. 15 September: useful energy as a function of mass flow rate

Time Hours	Ambient Temperature °C	Incident energy KJ/m^2	Useful energy KJ/m^2		
			Flow rate		
			0.01 kg/Sm^2	0.015 kg/Sm^2	0.02 kg/Sm^2
5 - 6	9.97	0017.1	0000.0	0000.0	0000.0
6 - 7	10.55	0172.1	0076.8	0078.9	0080.0
7 - 8	11.81	0527.6	0366.2	0376.5	0381.8
8 - 9	13.01	0939.8	0717.1	0737.2	0747.6
9 - 10	14.19	1354.8	1049.7	1079.2	1094.4
10 - 11	15.10	1555.4	1211.9	1246.0	1263.5
11 - 12	15.74	1646.5	1289.2	1325.4	1344.1
12 - 13	16.29	1613.9	1279.7	1315.7	1334.2
13 - 14	16.61	1452.0	1176.3	1209.3	1226.3
14 - 15	16.63	1205.6	1004.7	1032.9	1047.4
15 - 16	16.34	0870.5	0749.4	0770.5	0781.4
16 - 17	15.97	0481.3	0437.6	0449.9	0456.3
17 - 18	15.09	0151.3	0000.0	0000.0	0000.0
18 - 19	13.79	0017.1	0000.0	0000.0	0000.0
Total		12005.0	9358.6	9621.5	9757

TABLE 23. 15 October: useful energy as a function of mass flow rate

Time Hours	Ambient Temperature °C	Incident energy KJ/m^2	Useful energy KJ/m^2		
			Flow rate		
			0.01 kg/Sm^2	0.015 kg/Sm^2	0.02 kg/Sm^2
6 - 7	8.48	0017.1	0000.0	0000.0	0000.0
7 - 8	8.99	0239.7	0163.0	0167.6	0170.0
8 - 9	9.98	0567.7	0429.0	0441.1	0447.3
9 - 10	11.11	0904.9	0700.1	0719.8	0729.9
10 - 11	11.98	1180.8	0915.7	0941.4	0954.7
11 - 12	12.71	1332.2	1037.4	1066.6	1081.6
12 - 13	13.14	1323.6	1041.1	1070.3	1085.4
13 - 14	13.31	1142.8	0920.9	0946.8	0960.1
14 - 15	13.33	0921.3	0763.3	0784.7	0795.8
15 - 16	12.92	0567.7	0498.5	0512.5	0519.7
16 - 17	12.22	0239.7	0000.0	0000.0	0000.0
17 - 18	11.33	0017.1	0000.0	0000.0	0000.0
Total		8454.6	6469	6650.8	6744.5

TABLE 24. 15 November: useful energy as a function of mass flow rate

Time Hours	Ambient Temperature °C	Incident energy KJ/m^2	Useful energy KJ/m^2		
			Flow rate		
			0.01 kg/Sm^2	0.015 kg/Sm^2	0.02 kg/Sm^2
7 - 8	4.90	008.5	0	0	0
8 - 9	5.28	323.4	165.7	170.4	172.8
9 - 10	6.11	619.6	411.2	422.8	428.8
10 - 11	6.83	822.4	575.2	591.4	599.7
11 - 12	7.41	910.7	649.6	667.9	677.3
12 - 13	7.78	881.9	638.5	656.5	665.7
13 - 14	7.91	752.9	552.7	568.2	576.2
14 - 15	7.69	571.8	416.9	428.6	434.6
15 - 16	7.23	263.9	175.9	180.9	183.4
16 - 17	6.57	008.5	000.0	000.0	000.0
Total		5163.6	3585.7	3686.7	3738.5

TABLE 25. 15 December: useful energy as a function of mass flow rate.

Time Hours	Ambient Temperature °C	Incident energy KJ/m^2	Useful energy KJ/m^2		
			Flow rate		
			0.01 kg/Sm^2	0.015 kg/Sm^2	0.02 kg/Sm^2
8 - 9	3.07	034.1	0	0	0
9 - 10	3.61	373.6	197.1	202.7	205.5
10 - 11	4.21	620.8	384.8	395.6	401.2
11 - 12	4.74	686.2	443.7	456.1	462.6
12 - 13	5.06	686.2	451.2	463.9	470.4
13 - 14	5.12	573.0	373.4	383.9	389.3
14 - 15	4.95	373.6	228.8	235.2	238.5
15 - 16	4.44	034.1	0	0	0
Total		3381.6	2079	2137.4	2167.5

3.7 Discussion

The calculations were carried out on the basis of one square metre of collector area so that the results can be adapted to collectors of different sizes.

Since the radiation income used in the computation is based on hourly totals, it is necessary to consider the useful energy gain as hourly energy totals, and the sum total of useful energy gain for all hours, whenever there is a positive gain, would give the daily total useful energy gain.

A few negative values of useful energy gain were observed in the results, the reason is that if the right-hand side of equation 3.1 is negative, the collector will be losing heat to the atmosphere and therefore these values must be set at zero.

It is interesting to note that all incident angles were near normal whenever there was significant useful energy gain.

The collector model could also be used to simulate different types of flat-plate collectors by defining their characteristic parameters.

CHAPTER 4. THE SIMULATOR AND EXPERIMENTAL EQUIPMENT

4.1 The Simulator

4.1.1 Introduction

The general brief for the simulator was that it should behave, in terms of heat transfer, in a very similar manner to a flat plate collector system when connected to the storage vessel under test. This meant that consideration had to be given to:

a) appropriate solar radiation data

b) the characteristics of the particular flat-plate collector being simulated

c) other important system variables such as ambient temperature, water supply temperature, fluid flow rate, and differential temperature control.

This simulator was intended to be representative of the long term system performance. The analysis of chapter 1 and 2 produced the basic energy profiles to be transferred, by the similator, to storage vessels to study stratification.

4.1.2 Description of the simulator

A line diagram, showing the various elements of the simulator[43] is shown in figure 20. Plate 1 shows a close-up of the power regulator. The simulator consists of a microcomputer interfacing a main power regulator with an 8-bit

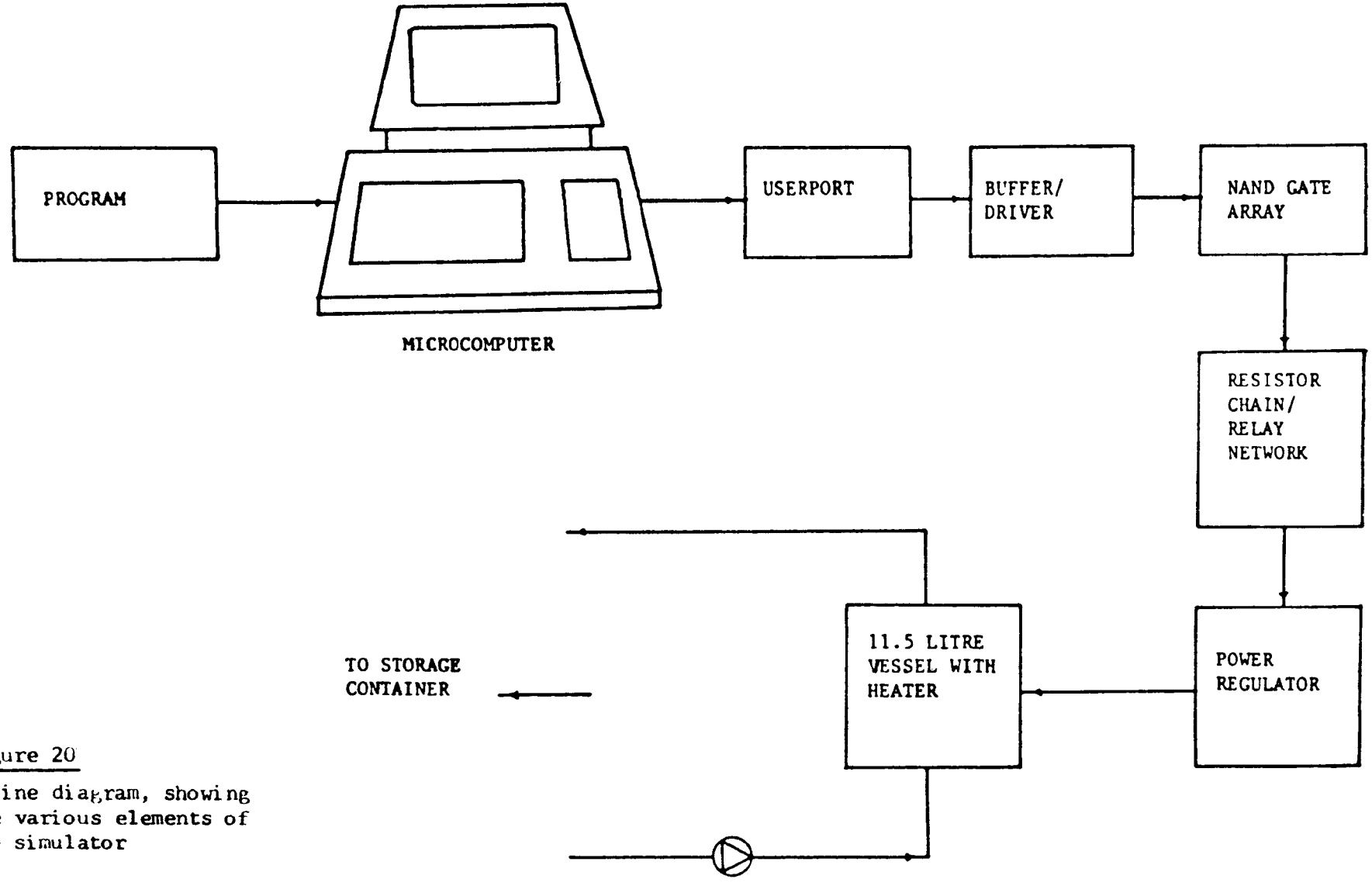

Figure 20

A line diagram, showing the various elements of the simulator

Plate 1 The Simulator

digital control system (0-255 useful states) which drives a resistor chain. The output from this network is a voltage which determines the power level of an electrical heater in an 11.5 litre water filled copper vessel. With any useful energy profile of interest, the user is able to control, through the micro-computer, the logic level of the userport and decide on the time step interval for the test by accessing the internal clock of the micro-computer. It was decided to use a 10 minute stepping interval based on the hourly profiles, which have been generated in chapter 3 as shown in tables 26-43, and are given in Appendix 1.

The details of the calibration are given in Appendix 2.

4.2 Making the temperature probes

It was very difficult to decide which material was to be employed for the construction of the temperature probes.

However, the material to be employed needed to have low thermal conductivity. It had to be rigid enough to be used with temperatures up to 85 ^{o}C, and be chemically resistant to attack by water. The material had to have a low coefficient of thermal expansion. It had to have good impact resistance and be tough and durable.

It was decided to investigate which material had these properties. It was found that "perspex" had almost the

required properties, and therefore it was preferred. A 1783 mm* perspex tube was employed having a 25 mm outside diameter and 19 mm inside diameter. One end of the perspex tube was filled with a perspex rod, having a length of 25 mm and diameter of 19 mm. The other end of the perspex tube was left free to allow the thermocouples to come out of the perspex tube. Fifty two holes were drilled on a straight line along the tube, each hole being 3 mm in diameter and 25 mm apart. Thermocouples were threaded one by one into the perspex tube from the open end, and were allowed to come out through the holes above the surface of the perspex tube to a height of 25 mm. This was done to avoid the boundary layer effect on the thermocouples at the measuring points.

Each end of the thermocouples above the surface of the perspex tube was stripped, and soldered at the top end with a soldering iron. The thermocouples protruding from the perspex temperature probe is shown in plate 2. The other end of the thermocouples were free to connect to the DATA LOGGER. The holes on the surface of the perspex tube were sealed with M890 rapid bonding adhesive. This method of bonding was recommended by Bostik Ltd. after private communication.

Unfortunately two days later it was found that the perspex tube had cracked around the holes. This suggested that the expansion of the perspex tube was different from the expansion of the bonding adhesive, and therefore a strain was produced

* For L/D = 3/1 tank

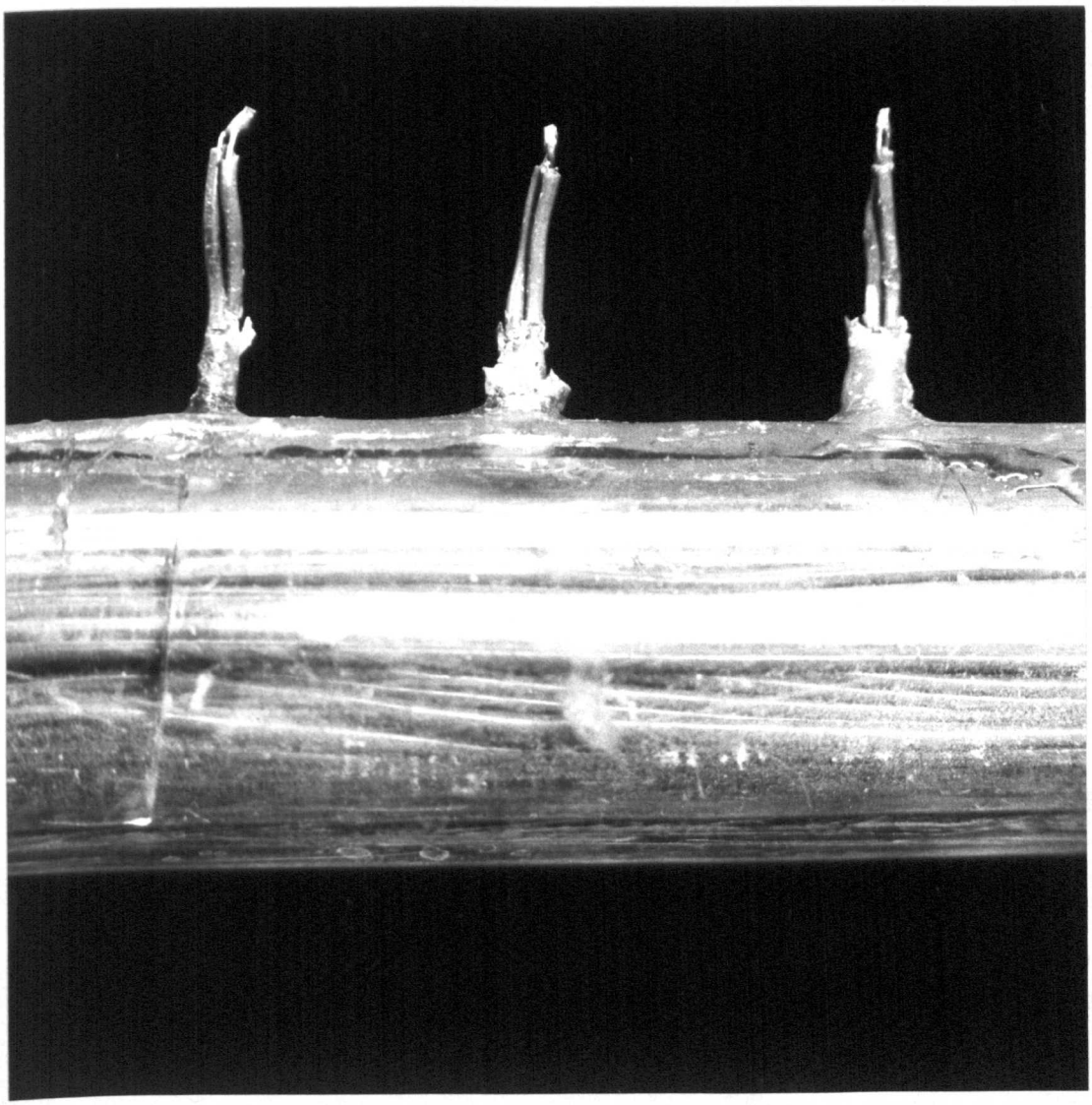

Plate 2 Thermocouples protruding from the perspex temperature probe.

and the perspex tube cracked around the holes. It was decided to do the same procedure again and change the adhesive from M890 rapid bonding adhesive to Araldite.

Unfortunately four days later it was found that the perspex tube had cracked again around the holes, exactly as when the M890 rapid bonding adhesive was used. It was then decided to strengthen the cracked perspex tube by inserting a larger diameter perspex tube over the cracked one after making a split along the length to allow the thermocouples to come out. The split was then sealed with araldite, as shown in plate 3.

4.2.1 Testing the temperature probe

A p.v.c. tube was employed having a 10 cm diameter and 2 metre length, a 25 mm split was cut along the plastic tube. Both ends of the plastic tube were sealed with a blank flange and solvent.

A wooden box was made having a length of 2 metres, width of 15 cm and depth of 17.5 cm to house the p.v.c. tube and allow enough space round the tube for insulation. The space was filled with a micafil insulation to prevent heat losses. The p.v.c. tube was filled with hot water and then the temperature probe put on the top of the p.v.c. tube allowing the tips of the thermocouples to be fully immersed into the hot water. The thermocouples wires passed through a 25 mm diameter hole at the side of the wooden box. The other end of the

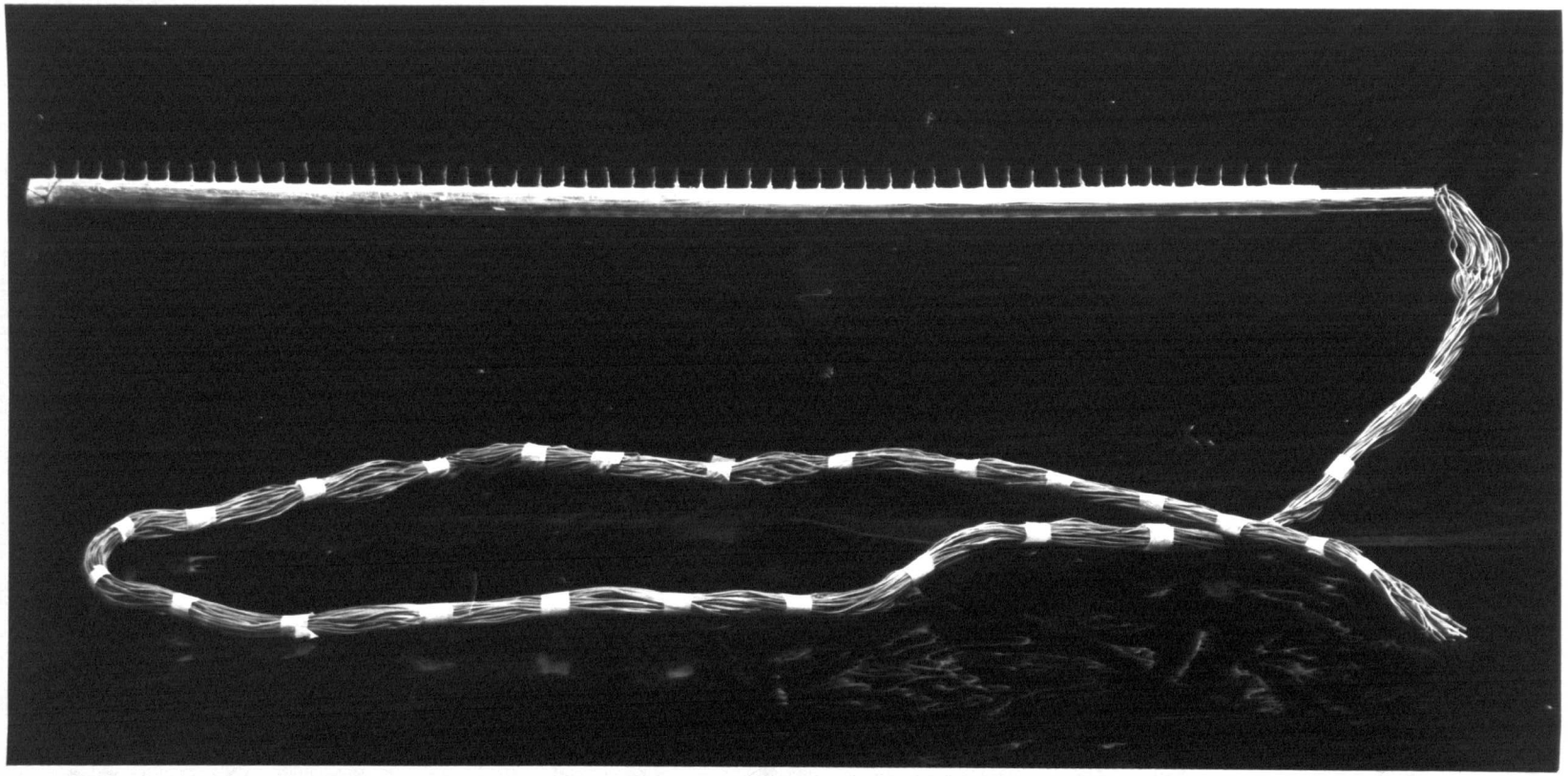

Plate 3 The perspex temperature probe.

thermocouples was connected to the data logger. A top layer of micafil covered the temperature probe and the lid was placed on the box.

During the test there was a leak from the p.v.c. tube and by examining the situation it was found that the temperature probe was bent and the araldite had become soft.

It was concluded that neither the perspex tube nor the araldite was suitable for use in the construction of the temperature probe.

4.2.2 The second attempt at making the temperature probes

It was decided to look for a more suitable material to make the temperature probe. After private communication with the Institute of Plastic they recommended use of a poltruded glass reinforced tube, and plastic filler paste commercially called "David's Isopon" to fill the holes.

The properties of the glass reinforced tube were obtained from Fothergill & Harvey Ltd. It was found out that the properties of the glass reinforced tube were much better than the perspex tube and therefore it was selected.

In this investigation three probes were needed since there were three solar storage containers for experimentation. It was decided to make one at a time, and having gained experience with the first one, the other two could be manufactured with less difficulty. Three poltruded glass reinforced tubes were

employed having length of 2499 mm, 2163 mm and 1783 mm respectively.*

The inside diameter of the tubes was 19 mm, the outside diameter was 25 mm, and the wall thickness was 3 mm. It was decided to locate the thermocouples on the surface of the tubes in a way dependent on the expected stratification within the solar storage containers. In the light of the literature survey, it was found out that the most stratification was expected to take place in the top third of the solar storage container, and less was expected to take place at the middle third of the storage container, and none was expected to take place in the bottom third of the storage container. On the basis of that finding, it was decided to locate 18 thermocouples at the top third of the tube at equal intervals as shown in plate 4, and 8 thermocouples in the middle third of the tube, and 1 thermocouple in the bottom third of the tube. One end of the tube was filled with plastic filler paste. The other end of the tube was left free to allow thermocouples to come out of the tube.

26 holes were drilled on a straight line along the tube, each hole having a 3mm diameter. As the glass reinforced tube was opaque, a thin wire rod was pushed into the hole until it reached the open end of the tube. The thermocouple tip was soldered to it and then pulled out of the hole on the surface of the tube. The wire rod was then cut. This procedure was repeated until all the thermocouples were threaded

* for L/D ratio = 5/1, 4/1 and 3/1 respectively.

Plate 4 The glass reinforced temperature probe.

onto the glass reinforced tube. The thermocouples were above the surface of the tube to a height of 25 mm. This was done to avoid the boundary layer effect on the thermocouples at the measuring points.

Each end of the thermocouples above the surface of the tube were stripped and soldered at the top end with a soldering iron. A thin plastic tube was put over the thermocouples to support them. A typical thermocouple tip along the glass reinforced temperature probe is shown in plate 5.

The other end of the thermocouples were free to connect to the data logger. The holes on the surface of the tube were sealed with plastic filler paste and then the tube was brushed with resin commercially called "David's Isopon Resin". This was done to make sure no leak occurred through the tube.

The same procedure was repeated for the other two tubes.

4.3 The Calibration of Copper-Constantan Thermocouple by Freezing-point Baths

4.3.1 Introduction

Calibration of a thermocouple is the process of determining the electromotive force developed by the thermocouple as a function of the temperature difference between its measuring junction and a standard reference junction.

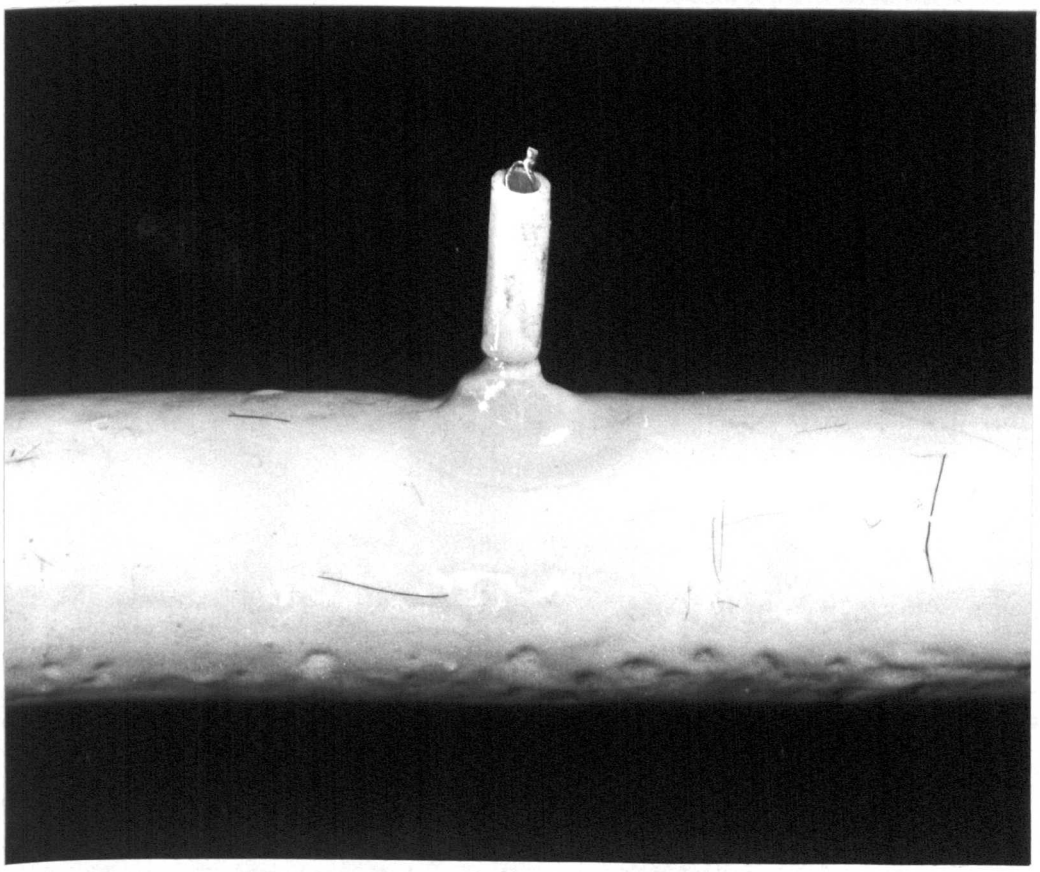

Plate 5 Typical thermocouple tip along the glass reinforced temperature probe.

4.3.2 Description of Terms

4.3.2.1 Thermocouple

A thermocouple is a temperature-sensing device generally consisting of two dissimilar electrical conductors (usually wires). These wires are joined together at one end to form a measuring junction. The other end of the thermocouple is called a reference junction. When the measuring junction and the reference junctions are at different temperatures, an electromotive force is generated in the system; the magnitude of this electromotive force depends on the temperature difference.

4.3.2.2 Selection of the thermocouple

The temperature range will determine the type of thermocouple to be used. The range of this investigation was approximately between $0^{o}C$ - $60^{o}C$ for which a copper-constantan thermocouple was employed.

4.3.3 Apparatus

4.3.3.1 The Liquid Bath

The success of the calibration depended upon the ability to bring the thermocouple being calibrated and the platinum resistance thermometer to the same temperature within the required limits of accuracy. This was achieved by using a well stirred, insulated liquid bath provided with controls for maintaining the temperature constant.

4.3.3.2 The Digital Voltmeter

A Solartron A212 digital voltmeter was used to measure the electromotive force of the thermocouple being calibrated. It gives an accurate and sensitive range of voltages and permits fast readings.

4.3.3.3 The Standard platinum resistance thermometer

A standard platinum resistance thermometer was used. This was the most accurate standard for use in a stirred liquid bath. Temperatures were not measured directly with this instrument. Its electrical resistance was determined by comparison with a standard resistor using Inductively Coupled Ratio Bridge Type 5650.

4.3.3.4 Ice-point reference junction bath

An ice-point reference junction bath was used. This provided a relatively simple and reliable means for maintaining the reference junction at $0^{o}C$ ($32^{o}F$). A wide mouthed thermos bottle filled with shaved ice saturated with water was used.

4.4 Calibration procedures

A copper-constantan thermocouple was prepared for calibration. The thermocouple was stripped and soldered at one end with a soldering iron.

The standard resistance thermometer was wrapped with calibrated thermocouple by a fine wire and clamped into the

liquid bath two inches above the bottom of the bath. The sensor of the standard resistance thermometer was level with the thermocouple reference junctions. The standard resistance thermometer was connected to Inductively Coupled Double Ratio Bridge Type 5650. Electrical Connection between the thermocouple wire and its copper connecting wire was made by inserting them in small glass tube containing about 20 mm (.075 in) of mercury. The glass tube was mounted in hole in a stopper fitted into the mouth of the thermos bottle and extending below the surface of the ice slush near to the bottom of the thermos bottle. The copper connecting wire was electically insulated to a point about 6 mm (0.25 in) below the mercury surface. In the preparation of the ice bath, the spaces between the ice particles were filled with water (to prevent air pockets), and the ice was extended to a depth of at least 25 mm (1 in) below the bottom of the tube, water being drawn off from time to time, and ice added as needed. The digital voltemeter was connected to the thermocouple. When the bath was stabilized at $-1^{o}C$ for about 10 minutes by means of a stirrer and a thermometer, the electromotive force of the thermocouple was recorded, and the corresponding resistance ratio of the standard platinum thermometer was recorded, immediately after the reading of the electromotive force of the thermocouple these procedures were repeated at each of a series of selected calibration points, these were $-1^{o}C$, $5^{o}C$, $18^{o}C$, $23^{o}C$, $29^{o}C$, $36^{o}C$, $41^{o}C$, $48^{o}C$, $53^{o}C$, $60^{o}C$, $75^{o}C$ respectively.

4.5 Results

The electromotive force of the thermocouple and twelve calibration points and the corresponding resistance ratio of the platinum resistance thermometer are shown in table 44.

Table 44: Calibration of Copper-constant thermocouple

Temperature (^{o}C)	Resistance Ratio	Equivalent Temperature for Resistance Ratio	Soldered Thermocouple E.M.F./MV
-1	0.505578	0.39	10
5	0.509477	4.35	168
18	0.522001	17.53	687
23	0.527713	23.80	953
29	0.532374	29.03	1168
36	0.538851	36.49	1483
41	0.543177	41.61	1698
48	0.548213	47.69	1968
53	0.552953	53.55	2220
60	0.557890	59.80	2494
75	0.569152	74.64	3157

4.6 Reading between test points

Interpolation was required to obtain a continuous temperature electromotive force relationship. The experimental data were treated mathematically. In consideration of each point, one weighs its relative value according to the laws of probability then passes a precisely determined equation of a prescribed form through the data. The well-known least-square

principle for treating data fulfils the foregoing requirements. It was found that there was no improvement gained by going to a fourth order fit. The equation used was as follows: E.M.F./mv = $t(0.0389566 + 4.5525 \times 10^{-5}t)$. The cubic fit representing the thermocouple characteristic was determined at appropriate intervals and the results are shown in table 45 as a photocopy of the computer print out.

4.7 Differential Temperature Controller

The purpose of the controller is to ensure that fluid is pumped through the collector only when useful heat can be gained, that is, when the temperature of the fluid at the collector output is higher than that of a reference point at the bottom of the storage container. Close[44] has shown that the best (i.e. highest energy collection) control strategy for pump operation is achieved by the use of an on-off differential controller. Therefore a differential temperature controller TYPE B-18 was employed. It is manufactured by Air Distribution Equipment Limited. The controller is provided with two temperature sensors which are suitably housed thermisters. One sensor was located at the bottom of the storage container and the other was located at the outlet of the heater. The differential temperature controller senses T_{so}, the fluid temperature at the bottom of the storage container and T_{co}, the fluid temperature at the outlet of the heater, and then controls the operation of the pump as recommended by British Standard[40].

Table 45 COPPER CONSTANTAN THERMOCOUPLE E.M.F./mV

T/°C	0.0	0.1	0.2	0.3	0.4	0.5	0.6	0.7	0.8	0.9
0.0	0.000	0.004	0.008	0.012	0.016	0.019	0.023	0.027	0.031	0.035
1.0	0.039	0.043	0.047	0.051	0.055	0.059	0.062	0.066	0.070	0.074
2.0	0.078	0.082	0.086	0.090	0.094	0.098	0.102	0.106	0.109	0.113
3.0	0.117	0.121	0.125	0.129	0.133	0.137	0.141	0.145	0.149	0.153
4.0	0.157	0.160	0.164	0.168	0.172	0.176	0.180	0.184	0.188	0.192
5.0	0.196	0.200	0.204	0.208	0.212	0.216	0.220	0.224	0.227	0.231
6.0	0.235	0.239	0.243	0.247	0.251	0.255	0.259	0.263	0.267	0.271
7.0	0.275	0.279	0.283	0.287	0.291	0.295	0.299	0.303	0.307	0.311
8.0	0.315	0.319	0.323	0.326	0.330	0.334	0.338	0.342	0.346	0.350
9.0	0.354	0.358	0.362	0.366	0.370	0.374	0.378	0.382	0.386	0.390
10.0	0.394	0.398	0.402	0.406	0.410	0.414	0.418	0.422	0.426	0.430
11.0	0.434	0.438	0.442	0.446	0.450	0.454	0.458	0.462	0.466	0.470
12.0	0.474	0.478	0.482	0.486	0.490	0.494	0.498	0.502	0.506	0.510
13.0	0.514	0.518	0.522	0.526	0.530	0.534	0.538	0.542	0.546	0.550
14.0	0.554	0.558	0.562	0.566	0.570	0.574	0.578	0.582	0.587	0.591
15.0	0.595	0.599	0.603	0.607	0.611	0.615	0.619	0.623	0.627	0.631
16.0	0.635	0.639	0.643	0.647	0.651	0.655	0.659	0.663	0.667	0.671
17.0	0.675	0.679	0.684	0.688	0.692	0.696	0.700	0.704	0.708	0.712
18.0	0.716	0.720	0.724	0.728	0.732	0.736	0.740	0.744	0.748	0.753
19.0	0.757	0.761	0.765	0.769	0.773	0.777	0.781	0.785	0.789	0.793
20.0	0.797	0.801	0.805	0.810	0.814	0.818	0.822	0.826	0.830	0.834
21.0	0.838	0.842	0.846	0.850	0.855	0.859	0.863	0.867	0.871	0.875
22.0	0.879	0.883	0.887	0.891	0.895	0.900	0.904	0.908	0.912	0.916
23.0	0.920	0.924	0.928	0.932	0.937	0.941	0.945	0.949	0.953	0.957
24.0	0.961	0.965	0.969	0.974	0.978	0.982	0.986	0.990	0.994	0.998
25.0	1.002	1.006	1.011	1.015	1.019	1.023	1.027	1.031	1.035	1.040
26.0	1.044	1.048	1.052	1.056	1.060	1.064	1.068	1.073	1.077	1.081
27.0	1.085	1.089	1.093	1.097	1.102	1.106	1.110	1.114	1.118	1.122
28.0	1.126	1.131	1.135	1.139	1.143	1.147	1.151	1.156	1.160	1.164
29.0	1.168	1.172	1.176	1.181	1.185	1.189	1.193	1.197	1.201	1.206
30.0	1.210	1.214	1.218	1.222	1.226	1.231	1.235	1.239	1.243	1.247
31.0	1.251	1.256	1.260	1.264	1.268	1.272	1.276	1.281	1.285	1.289
32.0	1.293	1.297	1.302	1.306	1.310	1.314	1.318	1.323	1.327	1.331

33.0	1.335	1.339	1.344	1.348	1.352	1.356	1.360	1.365	1.369	1.373
34.0	1.377	1.381	1.386	1.390	1.394	1.398	1.402	1.407	1.411	1.415
35.0	1.419	1.423	1.428	1.432	1.436	1.440	1.445	1.449	1.453	1.457
36.0	1.461	1.466	1.470	1.474	1.478	1.483	1.487	1.491	1.495	1.499
37.0	1.504	1.508	1.512	1.516	1.521	1.525	1.529	1.533	1.538	1.542
38.0	1.546	1.550	1.555	1.559	1.563	1.567	1.572	1.576	1.580	1.584
39.0	1.589	1.593	1.597	1.601	1.606	1.610	1.614	1.618	1.623	1.627
40.0	1.631	1.635	1.640	1.644	1.648	1.652	1.657	1.661	1.665	1.669
41.0	1.674	1.678	1.682	1.687	1.691	1.695	1.699	1.704	1.708	1.712
42.0	1.716	1.721	1.725	1.729	1.734	1.738	1.742	1.746	1.751	1.755
43.0	1.759	1.764	1.768	1.772	1.776	1.781	1.785	1.789	1.794	1.798
44.0	1.802	1.807	1.811	1.815	1.819	1.824	1.828	1.832	1.837	1.841
45.0	1.845	1.850	1.854	1.858	1.862	1.867	1.871	1.875	1.880	1.884
46.0	1.888	1.893	1.897	1.901	1.906	1.910	1.914	1.919	1.923	1.927
47.0	1.932	1.936	1.940	1.944	1.949	1.953	1.957	1.962	1.966	1.970
48.0	1.975	1.979	1.983	1.988	1.992	1.996	2.001	2.005	2.009	2.014
49.0	2.018	2.023	2.027	2.031	2.036	2.040	2.044	2.049	2.053	2.057
50.0	2.062	2.066	2.070	2.075	2.079	2.083	2.088	2.092	2.096	2.101
51.0	2.105	2.110	2.114	2.118	2.123	2.127	2.131	2.136	2.140	2.144
52.0	2.149	2.153	2.158	2.162	2.166	2.171	2.175	2.179	2.184	2.188
53.0	2.193	2.197	2.201	2.206	2.210	2.214	2.219	2.223	2.228	2.232
54.0	2.236	2.241	2.245	2.250	2.254	2.258	2.263	2.267	2.272	2.276
55.0	2.280	2.285	2.289	2.294	2.298	2.302	2.307	2.311	2.316	2.320
56.0	2.324	2.329	2.333	2.338	2.342	2.346	2.351	2.355	2.360	2.364
57.0	2.368	2.373	2.377	2.382	2.386	2.391	2.395	2.399	2.404	2.408
58.0	2.413	2.417	2.421	2.426	2.430	2.435	2.439	2.444	2.448	2.452
59.0	2.457	2.461	2.466	2.470	2.475	2.479	2.484	2.488	2.492	2.497
60.0	2.501	2.506	2.510	2.515	2.519	2.524	2.528	2.532	2.537	2.541
61.0	2.546	2.550	2.555	2.559	2.564	2.568	2.572	2.577	2.581	2.586
62.0	2.590	2.595	2.599	2.604	2.608	2.613	2.617	2.622	2.626	2.630
63.0	2.635	2.639	2.644	2.648	2.653	2.657	2.662	2.666	2.671	2.675
64.0	2.680	2.684	2.689	2.693	2.698	2.702	2.707	2.711	2.716	2.720
65.0	2.725	2.729	2.733	2.738	2.742	2.747	2.751	2.756	2.760	2.765
66.0	2.769	2.774	2.778	2.783	2.787	2.792	2.796	2.801	2.805	2.810
67.0	2.814	2.819	2.823	2.828	2.832	2.837	2.842	2.846	2.851	2.855

68.0	2.860	2.864	2.869	2.873	2.878	2.882	2.887	2.891	2.896	2.900
69.0	2.905	2.909	2.914	2.918	2.923	2.927	2.932	2.936	2.941	2.946
70.0	2.950	2.955	2.959	2.964	2.968	2.973	2.977	2.982	2.986	2.991
71.0	2.995	3.000	3.004	3.009	3.014	3.018	3.023	3.027	3.032	3.036
72.0	3.041	3.045	3.050	3.055	3.059	3.064	3.068	3.073	3.077	3.082
73.0	3.086	3.091	3.096	3.100	3.105	3.109	3.114	3.118	3.123	3.128
74.0	3.132	3.137	3.141	3.146	3.150	3.155	3.160	3.164	3.169	3.173
75.0	3.178	3.182	3.187	3.192	3.196	3.201	3.205	3.210	3.214	3.219
76.0	3.224	3.228	3.233	3.237	3.242	3.247	3.251	3.256	3.260	3.265
77.0	3.270	3.274	3.279	3.283	3.288	3.293	3.297	3.302	3.306	3.311
78.0	3.316	3.320	3.325	3.329	3.334	3.339	3.343	3.348	3.352	3.357
79.0	3.362	3.366	3.371	3.376	3.380	3.385	3.389	3.394	3.399	3.403
80.0	3.408	3.413	3.417	3.422	3.426	3.431	3.436	3.440	3.445	3.450
81.0	3.454	3.459	3.463	3.468	3.473	3.477	3.482	3.487	3.491	3.496
82.0	3.501	3.505	3.510	3.514	3.519	3.524	3.528	3.533	3.538	3.542
83.0	3.547	3.552	3.556	3.561	3.566	3.570	3.575	3.580	3.584	3.589
84.0	3.594	3.598	3.603	3.608	3.612	3.617	3.622	3.626	3.631	3.636
85.0	3.640	3.645	3.650	3.654	3.659	3.664	3.668	3.673	3.678	3.682
86.0	3.687	3.692	3.696	3.701	3.706	3.710	3.715	3.720	3.724	3.729
87.0	3.734	3.738	3.743	3.748	3.753	3.757	3.762	3.767	3.771	3.776
88.0	3.781	3.785	3.790	3.795	3.800	3.804	3.809	3.814	3.818	3.823
89.0	3.828	3.832	3.837	3.842	3.847	3.851	3.856	3.861	3.865	3.870
90.0	3.875	3.880	3.884	3.889	3.894	3.898	3.903	3.908	3.913	3.917
91.0	3.922	3.927	3.931	3.936	3.941	3.946	3.950	3.955	3.960	3.965
92.0	3.969	3.974	3.979	3.984	3.988	3.993	3.998	4.002	4.007	4.012
93.0	4.017	4.021	4.026	4.031	4.036	4.040	4.045	4.050	4.055	4.059
94.0	4.064	4.069	4.074	4.078	4.083	4.088	4.093	4.097	4.102	4.107
95.0	4.112	4.116	4.121	4.126	4.131	4.136	4.140	4.145	4.150	4.155
96.0	4.159	4.164	4.169	4.174	4.178	4.183	4.188	4.193	4.198	4.202
97.0	4.207	4.212	4.217	4.221	4.226	4.231	4.236	4.241	4.245	4.250
98.0	4.255	4.260	4.265	4.269	4.274	4.279	4.284	4.289	4.293	4.298
99.0	4.303	4.308	4.312	4.317	4.322	4.327	4.332	4.336	4.341	4.346

This was as follows:

pump switched ON when approximately $T_{co} - T_{so} \geq 2^{o}C$ and

pump switched OFF when approximately $T_{co} - T_{so} \leq 1^{o}C$.

4.8 The Pump

A variable speed centrifugal pump ensures forced circulation of the water through the heater. It is a Commodor Bronze type, and is manufactured by Sealed Motor Construction Company Limited. The pump is controlled by the differential temperature controller.

4.9 Flow rate measurements

A turbine flowmeter was fitted in the heater circuit. It is a Q-flo turbine flowmeter part number QE6/J and is manufactured by Quadrina Limited. It is an instrument for accurately measuring liquid flows in pipes and produces pulse output information directly proportional to volumetric fluid flow, the rotation being sensed by the pickup unit producing pulse output information. This pulse output is transferred to a Quadrina QD instrument. This is specifically designed for use in turbine flow metering application where accurate flow rate measurements are required.

4.10 The Filter

A general purpose filter type WF-101-S-005, supplied with 5 micrometre polypropylene cartridge fitted with transparent

bowel was employed. It is manufactured by IMI Mouldings Limited. The filter was used in the system for sediment removal before the turbine flow meter, since the turbine rotation could be effected by any sediment on it.

4.11 The Data recording unit

The data recording unit consists of a data logger, a digital voltmeter and a tape punch.

a) The data logger

The data logger is a modular versatile, data acquisition and recording system. It could be used with any digital voltmeter. Data are transferred from an input interface via one or two output driver modules to data recording devices "Facit 4070 Tape Punch". It is manufactured by Solartron Electronic Group Limited.

b) The Digital Voltmeter

The Solartron A212 Digital Voltmeter gives an accurate and sensitive range of voltages. It is also manufactured by Solartron Electronic Group Limited.

c) The Facit 4070 Tape Punch

The Facit 4070 is a compact, quiet running tape punch operating at speeds up to 75 characters per second. It punches all types of standard tape. It is well suited for all kinds of data recording application.

CHAPTER 5. STORAGE OF THERMAL ENERGY

5.1 Introduction

While considerable work has been done on the measurement of thermal characteristics of solar panels, comparatively little has been published on thermal storage designs, particularly those depending upon the thermal capacity of water to store sensible heat.

The function of an energy storage system is to hold some or all of the solar energy collected during sunny periods for use at night or during subsequent cloudy days. Therefore effective utilization of solar energy will be greatly aided by the development of efficient energy storage systems.

Storage systems may be considered in three parts:

(i) The choice of storage medium

(ii) The determination of the storage capacity

(iii) The storage container design.

Each of these sections will be considered in this chapter.

5.2 The storage medium

Materials available for storage of thermal energy are water and crushed solids which store the energy as sensible heat, and certain chemicals which undergo a change of phase permitting storage of energy as latent heat (heat of fusion).

Table 46 was presented by Telkes[45] and compares thermal

storage data and shows the weight and volume of rock-like solids, water and heat of fusion materials for storing of 1 GJ.

Table 46: Thermal Storage of 1 GJ

	Rock	Water	Heat of fusion materials
Specific heat, KJ/Kg^{o}C	0.837	4.187	2.09
Heat of fusion, KJ/Kg	-	-	232.6
Density, Kg/m^{3}	2242	1000	1602
Storage of 1 GJ, weight, Kg	59737	11941	3644
Relative weight	16.4	3.27	1
Volume, m^{3}	26.6	11.941	2.274
Relative volume	11.69	5.25	1

A comparison of water and rocks from table 46 from which the superiority of water is clearly shown.

A comparison of water and heat of fusion materials were studied by Joy and Shelpuk[46], they concluded that water thermal storage is cheaper than phase change and phase change-water slurries, in addition they pointed out that further study and development work with phase change materials should focus on the solar air conditioning where the technical advantages of phase change storage over water storage is greatest. However, the choice of medium for energy storage depends on the nature

of the process. For water heating, energy storage as sensible heat of stored water is logical.

Churchliff[47] has pointed out that most of the solar houses presently in the United States utilize hot water storage. The advantages of using hot water storage has been summarized by Szego[48]. These advantages are:

1. Water is the most available storage material, it is also the least expensive.

2. Water is a substance for which we have the greatest amount of technical, physical, chemical and thermodynamic data.

3. Water is one of the few thermal storage materials which can be used as both the collector transfer and the load transfer medium at the same time.

4. Water has the highest specific heat of any common substance and of any generally usable fluid.

5. Its vapour-liquid equilibrium temperature/pressure relationship is appropriate for attainable nonfocusing solar collector performance characteristics.

6. Water has relatively excellent heat transfer and fluid dynamic characteristics - especially viscosity, thermal conductivity, density, and coefficient of thermal expansion which enhance natural convection.

7. Water is transparent and admits to easy level identification and flow instrumentation.

8. Water is nontoxic, and is not flammable.

9. Water-based corrosion inhibitor art is very advanced and there is an experienced background of many decades in this area.

The above are not the only advantages of water but these were the principle ones. However, there are some disadvantages of using hot water storage systems. These disadvantages are:

1. Water is a medium for electrolytic corrosion.

2. Water freezes in climates where solar heating is most desirable, and furthermore, it expands on freezing, leading to possible damage.

3. It can be a solvent for gases, especially oxygen, which can be the cause of corrosion.

Although there are some disadvantages, it can be seen that water is a superior storage medium for solar water heating systems, than other mediums previously mentioned.

5.3 The Storage Container Designs

The designs[49] were based on the following principles.

a) Capacity

Optimum storage capacity in solar water heating systems has been the subject of much research. Some of the more notable publications and their results are summarized in table 47. Within the ranges of storage capacities suggested by the authors (24, 13, 50, 30, 12, 3, 2, 51), it was difficult to decide upon an "optimum" for this work. 100 kg/m^2 collector area was adopted for storage containers tested, mainly because Buckles, Klein and Duffie[51] were able to show that this basis of sizing gave a greater efficiency than a system sized at 75 kg/m^2. Additionally, it would be sufficient to cover at least 2 or 3 days usage. This is based on 45 kg per person per day as recommended by Whittle and Warren.[52]

Table 47. Recommended Capacities of Storage Containers

AUTHOR(S)	STORAGE CAPACITY kg/m^2 Collector area
Heywood[24]	50
Brinkworth[13]	30-60
Jesch and Soldatos[50]	45
Lof and Tybout[30]	50-75
Carter[12]	208
Sharp and Loehrke[3]	125
Duffie and Beckman[2]	50-100
Buckles, Klein and Duffie[51]	100

b) Configuration

Klein[53] and Lavan and Thompson[11] have pointed out that a cylindrical storage tank is the best configuration. The shape promotes thermal stratification and because of its lower surface area offers greater resistance to heat loss than its rectangular counterpart for a given level of insulation.

c) Heat Exchanger

Consideration was given to the use of a heat exchanger in the storage container but the disadvantages significantly outweigh the advantages. Duffie and Beckman[2] and Davis and Bartera[4] have shown that for every degree celsius temperature drop across the exchanger the collection efficiency reduces by 1-2%.

Brinkworth[13] has concluded that convection motions induced by heat exchanger coils are often sufficient to prevent stratification taking place to any significant extent. Heat exchangers will also add significantly to the capital costs of solar storage systems.

If maximum stratification is the goal, it would appear that a heat exchanger can be a positive disadvantage, and one was not employed in this work.

d) Inlet/Outlet Arrangements

The store take-off point for the transportation fluid has been shown by Whillier[54] to be very important. The heat

transportation fluid enters the collector at the same temperature that it leaves the store, and for maximum collection efficiency this fluid should be at the lowest possible temperature. Wherever possible the transportation fluid should leave the store at its lowest point.

Provision was not made to change the point of entry of the transportation fluid, to the store, with changes in temperature, and the entry was located at the top of the store. Lavan and Thompson[11] reached similar conclusions with their studies on small-scale model storage containers.

e) Variation of length-to-diameter ratio (L/D)

Having determined the capacity and configuration of storage containers, the next step was to vary length-to-diameter ratio (L/D). These were as follows:

1) TYPE I Storage Container

L/D = 1:3, volume = 0.5 m^3

$\therefore \frac{\pi x^2}{4} \times 3x = 0.5 \qquad x = 0.596$ m

$\therefore$ D = 596 mm and L = 1788 mm

2) TYPE II Storage Container

L/D = 1:4, volume = 0.5 m^3

$\therefore \frac{\pi x^2}{4} \times 4x = 0.5 \qquad x = 0.542$ m

$\therefore$ D = 542 mm and L = 2168 mm

3) TYPE III Storage Container

$L/D = 1:5$, volume $= 0.5\ m^3$

$\therefore \quad \frac{\pi x^2}{4} \times 5x = 0.5$

$\therefore$ D = 503 mm and L = 2515 mm

Three copper cylindrical storage containers were manufactured having L/D equal to 3/1, 4/1 and 5/1 respectively.

Storage containers having length to diameter equal to 3/1 were designated as TYPE I, 4/1 as TYPE II, and 5/1 as TYPE III.

The bottom of the storage containers were fixed and the tops were movable. These containers were employed to study the effect of length-to-diameter ratio on stratification.

5.4 Storage Tank Losses

The amount of energy lost by the storage unit to its surroundings is represented as a function of time by $L_{(t)}$ in the equation:

$$L_{(t)} = U_s A_s (T_{(t)} - T_a) \qquad 5.1$$

Where:

U_s = the heat transfer coefficient of the storage unit

A_s = the surface area of the storage unit

T_a = the air temperature surrounding the storage unit

$T_{(t)}$ = average water temperature in the storage unit.

The numerical value of U_s depends on the thickness of the insulation surrounding the storage tank. A_s is related to the storage volume (V) by the equation

$$A_s = K(V)^{2/3} \qquad 5.2$$

where K is a constant which depends on the shape of the storage tank.

When the tank is cylindrical, K is given by the equation

$$K = 2\pi \left[2\left(\frac{h}{d}\right) + 1\right] \Big/ \left[2\pi\left(\frac{h}{d}\right)\right]^{2/3} \qquad 5.3$$

where (h/d) is the ratio of the height of the cylinder to the diameter of the cylinder.

CHAPTER 6. EXPERIMENTAL PROCEDURE AND RESULTS

6.1 INTRODUCTION

The experimental programme was divided into three sections:

(i) A study of the effects of each of three flow rates (0.01 kg/sm^2, 0.015 kg/sm^2, 0.02 kg/sm^2 of Collector area).

(ii) An investigation into the effect of length-to-diameter ratio (L/D) on stratification. Three storage containers were employed having a length-to-diameter ratios 3/1, 4/1 and 5/1 respectively. Storage containers having length-to-diameter ratios equal to 3/1 were designated as TYPE I, 4/1 as TYPE II, and 5/1 as TYPE III.

(iii) An assessment of the long term system performance for the storage containers.

Each of these three sections is discussed separately and the results are presented in a variety of ways. A discussion of the results for each section is also included.

6.2 Flow rate tests

The general testing arrangement is shown in Figure 21, and in Plate 6.

The simulator[43] is intended to be representative of the long term energy delivery averaged over most cloud conditions

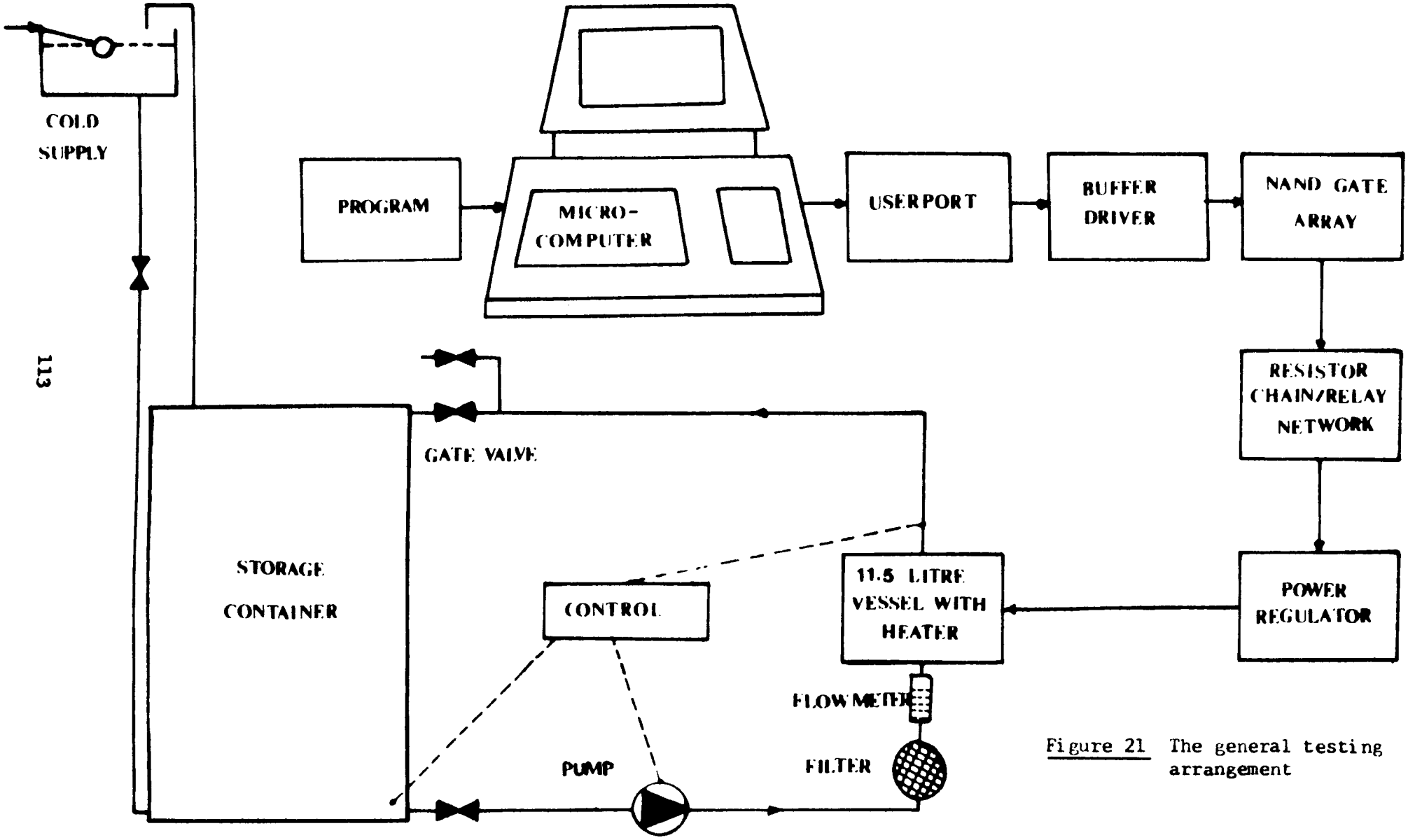

Figure 21 The general testing arrangement

PLATE 6 The general testing arrangement.

and incident angles. Tests were first conducted on the cylindrical water filled storage container of L/D equal to 3/1 and capacity of 500 kg, designated as TYPE I storage container.

The storage container had a uniform layer of insulation ($U = 1.65$ kJ/hr m^2 ^oC).

Useful energy profiles for 15 March, 15 June, and 15 December were simulated for each of three mass flow rates (0.01 kg/sm^2 (Tables 26, 29, 32), 0.015 kg/sm^2 (Tables 27, 30, 33), and 0.02 kg/sm^2 (Tables 28, 31, 34)) and temperatures throughout the store were monitored at hourly intervals. No draw-off was superimposed.

Twenty-eight calibrated thermocouples (copper-constantan) on the central axis of the store were used for temperature measurement in conjunction with a central data-logger. Data were stored on punched tape for later analysis. The pump switched on at a differential approximately $\geqslant 2^oC$ and switched off at a differential approximately $\leqslant 1^oC$ according to British Standard[40].

An example of a simulator control program is given in Appendix 3.

The arrangement of thermocouples in the TYPE I storage tank is shown in Figure 22, and the distance of each thermocouple from the bottom of the storage container is given in Table 48.

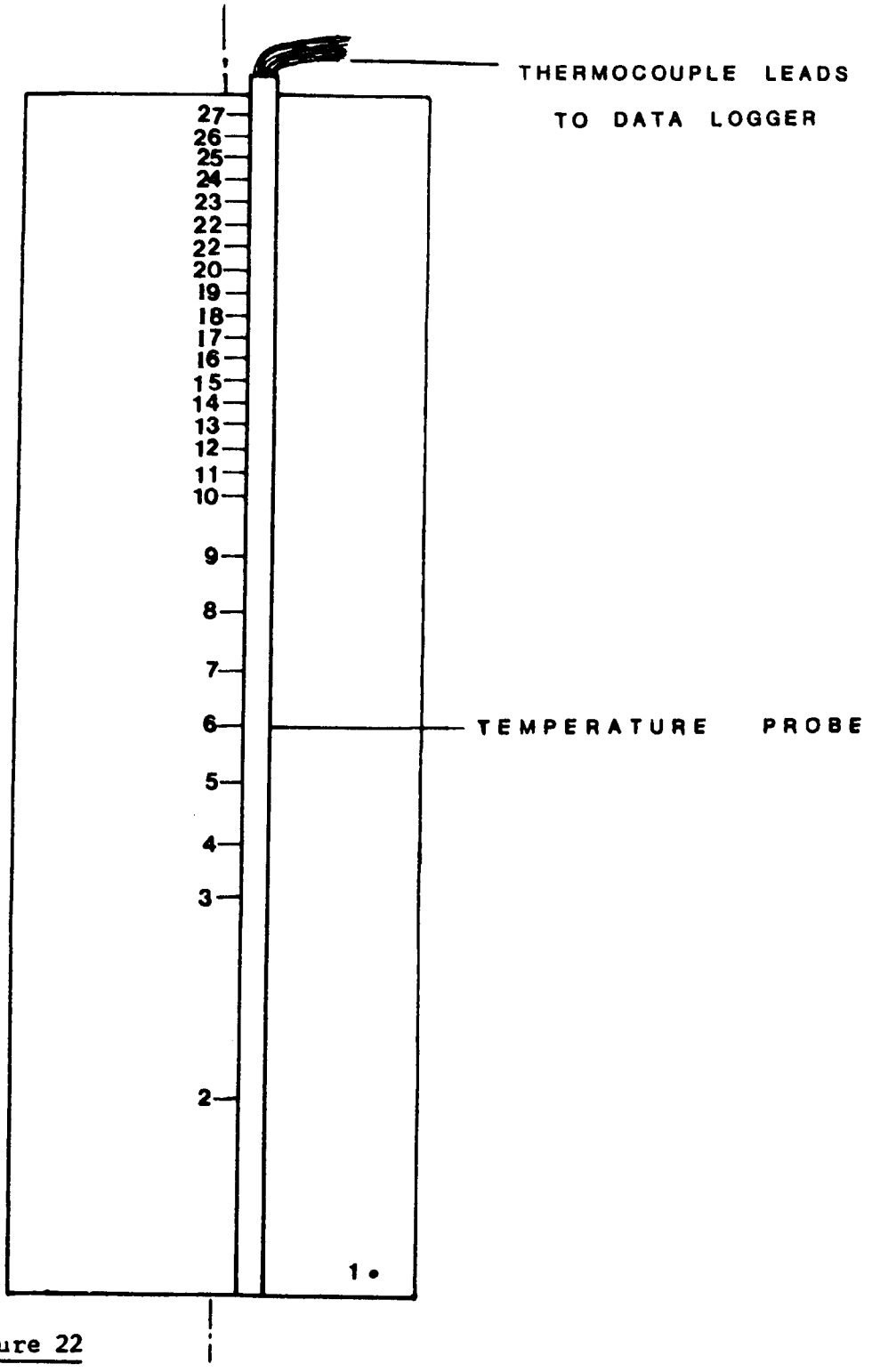

Figure 22

ARRANGEMENT OF THERMOCOUPLES
IN TYPE I STORAGE

TABLE 48. Thermocouples location in the TYPE I storage container

Thermocouples Number	Distance from the bottom of the storage container (M)
27	1.754
26	1.721
25	1.688
24	1.655
23	1.622
22	1.589
21	1.556
20	1.523
19	1.490
18	1.456
17	1.423
16	1.390
15	1.357
14	1.324
13	1.291
12	1.258
11	1.225
10	1.192
9	1.106
8	1.021
7	0.936
6	0.851
5	0.766
4	0.681
3	0.596
2	0.298
1	0.040

6.2.1 Interpretation of temperature measurements

It was difficult to decide how the temperature data of the storage container were to be interpreted. Several authors[10,12,55] have used single temperature readings at different positions to demonstrate the temperature histories of the storage container. It was decided to use an average value around groups of thermocouples to demonstrate the temperature histories of the storage container. In order to relate these results with the existing mathematical models of Duffie and Beckman[2] and Close[44], it was necessary to define segments within the storage container because the energy balance around each segment is taken as a basis for the analysis in their mathematical models. It transpired, however, that during the course of this series of tests, the temperatures around groups of chosen thermocouples on the probe Figure 22 produced similar results. A closer examination of this phenomenon revealed that the tank was behaving as a three-segment tank, producing three regions within which the water temperature was relatively constant. To exemplify this feature, the author has chosen to illustrate the December profile at times 11.30 hours and 13.30 hours; Table 49 shows the results from each thermocouple at these specified times. An inspection of this table demonstrates that thermocouple numbers 27 to 8 give a relatively constant temperature (average value = 14.94 ^{o}C and standard deviation = 0.85 ^{o}C at 11.30 hours; at 13.30 hours the average value = 15.74 ^{o}C and standard deviation = 0.38 ^{o}C). The temperature then differed slightly more around thermocouple number 8 and a second segment was defined by thermocouples 8 to

2 (average value = 11.48 °C and standard deviation = 0.60 °C at 11.30 hours; at 13.30 hours the average value = 12.88 °C and standard deviation 1.32°C). The temperature again differed slightly around thermocouple number 2 and a third segment was defined by thermocouples 2 to 1 (average value = 10.65 °C and standard deviation = 0.13 °C at 11.30 hours; at 13.30 hours the average value = 10.85 °C and standard deviation = 0.3 °C).

The limit at which temperatures around groups of thermocouples have been adopted for averaging purposes in relation to the height of the storage container are illustrated in each of the figures which follow (Figures 23-31).

6.2.1.1 Repeatability

The repeatability of the temperature histories within the storage containers under test was demonstrated through 3 tests on the TYPE III storage container for the March profile (Table 26). Similar starting conditions were arranged for each test and the results demonstrated that the temperature histories were reproducable and constant within $\pm$ 0.5 °C at each hourly interval throughout the entire series of tests. On this basis it was decided to accept all other test results on a one-off basis.

TABLE 49 Results from each thermocouple for TYPE I storage container

Thermocouples Number	Thermocouples reading at 11.30 hrs				Thermocouples reading at 13.30 hrs			
	Reading (°C)	Average Value	Standard deviation	Segment number	Reading (°C)	Average Value	Standard deviation	Segment number
27	15.52	14.94	0.85	1	16.26	15.74	0.38	1
26	15.37				16.26			
25	15.52				15.84			
24	15.47				16.34			
23	15.50				15.82			
22	15.52				15.77			
21	15.52				15.84			
20	15.37				15.87			
19	15.44				15.84			
18	15.55				15.89			
17	15.45				15.72			
16	15.17				15.82			
15	15.17				15.82			
14	14.95				15.84			
13	14.95				15.22			
12	14.33				15.65			
11	14.23				15.55			
10	14.03				15.45			
9	13.34				15.22			
8	12.46				14.70			
7	11.96	11.48	0.60	2	14.21	12.88	1.32	2
6	11.66				13.46			
5	11.42				12.79			
4	11.14				12.14			
3	10.99				11.81			
2	10.74				11.06			
1	10.56	10.65	0.13	3	10.64	10.85	0.3	3

6.2.2 Results

The temperature histories of the TYPE I storage container for each of the nine series of tests are shown in Figures 23-31.

6.2.3 Discussion

The general conclusions to be drawn from these tests are:

1. The TYPE I storage container behaves as a three segment tank.

2. Overall the lowest flow rate, 0.01 kg/Sm^2, gives the better series of results. In general terms, the greater the temperature separation of the segments, the more stable they become, and conversely, the nearer the temperatures are to each other, the more the system moves towards a mixed tank. The most stable case was 15 December profile (0.01 kg/Sm^2) and the least stable case was 15 June (0.02 kg/Sm^2).

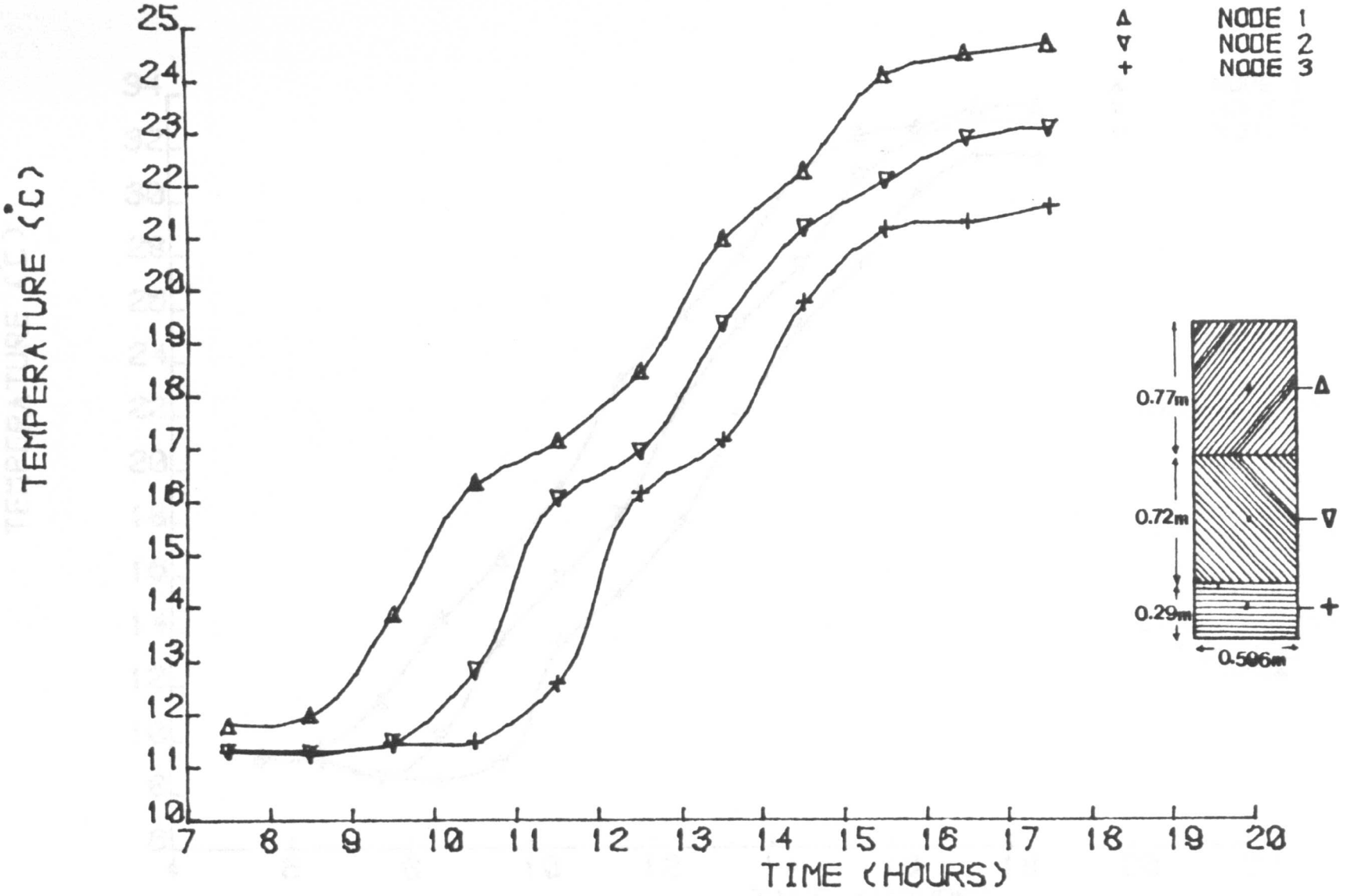

Figure 23

TEMPERATURE DISTRIBUTION IN TYPE I STORAGE TANK FOR 15TH MARCH
,NO DRAW OFF,FLOW RATE = 0.01 KG/SM**2

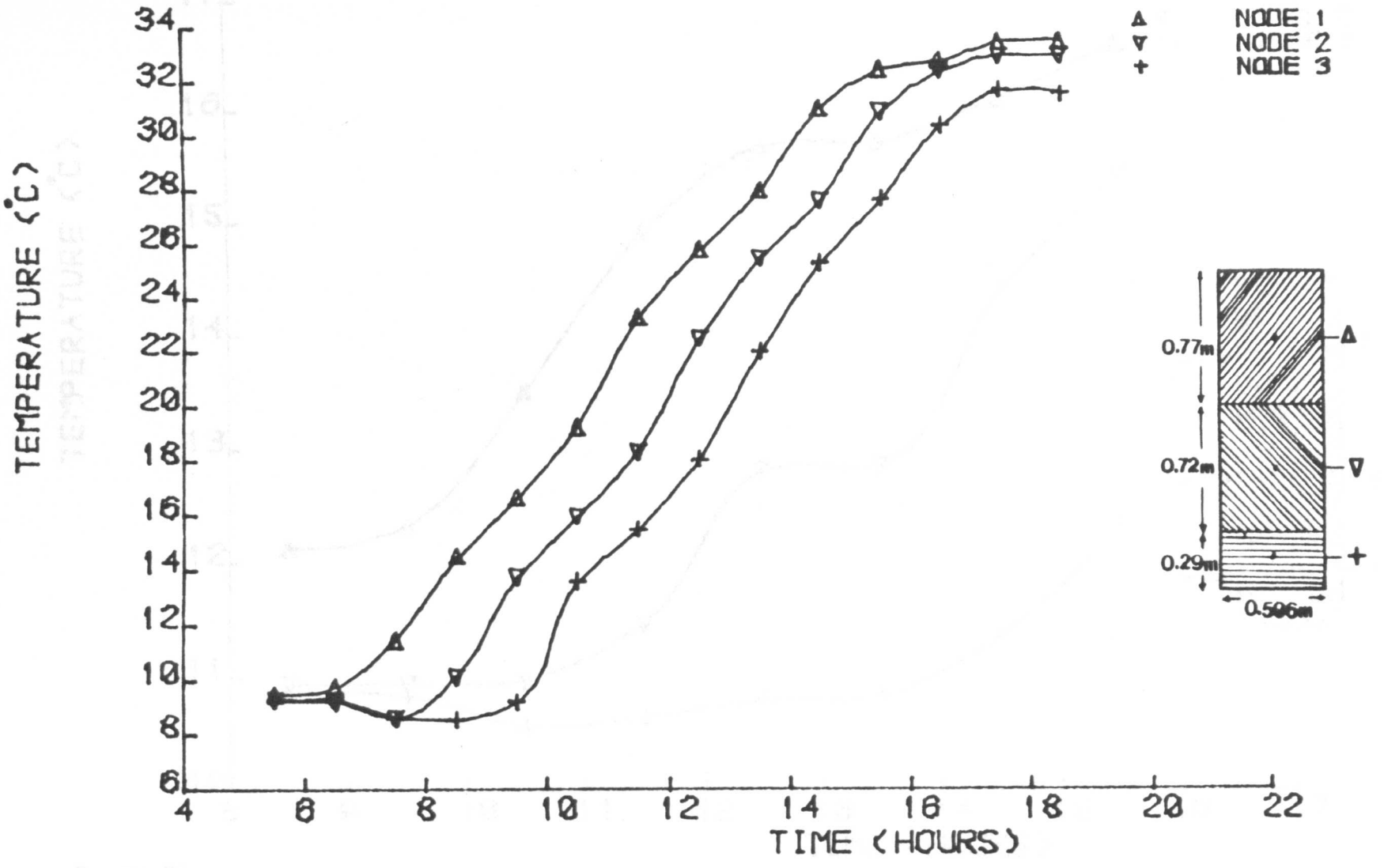

Figure 24

TEMPERATURE DISTRIBUTION IN TYPE I STORAGE TANK FOR 15TH JUNE ,NO DRAW OFF,FLOW RATE = 0.01 KG/SM**2

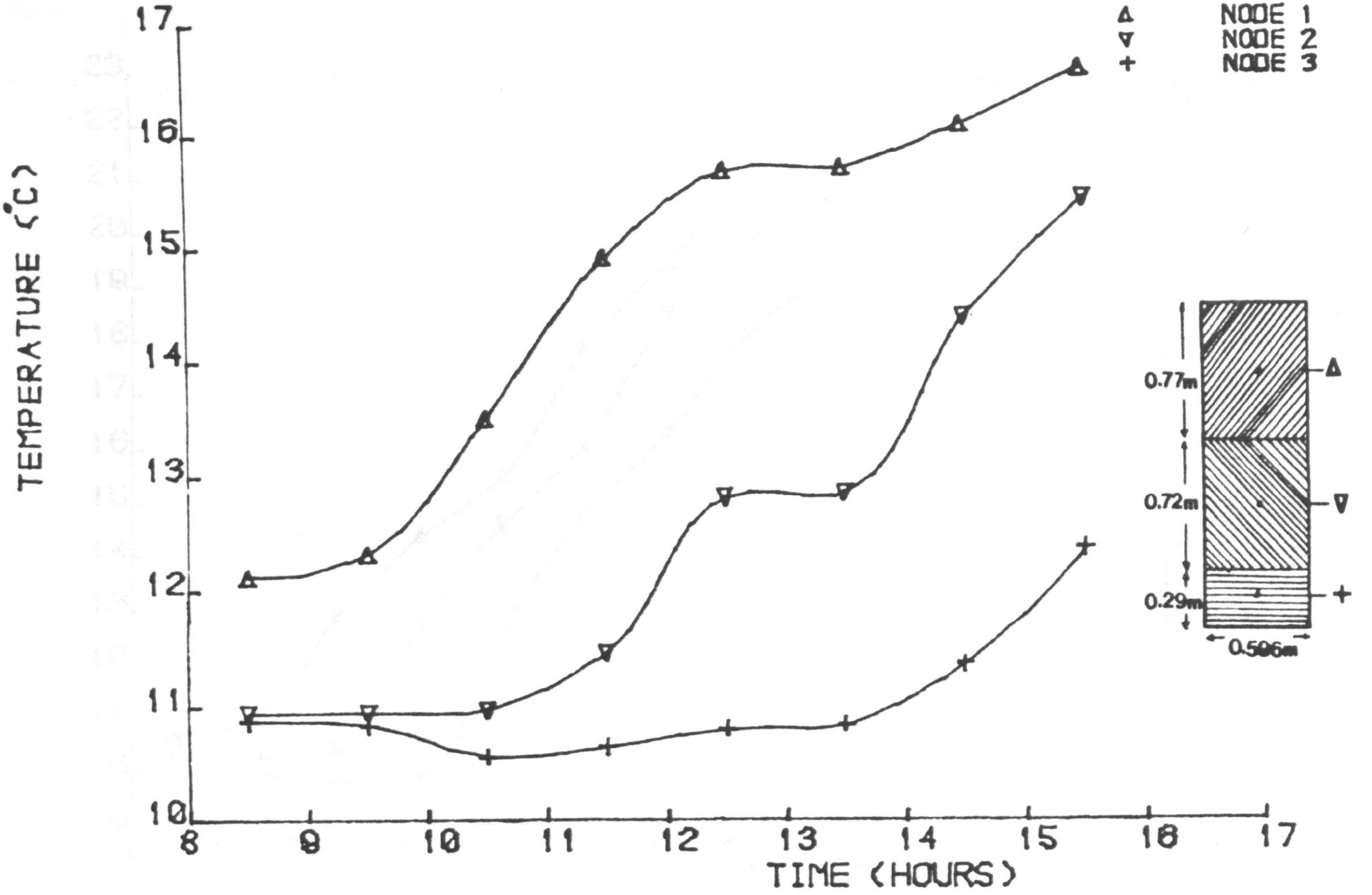

Figure 25

TEMPERATURE DISTRIBUTION IN TYPE I STORAGE TANK FOR 15TH DECEMBER ,NO DRAW OFF,FLOW RATE = 0.01 KG/SM**2

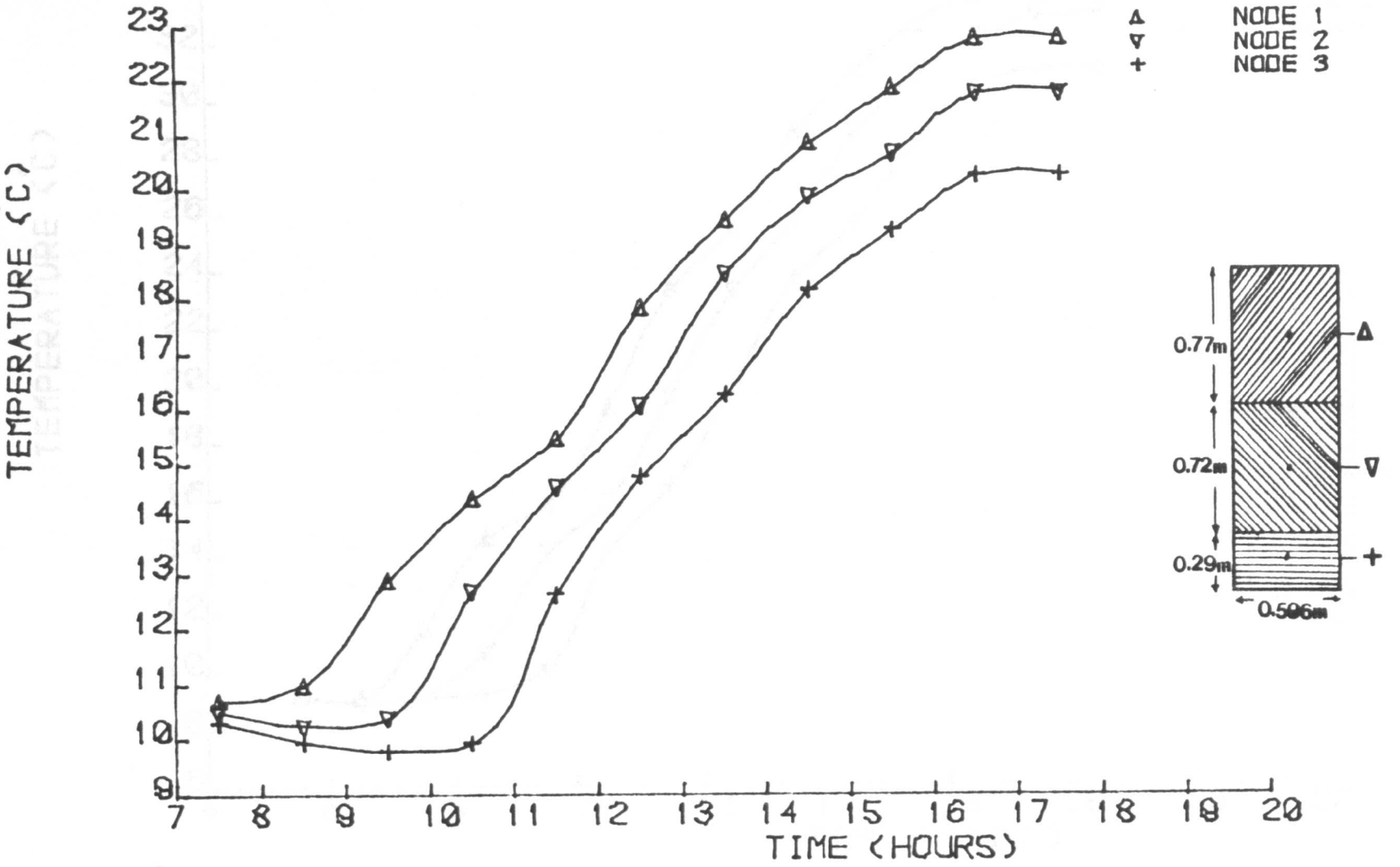

Figure 26

TEMPERATURE DISTRIBUTION IN TYPE I STORAGE TANK FOR 15TH MARCH
,NO DRAW OFF,FLOW RATE = 0.015 KG/SM**2

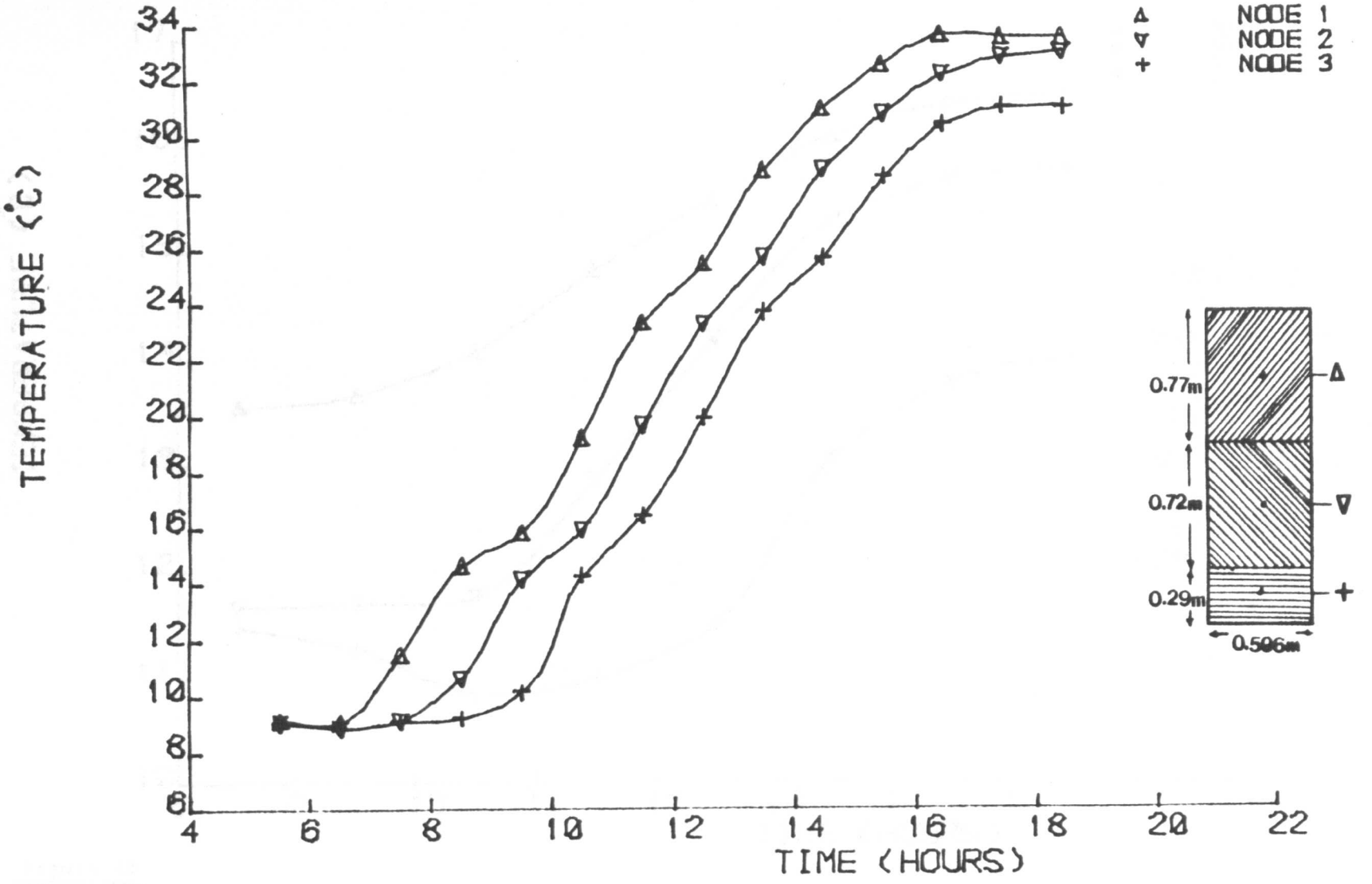

Figure 27

TEMPERATURE DISTRIBUTION IN TYPE I STORAGE TANK FOR 15TH JUNE ,NO DRAW OFF, FLOW RATE = 0.015 KG/SM**2

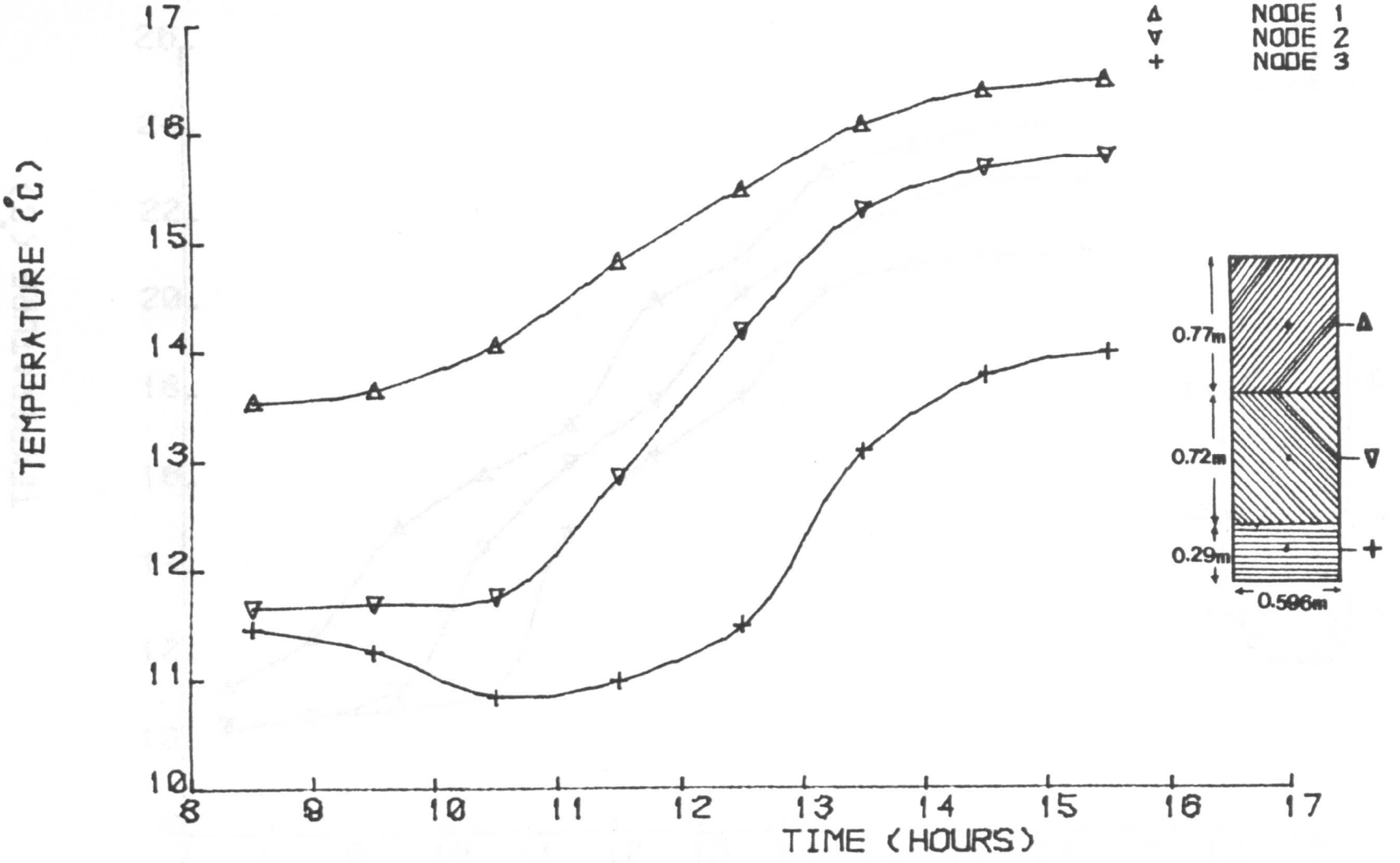

Figure 28

TEMPERATURE DISTRIBUTION IN TYPE I STORAGE TANK FOR 15TH DECEMBER ,NO DRAW OFF,FLOW RATE = 0.015 KG/SM**2

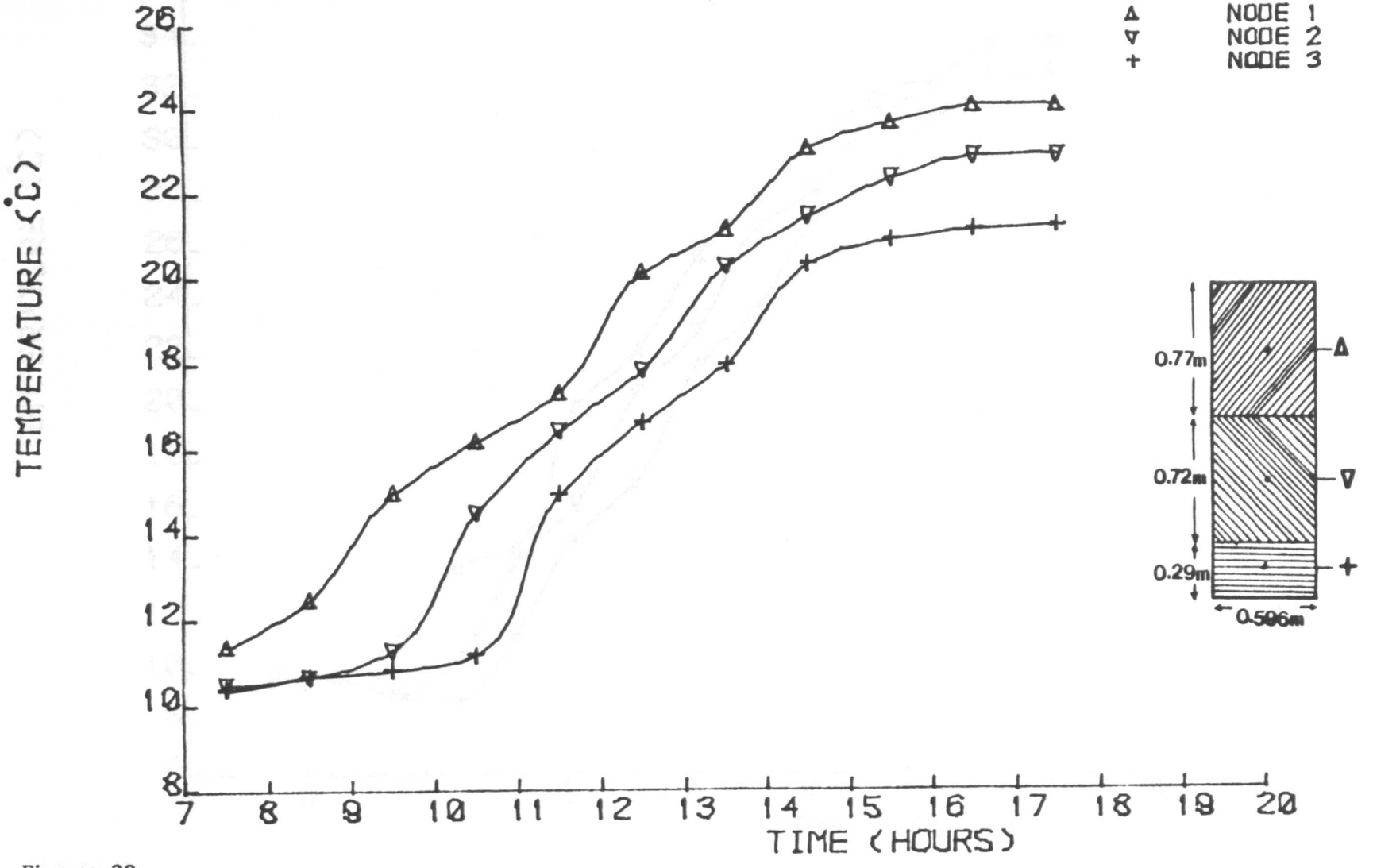

Figure 29

TEMPERATURE DISTRIBUTION IN TYPE I STORAGE TANK FOR 15TH MARCH
,NO DRAW OFF,FLOW RATE = 0.02 KG/SM**2

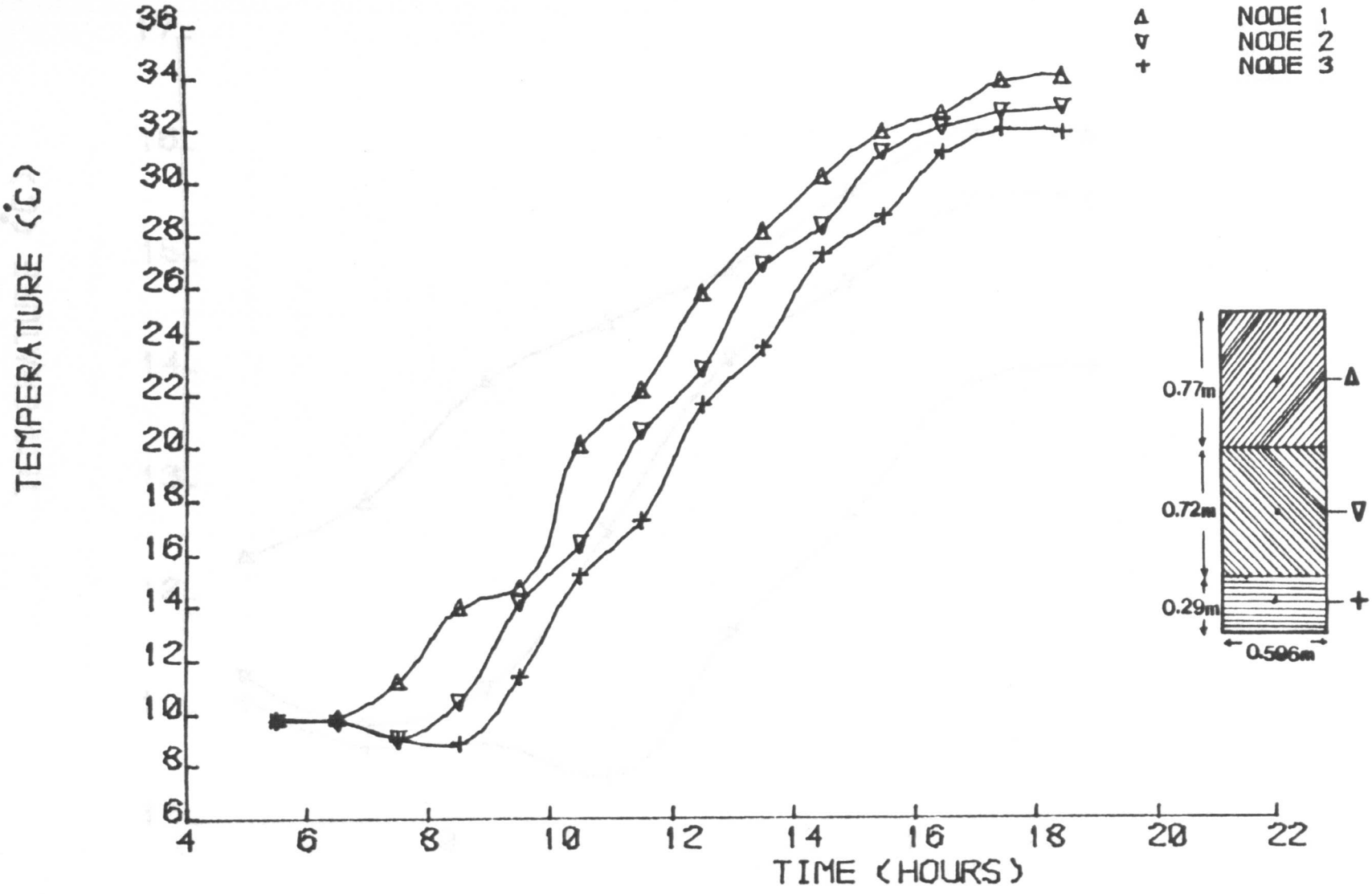

Figure 30

TEMPERATURE DISTRIBUTION IN TYPE I STORAGE TANK FOR 15TH JUNE ,NO DRAW OFF,FLOW RATE = 0.02 KG/SM**2

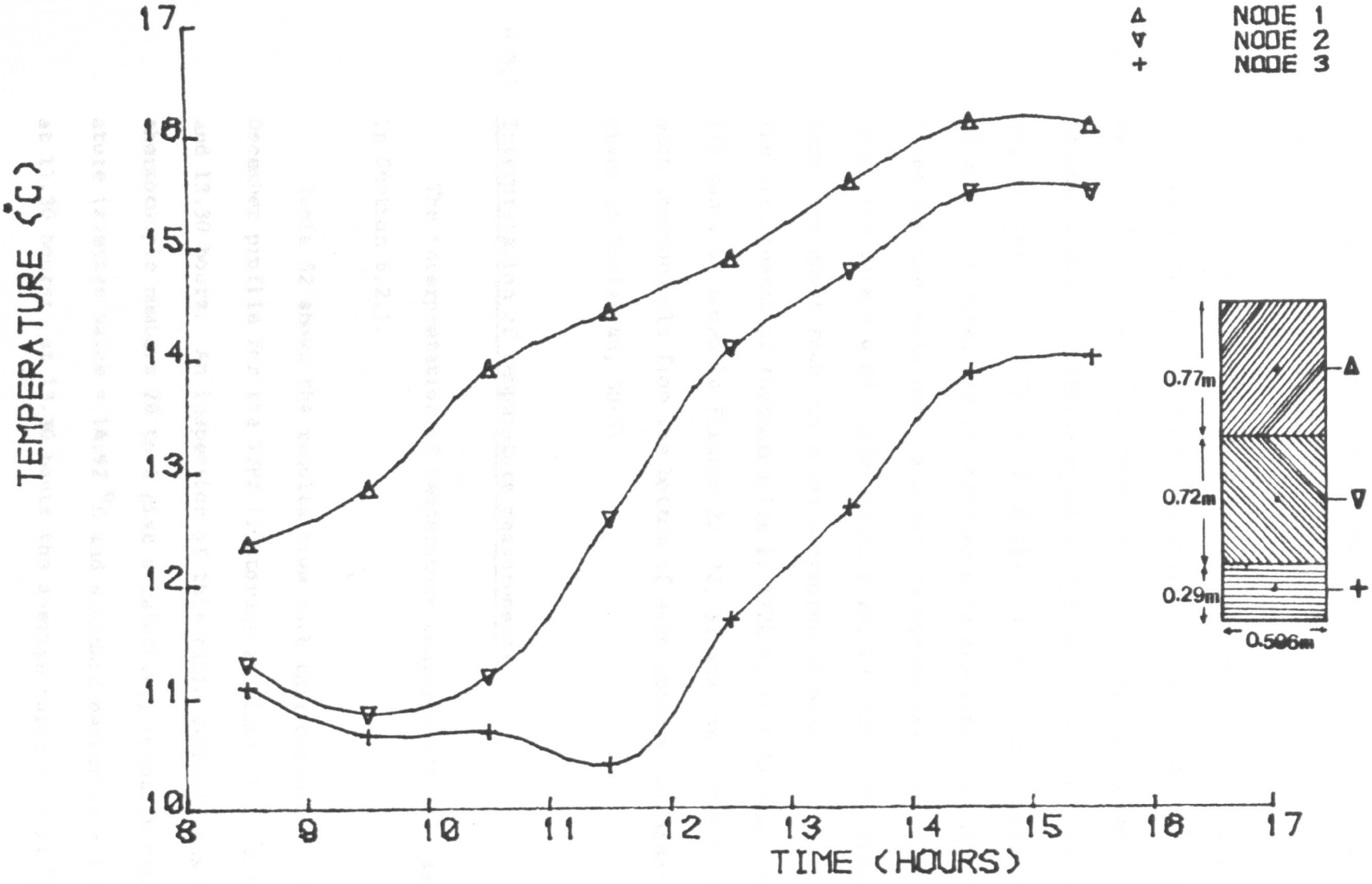

Figure 31

TEMPERATURE DISTRIBUTION IN TYPE I STORAGE TANK FOR 15TH DECEMBER
,NO DRAW OFF,FLOW RATE = 0.02 KG/SM**2

6.3 Length to diameter ratio (L/D) tests

The general testing arrangement was as previously described (Figure 21 and Plate 6).

Tests were conducted on three cylindrical water filled storage containers (500 kg capacity), having length-to-diameter ratios 3/1, 4/1 and 5/1 respectively. Storage containers having length to diameter ratios equal to 3/1 were designated as TYPE I, 4/1 as TYPE II, and 5/1 as TYPE III. Useful energy profiles for 15 March, 15 June, and 15 December were simulated for each of the three storage containers, and for the previously derived optimum mass flow rate = 0.01 kg/Sm^2 (Tables 26, 29, 32). The temperature throughout each store was monitored at hourly intervals. The arrangement of thermocouples in TYPE I, TYPE II and TYPE III tanks is shown in Figures 22, 32, 33 and the distance of each thermocouple from the bottom of each storage container is given in Tables 48, 50-51.

6.3.1 Interpretation of temperature measurements

The interpretation of temperature measurements were as in Section 6.2.1.

Table 52 shows the results from each thermocouple for the December profile for the TYPE II storage at times 11.30 hours and 13.30 hours. An inspection of this table demonstrates that thermocouple numbers 26 to 6 give a relatively constant temperature (average value = 14.92 ^{o}C and standard deviation = 1.73 ^{o}C at 11.30 hours; at 13.30 hours the average value = 16.71 ^{o}C and

standard deviation = 0.66 °C). The temperature then differed slightly more around thermocouple number 6 and a second segment was defined by thermocouples 6 to 2 (average value = 11.64 °C and standard deviation = 0.83 °C at 11.30 hours; at 13.30 hours the average value = 12.45 °C and standard deviation = 1.2 °C).

Table 53 shows the results from each thermocouple for the December profile for the TYPE III storage at times 11.30 hours and 13.30 hours. An inspection of this table demonstrates that thermocouple numbers 28 to 6 give a relatively constant temperature (average value = 18.43 °C and standard deviation = 0.9 °C at 11.30 hours; at 13.30 hours the average value = 19.29 °C and standard deviation = 0.45 °C). The temperature then differed slightly more around thermocouple number 6 and a second segment is defined by thermocouples 6 to 2 (average value = 16.86 °C and standard deviation = 0.06 °C at 11.30 hours; at 13.30 hours the average value = 17.29 °C and standard deviation = 0.38 °C at 13.30 hours).

The limit at which temperatures around groups of thermocouples have been adopted for averaging purposes in relation to the height of the storage container are illustrated in each of the figures which follow (figures 34-36 for Type II storage) and (figures 37-39 for Type III storage).

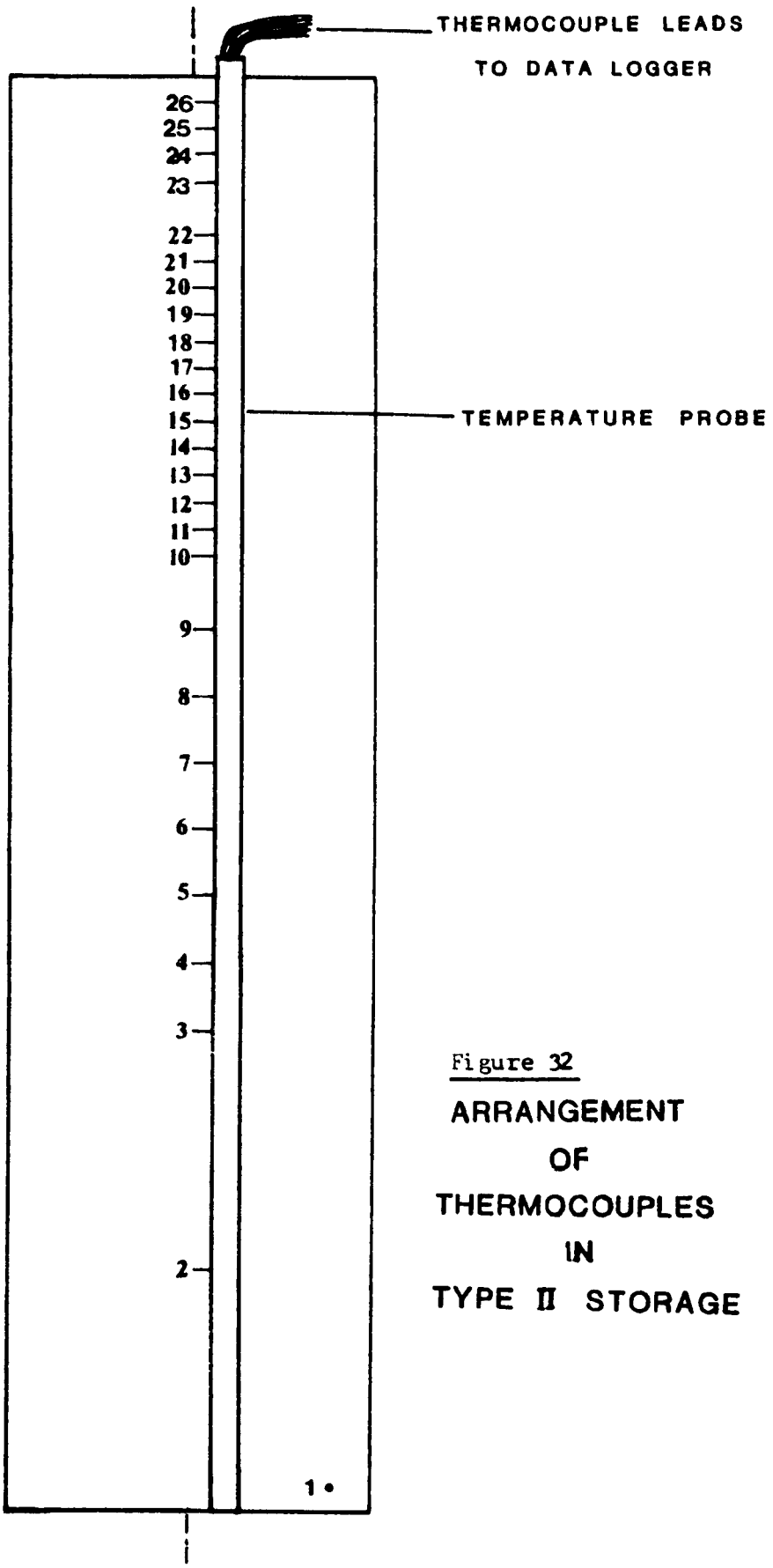

Figure 32

ARRANGEMENT OF THERMOCOUPLES IN TYPE II STORAGE

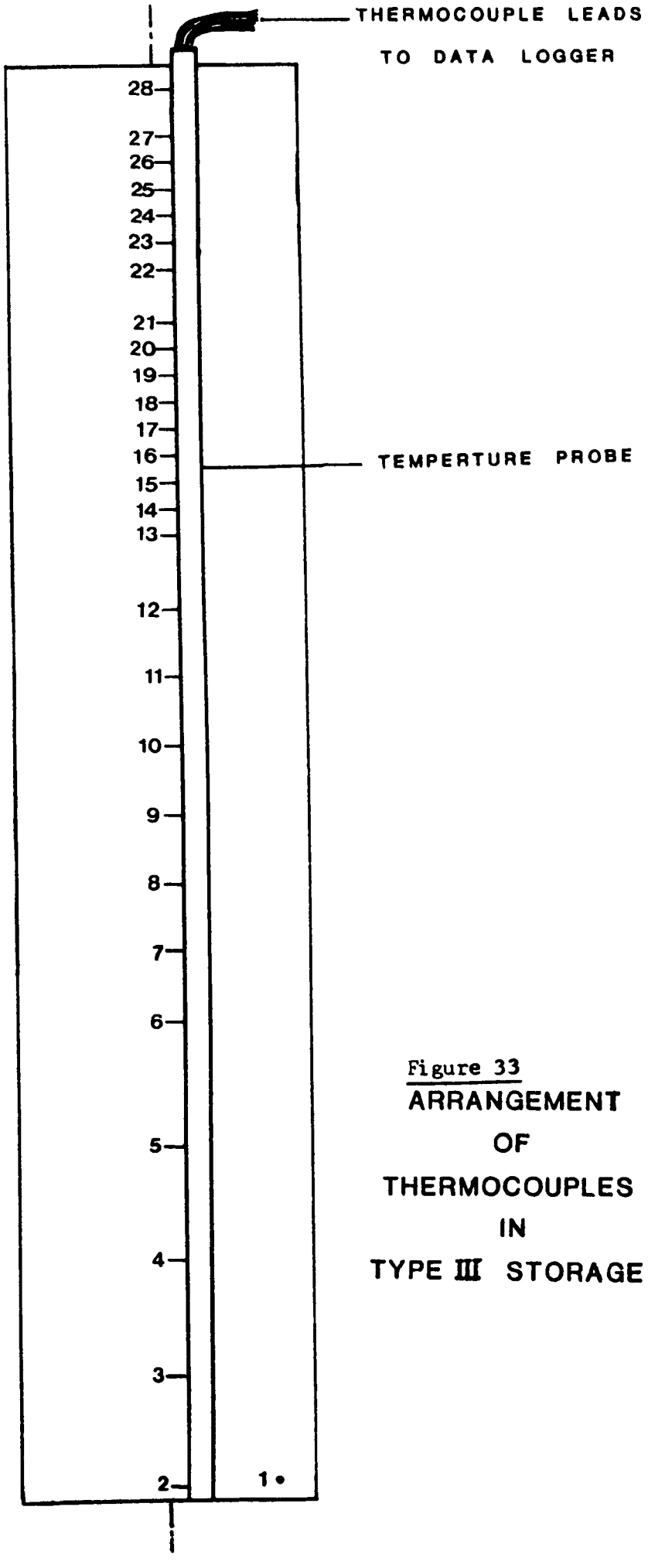

Figure 33
ARRANGEMENT
OF
THERMOCOUPLES
IN
TYPE III STORAGE

TABLE 50. Thermocouples location in the TYPE II storage container

Thermocouples Number	Distance from the bottom of the storage container (M)
26	2.127
25	2.087
24	2.047
23	2.007
22	1.927
21	1.886
20	1.846
19	1.806
18	1.766
17	1.726
16	1.686
15	1.646
14	1.605
13	1.565
12	1.525
11	1.485
10	1.445
9	1.342
8	1.238
7	1.135
6	1.032
5	0.929
4	0.825
3	0.722
2	0.361
1	0.040

TABLE 51. Thermocouples location in the TYPE III storage container

Thermocouple Number	Distance from the bottom of the storage container (M)
28	2.468
27	2.375
26	2.328
25	2.282
24	2.235
23	2.188
22	2.142
21	2.049
20	2.002
19	1.956
18	1.909
17	1.862
16	1.816
15	1.769
14	1.723
13	1.676
12	1.556
11	1.437
10	1.317
9	1.197
8	1.077
7	0.958
6	0.838
5	0.629
4	0.419
3	0.226
2	0.032
1	0.040

TABLE 52 Results from each thermocouple for TYPE II storage container

Thermo-couples Number	Thermocouples reading at 11.30 hrs				Thermocouples reading at 13.30 hrs			
	Read-ing (^{o}C)	Aver-age Value	Stan-dard devi-ation	Seg-ment num-ber	Read-ing (^{o}C)	Aver-age Value	Stan-dard devi-ation	Seg-ment num-ber
26	16.63	14.92	1.73	1	16.98	16.71	0.66	1
25	16.66				17.00			
24	16.66				17.13			
23	16.51				16.98			
22	16.59				17.08			
21	16.54				17.10			
20	16.46				16.98			
19	16.39				16.96			
18	16.29				16.98			
17	16.19				17.05			
16	15.77				16.96			
15	15.27				16.91			
14	14.90				16.96			
13	14.31				16.86			
12	13.86				16.83			
11	13.46				16.88			
10	13.01				16.73			
9	12.54				16.46			
8	12.44				16.16			
7	12.31				15.45			
6	12.14				14.38			
5	12.06	11.64	0.83	2	12.09	12.45	1.2	2
4	10.16				11.01			
3	11.96				12.58			
2	11.86				12.16			

TABLE 53 Results from each thermocouple for TYPE III storage container

Thermocouples Number	Thermocouples reading at 11.30 hrs				Thermocouples reading at 13.30 hrs			
	Reading (^{o}C)	Average Value	Standard deviation	Segment number	Reading (^{o}C)	Average Value	Standard deviation	Segment number
28	19.37	18.43	0.90	1	19.75	19.29	0.45	1
27	19.25				19.69			
26	19.27				19.69			
25	19.27				19.69			
24	19.27				19.74			
23	19.27				19.71			
22	19.27				19.74			
21	19.27				19.71			
20	19.12				19.76			
19	18.95				19.69			
18	18.85				19.66			
17	18.71				19.64			
16	18.66				19.74			
15	18.46				19.69			
14	18.26				19.61			
13	18.21				19.71			
12	17.75				19.64			
11	17.52				19.64			
10	17.28				19.64			
9	17.13				19.64			
8	16.98				19.61			
7	17.01				19.61			
6	16.86				19.54			
5	16.83	16.86	0.06	2	19.42	17.29	0.38	2
4	16.88				19.05			
3	16.93				18.61			
2	16.79				17.87			

6.3.2 Results

The temperature histories of each of the storage containers TYPE I, TYPE II and TYPE III are shown in Figures 23-25, 34-36 and 37-39 for each of the three series of tests.

Figure 40 shows the results plotted as a histogram for the three storage containers. It can be seen that heat collected for TYPE I storage container is slightly greater than TYPE II and TYPE III for each of the three series of tests.

Tables 54-56 show the starting temperature and the final temperature for each node of the three storage containers as well as heat collected in each one for each of the three series of tests. Heat collected was based on the standard formula

$$Q = m \times C_p \times \Delta T \quad KJ$$

where,

m = mass of water kg

C_p = specific heat of water $KJ/kg^{o}C$

ΔT = temperature difference ^{o}C.

Temperature correcting variables were also taken into account, i.e. m and C_p vary with temperature.

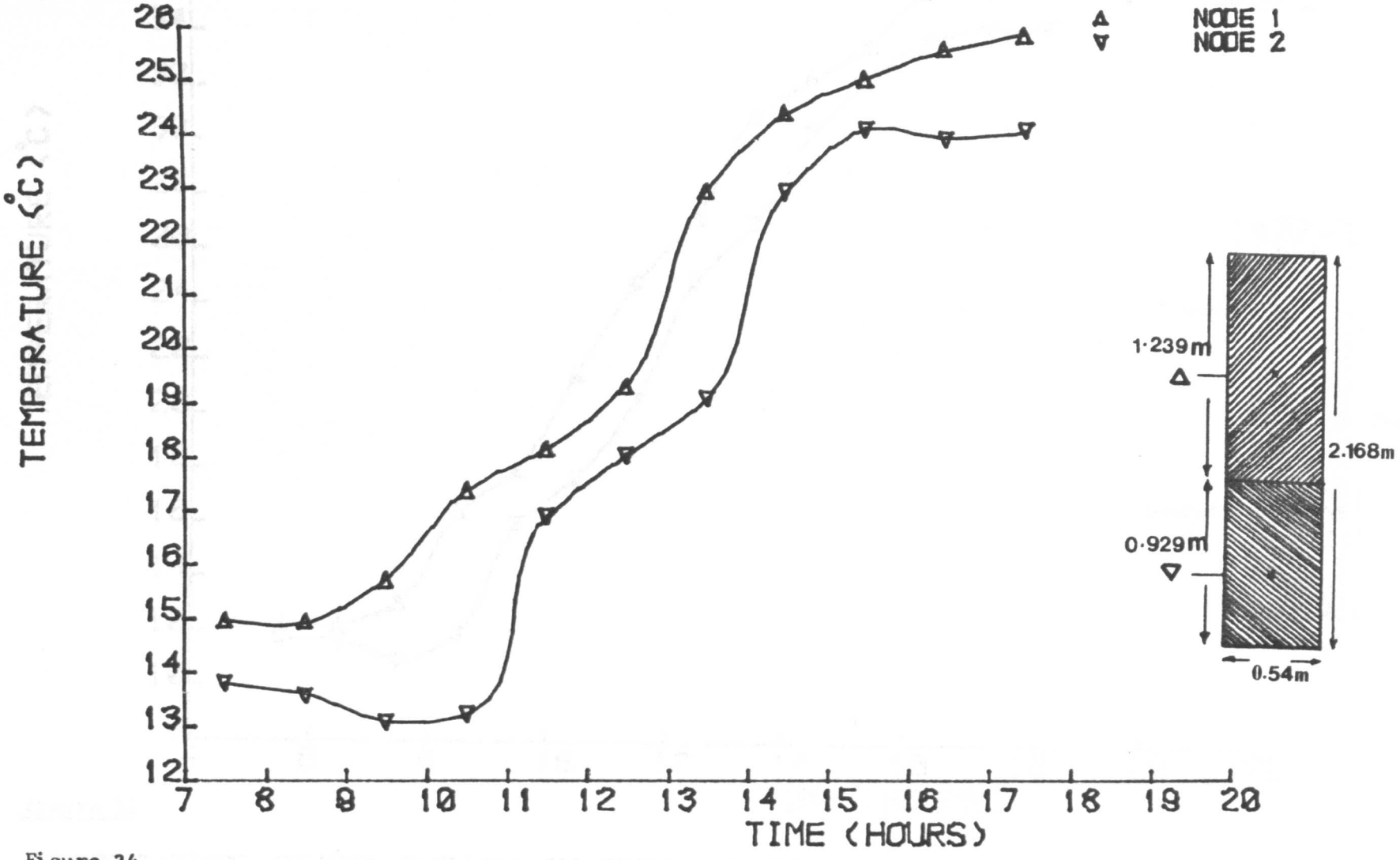

Figure 34

TEMPERATURE DISTRIBUTION IN TYPE II STORAGE TANK FOR 15TH MARCH ,NO DRAW OFF,FLOW RATE = 0.01 KG/SM**2

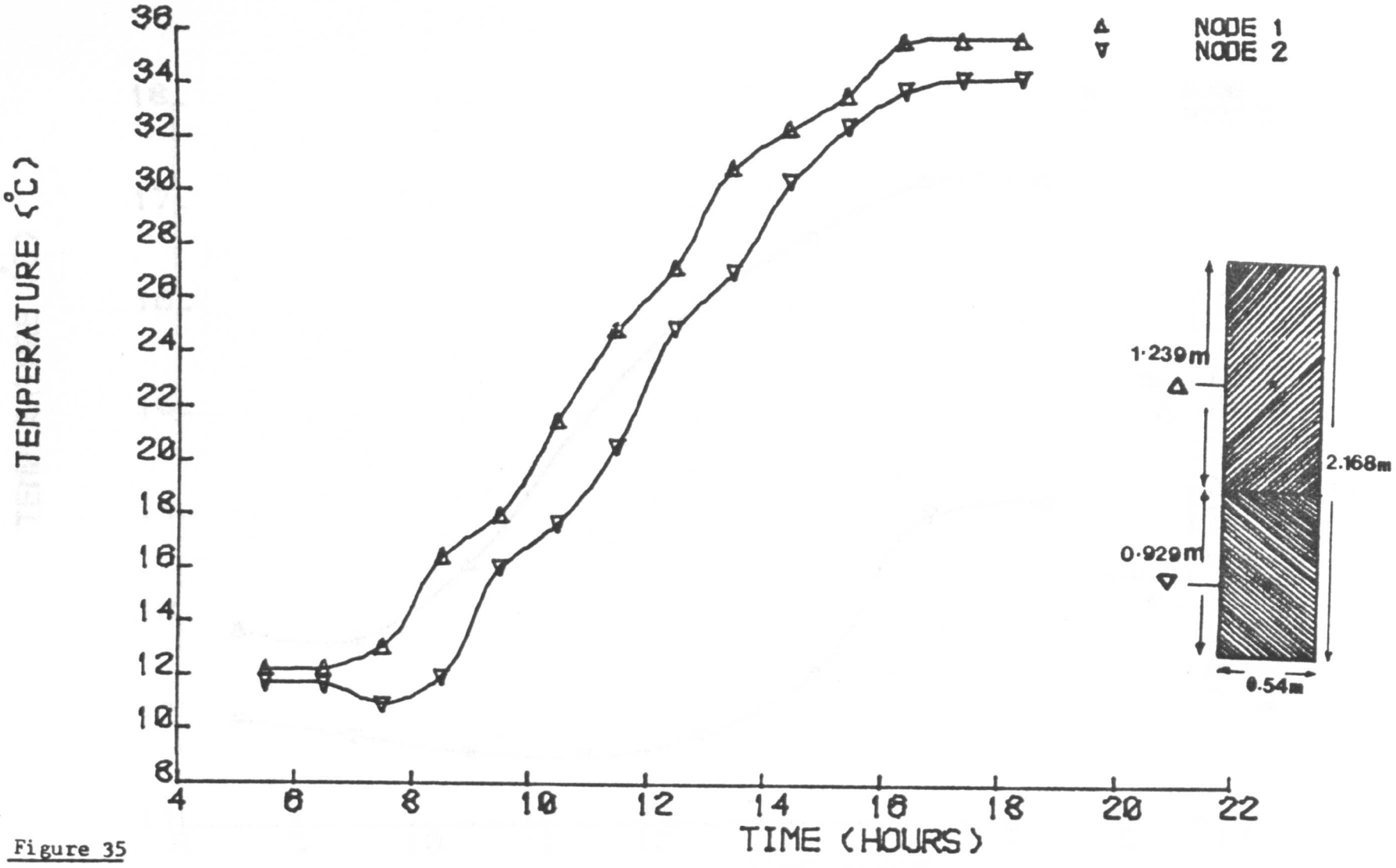

Figure 35

TEMPERATURE DISTRIBUTION IN TYPE II STORAGE TANK FOR 15TH JUNE
,NO DRAW OFF,FLOW RATE = 0.01 KG/SM**2

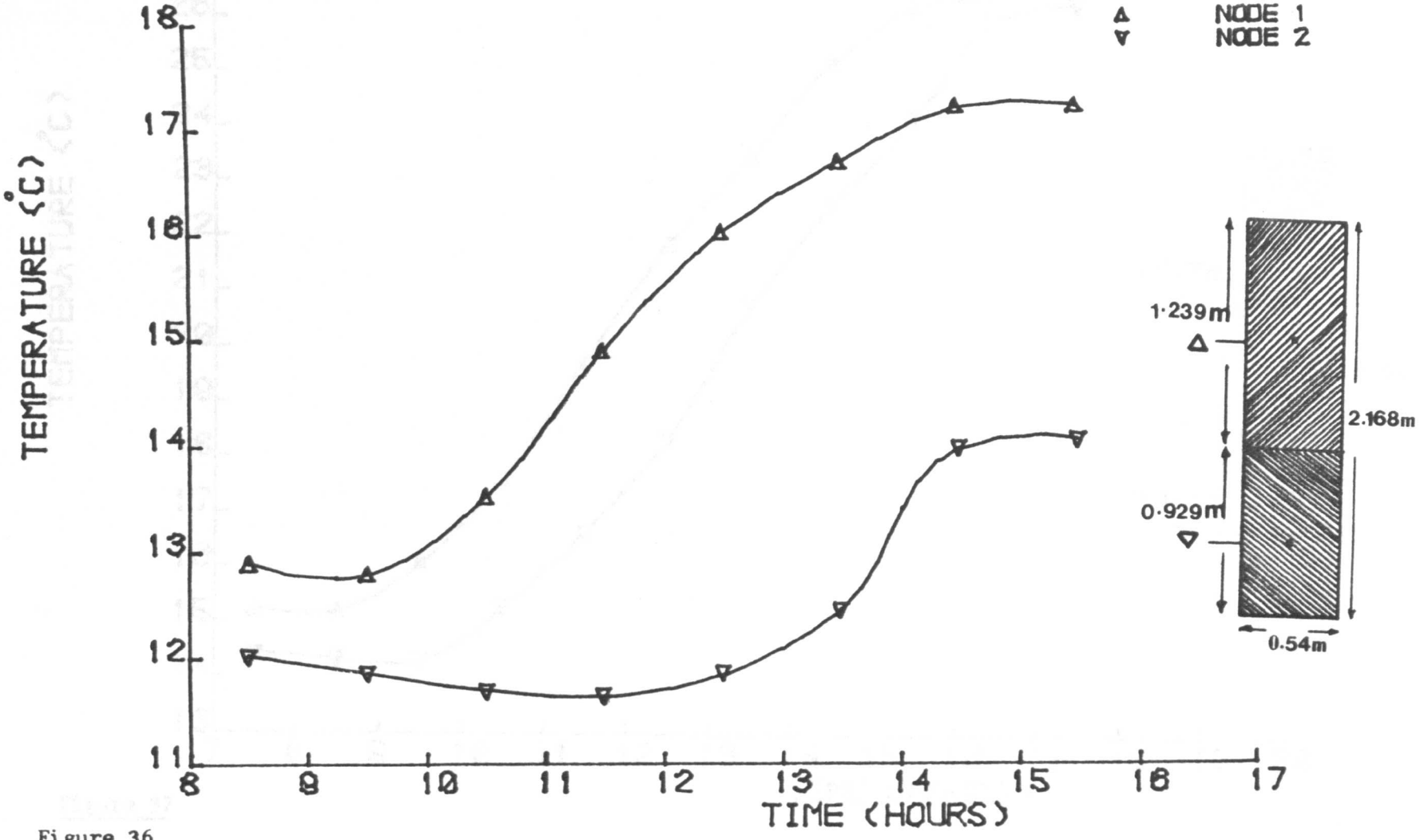

Figure 36

TEMPERATURE DISTRIBUTION IN TYPE II STORAGE TANK FOR 15TH DECEMBER ,NO DRAW OFF,FLOW RATE = 0.01 KG/SM**2

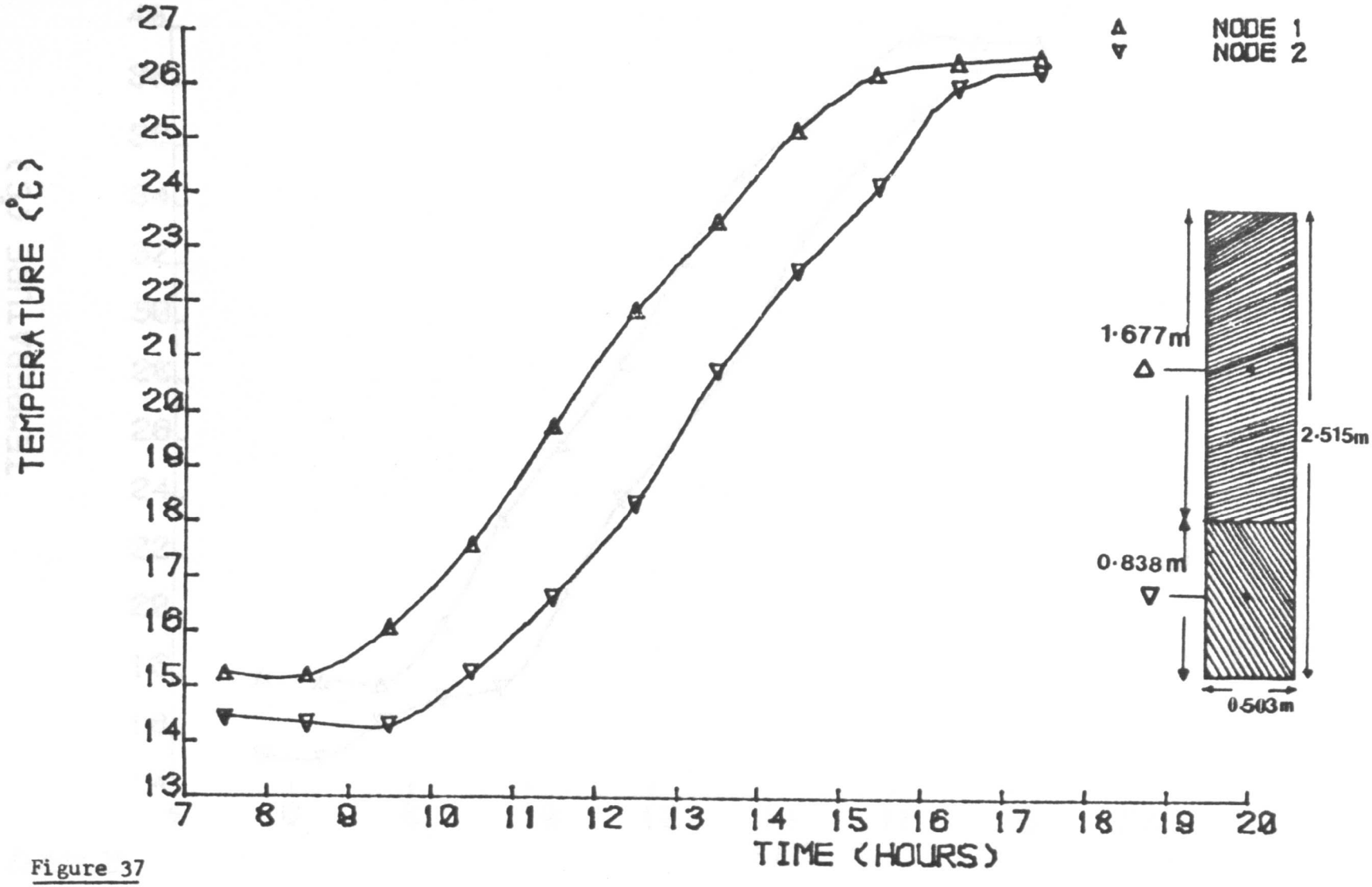

Figure 37

TEMPERATURE DISTRIBUTION IN TYPE III STORAGE TANK FOR 15TH MARCH ,NO DRAW OFF,FLOW RATE = 0.01 KG/SM**2

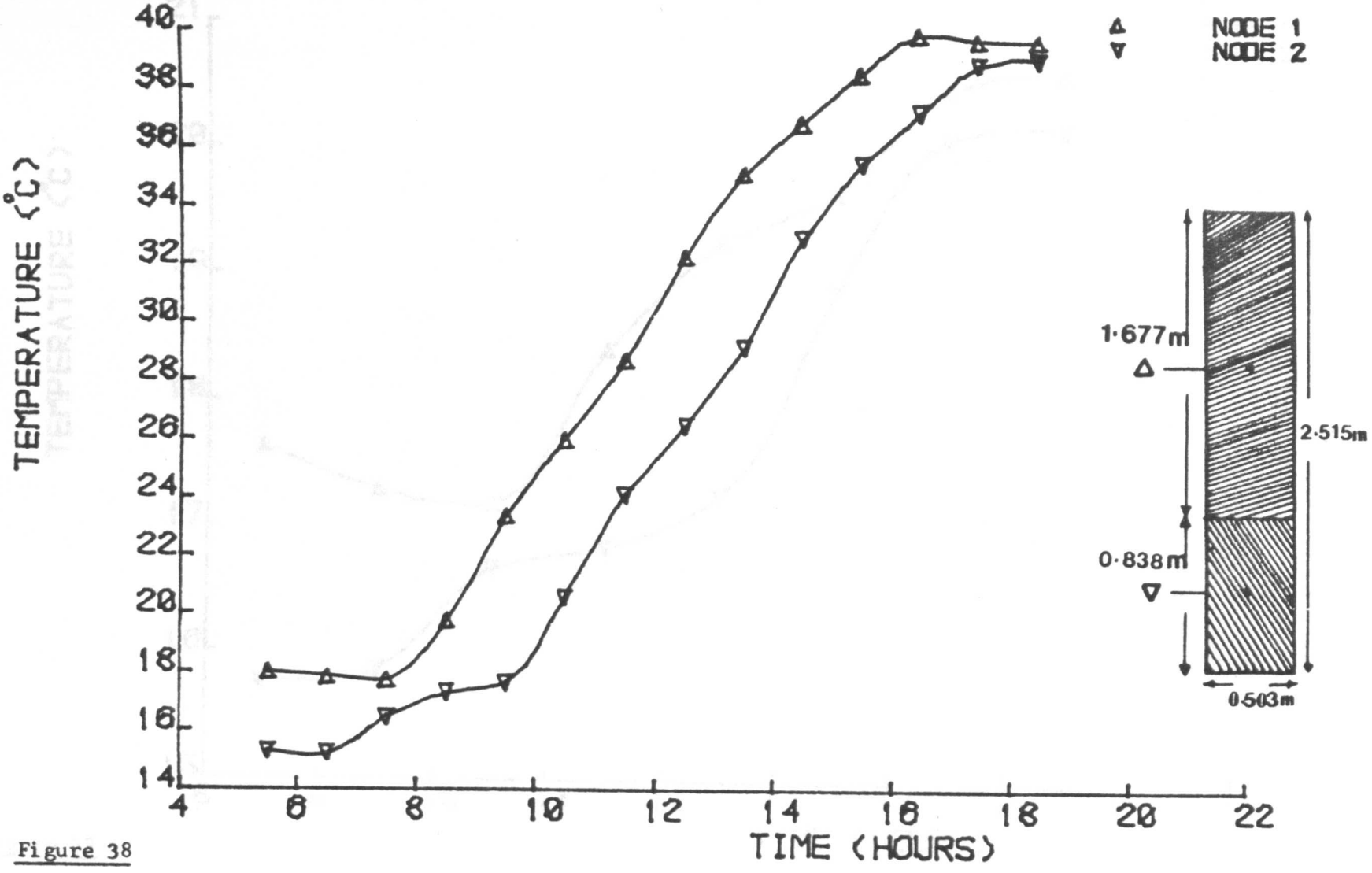

Figure 38

TEMPERATURE DISTRIBUTION IN TYPE III STORAGE TANK FOR 15TH JUNE
,NO DRAW OFF,FLOW RATE = 0.01 KG/SM**2

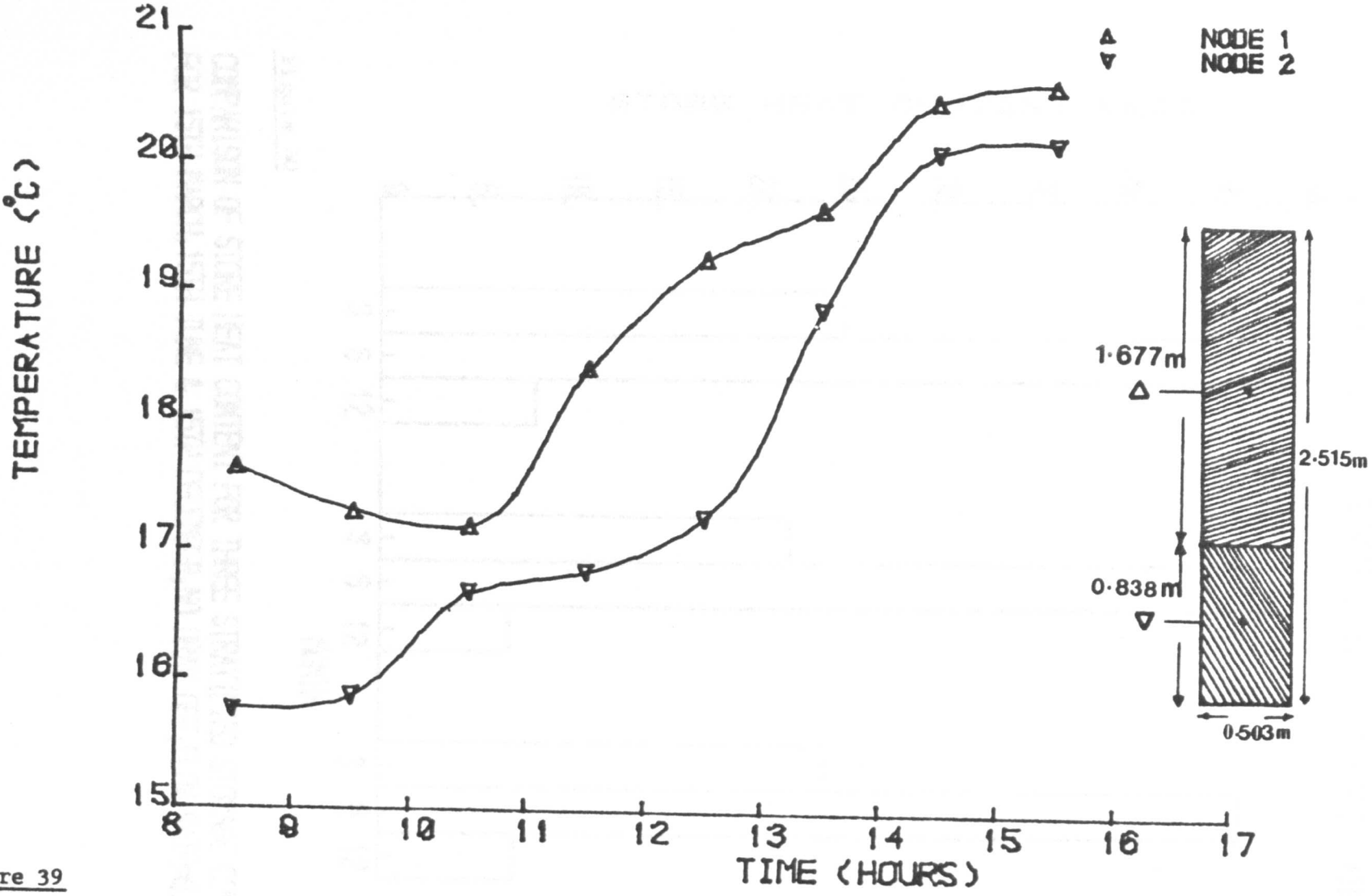

Figure 39

TEMPERATURE DISTRIBUTION IN TYPE III STORAGE TANK FOR 15TH DECEMBER ,NO DRAW OFF,FLOW RATE = 0.01 KG/SM**2

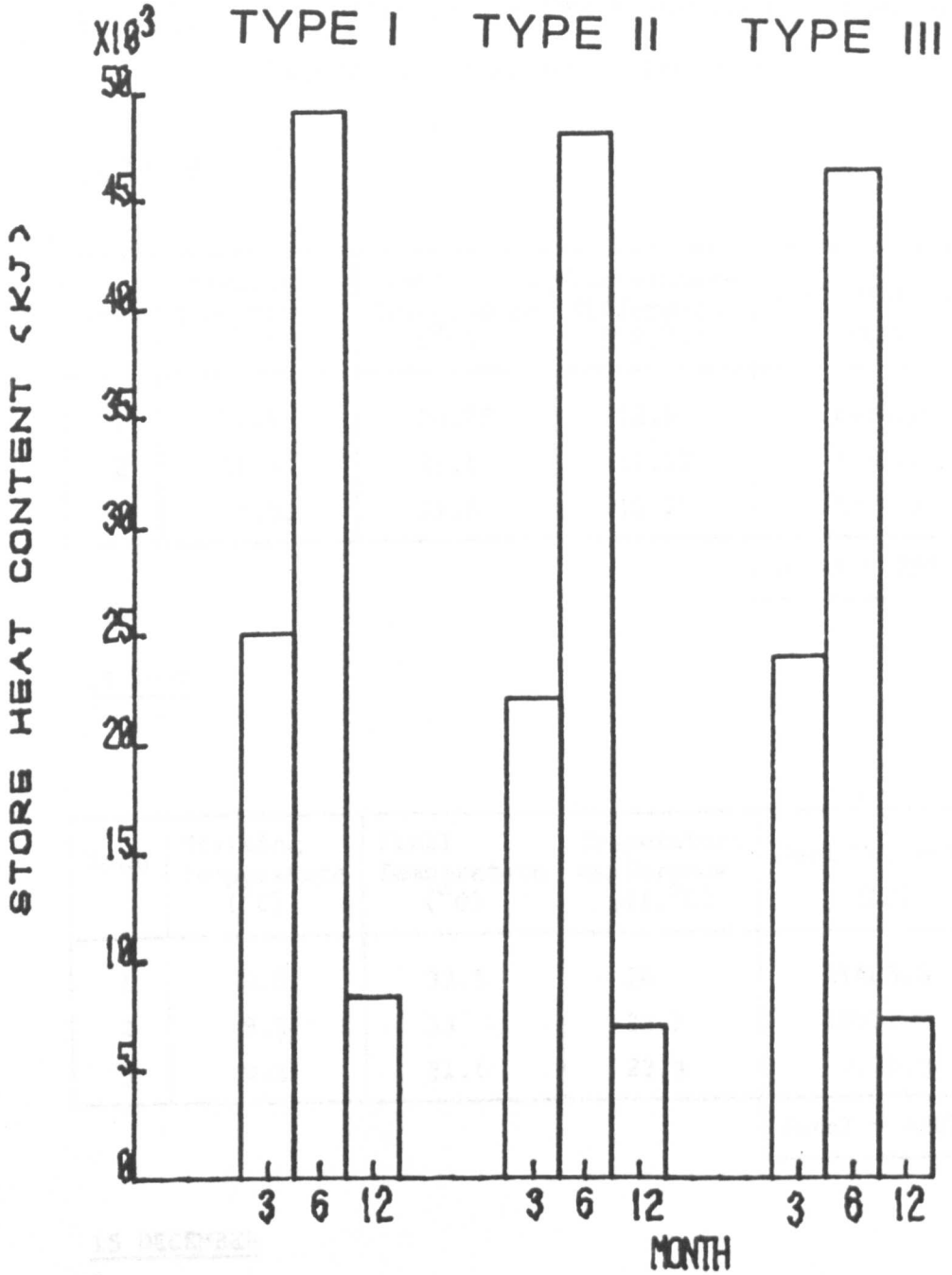

Figure 40

COMPARISON OF STORE HEAT CONTENT FOR THREE STRATIFIED STORAGE CONTAINERS FOR 15TH MARCH, 15TH JUNE & 15TH DECEMBER, NO DRAW OFF, FLOW RATE=0.01 KG/SM**2

TABLE 54. Heat collected for TYPE I storage container for 15 March, 15 June, and 15 December

15 MARCH

Node	Starting Temperature (^{o}C)	Final Temperature (^{o}C)	Temperature difference (ΔT,^{o}C)	Heat Collected (KJ)
1	11.8	24.75	12.95	11606.2
2	11.33	23.1	11.77	9957.1
3	11.32	21.6	10.28	3574.1
				Total = 25137.4

15 JUNE

Node	Starting Temperature (^{o}C)	Final Temperature (^{o}C)	Temperature difference (ΔT,^{o}C)	Heat Collected (KJ)
1	9.5	33.5	24	21405.8
2	9.3	33	23.7	19952.9
3	9.3	31.6	22.3	7719.8
				Total = 49078.5

15 DECEMBER

Node	Starting Temperature (^{o}C)	Final Temperature (^{o}C)	Temperature difference (ΔT,^{o}C)	Heat Collected (KJ)
1	12.13	16.62	4.49	4035.6
2	10.95	15.46	4.51	3826.3
3	10.87	12.4	1.53	533.3
				Total = 8395.2

TABLE 55. Heat collected for TYPE II storage container for 15 March, 15 June and 15 December

15 MARCH

Node	Starting Temperature (°C)	Final Temperature (°C)	Temperature difference (ΔT, °C)	Heat Collected (KJ)
1	14.98	25.84	10.85	12998.5
2	13.81	24.07	10.26	9197.3
				Total = 22195.8

15 JUNE

Node	Starting Temperature (°C)	Final Temperature (°C)	Temperature difference (ΔT, °C)	Heat Collected (KJ)
1	12.23	35.71	23.48	27988.0
2	11.72	34.30	22.58	20149.0
				Total = 48137

15 DECEMBER

Node	Starting Temperature (°C)	Final Temperature (°C)	Temperature difference (ΔT, °C)	Heat Collected (KJ)
1	12.9	17.23	4.33	5201.2
2	12.02	14.06	2.04	1833.5
				Total = 7034.7

TABLE 56. Heat collected for TYPE III storage container for 15 March, 15 June, and 15 December

15 MARCH

Node	Starting Temperature (^{o}C)	Final Temperature (^{o}C)	Temperature difference (ΔT,^{o}C)	Heat Collected (KJ)
1	15.24	26.57	11.33	15800.8
2	14.43	26.3	11.87	8301.8
				Total = 24102.6

15 JUNE

Node	Starting Temperature (^{o}C)	Final Temperature (^{o}C)	Temperature difference (ΔT,^{o}C)	Heat Collected (KJ)
1	18.02	39.6	21.58	29972.0
2	15.3	39.0	23.7	16495.7
				Total = 46467.7

15 DECEMBER

Node	Starting Temperature (^{o}C)	Final Temperature (^{o}C)	Temperature difference (ΔT,^{o}C)	Heat Collected (KJ)
1	17.63	20.64	3.01	4209.8
2	15.77	20.2	4.43	3107.2
				Total = 7317

6.3.3 Discussion

The general conclusions to be drawn from these tests are:

1. TYPE I storage container behaves as a three-segment tank (see Section 6.2.2).

2. TYPE II storage container behaves as a two-segment tank with a thermocline occupying approximately half of the height of the storage container.

3. TYPE III storage container behaves as a two-segment tank with a thermocline occupying two thirds of the height of the storage container.

4. TYPE I storage container with a L/D equal to 3/1, gave the best result in terms of heat collected, and also had the maximum stratification which was the main goal of this part of the study.

6.4 Long term system performance tests

Having concluded that the TYPE I storage container with a L/D equal to 3/1 gave the best result in terms of heat collected, and also had the maximum stratification which was the main goal of this study, the next stage was to determine the long term system performance (see Chapter 4).

The general testing arrangement was as previously described (Figure 21 and Plate 6).

Useful energy profiles for 15 January, 15 February, 15 March, 15 April, 15 May, 15 June, 15 July, 15 August, 15 September, 15 October, 15 November and 15 December for mass flow rate = 0.01 kg/Sm^2 (Tables 35, 36, 26, 37, 38, 29, 39-43, 32) and temperatures throughout the store were monitored at hourly intervals.

6.4.1 Results

The temperature histories of TYPE I storage container for each of the twelve series of tests are shown in Figures 23-25 and 41-49. Tables 54, 57-59 show the starting temperature and the final temperature for the twelve series of tests as well as heat collected.

Table 60 shows a summary of the monthly averaged daily performance.

Table 61 shows monthly long term average performance of the system.

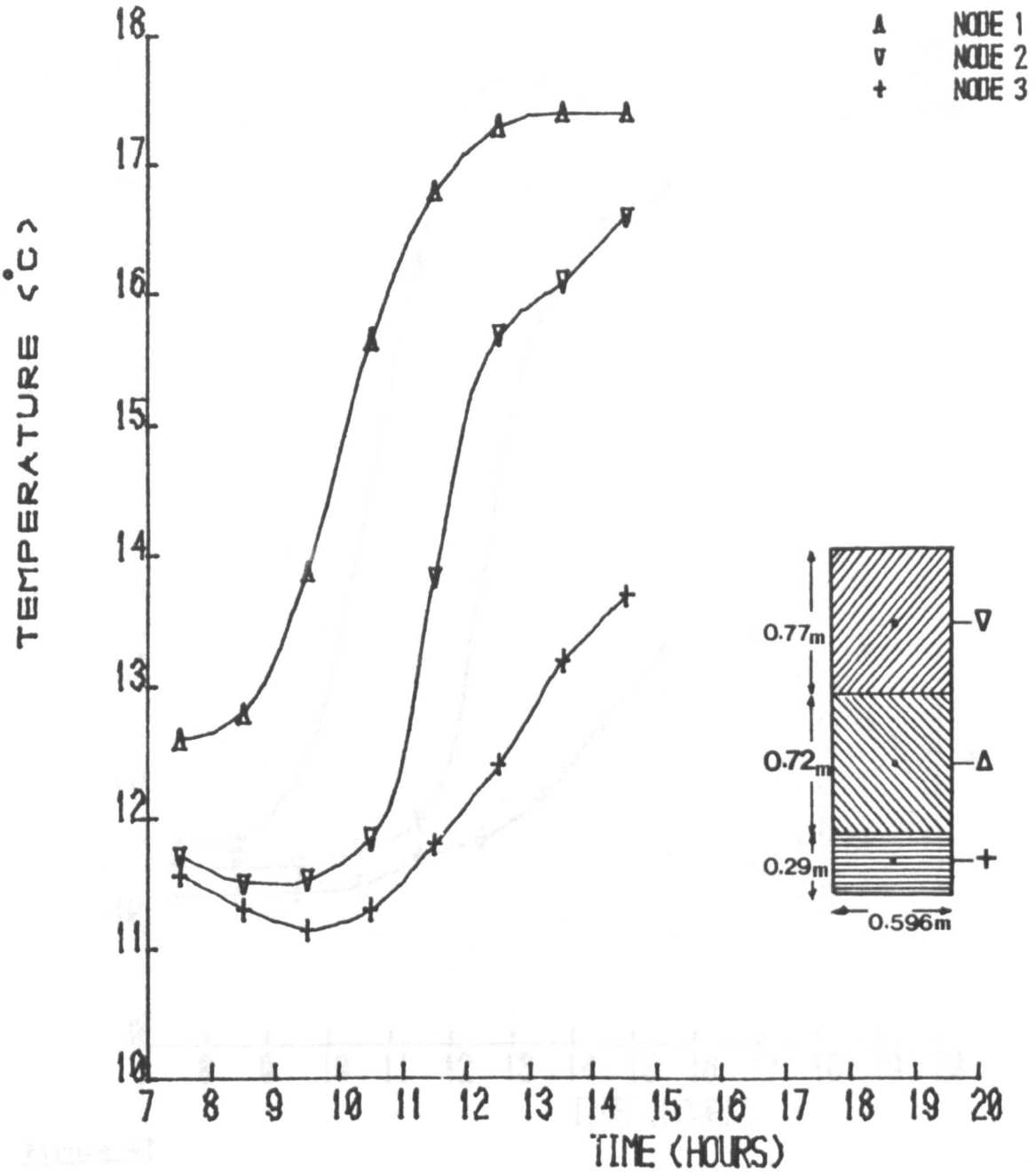

Figure 41

TEMPERATURE DISTRIBUTION IN TYPE I STORAGE TANK FOR 15TH JANUARY ,NO DRAW OFF,FLOW RATE = 0.01 KG/SM**2

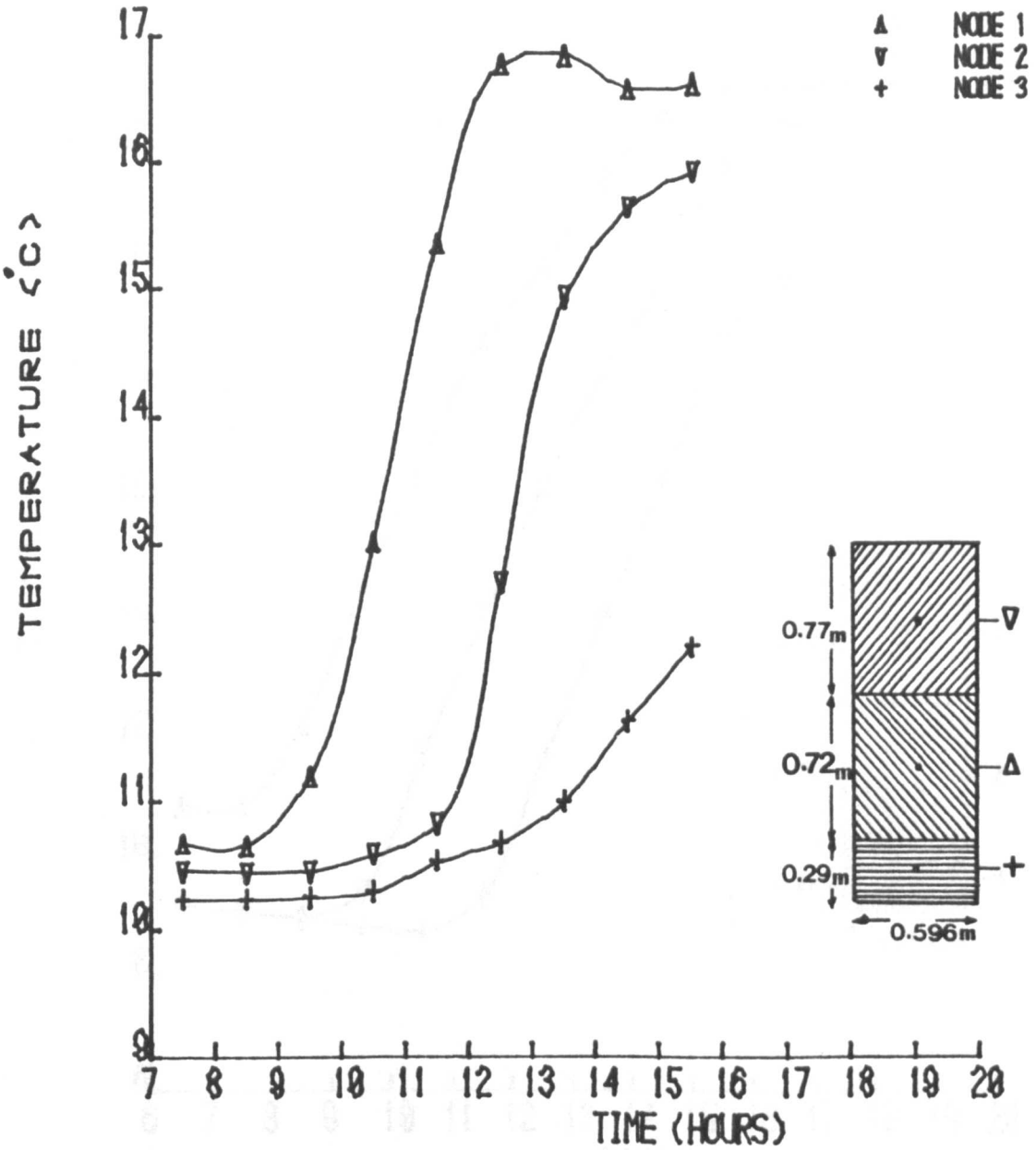

Figure 42

TEMPERATURE DISTRIBUTION IN TYPE I STORAGE TANK FOR 15TH FEBRUARY ,NO DRAW OFF,FLOW RATE = 0.01 KG/SM**2

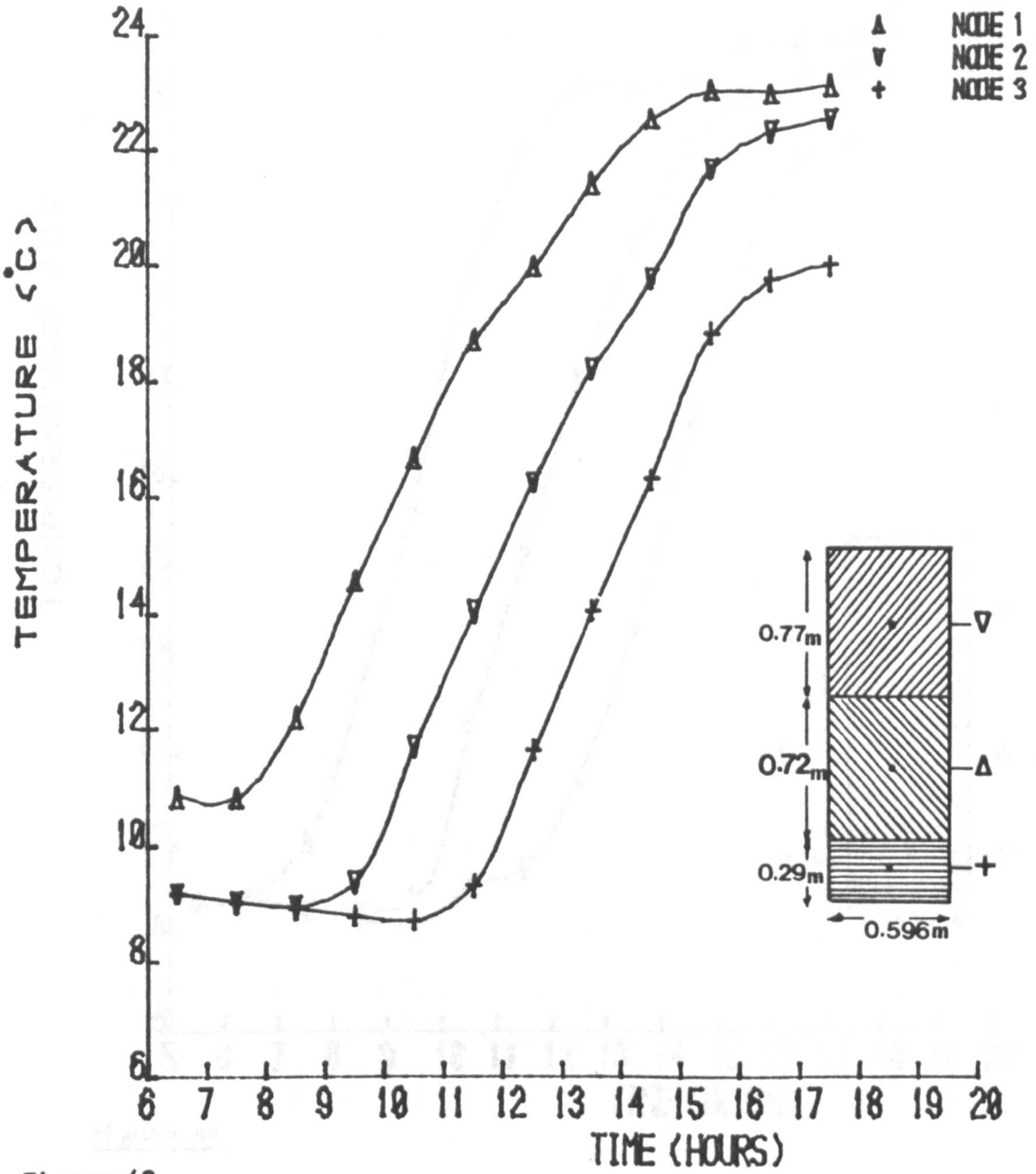

Figure 43

TEMPERATURE DISTRIBUTION IN TYPE I STORAGE TANK FOR 15TH APRIL ,NO DRAW OFF, FLOW RATE = 0.01 KG/SM**2

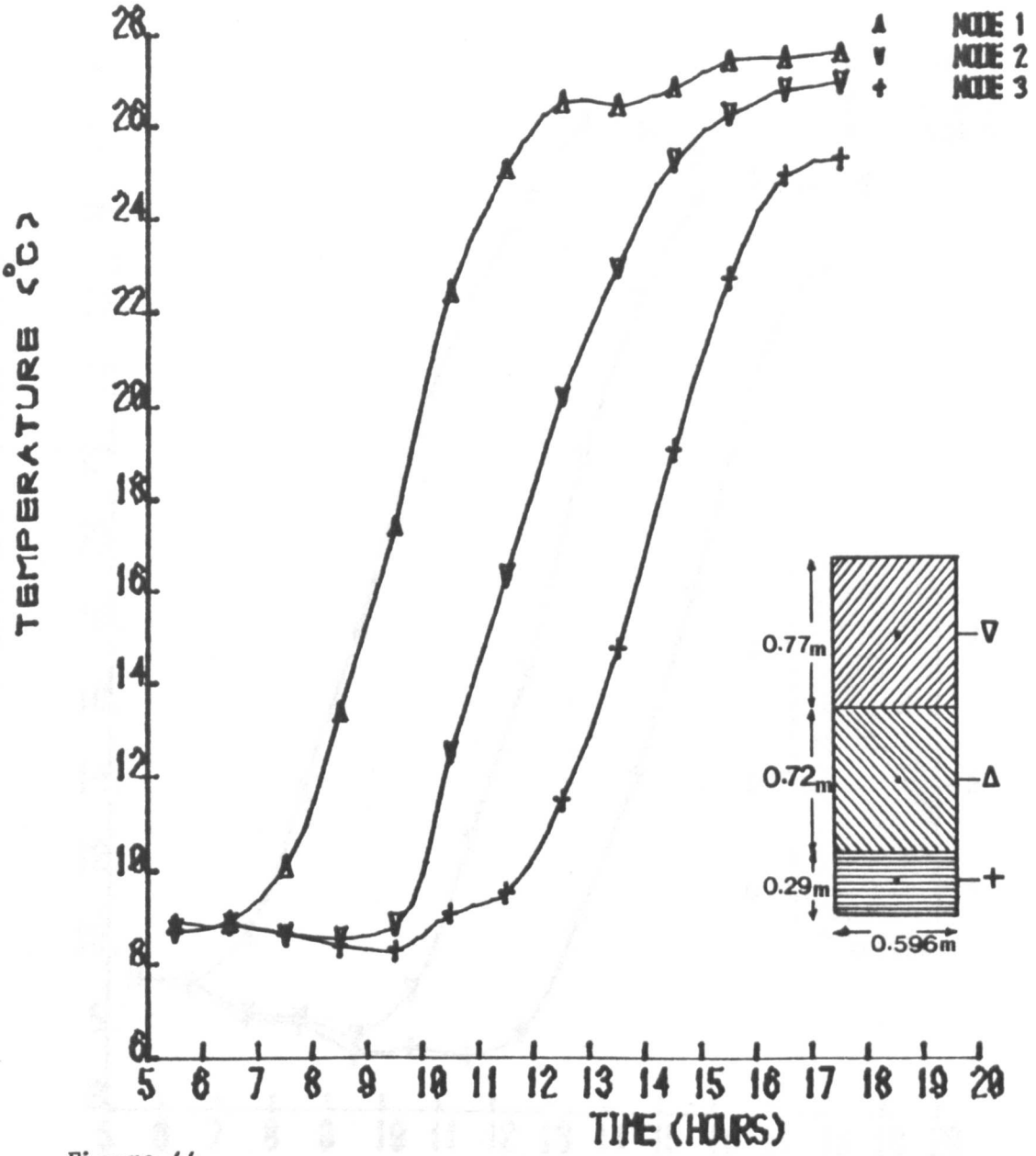

Figure 44

TEMPERATURE DISTRIBUTION IN TYPE I STORAGE TANK FOR 15TH MAY ,NO DRAW OFF,FLOW RATE = 0.01 KG/SM**2

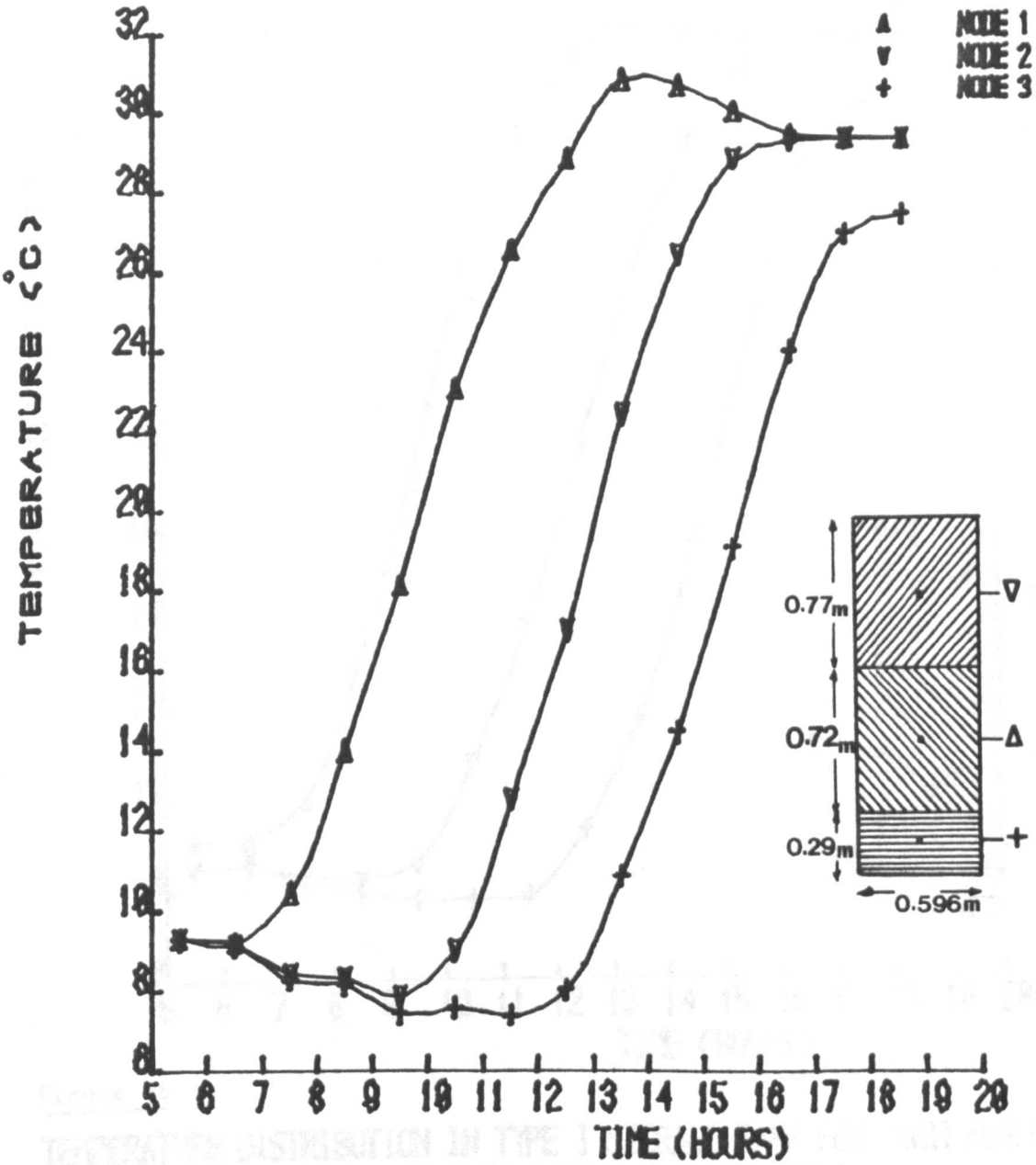

Figure 45

TEMPERATURE DISTRIBUTION IN TYPE I STORAGE TANK FOR 15TH JULY
,NO DRAW OFF,FLOW RATE = 0.01 KG/SM**2

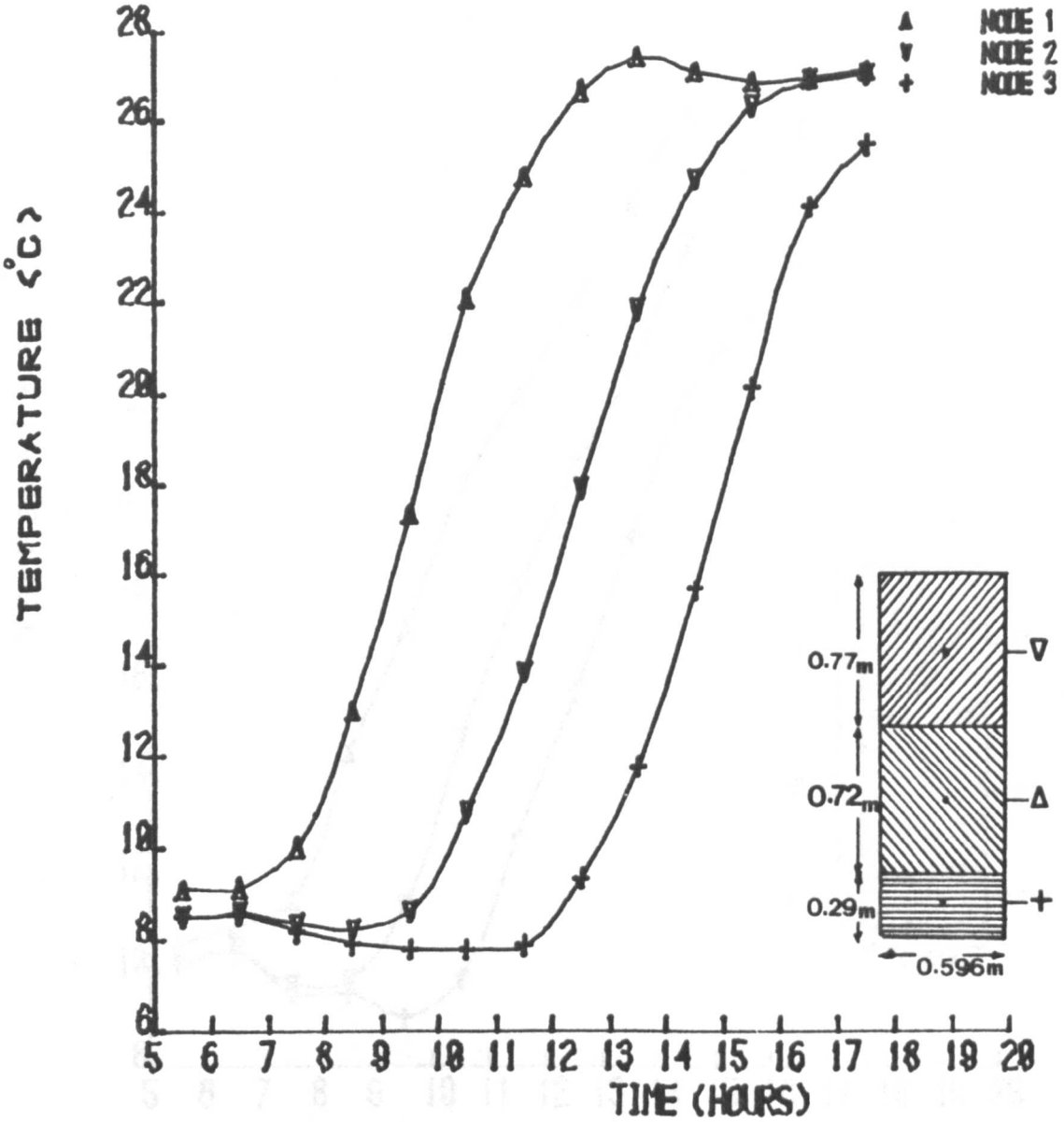

Figure 46

TEMPERATURE DISTRIBUTION IN TYPE I STORAGE TANK FOR 15TH AUGUST ,NO DRAW OFF,FLOW RATE = 0.01 KG/SM**2

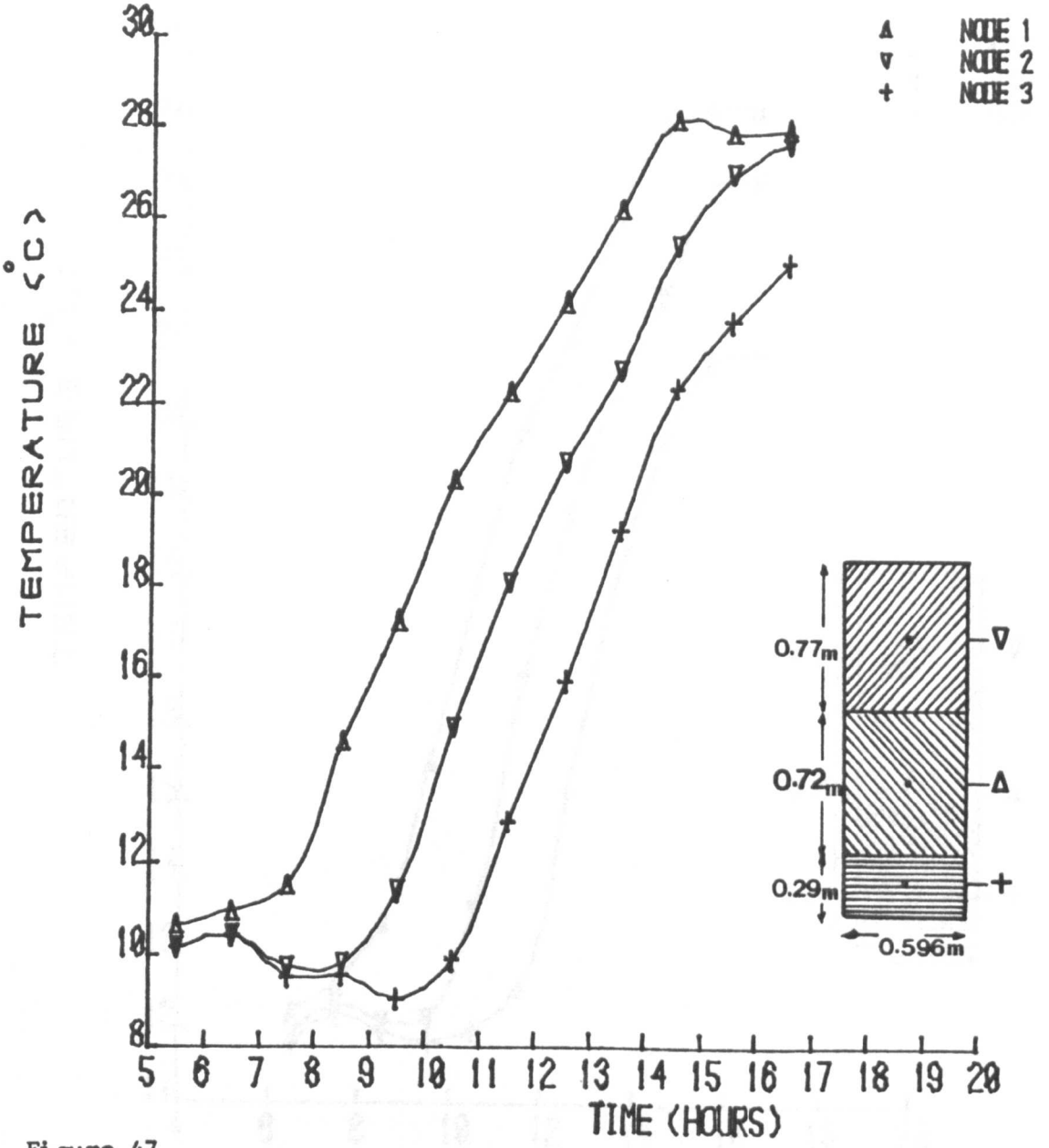

Figure 47

TEMPERATURE DISTRIBUTION IN TYPE I STORAGE TANK FOR 15TH SEPTEMBER ,NO DRAW OFF,FLOW RATE = 0.01 KG/SM**2

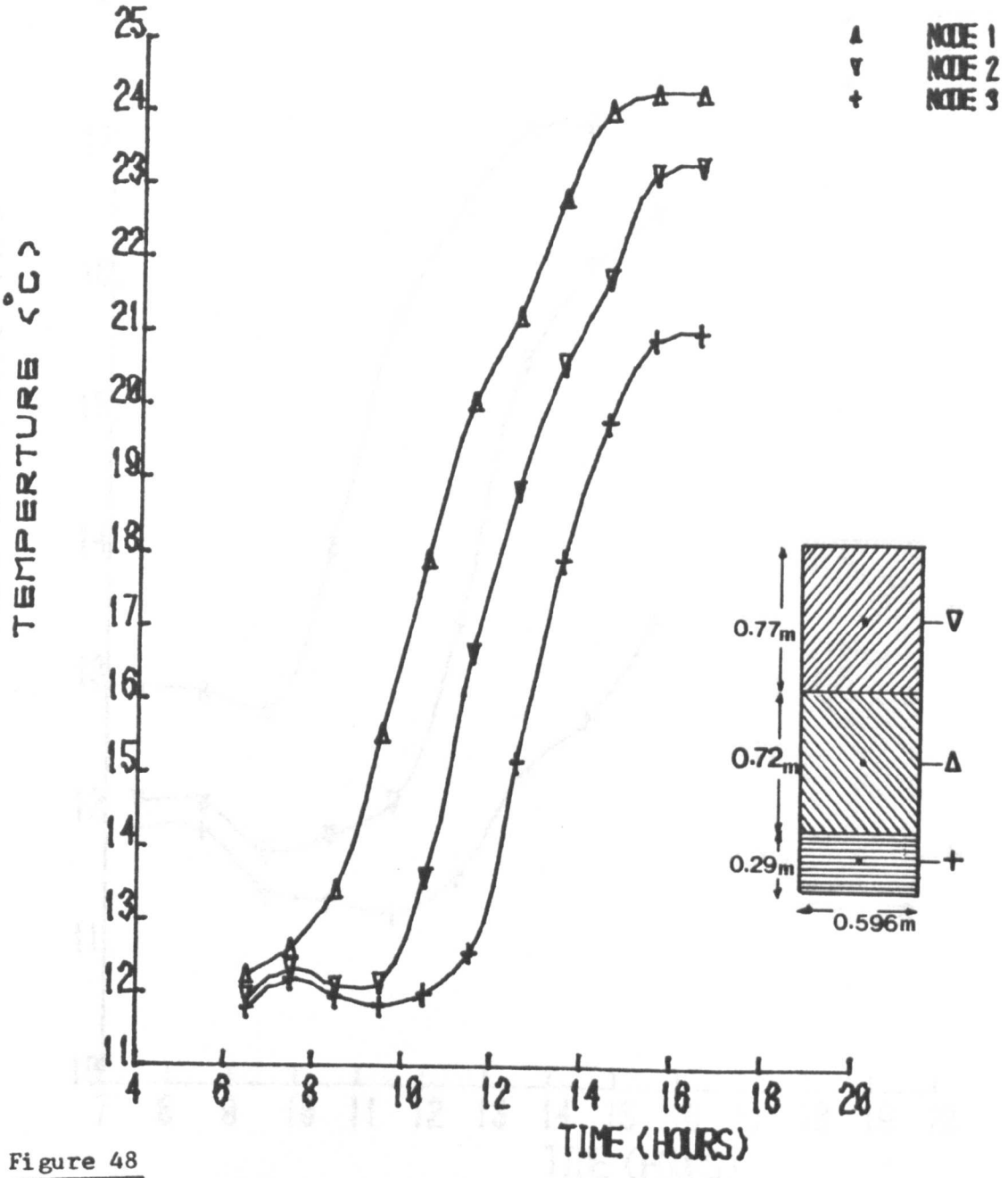

Figure 48

TEMPERTURE DISTERBUTION IN TYPE I STORAGE TANK FOR 15TH OCTOBER ,NO DRAW OFF,FLOW RATE =0.01 KG/SM**2

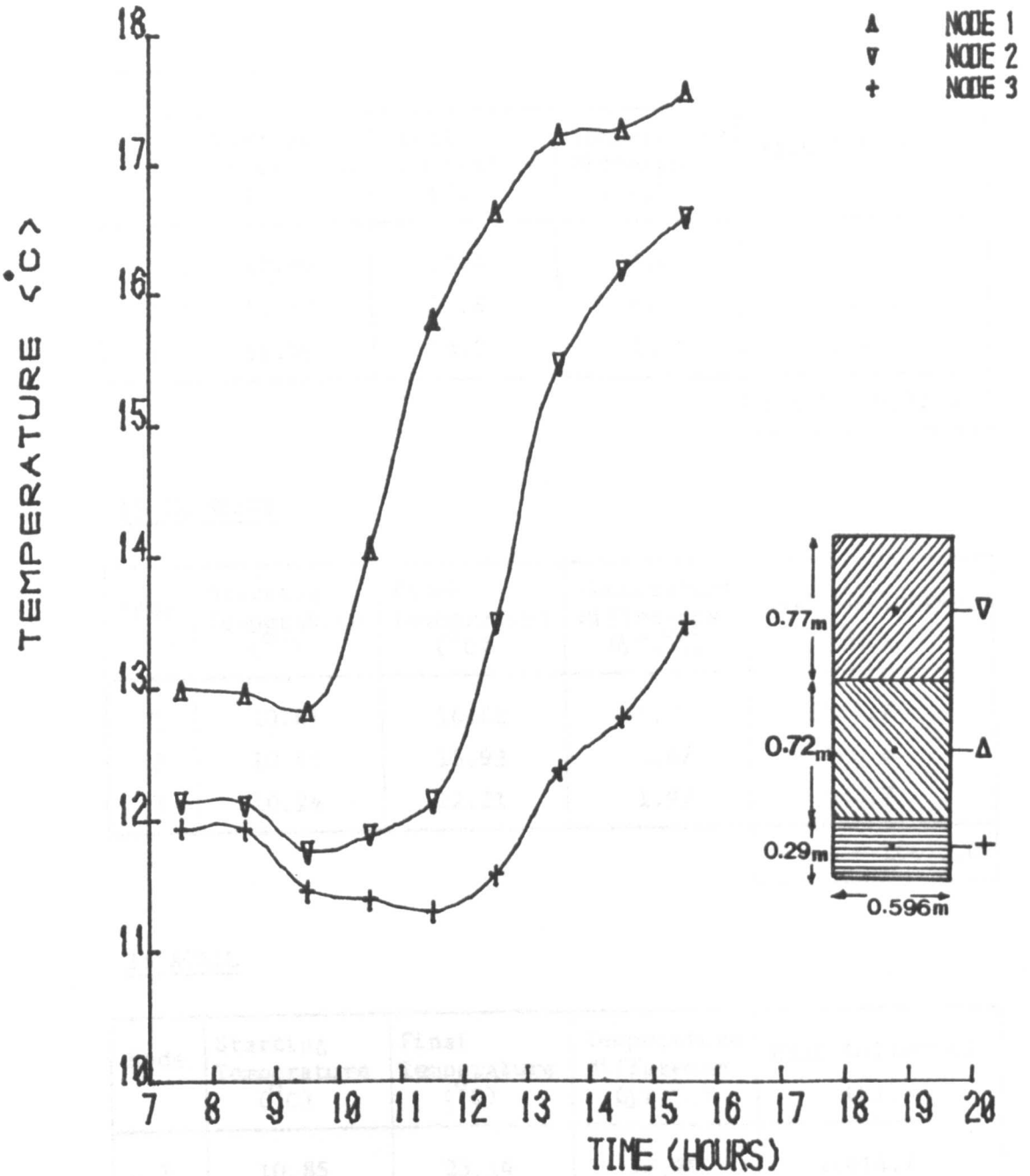

Figure 49

TEMPERATURE DISTRIBUTION IN TYPE I STORAGE TANK FOR 15TH NOVEMBER ,NO DRAW OFF,FLOW RATE = 0.01 KG/SM**2

TABLE 57. Heat collected for TYPE I storage container for 15 January, 15 February, and 15 April

15 JANUARY

Node	Starting Temperature (°C)	Final Temperature (°C)	Temperature difference (ΔT, °C)	Heat Collected (KJ)
1	12.60	17.4	4.8	4314.2
2	11.70	16.6	4.9	4157.2
3	11.56	13.7	2.14	746.0
				Total = 9217.4

15 FEBRUARY

Node	Starting Temperature (°C)	Final Temperature (°C)	Temperature difference (ΔT, °C)	Heat Collected (KJ)
1	10.67	16.62	5.95	5347.7
2	10.46	15.93	5.47	4640.6
3	10.24	12.21	1.97	686.7
				Total = 10675.0

15 APRIL

Node	Starting Temperature (°C)	Final Temperature (°C)	Temperature difference (ΔT, °C)	Heat Collected (KJ)
1	10.85	23.14	12.29	11014.7
2	9.19	22.56	13.37	11283.7
3	9.19	19.99	10.80	3754.9
				Total = 26053.3

TABLE 58. Heat collected for TYPE I storage container for 15 May, 15 July and 15 August

15 MAY

Node	Starting Temperature (^{o}C)	Final Temperature (^{o}C)	Temperature difference (ΔT,^{o}C)	Heat Collected (KJ)
1	8.90	27.63	18.73	16731.2
2	8.76	27.00	18.24	15379.9
3	8.74	25.34	16.60	5760.2
				Total = 37871.3

15 JULY

Node	Starting Temperature (^{o}C)	Final Temperature (^{o}C)	Temperature difference (ΔT,^{o}C)	Heat Collected (KJ)
1	9.33	29.40	20.07	17921.2
2	9.31	29.40	20.09	16933.2
3	9.30	27.48	18.18	6298.7
				Total = 41153.1

15 AUGUST

Node	Starting Temperature (^{o}C)	Final Temperature (^{o}C)	Temperature difference (ΔT,^{o}C)	Heat Collected (KJ)
1	9.12	26.98	17.86	15954.1
2	8.54	26.92	18.38	15497.9
3	8.53	24.13	15.6	5414.8
				Total = 36866.8

TABLE 59. Heat collected for TYPE I storage container for 15 September, 15 October, and 15 November

15 SEPTEMBER

Node	Starting Temperature (°C)	Final Temperature (°C)	Temperature difference (T,°C)	Heat Collected (KJ)
1	10.68	28.00	17.32	15495.6
2	10.19	27.68	17.49	14770.3
3	10.18	25.03	14.85	5154.5
				Total = 35420.4

15 OCTOBER

Node	Starting Temperature (°C)	Final Temperature (°C)	Temperature difference (T,°C)	Heat Collected (KJ)
1	12.27	24.3	12.03	10781.6
2	11.95	23.3	11.35	9601.8
3	11.80	21.0	9.20	3199.1
				Total = 23582.5

15 NOVEMBER

Node	Starting Temperature (°C)	Final Temperature (°C)	Temperature difference (T,°C)	Heat Collected (KJ)
1	12.99	17.56	4.57	4107.5
2	12.14	16.60	4.46	3783.9
3	11.94	13.50	1.56	543.8
				Total = 8435.2

TABLE 60. Summary of the monthly averaged daily performance for TYPE I storage container

Mid Month day	Incident Energy for 5 m^2 collector (KJ)	Heat Collected (KJ)
15 January	20700.5	9217.4
15 February	31956.0	10675.0
15 March	49717.5	25137.4
15 April	58631.5	26053.3
15 May	74597.5	37871.3
15 June	81136.0	49078.5
15 July	72700.5	41153.1
15 August	64137.0	36866.8
15 September	60025.0	35420.4
15 October	42273.0	23582.5
15 November	25818.0	8435.2
15 December	16908.0	8395.2

TABLE 61. Monthly long term system performance for TYPE I storage container

Month	Incident Energy for 5 m^2 Collector (KJ)	Heat Collected (KJ)
January	641715.5	285739.4
February	894768.0	298900.0
March	1541242.5	779259.4
April	1758945.0	781599.0
May	2312522.5	1174010.3
June	2434080.0	1472355.0
July	2253715.5	1275746.1
August	1988247.0	1142870.8
September	1800750.0	1062612.0
October	1310463.0	731057.5
November	774540.0	253056.0
December	524148.0	260251.2
TOTAL	18235137	9517456.7

long term system efficiency (η) = $\frac{9517456.7}{18235137}$ = 52%

6.4.2 Discussion

1. It can be seen from table 61 that the maximum heat collected is in June and the minimum is in December, and these correspond to the maximum and minimum radiation income on the collector surface (section 2.7).

2. Monthly long term average performance of the system for TYPE I storage has been determined, with long term system efficiency of 52%.

CHAPTER 7 THE COMPUTER MODEL OF THE STRATIFIED STORAGE CONTAINER

7.1 INTRODUCTION

Having concluded that the TYPE I storage container gave the best result in terms of heat collected with the maximum stratification, which was the main goal of this study, the next stage was to compare some of the experimental results with the theoretical predictions. The theoretical predictions were based on the two mathematical models of Duffie and Beckman[2] and Close[44]. In this chapter both models are compared using the hourly measured temperature as the initial condition.

7.2 The stratified storage mathematical model

The basic heat and mass transfer relations governing a storage container, subject to thermal stratification, are complicated. Two mathematical models exist, by Duffie and Beckman[2] and Close[44]; the basic form of each model is given below, and the nomenclature may be found in Appendix 4.

1. Duffie and Beckman mathematical model

The differential equation for section i of an n-section tank is

$$(mc_p)_i \frac{dT_i}{d\tau} = (\dot{m}c_p)_c \left[F_i^c (T_{c,o} - T_i) + (T_{i-1} - T_i) \sum_{J=1}^{i-1} F_j^c \right]$$

$$+ (\dot{m}c_p)_L \left[F_i^L (T_{L,r} - T_i) + (T_{i+1} - T_i) \sum_{j=i+1}^{n} F_j^L \right]$$

$$+ U_i A_i (T_a - T_i) \qquad (7.1)$$

where

F_i^c = Collector control function

$$F_i^c = \begin{cases} 1 & \text{if } T_{i+1} > T_{c,o} > T_i \\ 0 & \text{otherwise} \end{cases}$$

F_i^L = load control function

$$F_i^L = \begin{cases} 1 & \text{if } T_i > T_{L,r} > T_{i+1} \\ 0 & \text{otherwise} \end{cases}$$

For more details about the model see Duffie and Beckman[2].

2. Close's mathematical model

For a three-segment storage tank three differential equations can be written describing the transient behaviour of each.

The top segment equation is

$$(mc_p)_{s.1} \frac{dT_{s.1}}{d\tau} = R_1 R_2 \dot{m}_c \left[T_c - T_{s.1}\right] - R_5 \dot{m}_L \left[T_{s.1} - T_{s.2}\right] - UA_{s.1}\left[T_{s.1} - T_A\right] \qquad (7.2)$$

The middle segment equation is

$$(mc_p)_{s.2} \frac{dT_{s.2}}{d\tau} = R_1 R_3 \dot{m}_c \left[T_c - T_{s.2}\right] + R_1 R_2 \dot{m}_c \left[T_{s.1} - T_{s.2}\right] -$$

$$R_5 \dot{m}_L \left[T_{s.2} - T_{s.3} \right] -$$

$$UA_{s.2} \left[T_{s.2} - T_A \right] \qquad (7.3)$$

The bottom segment equation is

$$(mc_p)_{s.3} \frac{dT_{s.3}}{d\tau} = R_1 R_4 \dot{m}_c \left[T_c - T_{s.3} \right] +$$

$$R_1 R_3 \dot{m}_c \left[T_{s.2} - T_{s.3} \right] +$$

$$R_1 R_2 \dot{m}_c \left[T_{s.2} - T_{s.3} \right] -$$

$$R_5 \dot{m}_L \left[T_{s.3} - T_R \right] -$$

$$UA_{s.3} \left[T_{s.3} - T_A \right] \qquad (7.4)$$

Close's model incorporates three hypothetical values, or control functions, that either open or close, depending on the collector return temperatures and the bottom of the storage tank temperatures. These control functions are operated as in Table 62.

TABLE 62 Operation of valves governing flow into storage tank

Temperature Comparison	R_2	R_3	R_4
$T_c \gg T_{s.1}$	1	0	0
$T_{s.1} > T_c \gg T_{s.2}$	0	1	0
$T_{s.2} > T_c \gg T_{s.3}$	0	0	1

For more details about the model see Close[44].

7.3 The computation procedure for the stratified storage container model

The computation procedure is shown in Figures 50 and 51 which illustrate the flow charts for the stratified storage container models, based on the mathematical model of Duffie and Beckman[2], and Close[44].

7.4 Results

Tables 63-65 show comparison of measured and predicted (Duffie and Beckman) TYPE I storage temperature, no draw off, flow rate = 0.01 kg/Sm^2 for 15 March, 15 June and 15 December.

Tables 66-68 show comparison of measured and predicted (Close) TYPE I storage temperature, no draw off, flow rate = 0.01 kg/Sm^2 for 15 March, 15 June and 15 December.

Figures 52-54 compare the measured and predicted TYPE I storage temperature for 15 March, 15 June and 15 December using Duffie and Beckman[2] mathematical model.

Figures 55-57 compare the measured and predicted TYPE I storage temperature for 15 March, 15 June and 15 December using Close[44] mathematical model.

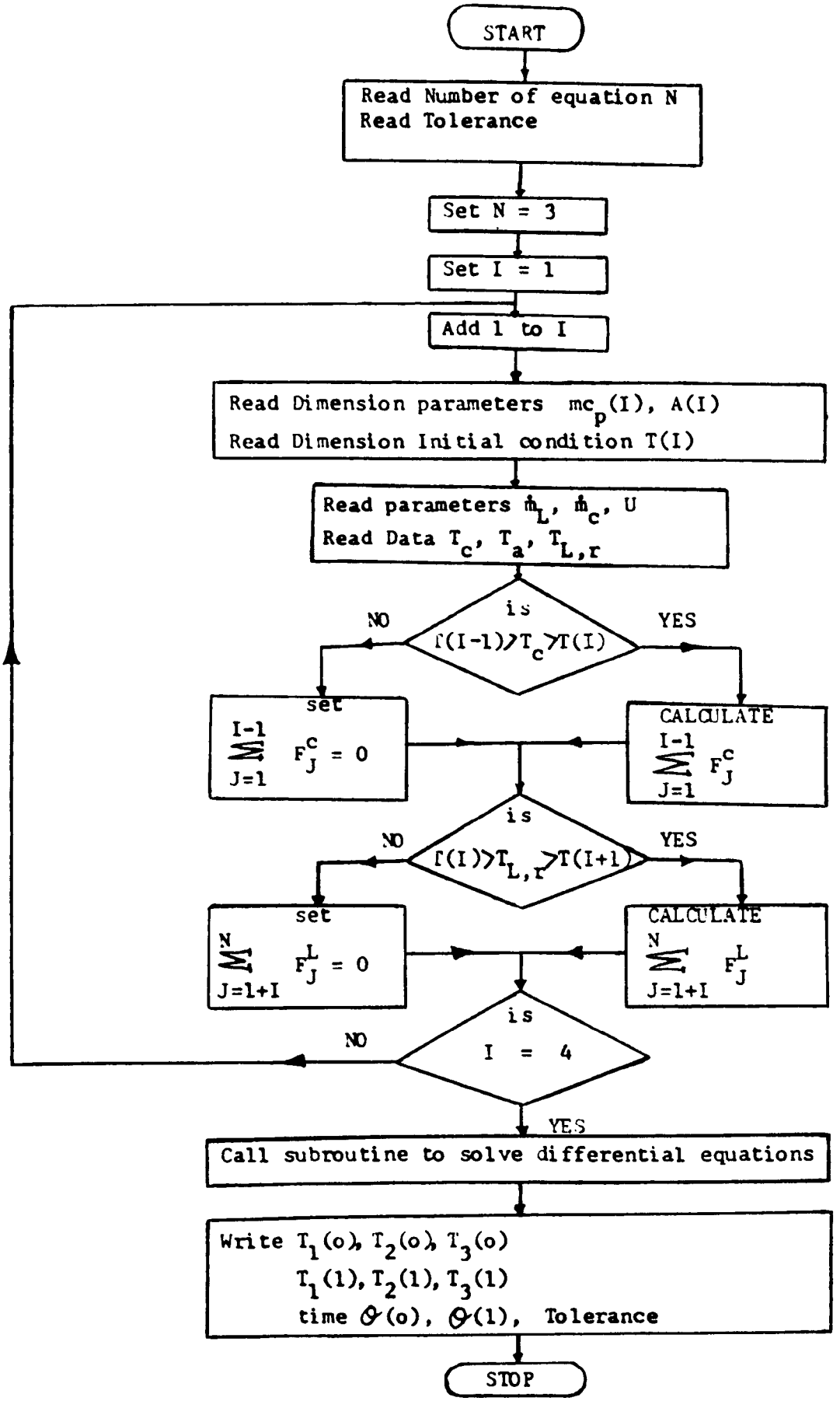

Figure 50

Flow chart for the stratified storage container model based on the mathematical model of Duffie and Beckman.

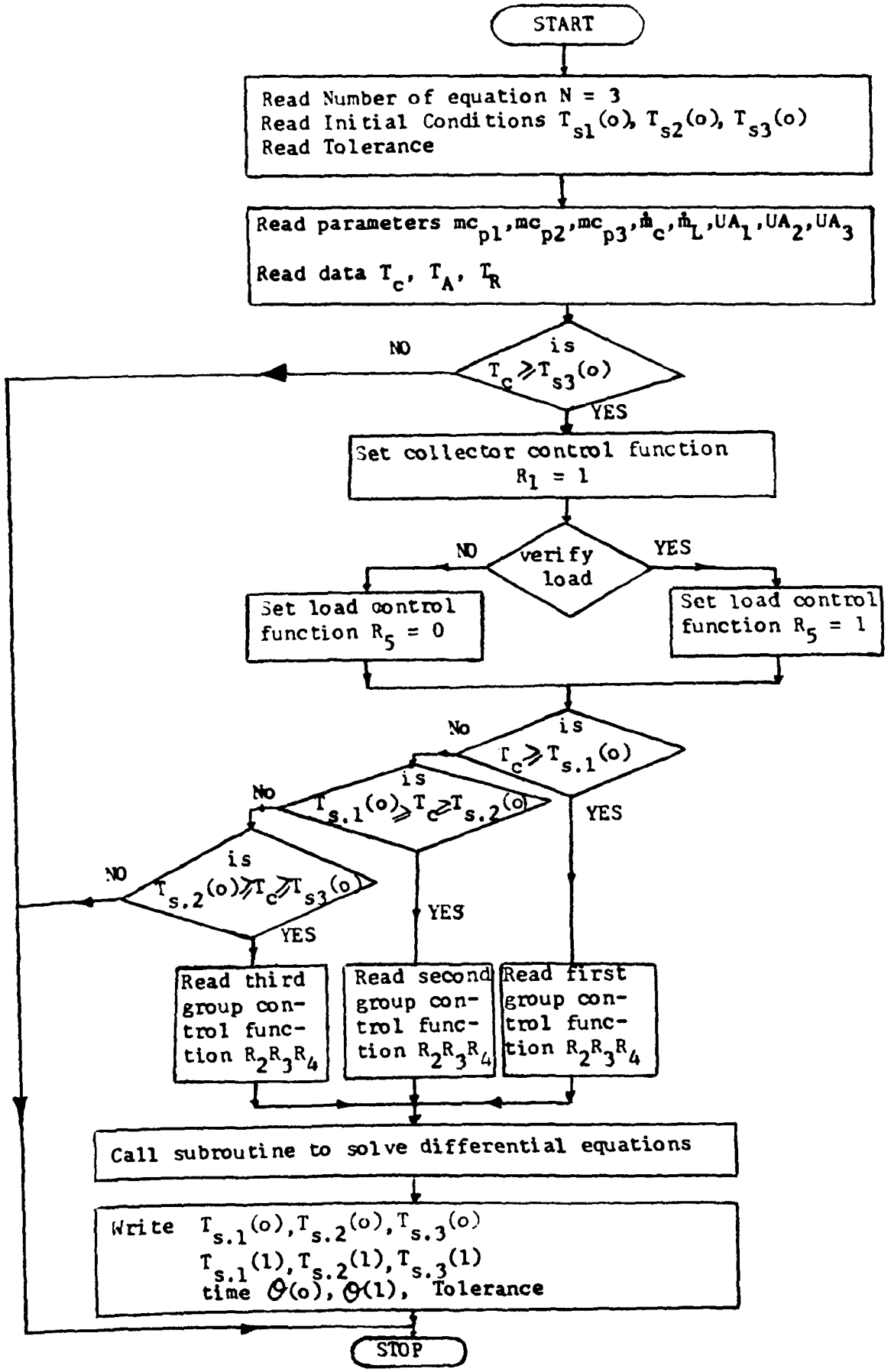

Figure 51

Flow chart for the stratified storage container model based on the mathematical model of Close

TABLE 63 15 March: Comparison of measured and predicted (Duffie and Beckman) TYPE I storage temperature, no draw off, flow rate = 0.01 kg/Sm^2

Time Hours	Measured Temperature (^oC)			Predicted Temperature (^oC)		
	Node 1	Node 2	Node 3	Node 1	Node 2	Node 3
7-8	11.80	11.33	11.32	11.80	11.33	11.32
8-9	12.00	11.30	11.25	11.82	11.35	11.32
9-10	13.90	11.50	11.45	12.02	11.32	11.25
10-11	16.40	12.85	11.50	13.92	11.53	11.45
11-12	17.20	16.10	12.60	16.40	12.87	11.50
12-13	18.50	17.00	16.20	17.20	16.11	12.60
13-14	21.00	19.40	17.20	18.50	17.00	16.20
14-15	22.30	21.20	19.80	20.99	19.40	17.20
15-16	24.10	22.10	21.17	22.28	21.88	19.80
16-17	24.50	22.90	21.30	24.08	22.08	21.17
17-18	24.70	23.10	21.60	24.48	22.88	21.30

TABLE 64 15 June: Comparison of measured and predicted (Duffie and Beckman) TYPE I storage temperature, no draw off, flow rate = 0.01 kg/Sm^2

Time Hours	Measured Temperature (^oC)			Predicted Temperature (^oC)		
	Node 1	Node 2	Node 3	Node 1	Node 2	Node 3
5-6	9.50	9.30	9.30	9.50	9.30	9.30
6-7	9.80	9.20	9.30	9.53	9.30	9.30
7-8	11.50	8.60	8.60	9.82	9.22	9.30
8-9	14.50	10.15	8.55	11.50	8.62	8.60
9-10	16.70	13.76	9.20	14.50	10.20	8.55
10-11	19.30	16.00	13.60	16.68	13.76	9.20
11-12	23.40	18.40	15.50	19.27	15.98	13.60
12-13	25.90	22.60	18.10	23.39	18.40	15.50
13-14	28.10	25.60	22.10	25.85	22.56	18.10
14-15	31.10	27.70	25.40	28.00	25.55	22.10
15-16	32.50	30.95	27.75	31.03	27.6	25.40
16-17	32.80	32.47	30.45	32.40	30.87	27.75
17-18	33.50	32.98	31.75	32.73	32.40	30.45
18-19	33.50	33.00	31.60	33.40	32.90	31.75

TABLE 65 15 December: Comparison of measured and predicted (Duffie and BecRman) TYPE I storage temperature, no draw off, flow rate = 0.01 kg/Sm^2

Time Hours	Measured Temperature (^oC)			Predicted Temperature (^oC)		
	Node 1	Node 2	Node 3	Node 1	Node 2	Node 3
8-9	12.13	10.95	10.87	12.13	10.95	10.87
9-10	12.34	10.95	10.83	12.14	10.90	10.80
10-11	13.53	10.98	10.56	12.36	10.97	10.80
11-12	14.94	11.48	10.65	13.54	11.00	10.56
12-13	15.71	12.84	10.81	14.90	11.50	10.65
13-14	15.74	12.88	10.85	15.72	12.80	10.80
14-15	16.12	14.42	11.38	15.70	12.90	10.80
15-16	16.62	15.46	12.40	16.13	14.40	11.40

TABLE 66 15 March: Comparison of measured and predicted (Close) TYPE I storage temperature, no draw off, flow rate = 0.01 kg/Sm^2

Time Hours	Measured Temperature (^oC)			Predicted Temperature (^oC)		
	Node 1	Node 2	Node 3	Node 1	Node 2	Node 3
7-8	11.80	11.33	11.32	11.80	11.33	11.32
8-9	12.00	11.30	11.25	11.82	11.35	11.35
9-10	13.90	11.50	11.45	12.02	11.32	11.28
10-11	16.40	12.85	11.50	13.92	11.53	11.49
11-12	17.20	16.10	12.60	16.40	12.87	11.50
12-13	18.50	17.00	16.20	17.20	16.11	12.63
13-14	21.00	19.40	17.20	18.50	17.01	16.21
14-15	22.30	21.20	19.80	20.99	19.40	17.21
15-16	24.10	22.10	21.17	22.30	21.10	19.80
16-17	24.50	22.90	21.30	24.07	22.08	21.14
17-18	24.70	23.10	21.60	24.50	22.90	21.30

TABLE 67 15 June: Comparison of measured and predicted (Close) TYPE I storage temperature, no draw off, flow rate = 0.01 kg/Sm^2

Time Hours	Measured Temperature (^{o}C)			Predicted Temperature (^{o}C)		
	Node 1	Node 2	Node 3	Node 1	Node 2	Node 3
5-6	9.50	9.30	9.30	9.50	9.30	9.30
6-7	9.80	9.20	9.30	9.53	9.33	9.34
7-8	11.50	8.60	8.60	9.80	9.20	9.30
8-9	14.50	10.15	8.55	11.50	8.60	8.63
9-10	16.70	13.76	9.20	14.49	10.16	8.57
10-11	19.30	16.00	13.60	16.68	13.75	9.20
11-12	23.40	18.40	15.50	19.27	15.98	13.59
12-13	25.90	22.60	18.10	23.38	18.40	15.50
13-14	28.10	25.60	22.10	25.80	22.56	18.10
14-15	31.10	27.70	25.40	28.04	25.55	22.10
15-16	32.50	30.95	27.75	31.02	27.60	25.33
16-17	32.80	32.47	30.45	32.40	31.05	27.66
17-18	33.50	32.98	31.75	32.70	32.40	30.40
18-19	33.50	33.00	31.60	33.40	32.90	31.65

TABLE 68 15 December: Comparison of measured and predicted (Close) TYPE I storage temperature, no draw off, flow rate = 0.01 kg/Sm^2

Time Hours	Measured Temperature (^oC)			Predicted Temperature (^oC)		
	Node 1	Node 2	Node 3	Node 1	Node 2	Node 3
8-9	12.13	10.95	10.87	12.13	10.95	10.87
9-10	12.34	10.95	10.83	12.15	10.97	10.90
10-11	13.53	10.98	10.56	12.36	10.97	10.86
11-12	14.94	11.48	10.65	13.54	11.00	10.60
12-13	15.71	12.84	10.81	14.95	11.50	10.69
13-14	15.74	12.88	10.85	15.72	12.86	10.85
14-15	16.12	14.42	11.38	15.75	12.90	10.93
15-16	16.62	15.46	12.40	16.13	14.43	11.42

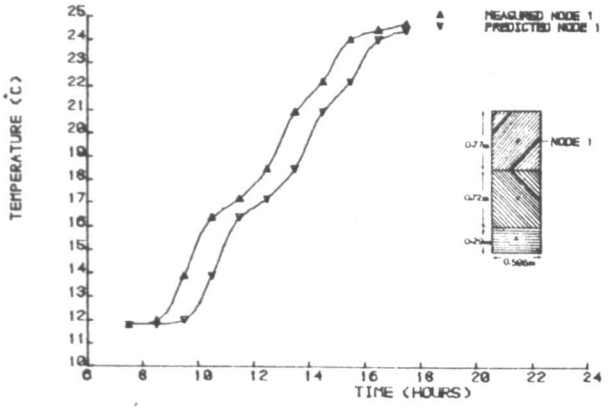

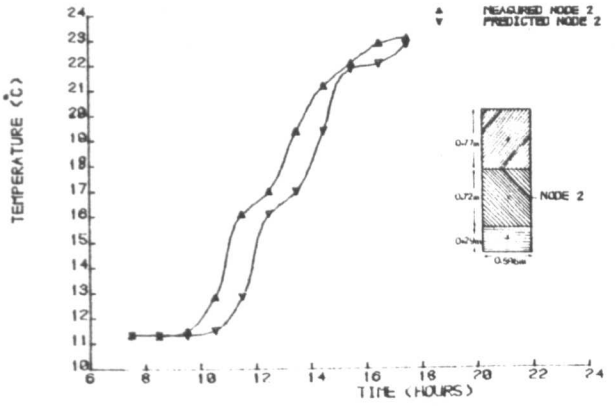

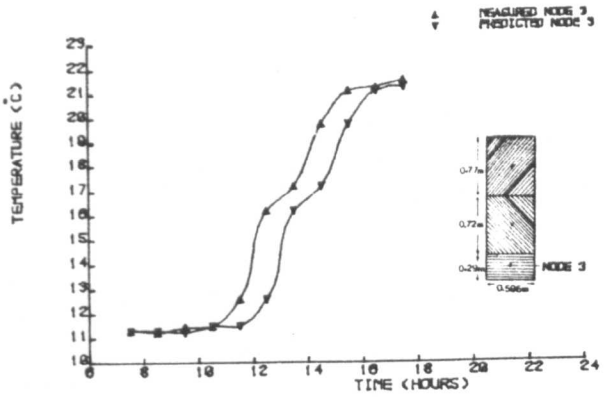

Figure 52

COMPARISON OF MEASURED & PREDICTED(DUFFIE&BECKMAN) TYPE I STORAGE TEMPERATURE FOR 15TH MARCH,NO DRAW OFF,FLOW RATE =0.01 KG/SM**2

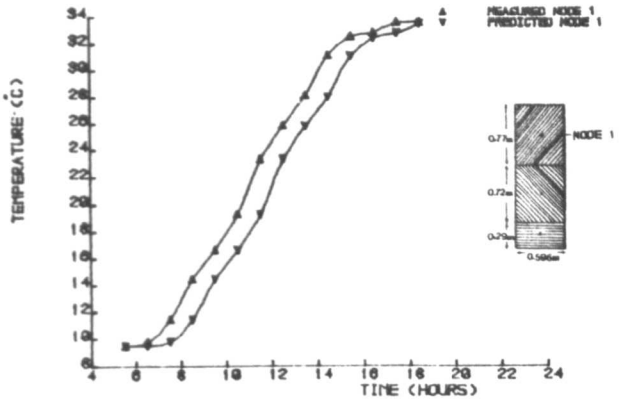

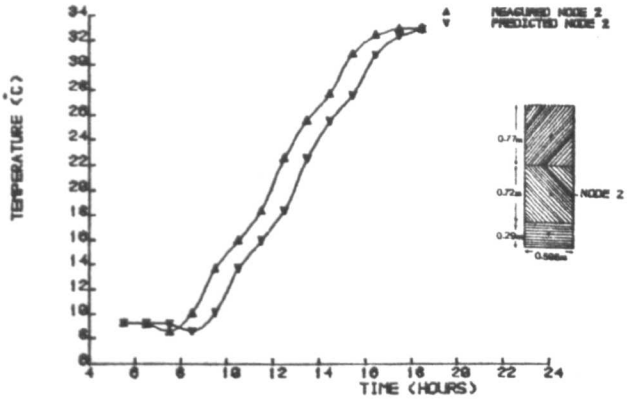

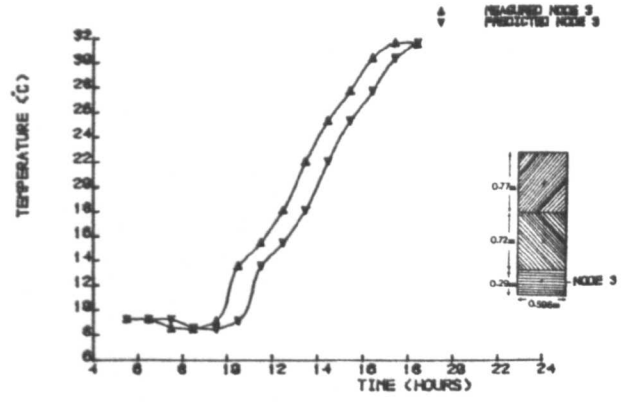

Figure 53

COMPARISON OF MEASURED & PREDICTED(DUFFIE&BECKMAN) TYPE I STORAGE TEMPERATURE FOR 15TH JUNE,NO DRAW OFF,FLOW RATE = 0.01 KG/SMM2

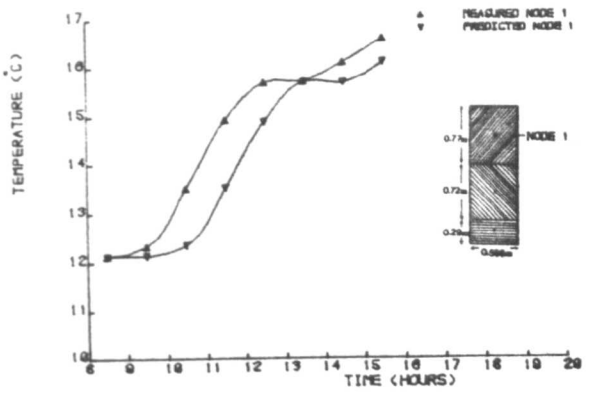

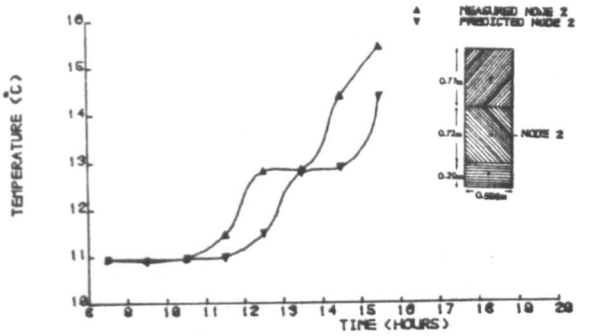

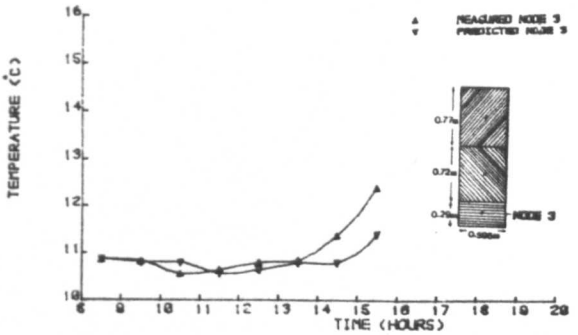

Figure 54

COMPARISON OF MEASURED & PREDICTED(DUFFIE&BECKMAN) TYPE I STORAGE TEMPERATURE FOR 15TH DECEMBER, NO DRAW OFF, FLOW RATE = 0.01 KG/SMMM2

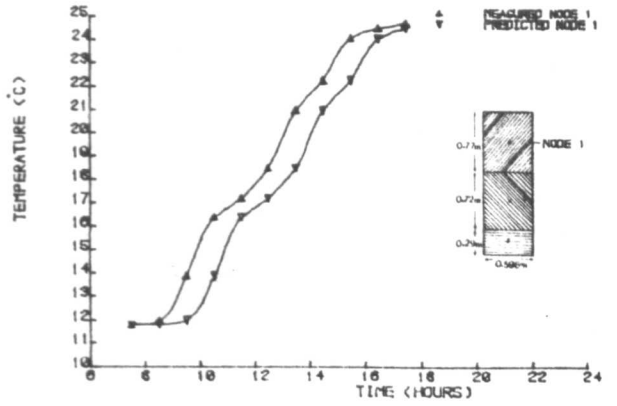

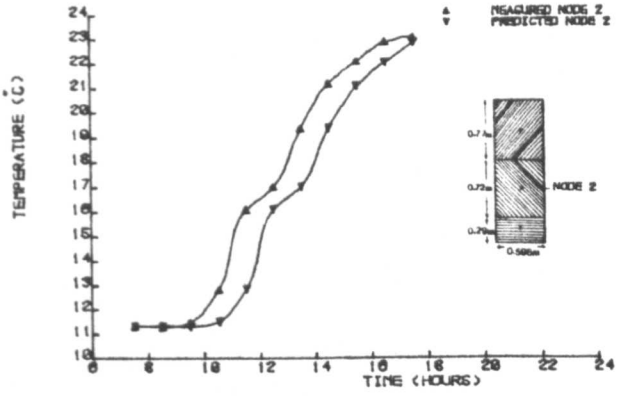

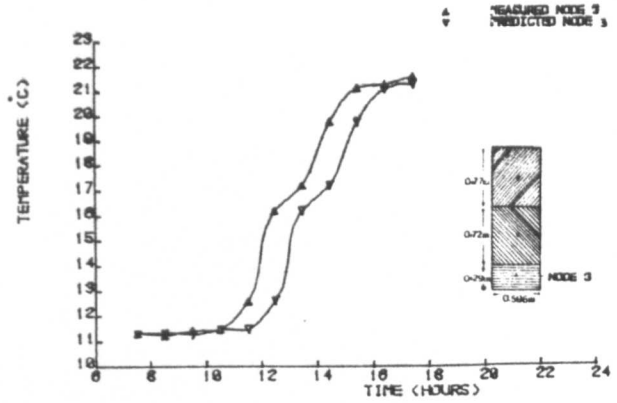

Figure 55

COMPARISON OF MEASURED & PREDICTED(CLOSE) TYPE I STORAGE TEMPERATURE
FOR 15TH MARCH,NO DRAW OFF,FLOW RATE = 0.01 KG/S

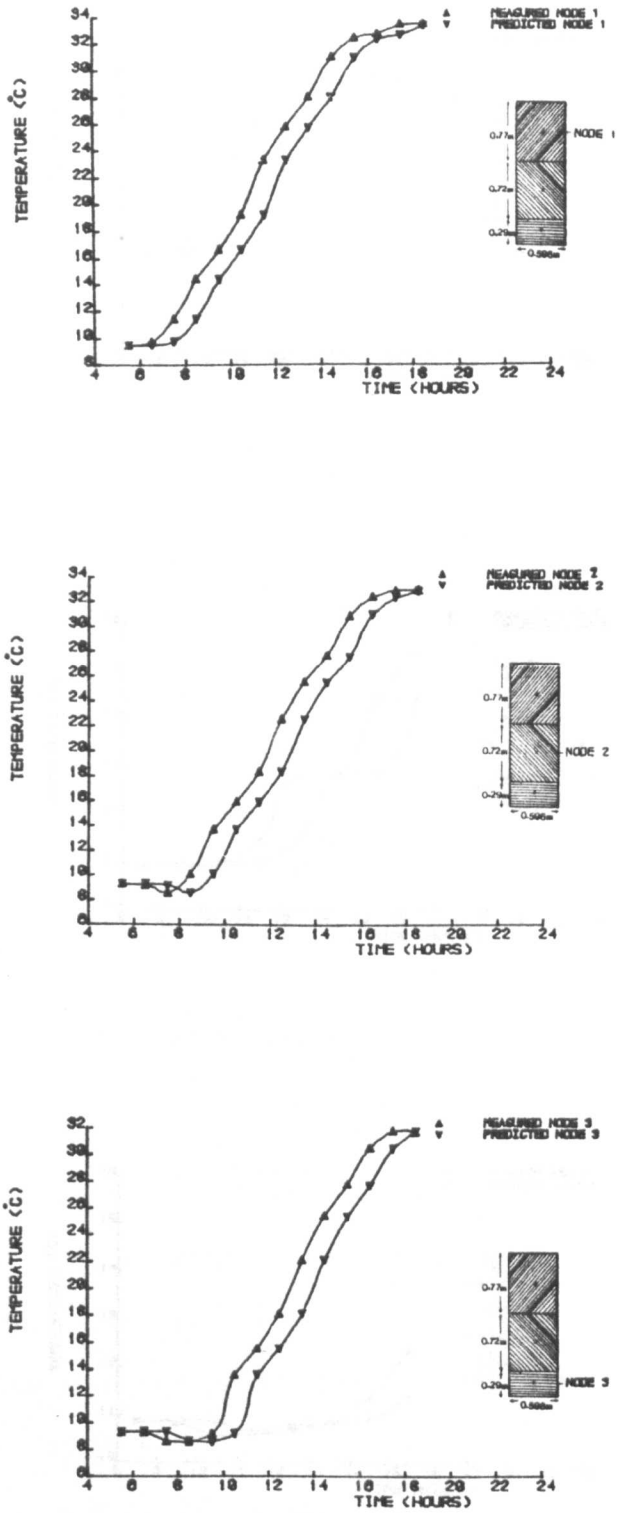

Figure 56

COMPARISON OF MEASURED & PREDICTED(CLOSE) TYPE I STORAGE TEMPERATURE
FOR 15TH JUNE,NO DRAW OFF,FLOW RATE = 0.01 KG/SM**2

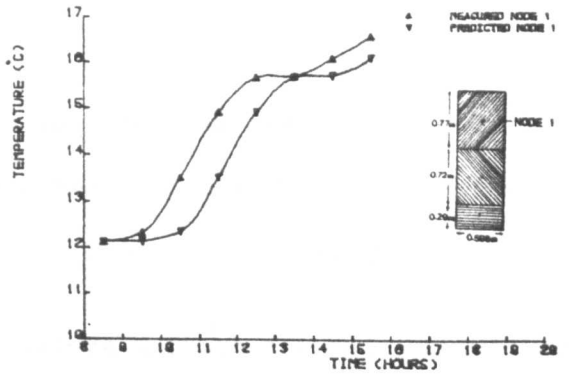

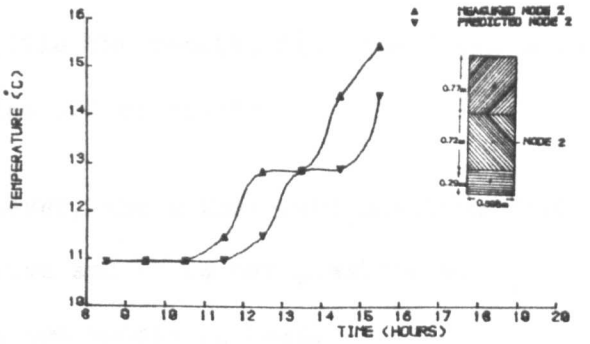

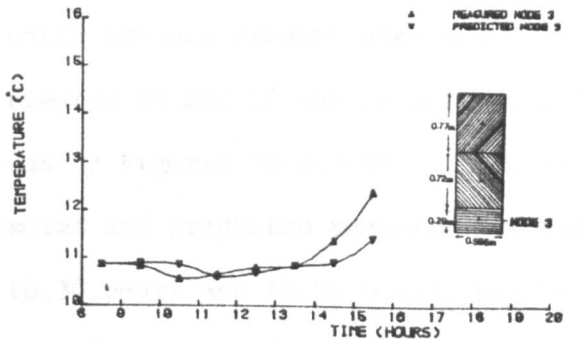

Figure 57

COMPARISON OF MEASURED & PREDICTED(CLOSE) TYPE I STORAGE TEMPERATURE FOR 15TH DECEMBER, NO DRAW OFF, FLOW RATE = 0.01 KG/SM**2

7.5 Discussion

1. Both the measured and predicted temperature differences for Duffie and Beckman, and Close for a given range of conditions, have been examined as given in Tables 69-71.

2. Average temperature differences and standard deviations have been shown in the tables overleaf.

3. The results demonstrate that both models give very similar results for the March and June profiles, although for the December profile the results from the Close model give marginally the better results.

4. Overall, however, the author must conclude that the evidence is inconclusive and it is not possible at this stage to say which of the two models is best.

5. In conclusion, both models produce very similar results and each model underestimates the measured temperatures.

6. Differences which are not evident when drawn to a small scale as in Figures 54 and 57 can be seen when drawn to a larger scale as in Figures 58 and 59. These figures emphasise the measured and predicted temperatures for node 3 at 9.30 hours, 10.30 hours and 11.30 hours, for both Duffie and Beckman, and Close. These however are small differences, and are perhaps not significant in terms of long term average performance of the system.

TABLE 69 15 March: Comparison of temperature difference (measured and predicted), Duffie and Beckman, and Close

Time Hours	Measured and predicted temperature difference, °C (Duffie and Beckman)			Measured and predicted temperature difference, °C (Close)		
	Node 1	Node 2	Node 3	Node 1	Node 2	Node 3
7-8	0	0	0	0	0	0
8-9	0.18	-0.05	-0.07	0.18	-0.05	-0.10
9-10	1.88	0.18	0.20	1.88	0.18	0.17
10-11	2.48	1.32	0.05	2.48	1.32	0.01
11-12	0.80	3.23	1.10	0.80	3.23	1.10
12-13	1.30	0.89	3.60	1.30	0.89	3.57
13-14	2.50	2.4	1.00	2.50	2.39	0.99
14-15	1.31	1.80	2.60	1.31	1.80	2.59
15-16	1.82	0.22	1.37	1.80	1.00	1.37
16-17	0.42	0.82	0.13	0.43	0.82	0.16
17-18	0.22	0.22	0.30	0.20	0.20	0.30
$\Delta T_{average}$	1.174	1.003	0.935	1.171	1.071	0.924
ΔT_{σ}	0.917	1.082	1.198	0.916	1.051	1.195

TABLE 70 15 June: Comparison of temperature difference (measured and predicted), Duffie and Beckman, and Close

Time Hours	Measured and predicted temperature difference, °C (Duffie and Beckman)			Measured and predicted temperature difference, °C (Close)		
	Node 1	Node 2	Node 3	Node 1	Node 2	Node 3
5-6	0	0	0	0	0	0
6-7	0.27	-0.10	0	0.27	-0.13	-0.04
7-8	1.68	-0.62	-0.70	1.70	-0.60	-0.70
8-9	3.00	1.53	-0.05	3.00	1.55	-0.08
9-10	2.20	3.56	0.65	2.21	3.60	0.63
10-11	2.62	2.24	4.40	2.62	2.25	4.40
11-12	4.13	2.42	1.90	4.13	2.42	1.91
12-13	2.51	4.2	2.60	2.52	4.20	2.60
13-14	2.25	3.04	4.00	2.30	3.04	4.00
14-15	3.10	2.15	3.30	3.06	2.15	3.30
15-16	1.47	3.35	2.35	1.48	3.35	2.42
16-17	0.40	1.60	2.70	0.40	1.42	2.79
17-18	0.77	0.58	1.30	0.80	0.58	1.35
18-19	0.10	0.10	-0.15	0.10	0.10	-0.05
$\Delta T_{average}$	1.750	1.718	1.593	1.756	1.709	1.609
ΔT_{σ}	1.291	1.534	1.677	1.289	1.540	1.682

TABLE 71 15 December: Comparison of temperature difference (measured and predicted), Duffie and Beckman, and Close

Time Hours	Measured and predicted temperature difference, ^{o}C (Duffie and Beckman)			Measured and predicted temperature difference, ^{o}C (Close)		
	Node 1	Node 2	Node 3	Node 1	Node 2	Node 3
8-9	0	0	0	0	0	0
9-10	0.20	0.05	0.03	0.19	-0.02	-0.07
10-11	1.17	0.01	-0.24	1.17	0.01	-0.30
11-12	1.40	0.48	0.09	1.40	0.48	0.05
12-13	0.81	1.34	0.16	0.76	1.34	0.12
13-14	0.02	0.08	0.05	0.02	0.02	0
14-15	0.42	1.52	0.58	0.37	1.52	0.45
15-16	0.49	1.06	1.00	0.49	1.03	0.98
$\Delta T_{average}$	0.564	0.568	0.209	0.55	0.548	0.154
ΔT_{σ}	0.521	0.643	0.393	0.521	0.655	0.394

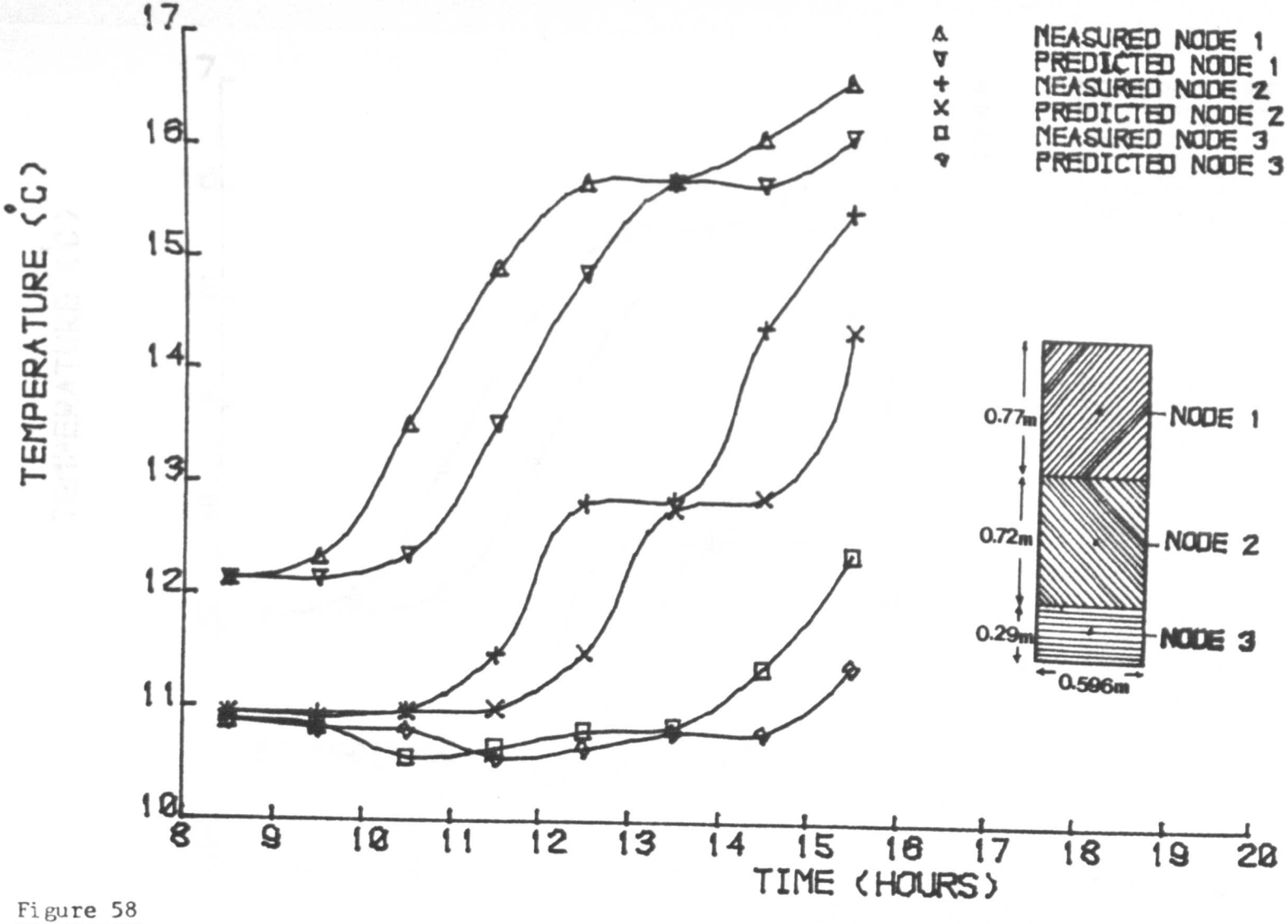

Figure 58

COMPARISON OF MEASURED & PREDICTED(DUFFIE&BECKMAN) TYPE I STORAGE TEMPERATURE FOR 15TH DECEMBER,NO DRAW OFF,FLOW RATE = 0.01 KG/SM**2

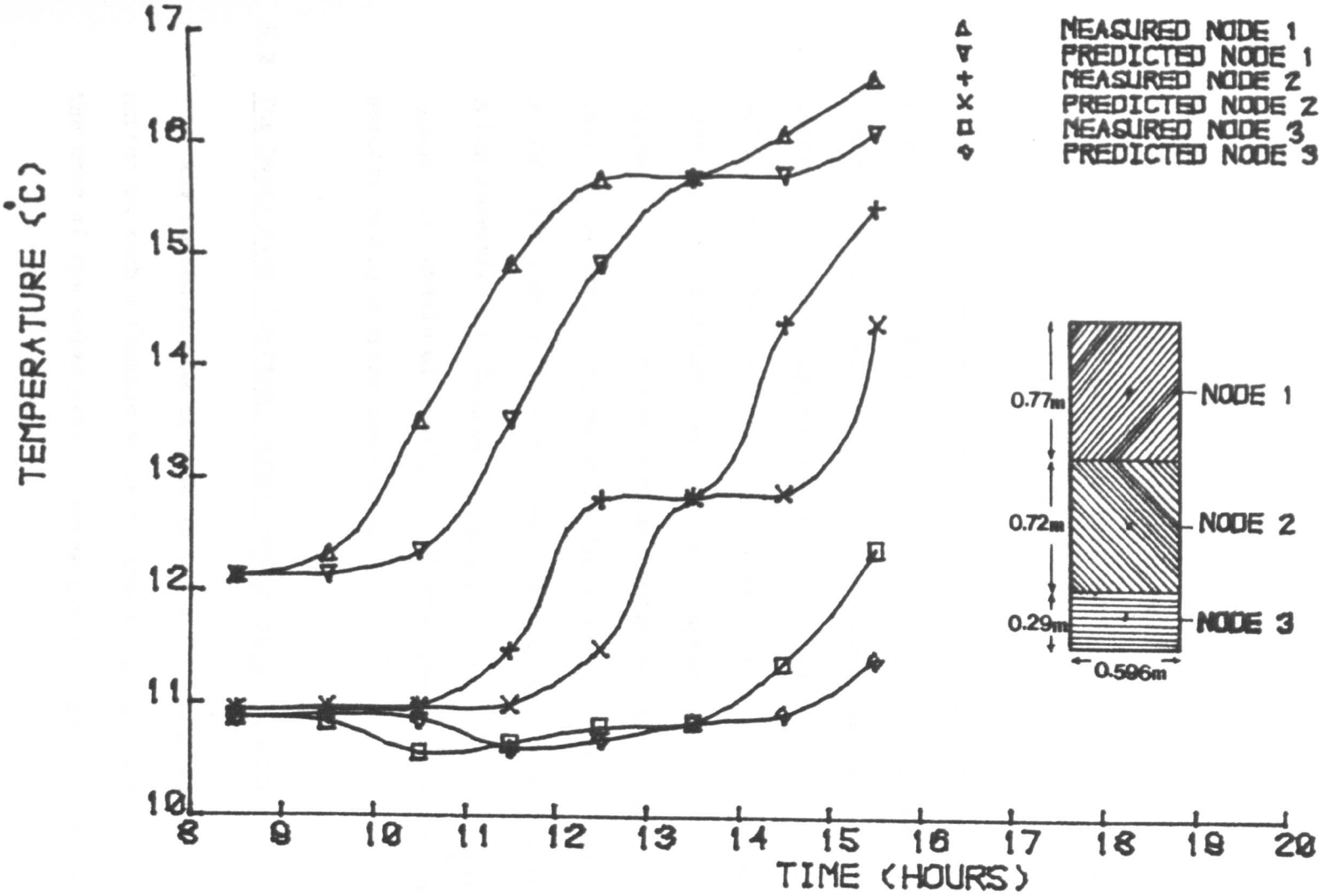

Figure 59

COMPARISON OF MEASURED & PREDICTED(CLOSE) TYPE I STORAGE TEMPERATURE FOR 15TH DECEMBER, NO DRAW OFF, FLOW RATE = 0.01 KG/SM**2

CHAPTER 8 The development of a computer system model to assist in the design of solar water heating systems

8.1 INTRODUCTION

It is apparent that a computer system model can be a powerful tool to assist in the design of solar water heating systems. However, experience has shown that the development of a computer system model is a complex task.

The computer system model, written in Fortran, has been designed specifically to assist in the design of solar water heating systems on a digital computer. The concepts employed in the computer system model are described in this chapter. The radiation model, the collector model and the stratified storage container model, which have been developed in Chapters 2, 3 and 7, together form the basis of the computer system model for solar water heating systems. Program Solar Water Heating System (SWHS) has so far been used to simulate the performance of the system undergoing investigation by dealing with each of the program components individually. It is capable of simulating alternative solar water heating systems having similar components.

8.2 The Solar Water heating system undergoing simulation

Any system may be defined as a set of components, interconnected in such a fashion so as to accomplish a specified task. In the case of the solar water heating system under investigation the

components consist of a solar collector, an energy storage unit, a pump and a differential controller. Because the system consists of components, it is possible to simulate the performance of the system as a whole by using the mathematical models of each of the system components. It is important to realize that the weather (i.e., solar radiation, ambient temperature, etc.) can be thought of as outputs of specialized system components and they can thus be treated in the same manner as any other component. The simulation technique used in this chapter reduces the complexity of system simulation because it essentially reduces a large problem into a number of smaller problems, each of which can be more easily solved independently. The entire problem of system simulation reduces then to one of identifying all of the components and formulating a general mathematical description of each.

8.3 Information flow in the computer system model

Once all the components of a system have been identified and a mathematical description of each component has been formulated, it is necessary to construct an information flow diagram of the system. Figures 60, 61, 62 and 63 illustrate the information flow diagram for the radiation model, the collector model, the stratified storage model and the computer system model. The nomenclature of the computer system model may be found in Appendix 5. An information flow diagram is a schematic representation of the flow of information into and out of each of the system components. In the diagrams, each component is represented as a box. Each piece of information required to completely describe the component is

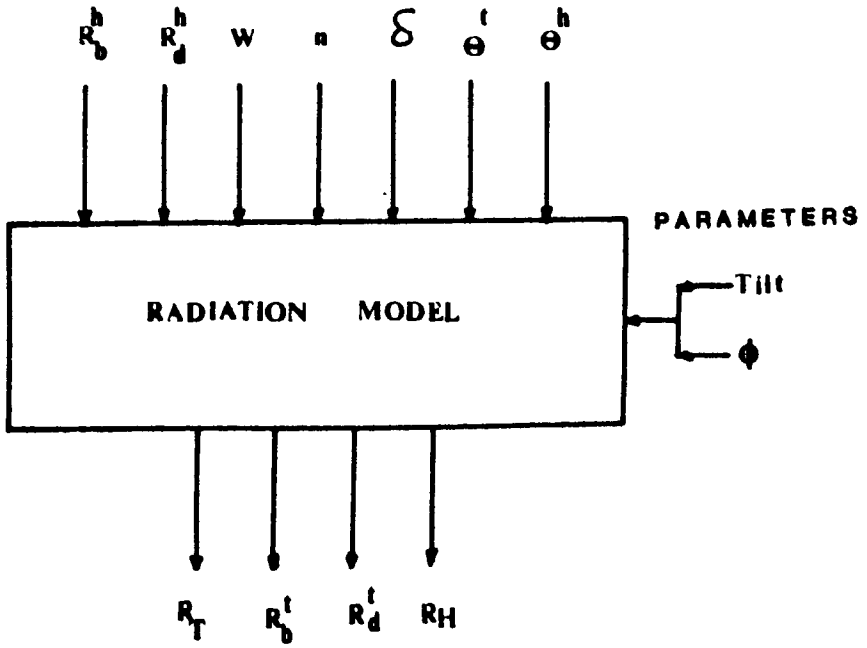

Figure 60

INFORMATION FLOW DIAGRAM FOR THE RADIATION MODEL

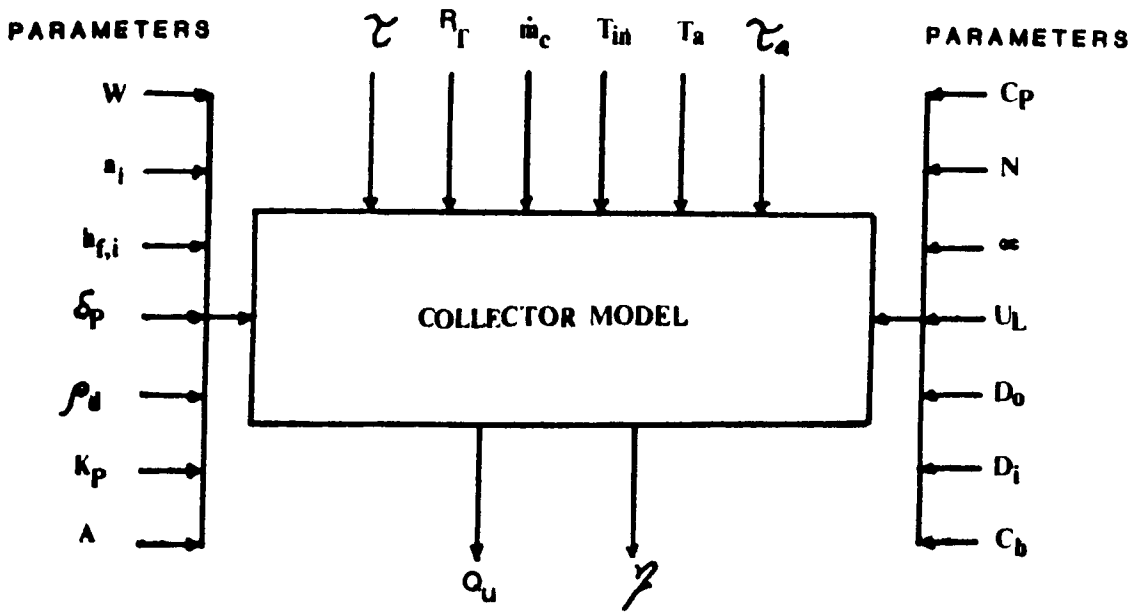

Figure 61

INFORMATION FLOW DIAGRAM FOR THE COLLECTOR MODEL

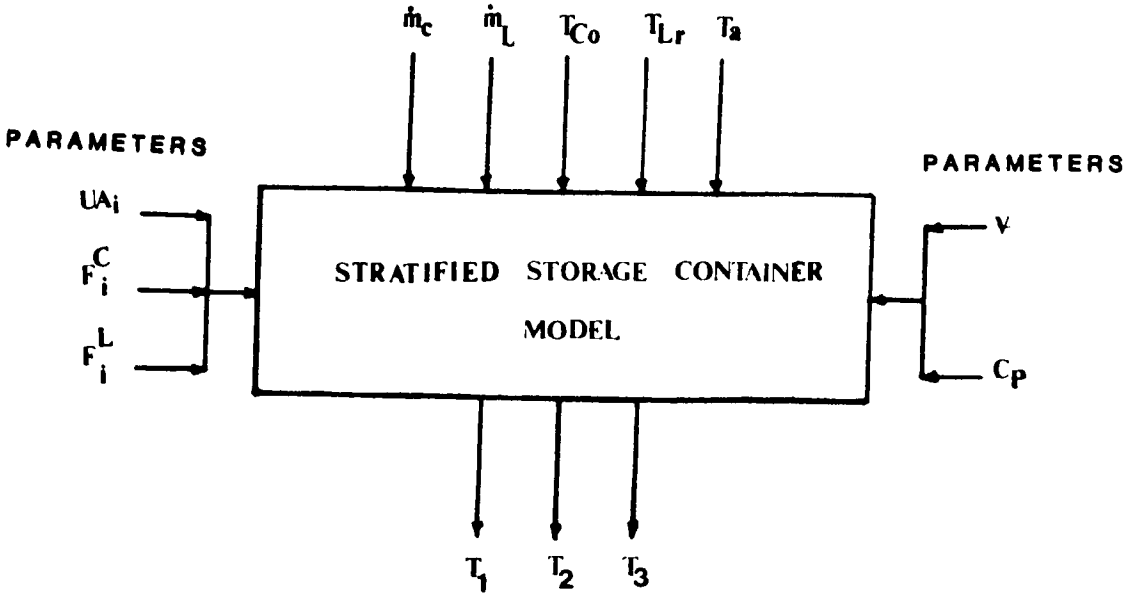

Figure 62

INFORMATION FLOW DIAGRAM FOR THE STRATIFIED STORAGE CONTAINER MODEL

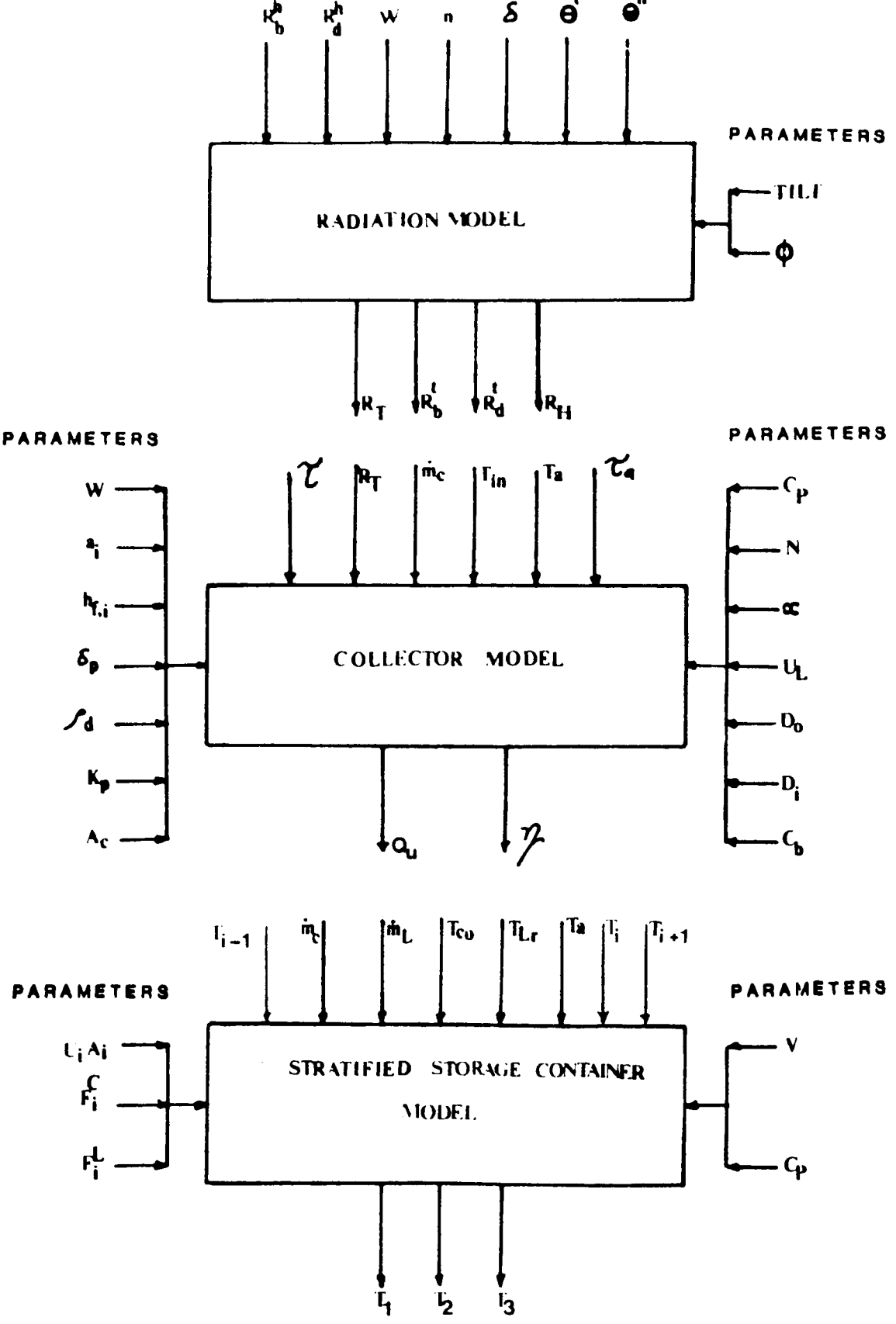

Figure 63

INFORMATION FLOW DIAGRAM FOR THE COMPUTER SYSTEM MODEL

represented as an arrow directed into the box. It is necessary to distinguish between several types of information flow which may occur in the information flow diagrams. The most obvious distinction is between information flowing into and that flowing out of a component. The set of information flowing out of a component, represented by outwardly directed arrows, is defined to be the output variable set for that component. For example the output variable for the collector model as shown in Figure 61, are Q_u, the rate of useful energy gain; η, the efficiency of the collector.

The information flowing into a component can be of three types:

1. Those pieces of information flowing into a component, which are output variables from any other component in the system, constitute what is defined to be the input variable set for the component. The input variables are those variables whose values may vary during the simulation. For a transient system, the input variables may vary with time. For example the input variables for the collector model as shown in Figure 61, represented by inwardly directed arrows are τ, the transmittance considering absorption and reflection; R_T, the solar radiation intensity; $\dot{m}_c$, the collector mass flow rate; T_{in}, the inlet fluid temperature; T_a, the ambient temperature; τ_a, the transmittance considering only absorption.

2. Those pieces of information which can be considered to be constant throughout the simulation and are of interest to the component form the parameters of the component. For example, the parameters for the collector model, as shown in Figure 61,

represented by side directed arrows are W, the distance between tube centres; a_i, the ratio of the overall loss coefficient to the loss coefficient from the i^{th} cover to the surrounding; $h_{f,i}$, the convection heat transfer coefficient between the fluid and the tube wall; δ_p, the plate thickness; ρ_d, the reflectance of the transparent covers for diffuse radiation; K_p, the plate conductivity; A_c, the collector area; c_p, the specific heat of fluid; N, the number of covers; α, the absorptance of the absorber plate; U_L, the collector overall loss coefficient; D_o, the outside tube diameter; D_i, the inside tube diameter; C_b, the bond conductivity.

3. Finally, the variable "time" which is neither an input variable nor a parameter, must be distinguished.

Output variables, Input variables, Parameters, and Time represent all of the types of information flow which may occur in the information flow diagram of a system.

CHAPTER 9 CONCLUSIONS AND SUGGESTIONS FOR FUTURE WORK

9.1 Present Investigation

The present investigation has involved a substantial experimental programme and the development of a computer system model for the prediction of system performance and to assist in the design of solar water heating systems.

9.1.1 Experimental Work

The experimental programme proceeded through several stages with results being presented as detailed in Chapter 6. Several conclusions may be drawn.

1. This work has demonstrated that it is possible to produce reliable and repeatable results using a low cost simulator. The design of the simulator was based on a relatively inexpensive micro-computer linking into a mains power regulator with an 8-bit digital control system. Meteorological data was used to compute radiation income on any inclined plane and the output to the power regulator is controlled by the computed instantaneous rate of energy gain from the collector system undergoing simulation.

   The simulator, or a modified version of it, could be used to simulate any solar water heating system , apart from the storage container; it is particularly useful in estimating long term system performance. Objective number 1 as

detailed in the introduction has therefore been accomplished, and was the subject of a paper which has been published[43].

2. Three domestic thermally stratified hot water storage containers were designed with the main object of improving and stabilizing thermal stratification of the stored water as a means of improving the overall efficiency of solar water heating systems. Testing of the three storage containers was carried out under similar conditions and the results showed that TYPE I storage container with a L/D equal to 3/1, behaves as a three-segment stratified system. TYPE II storage container with a L/D equal to 4/1, behaves as a two-segment stratified system with a thermocline occupying approximately half of the height of the storage container. TYPE III storage container with a L/D equal to 5/1, behaves as a two-segment stratified system with a thermocline occupying two thirds of the height of the storage container. It was found that TYPE I storage container gave the best result in terms of heat collected, and also had the maximum stratification which is the goal of this study. Therefore the long term system performance for TYPE I storage container was determined and the long term system efficiency was found to be of 52%.

3. The effect of each of three flow rates (0.01 kg/Sm^2), 0.015 kg/Sm^2, 0.02 kg/Sm^2) on stratification was studied and it was found that the flow rate of 0.01 kg/Sm^2 of collector area gave the better result. Objectives number 2, 3 as

detailed in the introduction have therefore been accomplished, and were the subjects of two papers which are going to be published in Sun at Work in Britain.

4. It is interesting to note that the general result of an L/D equal to 3:1 giving the better performance was within the range predicted by Lavan and Thompson[11] who suggest an L/D of between 3:1 and 4:1. These nearly similar results suggest that simple scale models may have further useful applications in solar storage work where the aim is to produce general trends concerning phenomena rather than detailed thermal behaviour as in this thesis.

9.1.2 Theoretical Work

A comparison has been made between some of the experimental and theoretical results for the TYPE I storage container using the two mathematical models of Duffie and Beckman[2], and Close[44]. Both models gave similar results, although both models underestimate the measured temperatures. Whilst the underestimate is on average less than $2^{o}C$, further work should be conducted to attempt to improve the accuracy of the model prediction. One area for further development could be the geometry of the storage container, and in particular the effect of length-to-diameter ratio on stratification. In addition the basis of their division of the tank into segments should be studied further (see 6.2.1). Duffie and Beckman[2], and Close[44] mathematical models are based on volume only, the shape of a container

surrounding this volume has not been considered. Therefore, if Duffie and Beckman[2], and Close[44] considered the geometrical shape of their volume container their theoretical prediction could possibly be closer to the experimental ones.

A computer system model has also been developed to assist in the design of solar water heating systems.

Objective number 4 as detailed in the introduction has therefore been accomplished, and will form the subject of an additional publication.

9.2 Suggestions for future work

1. The work so far has been carried out without taking into account draw-off profile. The future work should be directed toward the effect of draw-off on stratification and how draw-off would disturb stratification in the solar storage container. This study is required and worthwhile.

2. Study of the best draw off profile which maximises the heat collected from the storage container.

3. Study of methods which prevent kinetic disturbance of thermocline during fluid exchange such as diffuser designs, baffles, distributor and distribution manifold.

REFERENCES

1. Brumleve, T.D., "Sensible Heat Storage in Liquids", Sandia Lab. Energy Report, SLL-73-0263, 1974.

2. Duffie, J.A. and Beckman, W.A., "Solar Energy Thermal Processes", John Wiley, 1974.

3. Sharp, M.K. and Loehrke, R.I., "Stratified Thermal Storage in residential solar energy application", J. Energy, Vol. 3, No. 2, 1979.

4. Davis, E.S. and Bartera, R., "Stratification in solar water heaters storage tanks", proceedings of the workshop on solar energy storage sub-systems for heating and cooling, Virginia University, Charlottesville, U.S.A., 1975.

5. Brinkworth, B.J., "Thermal Storage in density-stratified fluids and phase-change material", Journal of the Institute of Energy, 193, 1979.

6. Sheridan, N.R., Bullock, K.M. and Duffie, J.A., "Study of solar processes by Analog Computer", Solar Energy, Vol. 11, No. 2, 1967.

7. Gutierrez, G., Hincapie, F., Duffie, J.A. and Beckman, W.A., "Simulation of forced circulation water heaters; Effects of Auxiliary Energy Supply, load type, and storage capacity", Solar Energy, Vol. 15, No. 4, 1974.

8. Loehrke, R.I., Gari, H.N., Sharp, M.K. and Haberstroh, R.D., "A passive technique for enhancing thermal stratification in liquid

storage tanks", ASME paper 78-HT-50, AIAA-ASME Thermophysics and Heat Transfer Conference, February, 1978.

9. Sharp, M.K. and Loehrke, R.I., "Stratified versus well-mixed sensible heat storage in a solar space heating application", ASME paper 78-HT-49, AIAA-ASME Thermophysics and Heat Transfer Conference, February, 1978.

10. Van Koppen, C.W.J., Fischer, L.S. and Dijkmans, I.A., "Stratification effects in the short and long term storage of solar heat", Sun-Mankinds future source of energy, ISES Conf., New Delhi, India, Vol. 1, 1978.

11. Lavan, Z. and Thompson, J., "Experimental study of thermally stratified hot water storage tanks", Solar Energy, Vol. 19, No. 5, 1977.

12. Carter, B., "Storing solar heated water without mixing the different temperatures of the flow from the collectors", Sun at Work in Britain, No. 7, 1978.

13. Brinkworth, B.J., "Active collection and use of Solar Energy", Sun at Work in Britain, No. 5, 1977.

14. Lin, E.I.H. and Sha, W.T., "Effects of Baffles on Thermal Stratification in Thermocline Storage Tanks", Silver Jubilee Congress, ISES Conf., ATLANTA, GEORGIA, U.S.A., Vol. 2, 1979.

15. Hamaker, J., Hoekstra, H.C.A., Van Koppen, C.W.J. and Van Wolde, J.T.T., "The Solar house of the Eindhoven University of Technology", Rep. WP53-77.6.R281, 1977.

16. Van Koppen, C.W.J., Simon Thomas, J.P. and Veltkamp, W.B., "The actual benefits of thermally stratified storage in a small and a medium size solar system", Silver Jubilee Congress, ISES Conf., ATLANTA, GEORGIA, U.S.A, Vol. 2, 1979.

17. Lin, E.I.H., Sha, W.T. and Michaels, A.I., "On thermal energy storage efficiency and the use of COMMIX-SA for its evaluation and enhancement", proceedings of Solar Energy Storage Options, SAN ANTONIO, TEXAS, U.S.A, Vol. 1, 1979.

18. Han, S.M. and Wu, S.T., "The effects of thermal stratification in water storage tank for the performance of a solar hot water system", proceedings of the fourteenth South Eastern seminar on Thermal Sciences, CAROLINA STATE UNIVERSITY, U.S.A., 1978.

19. Loehrke, R.I., Holzer, J.C., Gari, H.N., and Sharp, M.K., "Stratification Enhancement in Liquid Thermal Storage Tanks", J. Energy, Vol. 3, No. 3, 1978.

20. Brinkworth, B.,"Uses of Solar Energy", Chemistry in Britain, Vol. 11, 1975.

21. Page, J.K., "An interactive computer design methodology for the design of solar houses", Solar Energy for Building, RIBA, 1977.

22. Munroe, M.M., "Estimation of totals of irradiance on a horizontal surface from U.K. average meteorological data," Solar Energy, Vol. 24, No. 3, 1980.

23. Page, J.K., "The estimation of monthly mean values of daily short wave irradiation on vertical and inclined surfaces from sun shine records for latitudes 60°N - 40°S, B.S.32, University of Sheffield, 1976.

24. Heywood, H., "Solar Energy for Water and Space Heating", J. Inst. Fuel, 27, 1954.

25. Svendsen, D.A., "Some results of the measurement of inclined surface irradiance at Cardiff", UKISES Conference (C18) at the Royal Institution, 1979.

26. International Solar Energy Society - U.K. Section, U.K. Assessment, 1976.

27. Courtney, R.G., "An appraisal of solar water heating in the U.K.", BRE Current Paper CP7/76.

28. McVeigh, J.C., "Sun power - an introduction to the applications of solar energy", Pergamon, 1977.

29. Buchberg, H., Roulet, J.R., "Simulation and optimization of solar collection and storage for house heating", Solar Energy, Vol. 14, No. 3, 1973.

30. Log, G.O., Tybout, R.A., "Cost of house heating with solar energy", Solar Energy, Vol. 14, No. 3, 1973.

31. Courtney, R.G., "A computer study of solar water heating", BRE Current Paper CP 30/77.

32. Hottel, H.C. and Woertz, B.B., "Performance of flat-plate solar-heat collectors, ASME, Vol. 64, 1942.

33. Whillier, A., "Solar Energy Collection and its utilization for space heating", Ph.D. Thesis, Dept. of Mechanical Engineering, MIT, 1953.

34. Hottel, H.C. and Whillier, "Evaluation of Flate-Plate Solar Collector performance", Trans. of the Conference on the use of solar energy, Vol. II, Thermal processes, University of Arizona, 1955.

35. Klein, S.A., "The effects of thermal capacitance upon flat-plate solar collectors", M.S. Thesis, Dept. of Chemical Engineering, University of Wisconsin-Madison, 1973.

36. Klein, S.A., "Calculation of Flat-Plate Collector Loss Coefficients", Solar Energy, Vol. 17, No. 1, 1975.

37. Simon, F.F., "Flat-plate solar-collector performance evaluation with a solar simulator as a basis for collector selection and performance prediction", Solar Energy, Vol. 18, No. 5, 1976.

38. Kreith, F. and Kreider, J.F., "Principle of solar engineering", Hemisphere Publishing Corporation, 1978.

39. Hewitt, H.C., "Test for determining a best flow rate through solar collectors", J. Energy, Vol. 2, 1978.

40. Draft Standard Code of Practice - Solar Heating Systems for Domestic Hot Water, Document 78/75355DC, (British Standards Institution, London, 1978).

41. Tleimat, B.W., Howe, E.D. and Buckland, R.E., "A proposed method of rating the thermal performance of solar collectors", Solar Technology in the Seventies, ISES Conf., Winnipeg, Manitoba, Canada, Vol. 2, 1976.

42. Brinkworth, B.J., "Factors affecting the performance of solar water heating systems", Solar Technology for Building, Vol. 2, RIBA, 1977.

43. Bowman, N.T. and Eldessouky, E., "A low-cost simulator for studying the performance of solar energy storage containers", UKISES Conference, Solar Energy in the 80s: Technical and Economic Viability, University of Birmingham, 1980(Appendix 6).

44. Close, D.J., "A design approach for solar processes", Solar Energy, Vol. 11, No. 2, 1967.

45. Telkes, M., "Solar Energy Storage", Critical material problem in energy production, Academic Press, 1976.

46. Joy, P. and Shelpuk, B., "Solar Heating thermal storage feasibility", ASME paper 63-70-00, 1976.

47. Churchliff, W.A., "Solar Heated Buildings - a brief survey", 11th Edn. Cambridge, Massachussetts, 1975.

48. Szego, G.C., "Hot Water Storage Systems", proceedings of the workshop of solar energy storage sub-systems for heating and cooling, Virginia University, Charlottesville, U.S.A., 1975.

49. Bowman, N.T., Redferne, W.B. and Eldessouky, E., "Stratified Solar Storage for use in domestic scale systems", to be published in sun at work in Britain. (Appendix 7).

50. Jesch, L.F. and Soldatos, P., "Solar water heating: Engineering and Economic Analysis of a new Technology", Report No. 47, Dept. Mech. Eng., University of Birmingham, 1977.

51. Buckles, W.E., Klein, S.A. and Duffie, J.A., "Analysis of solar water heating systems", Silver Jubilee Congress, ISES Conf., ATLANTA, GEORGIA, U.S.A., Vol. 2, 1979.

52. Whittle, G.E. and Warren, P.R., "The efficiency of domestic hot water production out of the heating season", BRE Current paper CP44/78.

53. Klein, S.A., "Mathematical Model of Thermal Storage", proceedings of the workshop on solar energy storage sub-systems for heating and cooling. Virginia University, Charlottesville, U.S.A., 1975.

54. Whillier, A., "Solar Energy Collection and its utilization for house heating", DSc thesis, MIT, 1953.

55. Close, D.J., "The performance of solar water heaters with natural circulation", Solar Energy, Vol. 6, No. 1, 1962.

APPENDICES

CONTENTS

* publication

APPENDIX 1

TABLE 26. 15 March: useful energy and logic levels for mass flow rate = 0.01 kg/Sm^2

Time	Average hourly total of useful energy (KJ/m^2)	Average hourly total of useful energy for 5 m^2 collector (KJ)	Constant rate of energy delivery to provide the equivalent heating effect (W)	Logic level
6.30	0	0	0	-
6.40	10	50	13.9	-
6.50	21	105	29.2	-
7.00	34	170	47.2	-
7.10	48	240	66.7	17
7.20	64	320	88.9	20
7.30	83	415	115.3	24
7.40	112	560	155.6	29
7.50	156	780	216.7	36
8.00	216	1080	300.0	45
8.10	272	1360	377.8	53
8.20	334	1670	463.9	61
8.30	392	1960	544.4	67
8.40	436	2180	605.4	72
8.50	488	2440	677.8	78
9.00	534	2670	741.7	83
9.10	580	2900	805.6	88
9.20	630	3150	875.0	93
9.30	675	3375	937.5	98
9.40	718	3590	997.2	102
9.50	753	3765	1045.8	106
10.00	787	3935	1093.1	109
10.10	812	4060	1127.8	111
10.20	838	4190	1163.9	114
10.30	860	4300	1194.4	116
10.40	878	4390	1219.4	118
10.50	892	4460	1238.9	119

11.00	904	4520	1255.6	120
11.10	914	4570	1269.4	121
11.20	921	4605	1279.2	122
11.30	926	4630	1286.1	122
11.40	928	4640	1288.9	122
11.50	929	4645	1290.3	123
12.00	928	4640	1288.9	122
12.10	926	4630	1286.1	122
12.20	922	4610	1280.6	122
12.30	918	4590	1275.0	122
12.40	911	4555	1265.3	121
12.50	902	4510	1252.8	120
13.00	890	4450	1236.1	119
13.10	877	4385	1218.1	118
13.20	860	4300	1194.4	116
13.30	844	4220	1172.2	115
13.40	818	4090	1136.1	112
13.50	790	3950	1097.2	109
14.00	759	3795	1054.2	106
14.10	724	3620	1005.6	103
14.20	690	3450	958.3	100
14.30	656	3280	911.1	96
14.40	619	3095	859.7	92
14.50	586	2930	813.9	88
15.00	548	2740	761.1	84
15.10	510	2550	708.3	80
15.20	470	2350	652.8	76
15.30	428	2140	594.4	71
15.40	384	1920	533.3	66
15.50	340	1700	472.2	62
16.00	300	1500	416.7	57
16.10	254	1270	352.8	51
16.20	215	1075	298.6	45
16.30	178	890	247.2	40
16.40	140	700	194.4	34

16.50	105	525	145.8	28
17.00	75	375	104.2	22
17.10	45	225	62.5	16
17.20	20	100	27.8	-
17.30	0	0	0	-

TABLE 27. 15 March: useful energy and logic levels for mass flow rate = 0.015 kg/Sm^2

Time	Average hourly total of useful energy (KJ/m^2)	Average hourly total of useful energy for 5 m^2 collector (KJ)	Constant rate of energy delivery to provide the equivalent heating effect (W)	Logic level
6.30	0	0	0	-
6.40	9	45	12.5	-
6.50	20	100	27.8	-
7.00	34	170	47.2	-
7.10	49	245	68.1	17
7.20	66	330	91.7	21
7.30	85	425	118.1	24
7.40	110	550	152.8	29
7.50	150	750	208.3	35
8.00	201	1005	279.2	43
8.10	254	1270	352.8	51
8.20	326	1630	452.8	60
8.30	403	2015	559.7	68
8.40	458	2290	636.1	74
8.50	507	2535	704.2	80
9.00	558	2790	775.0	86
9.10	608	3040	844.4	91
9.20	657	3285	912.5	96
9.30	694	3470	963.9	100
9.40	736	3680	1022.2	104
9.50	773	3865	1073.6	108
10.00	804	4020	1116.7	110
10.10	830	4150	1152.8	113
10.20	857	4285	1190.3	116
10.30	884	4420	1227.8	118
10.40	902	4510	1252.8	120
10.50	918	4590	1275.0	122
11.00	931	4655	1293.1	123

11.10	941	4705	1306.9	124
11.20	948	4740	1316.7	124
11.30	952	4760	1322.2	125
11.40	954	4770	1325.0	125
11.50	956	4780	1327.8	125
12.00	955	4775	1326.4	125
12.10	953	4765	1323.6	125
12.20	949	4745	1318.1	125
12.30	944	4720	1311.1	124
12.40	934	4670	1297.2	123
12.50	923	4615	1281.9	122
13.00	912	4560	1266.7	121
13.10	900	4500	1250.0	120
13.20	886	4430	1230.6	119
13.30	868	4340	1205.6	117
13.40	842	4210	1169.4	114
13.50	814	4070	1130.6	111
14.00	782	3910	1086.1	108
14.10	746	3730	1036.1	105
14.20	712	3560	988.9	102
14.30	674	3370	936.1	98
14.40	634	3170	880.6	94
14.50	594	2970	825.0	89
15.00	558	2790	775.0	86
15.10	524	2620	727.8	82
15.20	480	2400	666.7	77
15.30	440	2200	611.1	73
15.40	397	1985	551.4	68
15.50	356	1780	494.4	64
16.00	309	1545	429.2	58
16.10	260	1300	361.1	52
16.20	223	1115	309.7	47
16.30	183	915	254.2	41
16.40	148	740	205.6	35
16.50	116	580	161.1	31
17.00	88	440	122.2	25
17.10	59	295	81.9	19
17.20	29	145	40.3	-
17.30	0	0	0	-

TABLE 28. 15 March: useful energy and logic levels for mass flow rate = 0.02 kg/Sm^2

Time	Average hourly total of useful energy (KJ/m^2)	Average hourly total of useful energy for 5 m^2 collector (KJ)	Constant rate of energy delivery to provide the equivalent heating effect (W)	Logic level
6.30	0	0	0	-
6.40	12	60	16.7	-
6.50	24	120	33.3	-
7.00	36	180	50.0	-
7.10	50	250	69.4	17
7.20	66	330	91.7	21
7.30	86	430	119.4	24
7.40	117	585	162.5	30
7.50	158	790	219.4	37
8.00	212	1060	294.4	45
8.10	283	1415	393.1	55
8.20	340	1700	472.2	62
8.30	409	2045	568.1	69
8.40	458	2290	636.1	74
8.50	506	2530	702.8	80
9.00	556	2780	772.2	86
9.10	608	3040	844.4	91
9.20	658	3290	913.9	96
9.30	704	3520	977.8	101
9.40	742	3710	1030.6	105
9.50	775	3875	1076.4	108
10.00	810	4050	1125.0	111
10.10	843	4215	1170.8	114
10.20	870	4350	1208.3	117
10.30	897	4485	1245.8	120
10.40	917	4585	1273.6	121
10.50	933	4665	1295.8	123

11.00	946	4730	1313.9	124
11.10	955	4775	1326.4	125
11.20	961	4805	1334.7	125
11.30	966	4830	1341.7	126
11.40	967	4835	1343.1	126
11.50	968	4840	1344.4	126
12.00	967	4835	1343.1	126
12.10	965	4825	1340.3	126
12.20	961	4805	1334.7	125
12.30	957	4785	1329.2	125
12.40	946	4730	1313.9	124
12.50	936	4680	1300.0	123
13.00	924	4620	1283.3	122
13.10	912	4560	1266.7	121
13.20	897	4485	1245.8	120
13.30	880	4400	1222.2	118
13.40	850	4250	1180.6	115
13.50	820	4100	1138.9	112
14.00	792	3960	1100.0	109
14.10	760	3800	1055.6	106
14.20	720	3600	1000.0	103
14.30	683	3415	948.6	99
14.40	640	3200	888.9	94
14.50	606	3030	841.7	90
15.00	564	2820	783.3	86
15.10	524	2620	727.8	82
15.20	488	2440	677.8	78
15.30	446	2230	619.4	73
15.40	408	2040	566.7	69
15.50	366	1830	508.3	64
16.00	324	1620	450.0	60
16.10	284	1420	394.4	55
16.20	236	1180	327.8	48
16.30	186	930	258.3	41
16.40	147	735	204.2	35
16.50	110	550	152.8	29

17.00	70	350	97.2	22
17.10	45	225	62.5	16
17.20	23	115	31.9	-
17.30	0	0	0	-

TABLE 29. 15 June: useful energy and logic levels for mass flow rate = 0.01 kg/Sm^2

Time	Average hourly total of useful energy (KJ/m^2)	Average hourly total of useful energy for 5 m^2 collector (KJ)	Constant rate of energy delivery to provide the equivalent heating effect (W)	Logic level
5.30	0	0	0	-
5.40	27	135	37.5	-
5.50	52	260	72.2	18
6.00	78	390	108.3	23
6.10	107	535	148.6	28
6.20	138	690	191.7	34
6.30	171	855	237.5	39
6.40	232	1160	322.2	48
6.50	258	1290	358.3	51
7.00	320	1600	444.4	59
7.10	398	1990	552.8	68
7.20	480	2400	666.7	77
7.30	574	2870	797.2	87
7.40	636	3180	883.3	93
7.50	700	3500	972.2	101
8.00	754	3770	1027.2	104
8.10	816	4080	1133.3	112
8.20	870	4350	1208.3	117
8.30	916	4580	1272.2	121
8.40	970	4850	1347.2	127
8.50	1024	5120	1422.2	130
9.00	1070	5350	1486.1	134
9.10	1114	5570	1547.2	138
9.20	1154	5770	1602.8	142
9.30	1189	5945	1651.4	145
9.40	1230	6150	1708.3	149
9.50	1260	6300	1750.0	152

10.00	1288	6440	1788.9	154
10.10	1312	6560	1822.2	156
10.20	1332	6660	1850.0	158
10.30	1350	6750	1875.0	160
10.40	1364	6820	1894.4	161
10.50	1376	6880	1911.1	162
11.00	1385	6925	1923.6	163
11.10	1395	6975	1937.5	164
11.20	1400	7000	1944.4	164
11.30	1405	7025	1951.4	164
11.40	1410	7050	1958.3	165
11.50	1413	7065	1962.5	165
12.00	1415	7075	1965.3	165
12.10	1414	7076	1963.9	165
12.20	1413	7065	1962.5	165
12.30	1411	7055	1959.7	165
12.40	1405	7025	1951.4	164
12.50	1397	6985	1940.3	164
13.00	1387	6935	1926.4	163
13.10	1372	6860	1905.6	162
13.20	1354	6770	1880.6	160
13.30	1331	6655	1848.6	158
13.40	1304	6520	1811.1	156
13.50	1278	6390	1775.0	153
14.00	1250	6250	1736.1	151
14.10	1220	6100	1694.4	148
14.20	1188	5940	1650.0	145
14.30	1154	5770	1602.8	142
14.40	1114	5570	1547.2	138
14.50	1076	5380	1494.4	135
15.00	1038	5190	1441.7	132
15.10	1002	5010	1391.7	129
15.20	962	4810	1336.1	126
15.30	919	4595	1276.4	122
15.40	870	4350	1208.3	117
15.50	820	4100	1138.9	112

16.00	780	3900	1083.3	108
16.10	730	3650	1013.9	103
16.20	680	3400	944.4	98
16.30	632	3160	877.8	93
16.40	560	2800	777.8	86
16.50	490	2450	680.6	78
17.00	440	2200	611.1	73
17.10	372	1860	516.7	65
17.20	320	1600	444.4	59
17.30	277	1385	384.7	54
17.40	240	1200	333.3	49
17.50	204	1020	283.3	44
18.00	170	850	236.1	39
18.10	144	720	200.0	35
18.20	122	610	169.4	31
18.30	102	510	141.7	28
18.40	82	410	113.9	24
18.50	64	320	88.9	20
19.00	47	235	65.3	17
19.10	32	160	44.4	-
19.20	16	80	22.2	-
19.30	0	0	0	-

TABLE 30. 15 June: useful energy and logic levels for mass flow rate = 0.015 kg/Sm^2

Time	Average hourly total of useful energy (KJ/m^2)	Average hourly total of useful energy for 5 m^2 collector (KJ)	Constant rate of energy delivery to provide the equivalent heating effect (W)	Logic level
5.30	0	0	0	-
5.40	16	80	22.2	-
5.50	45	225	62.5	16
6.00	60	300	83.3	19
6.10	90	450	125.0	25
6.20	130	650	180.5	32
6.30	175	875	243.1	40
6.40	236	1180	327.8	48
6.50	292	1460	405.6	56
7.00	355	1775	493.1	63
7.10	426	2130	591.6	71
7.20	500	2500	694.4	79
7.30	591	2955	820.8	89
7.40	660	3300	916.6	96
7.50	724	3620	1005.5	103
8.00	785	3925	1090.3	109
8.10	840	4200	1166.6	114
8.20	894	4470	1241.6	119
8.30	942	4710	1308.3	124
8.40	996	4980	1383.3	128
8.50	1046	5230	1452.7	132
9.00	1094	5470	1519.4	136
9.10	1142	5710	1586.1	141
9.20	1184	5920	1644.4	144
9.30	1223	6115	1698.6	148
9.40	1270	6350	1763.8	152
9.50	1304	6520	1811.1	156
10.00	1330	6650	1847.2	158

10.10	1350	6750	1875.0	160
10.20	1370	6850	1902.7	162
10.30	1388	6940	1927.8	163
10.40	1400	7000	1944.4	164
10.50	1410	7050	1958.3	165
11.00	1421	7105	1973.6	166
11.10	1429	7145	1984.7	167
11.20	1436	7180	1994.4	168
11.30	1444	7220	2005.6	168
11.40	1448	7240	2011.1	169
11.50	1453	7265	2018.1	169
12.00	1455	7275	2020.8	169
12.10	1458	7290	2025.0	170
12.20	1456	7280	2022.2	170
12.30	1451	7255	2015.3	169
12.40	1446	7230	2008.3	168
12.50	1440	7200	2000.0	168
13.00	1430	7150	1986.1	167
13.10	1414	7070	1963.8	165
13.20	1394	6970	1936.1	164
13.30	1369	6845	1901.4	161
13.40	1340	6700	1861.1	159
13.50	1314	6570	1825.0	156
14.00	1284	6420	1783.3	154
14.10	1250	6250	1736.1	151
14.20	1220	6100	1694.4	148
14.30	1186	5930	1647.2	145
14.40	1148	5740	1594.4	142
14.50	1110	5550	1541.6	138
15.00	1074	5370	1491.6	135
15.10	1032	5160	1433.3	131
15.20	990	4950	1375.0	128
15.30	945	4725	1312.5	124
15.40	900	4500	1250.0	120
15.50	852	4260	1183.3	115
16.00	800	4000	1111.1	110

16.10	752	3760	1044.4	106
16.20	704	3520	977.7	101
16.30	650	3250	902.8	95
16.40	580	2900	805.5	88
16.50	520	2600	722.2	82
17.00	450	2250	625.0	74
17.10	392	1960	544.4	67
17.20	334	1670	463.8	61
17.30	285	1425	395.8	55
17.40	234	1170	325.0	48
17.50	200	1000	277.7	43
18.00	172	860	238.8	39
18.10	146	730	202.7	35
18.20	124	620	172.2	31
18.30	105	525	145.8	28
18.40	84	420	116.6	24
18.50	64	320	88.8	20
19.00	46	230	63.8	16
19.10	30	150	41.6	-
19.20	14	70	19.4	-
19.30	0	0	0	-

TABLE 31. 15 June: useful energy and logic levels for mass flow rate = 0.02 kg/Sm^2

Time	Average hourly total of useful energy (KJ/m^2)	Average hourly total of useful energy for 5 m^2 collector (KJ)	Constant rate of energy delivery to provide the equivalent heating effect (W)	Logic level
5.30	0	0	0	-
5.40	20	100	27.7	-
5.50	50	250	69.4	17
6.00	80	400	111.1	23
6.10	110	550	152.7	29
6.20	140	700	194.4	34
6.30	178	890	247.2	40
6.40	220	1100	305.5	46
6.50	270	1350	375.0	53
7.00	340	1700	472.2	62
7.10	420	2100	583.3	71
7.20	500	2500	694.4	79
7.30	599	2995	831.9	90
7.40	670	3350	930.5	97
7.50	740	3700	1027.7	104
8.00	806	4030	1119.4	111
8.10	866	4330	1202.7	117
8.20	920	4600	1277.7	122
8.30	955	4775	1326.4	125
8.40	1010	5050	1402.7	129
8.50	1060	5300	1472.2	133
9.00	1106	5530	1536.1	138
9.10	1150	5750	1597.2	142
9.20	1200	6000	1666.6	146
9.30	1240	6200	1722.2	150
9.40	1276	6380	1772.2	153
9.50	1306	6530	1813.8	156

10.00	1330	6650	1847.2	158
10.10	1358	6790	1886.1	160
10.20	1384	6920	1922.2	163
10.30	1407	7035	1954.2	165
10.40	1420	7100	1972.2	166
10.50	1430	7150	1986.1	167
11.00	1440	7200	2000.0	168
11.10	1450	7250	2013.8	169
11.20	1456	7280	2022.2	170
11.30	1464	7320	2033.3	170
11.40	1468	7340	2038.8	171
11.50	1472	7360	2044.4	171
12.00	1474	7370	2047.2	171
12.10	1474	7370	2047.2	171
12.20	1473	7365	2045.8	171
12.30	1471	7355	2043.1	171
12.40	1460	7300	2027.7	170
12.50	1450	7250	2013.8	169
13.00	1436	7180	1994.4	168
13.10	1422	7110	1975.0	166
13.20	1406	7030	1952.7	164
13.30	1388	6940	1927.7	163
13.40	1370	6850	1902.7	161
13.50	1346	6730	1869.4	159
14.00	1318	6590	1830.5	157
14.10	1284	6420	1783.3	154
14.20	1248	6420	1733.3	151
14.30	1203	6015	1670.8	146
14.40	1166	5830	1619.4	143
14.50	1124	5620	1561.1	139
15.00	1080	5400	1500.0	135
15.10	1046	5230	1452.7	132
15.20	1002	5010	1391.6	128
15.30	958	4790	1330.5	125
15.40	914	4570	1269.4	121
15.50	870	4350	1208.3	117

16.00	820	4100	1138.8	112
16.10	774	3870	1075.0	108
16.20	720	3600	1000.0	103
16.30	659	3295	915.3	96
16.40	570	2850	791.6	87
16.50	490	2450	680.5	78
17.00	430	2150	597.2	72
17.10	380	1900	527.7	66
17.20	330	1650	458.3	61
17.30	289	1420	394.4	55
17.40	242	1210	336.1	49
17.50	206	1030	286.1	44
18.00	176	880	244.4	40
18.10	150	750	208.3	35
18.20	126	630	175.0	32
18.30	106	530	147.2	28
18.40	84	420	116.6	24
18.50	66	330	91.6	21
19.00	50	250	69.4	17
19.10	34	170	47.2	-
19.20	18	90	25.0	-
19.30	0	0	0	-

TABLE 32. 15 December: useful energy and logic levels for mass flow rate = 0.01 kg/Sm^2

Time	Average hourly total of useful energy (KJ/m^2)	Average hourly total of useful energy for 5 m^2 collector (KJ)	Constant rate of energy delivery to provide the equivalent heating effect (W)	Logic level
8.30	0	0	0	-
8.40	28	140	38.9	-
8.50	60	300	83.3	19
9.00	94	470	130.6	26
9.10	124	620	172.2	31
9.20	162	810	225.0	38
9.30	197	985	273.6	43
9.40	234	1170	325.0	48
9.50	271	1355	376.4	53
10.00	306	1530	425.0	58
10.10	338	1690	469.4	62
10.20	364	1820	505.6	64
10.30	385	1925	534.7	66
10.40	400	2000	555.0	68
10.50	412	2060	572.2	70
11.00	423	2115	587.2	71
11.10	432	2160	600.0	71
11.20	438	2190	608.3	72
11.30	444	2220	616.6	73
11.40	450	2250	625.0	74
11.50	453	2265	629.1	74
12.00	455	2275	631.9	74
12.10	456	2280	633.3	74
12.20	455	2275	631.9	74
12.30	451	2255	626.4	74
12.40	444	2220	616.6	73
12.50	434	2170	602.7	72
13.00	422	2110	586.1	71

13.10	408	2040	566.6	69
13.20	392	1960	544.4	67
13.30	373	1865	518.1	65
13.40	354	1770	491.7	64
13.50	332	1660	461.1	61
14.00	308	1540	427.8	58
14.10	284	1420	394.4	55
14.20	258	1290	358.3	51
14.30	229	1145	318.1	48
14.40	200	1000	277.8	43
14.50	160	800	222.2	37
15.00	124	620	172.2	31
15.10	82	410	113.9	24
15.20	44	220	61.1	-
15.30	0	0	0	-

TABLE 33. 15 December: useful energy and logic levels for mass flow rate = 0.015 kg/Sm^2

Time	Average hourly total of useful energy (KJ/m^2)	Average hourly total of useful energy for 5 m^2 collector (KJ)	Constant rate of energy delivery to provide the equivalent heating effect (W)	Logic level
8.30	0	0	0	-
8.40	38	190	52.8	-
8.50	70	350	97.2	21
9.00	100	500	138.9	27
9.10	138	650	180.6	32
9.20	170	850	236.1	39
9.30	203	1015	281.9	44
9.40	236	1180	327.8	48
9.50	270	1350	375.0	53
10.00	304	1520	422.2	57
10.10	338	1690	469.4	62
10.20	368	1840	511.1	64
10.30	396	1980	550.0	68
10.40	410	2050	569.4	69
10.50	424	2120	588.9	71
11.00	435	2175	604.2	72
11.10	444	2220	616.7	73
11.20	451	2255	626.4	74
11.30	456	2280	633.3	74
11.40	461	2305	640.3	75
11.50	465	2325	645.8	75
12.00	467	2335	648.6	76
12.10	468	2340	650.0	76
12.20	467	2335	648.6	76
12.30	464	2320	644.4	75
12.40	458	2290	636.1	74
12.50	450	2250	625.0	74
13.00	438	2190	603.3	72

13.10	422	2110	586.1	71
13.20	404	2020	561.1	69
13.30	384	1925	534.7	66
13.40	364	1820	505.5	64
13.50	341	1705	473.6	62
14.00	318	1590	441.6	59
14.10	292	1460	405.5	56
14.20	264	1320	366.6	52
14.30	235	1175	326.4	48
14.40	200	1000	277.7	43
14.50	160	800	222.2	37
15.00	120	600	166.6	31
15.10	80	400	111.1	23
15.20	40	200	55.5	-
15.30	0	0	0	-

TABLE 34. 15 December: useful energy and logic levels for mass flow rate = 0.02 kg/Sm^2

Time	Average hourly total of useful energy (KJ/m^2)	Average hourly total of useful energy for 5 m^2 collector (KJ)	Constant rate of energy delivery to provide the equivalent heating effect (W)	Logic level
8.30	0	0	0	-
8.40	32	160	44.4	-
8.50	66	330	91.6	21
9.00	100	500	138.8	27
9.10	132	660	183.3	33
9.20	172	860	238.8	39
9.30	206	1030	286.1	44
9.40	244	1220	338.8	49
9.50	278	1390	386.1	54
10.00	312	1560	433.3	58
10.10	346	1730	480.5	63
10.20	378	1890	525.0	65
10.30	401	2005	556.9	68
10.40	418	2090	580.5	70
10.50	430	2150	597.2	72
11.00	440	2200	611.1	73
11.10	450	2250	625.0	74
11.20	456	2280	633.3	74
11.30	463	2315	643.1	75
11.40	468	2340	650.0	76
11.50	472	2360	655.5	76
12.00	473	2365	656.9	76
12.10	474	2370	658.3	76
12.20	473	2365	656.9	76
12.30	470	2350	652.7	76
12.40	462	2310	641.6	75
12.50	454	2270	630.5	74
13.00	442	2210	613.8	73

13.10	429	2145	595.8	72
13.20	412	2060	572.2	70
13.30	389	1945	540.3	67
13.40	370	1850	513.8	65
13.50	344	1720	477.7	63
14.00	320	1600	444.4	60
14.10	294	1470	408.3	56
14.20	266	1330	369.4	52
14.30	239	1195	331.9	49
14.40	206	1030	286.1	44
14.50	172	860	238.8	39
15.00	132	660	183.3	33
15.10	86	430	119.4	24
15.20	40	200	55.5	-
15.30	0	0	0	-

TABLE 35. 15 January: useful energy and logic levels for mass flow rate = 0.01 kg/Sm^2

Time	Average hourly total of useful energy (KJ/m^2)	Average hourly total of useful energy for 5 m^2 collector (KJ)	Constant rate of energy delivery to provide the equivalent heating effect (W)	Logic level
7.30	0	0	0	-
7.40	40	200	55.5	16
7.50	86	430	119.4	24
8.00	124	620	172.2	31
8.10	160	800	222.2	37
8.20	194	970	269.4	42
8.30	227	1135	315.3	47
8.40	254	1270	352.8	51
8.50	280	1400	388.9	54
9.00	306	1530	425.0	58
9.10	333	1665	462.5	61
9.20	357	1785	495.8	63
9.30	380	1900	527.7	66
9.40	402	2010	558.3	68
9.50	423	2115	587.5	71
10.00	441	2205	612.5	73
10.10	458	2290	636.1	75
10.20	474	2370	658.3	76
10.30	486	2430	675.0	78
10.40	494	2470	686.1	79
10.50	497	2485	690.2	79
11.00	498	2490	691.6	79
11.10	498	2490	691.6	79
11.20	497	2485	690.2	79
11.30	494	2470	686.1	78
11.40	488	2440	677.7	78
11.50	482	2410	669.4	77
12.00	471	2355	654.2	75

12.10	460	2300	638.8	75
12.20	444	2220	616.6	73
12.30	424	2120	588.8	71
12.40	404	2020	561.1	69
12.50	380	1900	527.7	66
13.00	354	1770	491.6	63
13.10	326	1630	452.7	60
13.20	296	1480	411.1	56
13.30	260	1300	361.0	52
13.40	220	1100	305.5	46
13.50	176	880	244.4	40
14.00	132	660	183.3	33
14.10	88	440	122.2	25
14.20	44	220	61.0	16
14.30	0	0	0	-

TABLE 36. 15 February: useful energy and logic levels for mass flow rate = 0.01 kg/Sm^2

Time	Average hourly total of useful energy (KJ/m^2)	Average hourly total of useful energy for 5 m^2 collector (KJ)	Constant rate of energy delivery to provide the equivalent heating effect (W)	Logic level
7.30	0	0	0	-
7.40	20	100	27.7	-
7.50	40	200	55.5	16
8.00	60	300	83.3	19
8.10	82	410	113.9	24
8.20	106	530	147.2	28
8.30	130	650	180.5	32
8.40	160	800	222.2	37
8.50	194	970	269.4	42
9.00	232	1160	322.2	48
9.10	282	1410	391.6	54
9.20	325	1625	451.4	60
9.30	369	1845	512.5	64
9.40	400	2000	555.5	68
9.50	430	2150	597.2	72
10.00	464	2320	644.4	75
10.10	500	2500	694.4	79
10.20	530	2650	736.1	83
10.30	561	2805	779.2	86
10.40	588	2940	816.6	89
10.50	610	3050	847.2	91
11.00	628	3140	872.2	93
11.10	643	3215	893.1	94
11.20	653	3265	906.9	95
11.30	660	3300	916.6	96
11.40	662	3310	919.4	96
11.50	663	3315	920.8	96
12.00	662	3310	919.4	96

12.10	659	3295	915.2	96
12.20	655	3275	909.7	96
12.30	647	3235	898.6	95
12.40	638	3190	886.1	94
12.50	628	3140	872.2	93
13.00	615	3075	854.2	91
13.10	600	3000	833.3	90
13.20	584	2920	811.1	88
13.30	559	2795	776.4	86
13.40	534	2670	741.6	83
13.50	508	2540	705.5	80
14.00	484	2420	672.2	78
14.10	460	2300	638.8	75
14.20	432	2160	600.0	71
14.30	403	2015	559.7	68
14.40	368	1840	511.1	64
14.50	334	1670	463.8	61
15.00	300	1500	416.6	56
15.10	264	1320	366.6	52
15.20	226	1130	313.8	47
15.30	187	935	259.7	41
15.40	152	760	211.1	36
15.50	118	590	163.8	30
16.00	84	420	116.6	24
16.10	52	260	72.2	18
16.20	25	125	34.7	-
16.30	0	0	0	-

TABLE 37. 15 April: useful energy and logic levels for mass flow rate = 0.01 kg/Sm^2

Time	Average hourly total of useful energy (KJ/m^2)	Average hourly total of useful energy for 5 m^2 collector (KJ)	Constant rate of energy delivery to provide the equivalent heating effect (W)	Logic level
6.30	0	0	0	-
6.40	46	230	63.9	16
6.50	87	435	120.8	25
7.00	132	660	183.3	33
7.10	177	885	245.8	40
7.20	226	1130	313.8	47
7.30	268	1340	372.2	53
7.40	318	1590	441.6	59
7.50	368	1840	511.1	64
8.00	420	2100	583.3	71
8.10	466	2330	647.2	75
8.20	520	2600	722.2	82
8.30	567	2835	787.5	87
8.40	610	3050	847.2	91
8.50	649	3245	901.4	95
9.00	686	3430	952.8	99
9.10	720	3600	1000.0	103
9.20	754	3770	1047.2	106
9.30	783	3915	1087.5	108
9.40	813	4065	1129.2	111
9.50	840	4200	1166.6	114
10.00	864	4320	1200.0	116
10.10	887	4435	1231.9	119
10.20	907	4535	1259.7	120
10.30	924	4620	1283.3	122
10.40	940	4700	1305.5	124
10.50	954	4770	1325.0	125
11.00	968	4840	1344.0	126

11.10	980	4900	1361.0	127
11.20	990	4950	1375.0	128
11.30	1000	5000	1388.8	128
11.40	1009	5045	1401.4	128
11.50	1016	5080	1411.1	129
12.00	1020	5100	1416.6	130
12.10	1024	5120	1422.2	130
12.20	1026	5130	1425.0	130
12.30	1027	5135	1426.4	130
12.40	1021	5105	1418.1	130
12.50	1011	5055	1404.1	129
13.00	1000	5000	1388.8	128
13.10	988	4940	1372.2	128
13.20	972	4860	1350.0	127
13.30	953	4765	1323.6	125
13.40	931	4655	1293.1	123
13.50	908	4540	1261.1	121
14.00	884	4420	1227.7	118
14.10	858	4290	1191.6	116
14.20	830	4150	1152.7	113
14.30	801	4005	1112.5	110
14.40	774	3870	1075.0	108
14.50	742	3710	1030.5	105
15.00	710	3550	986.1	102
15.10	676	3380	938.8	98
15.20	636	3180	883.3	94
15.30	594	2970	825.0	89
15.40	550	2750	763.8	85
15.50	502	2510	697.2	79
16.00	446	2230	619.4	73
16.10	408	2040	566.6	69
16.20	360	1800	500.0	64
16.30	312	1560	433.3	58
16.40	266	1330	369.4	52
16.50	216	1080	300.0	46

17.00	162	810	225.0	38
17.10	110	550	152.7	29
17.20	59	295	81.9	19
17.30	0	0	0	-

TABLE 38. 15 May: useful energy and logic levels for mass flow rate = 0.01 kg/Sm^2

Time	Average hourly total of useful energy (KJ/m^2)	Average hourly total of useful energy for 5 m^2 collector (KJ)	Constant rate of energy delivery to provide the equivalent heating effect (W)	Logic level
5.30	0	0	0	-
5.40	12	60	16.6	-
5.50	24	120	33.3	-
6.00	36	180	50.0	16
6.10	48	240	66.6	17
6.20	61	305	84.7	20
6.30	74	370	102.8	22
6.40	92	460	127.7	25
6.50	118	590	163.8	30
7.00	166	830	230.5	38
7.10	246	1230	341.6	50
7.20	356	1780	494.4	63
7.30	452	2260	627.7	74
7.40	532	2660	738.8	83
7.50	590	2950	819.4	89
8.00	644	3220	894.4	94
8.10	700	3500	972.2	101
8.20	750	3750	1041.6	106
8.30	794	3970	1102.7	110
8.40	845	4225	1173.6	115
8.50	886	4430	1230.5	119
9.00	924	4620	1283.3	122
9.10	962	4810	1336.1	126
9.20	998	4990	1386.1	128
9.30	1042	5210	1447.2	132
9.40	1070	5350	1486.1	134
9.50	1100	5500	1527.7	137
10.00	1126	5630	1563.8	139

10.10	1150	5750	1597.2	142
10.20	1174	5870	1630.5	144
10.30	1196	5975	1659.7	145
10.40	1220	6100	1694.4	148
10.50	1239	6195	1720.8	150
11.00	1254	6270	1741.6	151
11.10	1267	6335	1759.7	152
11.20	1278	6390	1775.0	153
11.30	1285	6425	1784.7	154
11.40	1290	6450	1791.6	154
11.50	1293	6465	1795.8	155
12.00	1295	6475	1798.6	155
12.10	1296	6480	1800.0	155
12.20	1294	6470	1797.2	155
12.30	1291	6455	1793.1	155
12.40	1279	6395	1776.4	153
12.50	1265	6325	1756.9	152
13.00	1249	6245	1734.7	151
13.10	1230	6150	1708.3	149
13.20	1209	6045	1679.2	147
13.30	1186	5930	1647.2	145
13.40	1165	5825	1618.1	143
13.50	1142	5710	1586.1	141
14.00	1118	5590	1552.7	139
14.10	1094	5470	1519.4	137
14.20	1067	5335	1481.9	134
14.30	1036	5180	1438.8	131
14.40	1000	5000	1388.9	128
14.50	958	4790	1330.5	125
15.00	920	4600	1277.8	122
15.10	877	4385	1218.1	118
15.20	836	4180	1161.0	114
15.30	790	3950	1097.2	109
15.40	742	3710	1030.5	105
15.50	697	3485	968.1	100

16.00	648	3240	900.0	95
16.10	605	3025	840.3	90
16.20	558	2790	775.0	86
16.30	516	2580	716.6	81
16.40	440	2200	611.0	73
16.50	376	1880	522.0	65
17.00	315	1575	437.5	59
17.10	258	1290	358.3	51
17.20	212	1060	294.4	45
17.30	172	860	238.8	39
17.40	144	720	200.0	35
17.50	114	570	158.3	30
18.00	84	420	116.6	24
18.10	56	280	77.8	18
18.20	28	140	38.9	-
18.30	0	0	0	-

TABLE 39. 15 July: useful energy and logic levels for mass flow rate = 0.01 kg/Sm^2

Time	Average hourly total of useful energy (KJ/m^2)	Average hourly total of useful energy for 5 m^2 collector (KJ)	Constant rate of energy delivery to provide the equivalent heating effect (W)	Logic level
5.30	0	0	0	-
5.40	18	90	25.0	-
5.50	40	200	55.5	16
6.00	66	330	91.6	21
6.10	98	490	136.0	27
6.20	138	690	191.6	34
6.30	190	950	263.8	42
6.40	238	1190	330.5	49
6.50	292	1460	405.5	56
7.00	350	1750	486.1	63
7.10	414	2070	575.0	70
7.20	478	2380	661.0	77
7.30	540	2700	750.0	84
7.40	594	2970	825.0	89
7.50	650	3250	902.7	95
8.00	708	3540	983.3	101
8.10	756	3780	1050.0	106
8.20	806	4030	1119.4	111
8.30	854	4280	1188.8	115
8.40	900	4500	1250.0	120
8.50	944	4720	1311.1	124
9.00	988	4940	1372.2	128
9.10	1028	5140	1427.7	130
9.20	1066	5330	1480.5	134
9.30	1106	5530	1536.1	137
9.40	1136	5680	1577.7	140
9.50	1164	5820	1616.6	143
10.00	1188	5940	1650.0	145

10.10	1211	6055	1681.9	147
10.20	1230	6150	1708.3	149
10.30	1244	6220	1727.7	150
10.40	1256	6280	1744.4	151
10.50	1264	6320	1755.5	152
11.00	1272	6360	1766.6	153
11.10	1278	6390	1775.0	153
11.20	1285	6425	1784.7	154
11.30	1290	6450	1791.6	154
11.40	1297	6485	1801.3	155
11.50	1302	6510	1808.3	155
12.00	1308	6540	1816.6	156
12.10	1311	6555	1820.8	156
12.20	1314	6570	1825.0	156
12.30	1314	6570	1825.0	156
12.40	1312	6560	1822.2	156
12.50	1304	6520	1811.1	155
13.00	1292	6460	1794.4	154
13.10	1280	6400	1777.7	153
13.20	1265	6325	1756.9	152
13.30	1247	6235	1731.9	151
13.40	1232	6160	1711.1	149
13.50	1214	6070	1686.1	147
14.00	1194	5970	1658.3	145
14.10	1170	5850	1625.0	143
14.20	1144	5720	1588.8	141
14.30	1116	5580	1550.0	139
14.40	1084	5420	1505.5	136
14.50	1046	5230	1452.7	132
15.00	1010	5050	1402.7	129
15.10	977	4885	1356.9	127
15.20	944	4720	1311.1	124
15.30	902	4510	1252.7	120
15.40	860	4300	1194.4	116
15.50	814	4070	1130.5	111
16.00	770	3850	1069.4	107

16.10	724	3620	1005.5	103
16.20	674	3370	936.1	98
16.30	616	3080	855.5	91
16.40	550	2750	763.8	85
16.50	490	2450	680.5	78
17.00	430	2150	597.2	71
17.10	376	1880	522.2	65
17.20	330	1650	458.3	60
17.30	296	1480	411.1	56
17.40	264	1320	366.6	52
17.50	234	1170	325.0	48
18.00	208	1040	288.8	44
18.10	184	920	255.5	41
18.20	158	790	219.4	37
18.30	133	665	184.7	33
18.40	105	525	145.8	28
18.50	80	400	111.1	23
19.00	58	290	80.5	19
19.10	36	180	50.0	16
19.20	18	90	25.0	-
19.30	0	0	0	-

TABLE 40. 15 August: useful energy and logic levels for mass flow rate = 0.01 kg/Sm^2

Time	Average hourly total of useful energy (KJ/m^2)	Average hourly total of useful energy for 5 m^2 collector (KJ)	Constant rate of energy delivery to provide the equivalent heating effect (W)	Logic level
5.30	0	0	0	-
5.40	22	110	30.6	-
5.50	44	220	61.1	16
6.00	68	340	94.4	21
6.10	94	470	130.6	26
6.20	120	600	166.7	30
6.30	144	720	200.0	35
6.40	178	890	247.2	40
6.50	213	1065	295.8	45
7.00	255	1275	354.2	51
7.10	320	1600	444.4	59
7.20	402	2010	558.3	61
7.30	486	2430	675.0	70
7.40	545	2725	756.9	84
7.50	594	2970	825.0	89
8.00	650	3250	902.8	95
8.10	708	3540	983.3	101
8.20	768	3840	1066.7	107
8.30	815	4075	1131.9	112
8.40	870	4350	1208.3	117
8.50	912	4560	1266.7	121
9.00	953	4765	1323.6	125
9.10	997	4985	1384.7	128
9.20	1040	5200	1444.4	131
9.30	1082	5410	1502.8	135
9.40	1104	5520	1533.3	137
9.50	1124	5620	1561.1	139
10.00	1142	5710	1586.1	141

10.10	1158	5790	1608.3	143
10.20	1174	5870	1630.6	144
10.30	1188	5940	1650.0	145
10.40	1204	6020	1672.2	146
10.50	1216	6080	1688.8	147
11.00	1227	6135	1704.2	149
11.10	1237	6185	1718.1	149
11.20	1245	6225	1729.2	150
11.30	1252	6260	1738.8	151
11.40	1255	6275	1743.1	151
11.50	1257	6285	1745.8	152
12.00	1258	6290	1747.2	152
12.10	1257	6285	1745.8	151
12.20	1254	6270	1741.7	151
12.30	1249	6245	1734.7	151
12.40	1242	6210	1725.0	150
12.50	1232	6160	1711.1	149
13.00	1220	6100	1694.4	148
13.10	1206	6030	1675.0	147
13.20	1189	5945	1651.3	145
13.30	1167	5835	1620.8	143
13.40	1140	5700	1583.3	141
13.50	1112	5560	1544.4	138
14.00	1084	5420	1505.5	136
14.10	1056	5280	1466.6	133
14.20	1030	5150	1430.5	131
14.30	1001	5005	1390.3	129
14.40	974	4870	1352.8	127
14.50	946	4730	1313.9	124
15.00	916	4580	1272.2	121
15.10	882	4410	1225.0	118
15.20	850	4250	1180.5	116
15.30	816	4080	1133.3	112
15.40	776	3880	1077.7	108
15.50	724	3620	1005.5	103
16.00	678	3390	941.7	98

16.10	632	3160	877.7	93
16.20	583	2915	809.7	88
16.30	532	2660	738.8	83
16.40	480	2400	666.6	77
16.50	424	2120	588.8	71
17.00	380	1900	527.8	66
17.10	337	1685	468.1	62
17.20	290	1450	402.8	55
17.30	249	1245	345.8	50
17.40	202	1010	280.6	44
17.50	164	820	227.7	38
18.00	124	620	172.2	31
18.10	81	405	112.5	23
18.20	40	200	55.5	16
18.30	0	0	0	-

TABLE 41. 15 September: useful energy and logic levels for mass flow rate = 0.01 kg/Sm^2

Time	Average hourly total of useful energy (KJ/m^2)	Average hourly total of useful energy for 5 m^2 collector (KJ)	Constant rate of energy delivery to provide the equivalent heating effect (W)	Logic level
5.30	0	0	0	-
5.40	11	55	15.2	-
5.50	22	110	30.6	-
6.00	34	170	47.2	-
6.10	46	230	63.9	16
6.20	60	300	83.3	19
6.30	77	385	106.9	23
6.40	95	475	131.9	26
6.50	122	610	169.4	31
7.00	174	870	241.6	39
7.10	234	1170	325.0	48
7.20	305	1525	423.6	58
7.30	366	1830	508.3	64
7.40	420	2100	583.3	71
7.50	475	2375	659.7	77
8.00	532	2660	738.8	83
8.10	594	2970	825.0	89
8.20	660	3300	916.6	96
8.30	718	3590	997.2	102
8.40	774	3870	1075.0	108
8.50	836	4180	1161.0	114
9.00	895	4475	1243.0	119
9.10	950	4750	1319.4	125
9.20	998	4990	1386.0	128
9.30	1050	5250	1458.3	132
9.40	1080	5400	1500.0	135
9.50	1110	5550	1541.6	138
10.00	1135	5675	1576.3	140

10.10	1160	5800	1611.0	143
10.20	1184	5920	1644.0	144
10.30	1210	6050	1680.5	147
10.40	1230	6150	1708.3	149
10.50	1247	6235	1731.9	151
11.00	1260	6300	1750.0	152
11.10	1272	6360	1766.0	152
11.20	1282	6410	1780.5	154
11.30	1288	6440	1788.8	154
11.40	1292	6460	1794.4	154
11.50	1293	6465	1795.8	154
12.00	1292	6460	1794.4	154
12.10	1290	6450	1791.6	154
12.20	1286	6430	1786.1	154
12.30	1280	6400	1777.7	153
12.40	1266	6330	1758.3	152
12.50	1250	6250	1736.1	151
13.00	1234	6170	1713.8	149
13.10	1218	6090	1691.6	148
13.20	1200	6000	1666.6	146
13.30	1176	5880	1633.3	144
13.40	1152	5760	1600.0	142
13.50	1123	5615	1559.7	139
14.00	1096	5480	1522.2	137
14.10	1067	5335	1481.9	134
14.20	1026	5130	1425.0	130
14.30	1004	5020	1394.4	129
14.40	962	4810	1336.0	126
14.50	923	4615	1281.9	122
15.00	880	4400	1222.2	118
15.10	840	4200	1166.6	114
15.20	798	3990	1108.0	110
15.30	750	3750	1041.6	106
15.40	700	3500	972.0	101
15.50	640	3200	888.9	94
16.00	600	3000	833.3	90

16.10	558	2790	775.0	86
16.20	505	2525	701.4	80
16.30	404	2020	561.0	69
16.40	360	1800	500.0	64
16.50	280	1400	388.9	54
17.00	210	1050	292.0	45
17.10	138	690	191.2	34
17.20	66	330	91.6	21
17.30	0	0	0	-

TABLE 42. 15 October: useful energy and logic levels for mass flow rate = 0.01 kg/Sm^2

Time	Average hourly total of useful energy (KJ/m^2)	Average hourly total of useful energy for 5 m^2 collector (KJ)	Constant rate of energy delivery to provide the equivalent heating effect (W)	Logic level
6.30	0	0	0	-
6.40	22	110	30.5	-
6.50	47	235	65.3	16
7.00	74	370	102.7	22
7.10	102	510	141.6	28
7.20	130	650	180.5	32
7.30	163	815	226.4	38
7.40	204	1020	283.3	44
7.50	246	1230	341.7	50
8.00	292	1460	405.5	55
8.10	340	1700	472.2	62
8.20	386	1930	536.1	66
8.30	429	2145	595.8	70
8.40	476	2380	661.0	77
8.50	520	2600	722.2	81
9.00	564	2820	783.3	86
9.10	610	3050	847.2	91
9.20	660	3300	916.6	96
9.30	700	3500	972.2	101
9.40	744	3720	1033.3	105
9.50	788	3940	1094.4	109
10.00	824	4120	1144.4	112
10.10	858	4290	1191.7	116
10.20	886	4430	1230.5	119
10.30	916	4580	1272.2	121
10.40	936	4680	1300.0	123
10.50	960	4800	1333.3	126
11.00	982	4910	1363.8	127

11.10	1002	5010	1391.6	129
11.20	1020	5100	1416.6	129
11.30	1037	5185	1440.2	131
11.40	1043	5215	1448.6	132
11.50	1047	5235	1454.2	132
12.00	1049	5245	1456.9	132
12.10	1048	5240	1455.5	132
12.20	1046	5230	1452.7	132
12.30	1041	5205	1445.8	131
12.40	1028	5140	1427.7	130
12.50	1012	5060	1405.5	129
13.00	990	4950	1375.0	128
13.10	970	4850	1347.2	127
13.20	944	4720	1311.1	124
13.30	921	4605	1279.1	122
13.40	896	4480	1244.4	119
13.50	870	4350	1208.3	117
14.00	844	4220	1172.2	115
14.10	818	4090	1136.1	112
14.20	790	3950	1097.2	109
14.30	763	3815	1059.7	106
14.40	726	3630	1008.3	103
14.50	687	3435	954.2	99
15.00	646	3230	897.2	95
15.10	604	3020	838.8	90
15.20	550	2750	763.8	85
15.30	499	2495	693.1	79
15.40	430	2150	597.2	72
15.50	344	1720	477.7	63
16.00	270	1350	375.0	53
16.10	188	940	261.1	42
16.20	96	480	133.3	26
16.30	0	0	0	-

TABLE 43. 15 November: useful energy and logic levels for mass flow rate = 0.01 kg/Sm2

Time	Average hourly total of useful energy (KJ/m^2)	Average hourly total of useful energy for 5 m^2 collector (KJ)	Constant rate of energy delivery to provide the equivalent heating effect (W)	Logic level
7.30	0	0	0	-
7.40	28	140	38.8	-
7.50	56	280	77.7	18
8.00	82	410	113.8	24
8.10	108	540	150.0	29
8.20	136	680	188.8	33
8.30	166	830	230.5	38
8.40	195	975	270.8	43
8.50	228	1140	316.6	47
9.00	267	1335	370.8	53
9.10	311	1555	431.9	58
9.20	360	1800	500.0	64
9.30	411	2055	570.8	70
9.40	445	2225	618.1	73
9.50	480	2400	666.6	77
10.00	510	2550	708.3	80
10.10	536	2680	744.4	83
10.20	557	2785	773.6	85
10.30	575	2875	798.6	87
10.40	592	2960	822.2	89
10.50	606	3030	841.6	90
11.00	620	3100	861.1	92
11.10	631	3155	876.4	93
11.20	641	3205	890.3	94
11.30	650	3250	902.7	95
11.40	652	3260	905.5	95
11.50	653	3265	906.9	95
12.00	652	3260	905.5	95

12.10	650	3250	902.7	95
12.20	646	3230	897.2	95
12.30	639	3195	887.5	94
12.40	628	3140	872.2	93
12.50	616	3080	855.5	91
13.00	601	3005	834.7	90
13.10	586	2930	813.9	88
13.20	570	2850	791.6	87
13.30	553	2765	768.1	85
13.40	534	2670	741.6	83
13.50	512	2560	711.1	81
14.00	492	2460	683.3	78
14.10	472	2360	655.5	76
14.20	448	2240	622.2	74
14.30	417	2085	579.2	70
14.40	382	1910	530.5	66
14.50	343	1715	476.4	62
15.00	300	1500	416.6	56
15.10	257	1285	356.9	51
15.20	216	1080	300.0	46
15.30	176	880	244.4	40
15.40	145	725	201.4	35
15.50	117	585	162.5	30
16.00	86	430	119.4	24
16.10	56	280	77.7	18
16.20	26	130	36.1	-
16.30	0	0	0	-

APPENDIX 2

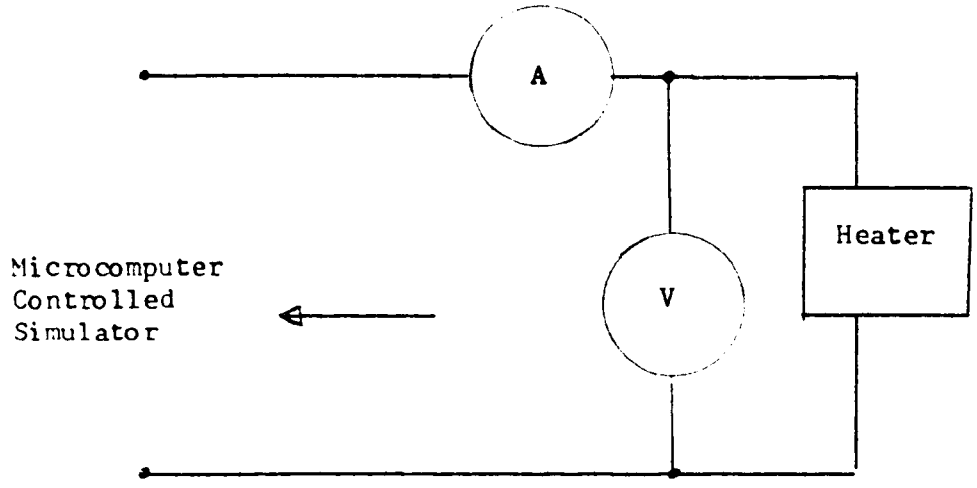

Figure 64 Calibration Circuit

Figure 64 shows the details of the circuit which was used for calibration. The basic procedure was as follows:-

The heater was checked for resistance and inductance and it was found that the inductance was negligible, hence the heater was purely resistive and therefore the power to load (heater) was equal to VI or I^2R or $\frac{V^2}{R}$.

The logic level was set from the PET and the voltage measured at each level. The power was then determined from the heater at each level. The calibration procedure was then repeated ten times, and the results are shown in Table 72 which gives the average and standard deviation values. This forms the basis of the monthly profiles calibration.

Table 72 Calibration results

logic level	Measured Power (watts)										Average Power	Standard Deviation
	Test Number											
	1	2	3	4	5	6	7	8	9	10		
16	88.65	76.56	49.19	87.62	54.21	43.07	55.40	55.80	72.88	50.73	63.41	16.56
17	93.77	81.78	51.86	91.21	59.44	48.85	60.68	60.68	78.45	51.88	67.86	16.90
18	102.69	87.62	60.67	99.00	65.28	55.40	66.64	67.51	85.20	55.80	74.58	17.58
19	110.48	94.29	64.05	107.10	71.43	61.10	74.25	73.33	91.21	65.34	81.26	18.12
20	116.73	98.49	70.10	110.48	77.89	67.51	79.39	79.39	101.15	70.62	87.18	17.95
21	124.32	104.33	75.63	119.60	86.19	73.79	86.19	84.22	108.25	75.64	93.80	18.80
22	132.82	114.99	79.32	128.52	95.31	79.87	93.78	92.24	119.06	80.83	101.66	20.46
23	138.36	131.59	85.68	134.05	103.31	86.69	99.02	99.55	128.55	88.18	109.49	21.27
24	144.10	140.31	93.77	143.48	110.99	92.24	107.14	106.59	136.54	94.82	116.98	21.73
25	154.55	145.33	99.51	153.83	116.73	94.82	112.74	113.87	144.12	101.69	123.69	23.35
26	163.26	152.50	108.14	161.93	123.09	103.31	121.40	120.22	148.64	110.48	131.35	22.91
27	166.03	159.16	113.25	168.80	130.36	108.25	128.55	133.44	153.23	117.32	137.82	22.39
28	171.57	166.65	123.09	177.20	136.51	119.06	136.54	145.41	166.73	121.99	146.46	22.33
29	177.92	174.33	127.29	184.38	144.10	126.15	145.44	151.91	172.28	126.15	152.99	22.81
30	188.68	180.79	135.90	193.91	153.22	131.60	151.91	158.56	180.07	133.44	160.80	23.58

31	193.9	197.6	144.1	202.9	160.5	138.4	157.9	163.3	190.2	142.2	169.10	24.81
32	202.2	203.7	148.6	212.2	170.1	148.0	164.0	177.2	203.7	150.6	178.03	25.50
33	207.9	207.9	159.9	219.2	179.4	158.6	173.0	186.6	212.2	157.2	186.19	24.09
34	223.1	219.2	172.3	231.2	185.1	164.7	183.7	192.5	220.0	165.3	195.88	23.98
35	233.7	227.1	177.2	237.0	193.2	170.9	191.0	203.0	228.8	172.3	203.42	26.29
36	241.9	236.1	188.0	249.4	202.9	177.9	200.7	211.4	237.8	179.4	212.55	26.97
37	252.1	144.3	189.5	260.4	211.1	185.1	210.6	219.2	246.9	189.5	220.93	28.39
38	254.5	256.2	199.1	271.8	216.1	192.5	216.9	228.8	256.2	193.9	228.60	29.31
39	264.1	262.2	206.0	280.6	227.9	205.2	225.6	236.1	262.2	205.2	237.50	28.08
40	282.5	265.7	220.0	290.6	239.4	212.2	240.3	244.4	272.7	216.8	248.46	28.11
41	291.5	276.2	227.9	297.9	246.9	223.2	245.2	255.4	283.4	225.6	257.30	28.18
42	291.5	303.5	234.5	305.3	255.3	231.2	250.3	262.2	292.4	235.3	266.15	29.47
43	298.9	317.5	243.5	316.6	265.7	239.4	261.4	270.1	300.7	245.2	275.90	30.19
44	308.1	329.1	249.4	327.2	275.3	248.6	272.7	278.9	308.1	254.5	285.19	30.91
45	316.6	341.8	257.9	334.9	280.6	256.2	281.6	287.0	315.7	262.2	293.45	31.73
46	323.3	350.7	268.3	347.8	294.3	264.8	289.7	300.7	323.3	271.8	303.47	31.62
47	339.8	352.7	275.3	358.7	302.6	271.8	297.9	308.2	336.9	283.4	312.73	32.16
48	351.8	365.9	286.1	370.0	311.0	279.9	308.2	318.5	347.7	296.1	323.52	33.02
49	359.7	385.5	295.2	377.2	323.3	298.9	316.6	329.1	356.8	303.5	334.58	33.01
50	370.0	399.2	305.3	392.9	333.0	307.2	329.1	338.9	363.8	311.9	345.13	34.55

51	385.5	408.9	315.7	402.5	339.8	315.7	332.0	348.8	375.1	316.6	354.06	36.28
52	394.0	417.6	321.4	415.4	349.7	328.1	340.8	357.8	387.6	339.8	365.22	35.63
53	404.6	430.8	331.1	423.1	358.7	337.9	353.8	362.8	399.3	360.8	376.29	35.35
54	418.7	436.3	340.8	431.9	371.0	348.8	382.4	373.1	411.1	373.0	388.71	33.77
55	426.4	447.6	352.7	441.9	383.4	358.8	395.0	381.4	419.8	384.5	399.15	33.21
56	441.9	458.9	359.7	452.1	396.0	367.9	400.4	396.1	429.7	398.2	410.09	34.14
57	448.7	469.2	374.1	464.6	405.7	377.2	407.9	406.8	439.7	403.6	419.75	33.92
58	455.5	472.7	386.4	476.2	414.3	388.7	415.4	416.5	449.8	413.3	428.88	32.51
59	465.8	485.6	398.2	490.3	427.5	399.3	426.4	424.2	458.9	422.0	439.82	33.25
60	480.9	499.8	405.7	504.6	437.4	411.1	428.6	433.0	470.4	430.8	450.23	35.87
61	492.7	509.4	417.6	514.2	448.7	425.3	437.5	442.0	484.4	440.8	461.25	35.52
62	499.8	526.4	430.8	525.2	449.8	436.4	444.2	449.8	490.3	453.2	470.59	36.45
63	514.2	536.2	440.8	541.2	461.2	446.5	449.8	461.2	501.0	461.2	481.33	38.19
64	541.2	563.7	469.2	572.6	486.7	467.0	475.1	484.4	526.4	485.6	507.19	40.13
65	552.4	576.5	479.7	581.6	496.2	479.7	478.6	501.0	536.2	508.2	519.01	39.39
66	561.2	586.8	492.7	592.0	502.2	486.8	498.6	514.2	549.9	517.8	530.22	39.23
67	566.3	602.3	502.2	601.1	514.2	507.0	522.7	524.0	558.7	527.6	542.61	37.24
68	584.2	611.6	513.0	615.6	525.2	509.4	530.1	537.5	573.9	536.2	553.67	39.53
69	597.1	623.6	530.1	627.6	533.8	516.7	542.4	548.7	582.9	548.7	565.16	39.82
70	607.7	639.7	546.2	642.3	546.2	530.1	549.9	561.2	594.6	557.4	577.53	40.70

71	619.6	651.8	546.2	653.2	558.7	542.4	581.6	568.9	605.0	568.8	589.62	40.88
72	627.6	665.5	559.9	668.2	575.2	558.7	593.3	584.2	620.9	582.9	603.64	40.17
73	642.3	665.5	580.3	680.8	597.1	568.9	614.3	593.3	632.9	591.9	616.73	37.37
74	647.7	671.0	592.0	696.1	610.2	588.1	630.2	610.3	642.3	605.0	629.29	35.14
75	664.1	679.3	606.3	707.4	620.9	601.1	635.6	627.6	655.9	616.9	641.51	34.35
76	679.3	691.8	614.2	723.2	631.6	605.0	642.3	647.8	668.3	627.5	653.10	37.15
77	689.2	700.3	623.6	729.0	643.6	615.6	647.8	665.5	679.4	638.3	663.23	36.09
78	700.3	717.4	660.0	743.4	653.2	631.6	650.5	682.2	690.5	658.7	678.78	34.51
79	711.7	726.1	676.5	760.9	664.1	646.4	671.1	696.2	703.2	671.0	692.72	34.01
80	726.1	740.5	686.3	772.8	679.3	655.9	676.6	710.3	717.4	683.5	704.87	35.24
81	736.1	758.0	697.6	792.2	683.5	669.7	687.8	720.3	728.9	693.3	716.74	38.01
82	750.7	768.3	713.1	796.7	691.8	682.2	699.0	734.7	741.9	707.5	728.59	36.49
83	768.3	780.2	730.4	813.3	706.1	692.0	706.1	749.2	753.6	718.9	741.81	38.25
84	777.2	792.2	746.2	827.1	718.9	710.3	724.6	762.4	768.3	736.1	756.33	36.44
85	780.2	808.8	756.5	842.5	734.7	723.2	737.6	774.3	780.2	746.3	768.43	36.81
86	789.2	830.2	765.3	854.9	743.4	740.5	747.8	784.7	789.2	758.0	780.32	37.94
87	800.5	842.5	783.1	865.9	759.5	749.2	761.0	798.2	801.2	766.9	792.80	37.65
88	810.3	858.1	796.7	880.1	769.8	762.4	775.8	811.8	813.3	783.2	806.15	38.06
89	822.5	869.0	808.8	897.5	787.6	775.8	786.2	825.6	830.2	807.3	821.08	37.93
90	836.3	884.8	822.5	907.2	800.5	786.2	798.2	834.8	844.0	816.4	833.09	39.25

91	850.3	897.5	837.9	928.2	833.3	798.2	811.8	847.2	858.0	834.8	849.72	38.36
92	961.1	908.8	854.9	944.6	850.3	811.8	827.1	861.2	872.2	842.5	863.45	38.59
93	880.1	921.7	870.6	966.0	867.5	819.5	837.9	876.9	878.5	858.1	877.68	41.16
94	897.5	933.1	881.6	981.0	873.7	834.8	851.8	889.6	897.6	869.0	890.97	[illegible]
95	902.3	952.8	891.2	966.0	886.4	847.2	864.3	899.2	912.0	881.7	900.31	36.44
96	913.6	967.6	907.2	982.6	897.5	859.6	880.1	913.7	925.0	889.6	913.65	37.64
97	931.4	979.3	921.7	1004.5	912.0	870.6	896.0	946.2	933.1	899.2	929.40	39.87
98	939.6	987.6	938.0	1009.5	916.9	884.9	908.8	956.1	956.0	905.6	940.30	38.50
99	952.8	1002.8	952.8	1005.2	928.2	896.0	923.4	969.3	977.6	913.6	952.17	37.08
100	969.3	1016.3	959.3	1016.3	936.4	908.8	941.3	987.7	992.7	928.2	975.63	37.25
101	982.6	1024.9	969.3	1033.4	944.6	921.7	954.4	1001.1	1007.9	941.3	978.12	37.98
102	987.6	1043.8	989.4	1048.9	959.3	934.7	967.7	1013.0	1021.5	956.1	992.2[illegible]	38.72
103	999.4	1061.1	999.4	1059.4	972.6	946.2	981.0	1024.9	1038.6	969.3	1005.13	39.51
104	1024.9	1082.0	1024.9	1073.3	989.3	961.0	992.7	1040.3	1045.5	980.9	1021.43	40.10
105	1042.0	1089.1	1043.8	1089.1	999.4	974.3	1011.3	1050.7	1057.6	999.4	1035.67	38.75
106	1059.4	1099.6	1048.9	1101.4	1021.4	984.3	1023.2	1066.3	1069.8	1009.6	1048.39	38.45
107	1076.8	1115.6	1066.3	1117.4	1031.7	1016.4	1038.6	1082.1	1089.0	1019.8	1065.37	37.30
108	1094.3	1131.7	1082.0	1140.7	1047.2	1024.9	1049.0	1097.9	1101.4	1035.2	1080.43	40.03
109	1094.3	1144.3	1094.3	1151.6	1061.1	1042.1	1062.8	1113.9	1117.4	1048.9	1093.07	38.82
110	1115.6	1158.8	1112.0	1167.9	1073.3	1059.4	1087.3	1126.4	1126.4	1061.1	1108.82	38.16

111	1130.0	1171.6	1130.0	1188.1	1087.3	1068.1	1105.0	1142.6	1128.2	1108.5	1125.94	36.28
112	1138.9	1186.2	1147.9	1195.5	1105.0	1087.3	1117.4	1155.2	1148.0	1117.4	1139.88	34.31
113	1144.3	1201.0	1158.8	1204.7	1121.0	1101.4	1131.8	1169.8	1157.0	1128.2	1151.80	33.53
114	1151.6	1215.8	1171.6	1223.2	1138.9	1110.3	1148.0	1184.4	1169.7	1142.5	1165.60	35.05
115	1151.6	1238.2	1184.4	1240.1	1157.0	1119.2	1160.7	1199.1	1175.2	1155.2	1178.07	38.57
116	1193.6	1268.4	1202.8	1255.2	1171.6	1131.8	1171.6	1212.1	1189.9	1166.1	1196.31	41.23
117	1210.3	1276.0	1212.1	1262.9	1186.2	1146.2	1184.4	1227.0	1199.1	1182.6	1208.67	38.86
118	1225.1	1291.4	1221.4	1283.7	1199.2	1164.3	1197.3	1238.3	1213.9	1197.3	1223.19	39.47
119	1238.2	1291.4	1238.2	1300.9	1201.0	1178.9	1210.3	1255.2	1240.1	1212.1	1236.63	38.57
120	1253.3	1300.9	1253.3	1316.4	1221.4	1189.9	1225.2	1270.4	1257.1	1236.4	1252.43	37.50
121	1264.6	1310.6	1272.2	1337.8	1230.7	1201.0	1245.8	1281.8	1274.2	1253.3	1267.20	38.77
122	1276.0	1322.2	1291.9	1347.6	1247.6	1202.8	1266.6	1295.2	1287.6	1266.6	1280.36	39.66
123	1293.2	1322.2	1306.8	1373.2	1253.3	1214.0	1279.9	1316.4	1302.9	1278.0	1293.99	42.58
124	1314.4	1335.9	1322.2	1387.0	1259.0	1232.6	1297.2	1326.1	1314.5	1291.4	1308.03	42.31
125	1322.2	1347.6	1337.8	1405.0	1295.2	1247.7	1312.6	1339.8	1332.0	1304.8	1324.47	40.51
126	1337.8	1363.2	1351.4	1409.0	1333.9	1262.8	1326.1	1351.5	1345.6	1324.2	1340.55	36.66
127	1347.6	1377.1	1365.3	1421.0	1351.5	1279.9	1343.7	1365.3	1361.3	1345.6	1355.85	34.99
128	1391.0	1433.0	1401.0	1465.6	1373.2	1316.4	1371.2	1387.1	1391.0	1379.1	1379.86	41.47
129	1418.0	1433.1	1425.0	1482.0	1399.0	1332.0	1387.1	1407.0	1409.0	1395.0	1408.82	37.97
130	1433.1	1433.1	1431.1	1498.4	1421.0	1345.6	1403.0	1421.0	1419.0	1413.0	1421.83	37.20

131	1449.3	1447.3	1443.2	1508.8	1433.1	1359.4	1419.0	1435.2	1431.1	1425.0	1435.14	36.45
132	1461.5	1455.4	1473.8	1523.3	1443.2	1383.1	1435.2	1451.4	1445.3	1443.2	1451.54	34.78
133	1475.9	1484.1	1484.1	1540.0	1461.5	1395.0	1451.4	1471.8	1457.5	1461.5	1468.29	35.87
134	1496.4	1498.4	1496.4	1552.6	1471.8	1413.0	1459.5	1482.0	1473.8	1471.8	1481.57	35.29
135	1506.7	1506.7	1508.8	1565.2	1494.3	1427.1	1473.8	1508.9	1486.1	1486.1	1496.37	34.62
136	1525.5	1529.6	1517.1	1584.3	1504.7	1439.2	1488.2	1525.5	1504.7	1500.6	1511.94	36.56
137	1538.0	1544.2	1523.3	1603.5	1521.3	1457.5	1504.7	1540.1	1515.0	1521.3	1526.89	36.50
138	1559.0	1561.0	1542.2	1622.8	1535.8	1482.0	1515.1	1554.8	1531.7	1533.8	1543.82	36.28
139	1575.9	1569.6	1546.4	1633.6	1544.2	1502.6	1527.6	1569.6	1548.5	1550.6	1556.86	34.57
140	1595.0	1590.8	1563.2	1644.4	1559.0	1517.2	1544.3	1584.4	1563.2	1561.1	1572.26	34.14
141	1612.1	1605.6	1580.1	1666.1	1573.8	1517.2	1559.0	1607.8	1575.9	1578.0	1587.56	39.08
142	1618.5	1620.7	1590.8	1668.3	1580.1	1527.6	1569.6	1631.5	1586.5	1590.7	1598.43	38.47
143	1637.9	1627.2	1603.5	1688.0	1592.8	1550.6	1580.1	1648.7	1601.4	1609.9	1614.01	38.48
144	1653.1	1644.4	1646.5	1701.2	1679.2	1563.2	1595.0	1663.9	1614.3	1620.7	1638.15	40.84
145	1674.8	1666.1	1659.5	1725.4	1685.8	1575.9	1614.3	1674.8	1627.1	1631.4	1653.51	42.24
146	1674.8	1679.2	1679.2	1738.8	1696.7	1595.0	1629.3	1688.0	1642.2	1648.7	1667.19	39.99
147	1685.8	1685.5	1690.1	1747.7	1714.4	1614.3	1642.2	1701.2	1659.6	1661.7	1680.28	37.83
148	1701.2	1705.6	1698.9	1761.0	1732.1	1031.5	1650.9	1714.4	1674.8	1681.4	1695.18	37.78
149	1716.5	1710.0	1714.4	1781.3	1747.7	1646.6	1661.8	1727.7	1685.8	1698.9	1709.07	39.33
150	1732.1	1725.4	1725.4	1797.1	1758.9	1663.9	1672.7	1745.4	1701.1	1721.0	1724.30	39.25

151	1745.4	1736.5	1738.8	1815.2	1772.3	1677.0	1685.8	1756.6	1716.6	1734.3	1737.85	40.08
152	1758.9	1745.4	1763.3	1835.7	1783.6	1692.4	1701.2	1776.8	1732.1	1754.4	1754.38	41.25
153	1794.8	1770.0	1776.8	1851.7	1803.8	1707.8	1716.6	1790.3	1745.4	1767.8	1772.50	42.37
154	1813.0	1792.6	1792.6	1872.5	1817.5	1723.2	1729.9	1803.9	1761.1	1776.8	1788.31	43.91
155	1822.0	1810.6	1794.8	1886.4	1833.5	1743.2	1743.2	1819.8	1776.8	1792.6	1802.29	42.94
156	1840.3	1822.0	1806.1	1900.3	1844.8	1754.4	1758.8	1835.8	1808.4	1803.9	1817.48	42.50
157	1856.3	1844.3	1833.5	1912.0	1865.5	1765.6	1774.5	1849.5	1819.8	1819.8	1834.08	42.87
158	1867.9	1860.9	1851.7	1930.6	1886.4	1776.8	1797.1	1865.6	1833.5	1838.0	1850.85	43.55
159	1879.4	1877.1	1860.9	1954.2	1893.3	1790.3	1813.0	1877.1	1840.3	1856.4	1864.20	45.01
160	1891.0	1900.3	1874.8	1968.3	1912.0	1801.6	1833.5	1891.0	1847.2	1867.9	1878.76	45.96
161	1937.7	1916.6	1884.0	1987.3	1925.9	1831.2	1851.8	1900.3	1861.0	1884.0	1897.98	45.99
162	1944.5	1928.3	1895.7	1996.8	1933.0	1842.6	1861.0	1914.3	1872.5	1898.0	1909.17	45.54
163	1961.3	1951.8	1912.0	2004.0	1947.1	1844.9	1877.1	1933.0	1886.4	1919.0	1923.66	46.21
164	1973.0	1961.3	1928.3	2023.2	1966.0	1874.8	1895.7	1961.3	1900.3	1933.0	1941.69	44.15
165	1973.0	1980.2	1944.8	2040.0	1982.6	1891.0	1912.0	1975.5	1912.0	1942.4	1955.33	43.98
166	1989.7	1989.7	1954.2	2054.4	1994.5	1905.0	1926.0	1992.1	1926.0	1963.6	1969.52	43.94
167	2001.7	2006.4	1963.6	2069.0	2008.8	1914.3	1937.7	2008.8	1940.1	1977.8	1982.82	45.51
168	2016.0	2013.5	1982.6	2093.4	2028.0	1928.3	1951.8	2025.6	1954.2	1987.4	1998.08	47.83
169	2028.0	2042.4	1999.2	2108.0	2049.6	1942.4	1961.3	2037.6	1973.1	2008.8	2015.04	48.85
170	2042.4	2054.4	2013.5	2120.3	2049.6	1954.2	1977.9	2054.5	1985.0	2032.8	2028,46	47.88

171	2052.1	2076.3	2028.0	2142.5	2071.5	1970.7	1992.1	2066.6	1999.3	2047.3	2044.64	49.89
172	2073.9	2088.5	2040.0	2157.3	2078.7	1985.0	2006.4	2081.2	2013.6	2059.4	2058.40	49.77
173	2093.4	2100.7	2088.5	2169.7	2100.7	1999.3	2020.8	2093.4	2028.0	2071.5	2076.60	49.46
174	2103.1	2120.3	2105.6	2179.7	2110.5	2008.8	2037.6	2108.1	2042.4	2086.1	2090.22	49.16
175	2113.0	2122.8	2127.1	2192.2	2130.2	2020.8	2054.5	2125.3	2056.9	2105.6	2104.90	48.88
176	2132.6	2147.4	2142.5	2209.7	2152.3	2030.4	2069.1	2135.1	2086.1	2117.9	2122.31	49.95
177	2144.9	2162.3	2157.3	2227.2	2167.3	2044.9	2081.2	2147.5	2091.0	2132.6	2136.62	51.63
178	2169.7	2172.2	2172.2	2204.7	2187.2	2056.9	2098.3	2157.4	2103.2	2137.6	2145.94	46.33
179	2182.0	2184.7	2182.2	2227.2	2222.2	2069.1	2117.9	2168.7	2120.3	2142.5	2161.79	49.39
180	2194.6	2204.7	2199.7	2232.2	2242.4	2154.9	2135.1	2182.2	2132.6	2149.9	2182.83	38.83
181	2209.7	2222.2	2222.2	2245.0	2255.0	2167.3	2149.9	2199.7	2149.9	2164.8	2198.57	38.64
182	2222.2	2232.3	2232.3	2262.7	2275.4	2184.7	2164.8	2214.7	2159.8	2174.7	2212.35	40.29
183	2239.8	2245.0	2250.0	2275.4	2285.6	2199.7	2179.7	2229.8	2172.2	2187.2	2256.2	39.96
184	2250.0	2265.2	2262.7	2295.8	2295.8	2214.7	2187.2	2245.0	2184.7	2209.7	2241.09	40.68
185	2262.7	2280.4	2283.0	2313.7	2303.5	2229.8	2204.7	2257.6	2202.2	2224.8	2256.24	39.64
186	2285.6	2298.4	2293.2	2334.2	2329.1	2245.0	2227.3	2270.3	2222.3	2239.9	2274.93	40.31
187	2298.4	2308.6	2300.9	2349.8	2344.6	2255.1	2245.0	2283.0	2234.9	2255.1	2287.54	40.25
188	2311.2	2329.1	2409.7	2365.3	2360.2	2265.2	2257.6	2300.9	2245.0	2270.3	2311.45	54.26
189	2318.8	2331.7	2331.7	2386.1	2383.5	2275.4	2270.3	2316.3	2262.7	2290.7	2316.73	43.70
190	2331.7	2352.4	2349.8	2401.8	2383.5	2303.5	2288.1	2318.9	2278.0	2303.5	2331.12	40.57
191	2339.5	2360.2	2360.2	2417.5	2394.0	2313.7	2303.5	2336.9	2295.8	2318.8	2344.01	39.46
192	2378.3	2401.8	2404.4	2457.0	2438.6	2339.5	2331.7	2373.2	2334.3	2382.40	2384.10	42.66

```
READY.

 100 OPEN3,4
 200 CMD3
 250 DIM A(81)
 300 PRINT#3,"JUNE A"
 400 PRINT#3
 1000 REM 424938=10MIN CLOCK
 2000 REM PROGRAM CLOSES ONE RELAY
 2010 REM THUS 7 RESISTORS IN SERIES
 2020 POKE 59459,255
 2030 RESTORE
 2050 FOR K=1 TO 81 : READ A(K)
 2060 POKE 59471,A(K)
 2070 REM OPEN ONE RELAY 255-A(K)
 2080 REM THUS 1 RESISTOR AT ONCE
 2090 PRINT#3:PRINT#3,K,PEEK(59471),TI$; TI
 2100 FOR X=0 TO 424938:NEXT X
 2110 NEXT K
 2120 PRINT#3:PRINT#3:PRINT#3
 2130 DATA 18,23,28,34,39,48,51,59,68
 2140 DATA 77,87,93,101,104,112,117
 2150 DATA 121,127,130,134,138,142,145
 2160 DATA 149,152,154,156,158,160,161
 2170 DATA 162,163,164,164,164,165,165
 2180 DATA 165,165,165,165,164,164,163
 2190 DATA 162,160,158,156,153,151,148
 2200 DATA 145,142,138,135,132,129,126
 2210 DATA 122,117,112,108,103,98,93
 2220 DATA 86,78,73,65,59,54,49,44,39
 2230 DATA 35,31,28,24,20,17,0.
  2240 END
READY.

JUNE A
```

1	18	011124	257043
2	23	012125	293104
3	28	013126	329165
4	34	014127	365225
5	39	015128	401286
6	48	020129	437346
7	51	021130	473406
8	59	022131	509467
9	68	023132	545528
10	77	024133	581588
11	87	025134	617648
12	93	030135	653710
13	101	031136	689770
14	104	032137	725831
15	112	033138	761891
16	117	034139	797952
17	121	035140	834012
18	127	040141	870073
19	130	041142	906134
20	134	042143	942194
21	138	043144	978255
22	142	044145	1014315
23	145	045146	1050376
24	149	050147	1086437
25	152	051148	1122497
26	154	052149	1158558
27	156	053150	1194618
28	158	054151	1230679
29	160	055152	1266740
30	161	060153	1302800
31	162	061154	1338861
32	163	062155	1374921
33	164	063156	1410982
34	164	064157	1447042
35	164	065158	1483103
36	165	070159	1519163
37	165	071200	1555224
38	165	072201	1591284
39	165	073202	1627345
40	165	074203	1663405
41	165	075204	1699466
42	164	080205	1735526
43	164	081206	1771587
44	163	082207	1807648
45	162	083208	1843708
46	160	084209	1879769
47	158	085210	1915829
48	156	090211	1951890
49	153	091212	1987951
50	151	092213	2024011
51	148	093214	2060072
52	145	094215	2096133
53	142	095216	2132194
54	138	100217	2168255
55	135	101218	2204315
56	132	102219	2240376
57	129	103220	2276436
58	126	104221	2312497
59	122	105222	2348558
60	117	110223	2384619
61	112	111224	2420679
62	108	112225	2456740
63	103	113226	2492801
64	98	114227	2528862
65	93	115228	2564922
66	86	120229	2600983
67	78	121230	2637043
68	73	122231	2673104
69	65	123232	2709164
70	59	124233	2745225
71	54	125234	2781285
72	49	130235	2817346
73	44	131236	2853406
74	39	132237	2889467
75	35	133238	2925528
76	31	134239	2961588
77	28	135240	2997649
78	24	140241	3033709
79	20	141242	3069770
80	17	142243	3105831
81	0	143244	3141891

APPENDIX 4

Symbol	Meaning of principal symbols	Units
R_1	pump control function	-
R_2	top-tank control function	-
R_3	middle-tank control function	-
R_4	bottom-tank control function	-
R_5	load control function	-
$T_{s.1}$	top tank temperature	^oC
$T_{s.2}$	middle tank temperature	^oC
$T_{s.3}$	bottom tank temperature	^oC
mc_{p_1}	thermal capacity of top tank section	$KJ/^oC$
mc_{p_2}	thermal capacity of middle tank section	$KJ/^oC$
mc_{p_3}	thermal capacity of bottom tank section	$KJ/^oC$
$\dot{m}_L$	thermal capacity rate of fluid transferred to load	$KJ/^oC$ hr
$\dot{m}_c$	thermal capacity rate of fluid passing through collector	$KJ/^oC$ hr
$UA_{s.1}$	product of loss coefficient and the surface area from top tank section	KJ/hr ^oC
$UA_{s.2}$	product of loss coefficient and the surface area from middle tank section	KJ/hr ^oC

$UA_{s.3}$	product of loss coefficient and the surface area from bottom tank section	KJ/hr ^{o}C
T_A	ambient temperature	^{o}C
γ	time	hour
F_i^C	collector control function	-
F_i^L	load control function	-
T_{Lr}	temperature of the fluid replacing that extracted to supply the load	^{o}C
UiAi	product of loss coefficient and the area available for losses for tank segment i	KJ/hr ^{o}C
T_{Co}	temperature of the fluid from the collector	^{o}C
$(\dot{m}c_p)_c$	thermal capacity rate of fluid passing through collector	KJ/^{o}C hr
$(\dot{m}c_p)_L$	thermal capacity rate of fluid transferred to load	KJ/^{o}C hr
T_a	ambient temperature	^{o}C
$(mc_p)_i$	thermal capacity for tank segment i	KJ/^{o}C
T_{i-1}	initial temperature of section 1	^{o}C
T_i	initial temperature of section 2	^{o}C
T_{i+1}	initial temperature of section 3	^{o}C

APPENDIX 5

Symbol	Meaning	Units
R_b^h	beam radiation on a horizontal plane	KJ/m^2
R_d^h	diffuse radiation on a horizontal plane	KJ/m^2
W	hour angle	-
n	the day of the year	-
δ	declination	-
θ^t	angle of incidence of beam radiation on a tilted plane	degree
θ^h	angle of incidence of beam radiation on a horizontal plane	degree
ϕ	latitude	degree
R_H	total radiation on a horizontal plane	KJ/m^2
R_d^t	diffuse radiation on a tilted plane	KJ/m^2
R_b^t	beam radiation on a tilted plane	KJ/m^2
R_T	total radiation on a tilted plane	KJ/m^2

τ	the transmittance considering absorption and reflection	-
$\dot{m}_c$	the collector mass flow rate	Kg/Sm^2
T_{in}	the inlet fluid temperature	^oC
T_a	the ambient temperature	^oC
τ_a	the transmittance considering only absorption	-
W	the distance between tube centres	m
a_i	the ratio of the overall loss coefficient to the loss coefficient from the i^{th} cover to the surrounding	-
$h_{f,i}$	the convection heat transfer coefficient between the fluid and the tube wall	$KJ/hrm^2{}^oC$
δ_p	the plate thickness	m
ρ_d	the reflectance of the transparent cover for diffuse radiation	-
K_p	the plate conductivity	KJ/hrm^oC
A_c	the collector area	m^2
C_p	the specific heat of fluid	KJ/kg^oC

N	the number of covers	-
α	the absorptance of the absorber plate	-
U_L	the collector overall loss coefficient	$KJ/hrm^2{}^oC$
D_o	the outside tube diameter	m
D_i	the inside tube diameter	m
C_b	the bond conductivity	-
Q_u	the rate of useful energy gain	KJ/m^2
η	the efficiency of the collector	-
$\dot{m}_L$	load flow rate	kg/S
T_{Co}	temperature of the fluid from the collector	^oC
T_{Lr}	temperature of the fluid replacing that extracted to supply the load	^oC
$U_i A_i$	product of the U value and the area available for losses for tank segment i	KJ/hr^oC
F_i^C	collector control function	-
F_i^L	load control function	-
V	tank volume	m^3

T_{i-1}	initial temperature of node 1 at each hour	^{o}C
T_{i}	initial temperature of node 2 at each hour	^{o}C
T_{i+1}	initial temperature of node 3 at each hour	^{o}C
T_{1}	final temperature of node 1 at each hour	^{o}C
T_{2}	final temperature of node 2 at each hour	^{o}C
T_{3}	final temperature of node 3 at each hour	^{o}C

REFERENCES

1. N. T. Bowman and E. Eldessouky, 'A low-cost simulator for studying the performance of solar energy storage containers', UKISES Conference, Solar Energy in the 80s: Technical and Economic Viability, University of Birmingham, 1980.

2. T. D. Brumleve, 'Sensible Heat Storage in Liquids', Sandia Lab. Energy Report, SLL-73-0263, 1974.

3. J. A. Duffie and W. A. Beckman, 'Solar Energy Thermal Processes', John Wiley, 1974.

4. H. Heywood, 'Solar Energy for Water and Space Heating', J. Inst. Fuel, 27, 1954.

5. B. J. Brinkworth, 'Active Collection and Use of Solar Energy', Sun at Work in Britain, No 5, 1977.

6. L. F. Jesch and P. Soldatos, 'Solar Water Heating: Engineering & Economic Analysis of a New Technology', Report No 47, Dept Mech. Eng., University of Birmingham, 1977.

7. G. O. G. Lof and R. A. Tybout, 'Cost of House Heating with Solar Energy', Solar Energy, 14, No 3, 1973.

8. B. Carter, 'Storing Solar heated water without mixing the different temperatures of the flow from the Collectors.' Sun at Work in Britain, No 7, 1978.

9. M. K. Sharp, R. I. Loehrke, 'Stratified thermal Storage in residential Solar energy application', J. Energy, Vol. 3, No 2, 1979.

10. W. E. Buckles, S. A. Klein and J. A. Duffie, 'Analysis of Solar Water Heating Systems', Silver Jubilee Congress, ISES Conf., ATLANTA, GEORGIA, U.S.A., Vol. 2, 1979

11. S. A. Klein, 'Mathematical Model of Thermal Storage', Proceedings of

the workshop on solar energy storage subsystems for heating and cooling. Virginia University, Charlottesville, U.S.A., 1975

12. E. S. Davis, R. Bartera, 'Stratification in Solar water heaters storage tanks,' Proceedings of the workshop on solar energy storage sybsystems for heating and cooling, Virginia University, Charlottesville, U.S.A. 1975.

13. Z. Lavan, J. Thompson, 'Experimental Study of thermally stratified hot water storage tanks', Solar Energy, 19, No 5, 1977.

14. A. Whillier, 'Solar Energy Collection and its Utilization for House Heating', DSc thesis, MIT, 1953.

15. BS5918: 1980, 'Code of Practice for Solar Heating Systems for Domestic Hot Water', BSI, London, 1980.